NASA CR-134738

QCSEE TASK II FINAL REPORT

Engine and Installation Preliminary Design

by

R. Neitzel
R. Lee
A.J. Chamay

GENERAL ELECTRIC COMPANY

prepared for

NATIONAL AERONAUTICS AND SPACE ADMINISTRATION

NASA-Lewis Research Center
Contract NAS 3-16726

TABLE OF CONTENTS

TABLE OF CONTENTS (Continued)

TABLE OF CONTENTS (Concluded)

LIST OF ILLUSTRATIONS

LIST OF ILLUSTRATIONS (Continued)

LIST OF ILLUSTRATIONS (Continued)

LIST OF ILLUSTRATIONS (Continued).

LIST OF ILLUSTRATIONS (Concluded)

LIST OF TABLES

LIST OF TABLES (Continued)

LIST OF TABLES (Continued)

LIST OF TABLES (Continued)

LIST OF TABLES (Continued)

LIST OF TABLES (Concluded)

INTRODUCTION

The QCSEE program (NAS3-16726) was initiated by NASA-Lewis Research Center in April, 1972.

The purpose of this program is to identify candidate AW and EBF experimental engines to be tested in the 1973-75 time period, which would be the base for a quiet, clean, commercial STOL propulsion system certified in the late 1970's to early 1980's.

The study and design phase of the program is divided into two parts, a sixteen week engine parametric study (TASK I), and a subsequent ten week preliminary design effort (TASK II), directed at a more detailed investigation of four engines selected from the parametric study.

This report documents the significant results from the Task II preliminary design study.

SUMMARY

The results of the General Electric Task II work in compliance with the NASA contract "STOL Aircraft Quiet Clean Propulsion System Study" are summarized below. Specific content of the Task II effort is shown on Figure S - 1. The study involved the preliminary design of four basic engines with alternate installations in several cases. The specific propulsion systems studied and their designations are listed on Figure S - 2. These propulsion systems were selected by NASA based on recommendations made by General Electric at the conclusion of the Task I parametric study. These designs were laid out around the F101 core which is designed to meet commercial standards in addition to its use in the military B-1 application.

The requirement which dominates the design of the engine and its installation is noise. Noise objectives were set for each of the cases ranging from 95 - 100 EPNdB. Low emissions which affect the core combustor design are also a major requirement for the study. Other requirements are described in Section I of this report.

The designs are pointed toward commercial operation in the approximately 1980 time period. Technology utilized in the GE19 designs is expected to be well in hand for this timing.

The primary focus of the Task I study and the requirements set for Task II were on powered lift STOL with 2000' (609.6 m) field length. However, the designs laid out in Task II are applicable to the range of short fields including both powered and nonpowered lift. For example, the augmentor

- PRELIMINARY DESIGN OF FOUR PROPULSION SYSTEMS
  - VARIABLE PITCH 1.25 FAN PRESS. RATIO, EBF GEARED & DIRECT DRIVE VERSIONS
  - FIXED PITCH 1.35 FAN PRESS. RATIO, OTW &EBF
  - TWO FLOW AUGMENTOR WING ENG., 3.0 FAN PRESS. RATIO
- NOISE 95 TO 100 EPNdB @ 500' SIDELINE
- LOW EMISSIONS
- PRODUCT TYPE DESIGNS, ~1980 TIMING
- ORIGINAL FOCUS ON 2000' (609.6M) STOL - BUT RESULTS APPLICABLE TO RANGE OF FIELD LENGTHS
- INPUT TO TASK III - PROGRAM PLANNING.

Figure S-1. Task II Content.

	NOMINAL F_N	FAN P/P	FEATURES
GE19/F6D	24000 LB (106757 N)	1.25	EBF - GEAR DRIVE - V.P.
GE19/F6E	24000 LB (106757 N)	1.25	EBF - DIRECT DRIVE - V.P.
GE19/F2C1	24000 LB (106757 N)	1.35	EBF
GE19/F2C2	24000 LB (106757 N)	1.35	EBF - DECAYER
GE19/F2C3	24000 LB (106757 N)	1.35	UPPER SURFACE BLOWING (OTW)
GE19/F9A2	14900 LB (66278.5 N)	3.0	AW - FIXED INLET
GE19/F9A3	14900 LB (66278.5 N)	3.0	AW - VARIABLE INLET

Figure S-2. Task II Summary Preliminary Designs Based on F101 Core.

wing engine (GE19/F9A) will be of most interest at field lengths below 2000' (609.6 m), the variable pitch engines EBF (GE19/F6D & E) will be of interest in the 2000 to 3000' (609.6 to 914.4 m) range, the fixed pitch engine in an upper surface blowing installation (GE19/F2C3) will be of interest in the 2000 to 3000' (609.6 to 914.4 m) range, and the fixed pitch engine in a nonpowered lift installation will be of interest for field lengths above 3000' (914.4 m).

The GE19 designs described in this report are used as input to the Task III planning study for the QCSEE program. The results of this study will be reported upon separately to NASA.

General characteristics of the GE19/F2C, GE19/F6D, GE19/F6E and the GE19/F9A are given in Tables S - 1, S - 2, S - 3, and S - 4, respectively. Engine cross section schematics are shown in Figures S - 3, S - 4, S - 5, and S - 6. Installation drawings are shown in Section VI.

A general performance summary showing takeoff and cruise lapse rates and SFC levels is given on Table S - 5. The installed values shown do not include any external drag or interference effects. The 80 kt (41.16 m/ 920) value is shown as being representative of a liftoff condition.

Basic engine and installation weights are given on Table S - 6. Installation weights shown reflect current practice now in commercial service.

Table S - 7 gives the overall noise results using the assumptions as shown. In the case of the augmentor wing engines, engine system noise only is given, NASA having provided a wing noise goal separately.

Table S-1. Task II Summary, GE19/F2C EBF Engine.

- DUAL ROTOR
- MIXED FLOW
- SINGLE STAGE, T1 FAN
- 4 STAGE LPT
- TWO-POSITION JET NOZZLE

T/O POWER SETTING 90°F (32.2°C) DAY, UNINSTALLED

FAN PRESSURE RATIO	1.35
OVERALL PRESSURE RATIO	22.7
CORRECTED FAN FLOW, LB/SEC	969 (4310 N/Sec.)
BYPASS RATIO	8.3
THRUST, LB	24,000 (106757 N)
SFC	.345

- FAN TIP DIAMETER 70" (177.8 cm)
- BASIC ENGINE WEIGHT, LB 3600 (1632.9 kg)

Table S-2. Task II Summary, GE19/F6D EBF Engine.

- DUAL ROTOR
- SEPARATE FLOW
- SINGLE STAGE VARIABLE PITCH, COMPOSITE FAN BLADE
- TWO STAGE LPT
- GEAR DRIVE RATIO = 3.24
- TWO-POSITION FAN DUCT NOZZLE
- REVERSE PITCH FOR REVERSE THRUST

T/O POWER SETTING 90°F (32.2°C) DAY, UNINSTALLED

FAN PRESSURE RATIO	1.25
OVERALL PRESSURE RATIO	15.5
CORRECTED FAN FLOW, LB/SEC	1200 (544.31 kg/sec)
BYPASS RATIO	15
THRUST, LB	24,000 (106757.31 N)
SFC	.286

- FAN TIP DIAMETER 83" (210.8 cm)
- BASIC ENGINE WEIGHT, LB 4050 (1837.1 kg)

Table S-3. Task II Summary, GE19/F6E EBF Engine.

- DUAL ROTOR
- SEPARATE FLOW
- SINGLE STAGE VARIABLE PITCH, COMPOSITE FAN BLADE.
- 5 STAGE LPT
- DIRECT DRIVE
- TWO-POSITION FAN DUCT NOZZLE
- REVERSE PITCH FOR REVERSE THRUST

T/O POWER SETTING 90°F (32.2°C) DAY, UNINSTALLED

FAN PRESSURE RATIO	1.25
OVERALL PRESSURE RATIO	16.2
CORRECTED FAN FLOW, LB/SEC	1200 (544.3 kg/sec)
BYPASS RATIO	14.4
THRUST, LB	24,000 (106757 N)
SFC	.289

- FAN TIP DIAMETER 83" (210.8 cm)
- BASIC ENGINE WEIGHT, LB 4200 (1905.1 kg)

Table S-4. Task II Summary, GE19/F9A Augmentor Wing Engine.

- DUAL ROTOR
- 2 FLOW
- TWO STAGE Ti FAN + WING FLOW BOOSTER
- TWO STAGE LPT
- TWO-POSITION JET NOZZLE
- WING FLOW THRUST ~ 80% OF TOTAL THRUST

T/O POWER SETTING 90°F (32.2°C) DAY, UNINSTALLED	
FAN PRESSURE RATIO	3.0
WING PRESSURE RATIO	3.0
OVERALL PRESSURE RATIO	25
CORRECTED FAN FLOW, LB/SEC	366 (166.0 kg/sec)
BYPASS RATIO	2.2
TOTAL THRUST, LB	14,880 (66189 N)
WING THRUST, LB	11,930 (53067 N)
CORE THRUST, LB	2,950 (13122 N)
SFC	.595

- FAN TIP DIAMETER 45" (114.3 cm)
- BASIC ENGINE WEIGHT, LB 3000 (1360.8 kg)

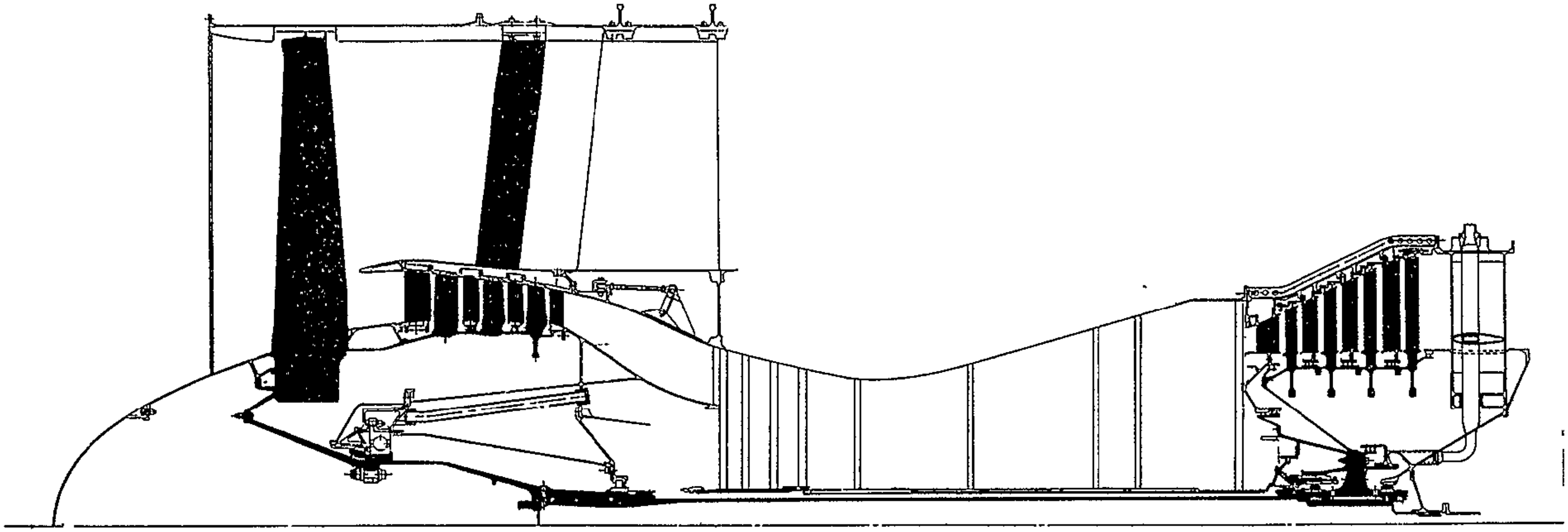

Figure S-3. GE19/F2C Cross Section.

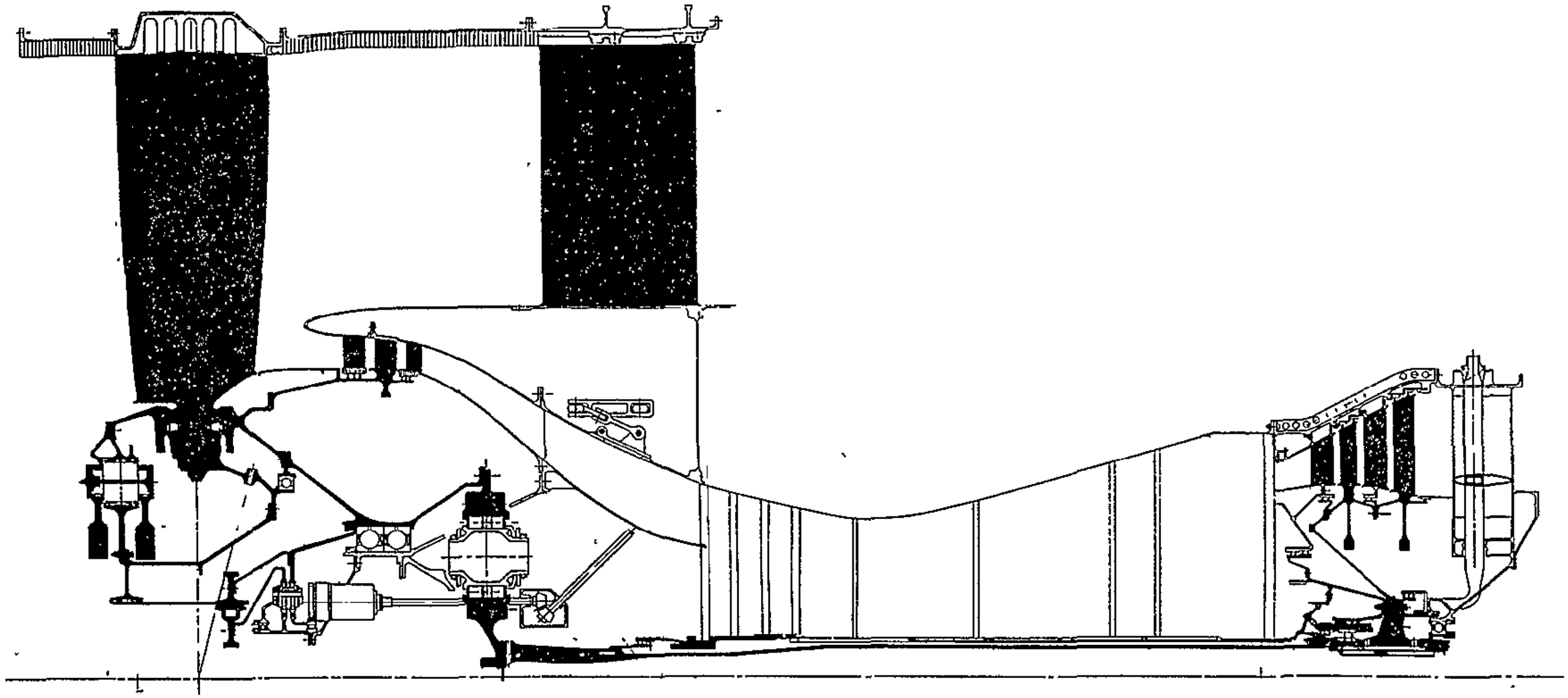

Figure S-4. GE19/F6D Cross Section.

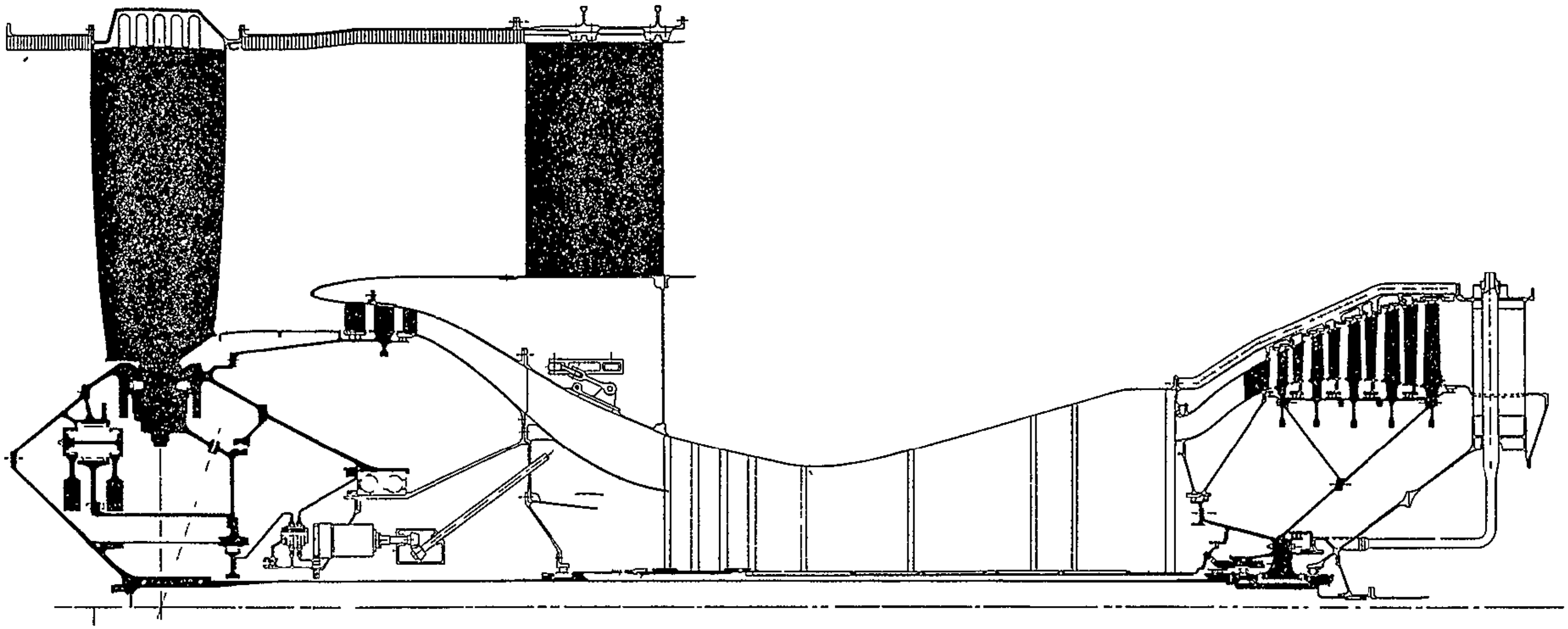

Figure S-5. GE19/F6E Cross Section.

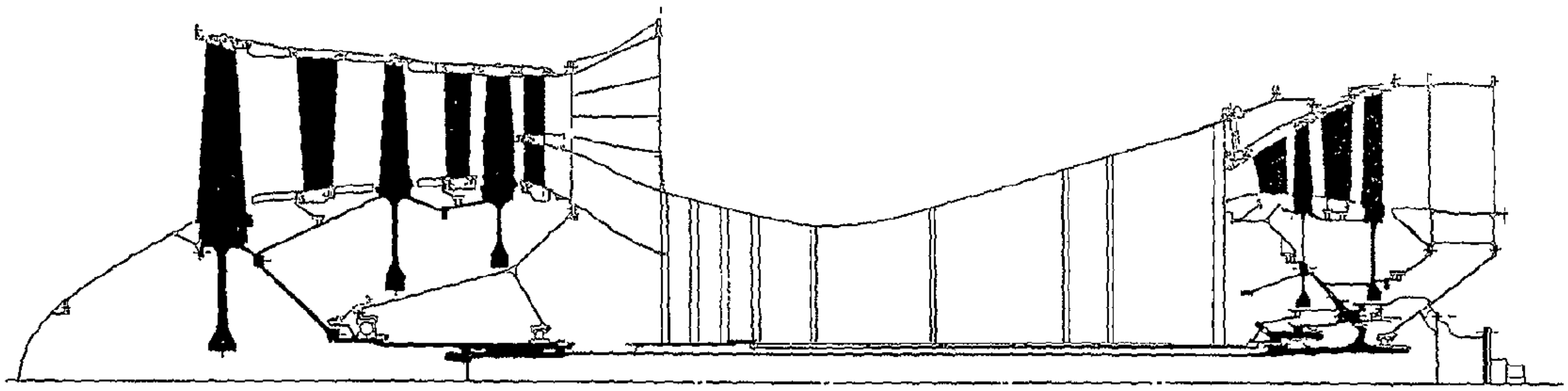

Figure S-6. GE19/F9A Cross Section.

Table S-5. Task II Summary, GE Performance Summary.

ENGINE	F2C1	F2C2	F2C3	F6D / F6E	F9A2 / F9A3
SEA LEVEL STATIC - TO RATED FN	24,000 (106757 N)	24,000 (106757 N)	24,000 (106757 N)	24,000 (106757 N)	14,900 (66279 N)
SEA LEVEL M = .1 - TO INSTALLED	19,800 (88250 N)	19,200 (85060N)	20,000 (89100 N)	19,100 (85030 N)	13,200 (58700 N)
M = .75, 30K, MAX. CR.					
UNINSTALLED FN	5,800 (25800 N)	5,800 (25800 N)	5,800 (25800 N)	5,000 (22241 N)	4,300 (19200 N)
INSTALLED* FN	5,400 (24020 N)	5,200 (23131 N)	5,400 (24020 N)	4,700 (18683 N)	4,000 (17850 N)
INSTALLED* SFC	.663	.682	.660	.671	.809

* INTERNAL LOSSES ONLY

Table S-6. Task II Summary, GE19 Series Weights.

	F2C1	F2C2	F2C3	F6D1	F6E1	F9A2	F9A3
BASIC ENGINE WT.	3600 (1632.9 kg)	3600 (1632.4 kg)	3600 (1632.9 kg)	4050 (1837 kg)	4200 (1905.1 kg)	3000 (1360.8 kg)	3000 (1360.8 kg)
BASIC ENGINE F_N/W	6.7 (1610.3 kg)	6.7 (65.7 N/kg)	6.7 (65.7 N/kg)	5.9 (57.9 N/kg)	5.7 (55.9 N/kg)	5.0 (49.0 N/kg)	5.0 (49.0 N/kg)
INSTALLATION WT.	3550 (1610.3 kg)	3960 (1796.2 kg)	3070 (1392.5 kg)	2420 (1097.7 kg)	2500 (1134 kg)	1500 (680.4 kg)	1730 (784.7 kg)
TOTAL WT.	7150 (3243.1 kg)	7560 (3429.2 kg)	6670 (3025.5 kg)	6470 (2934.7 kg)	6700 (3039.1 kg)	4500 (2040.7 kg)	4730 (2145.5 kg)

Table S-7. Task II Summary, Noise Results.

- 500' (152.4M) SIDELINE
- 100' (30.48.0M) ALTITUDE
- T/O POWER
- GRASS/GROUND ATTENUATION

	EPNdB
GE19/F6D	95
GE19/F6E	95
GE19/F2C1	100
GE19/F2C2	98
GE19/F2C3	97
GE19/F9A2*	90
GE19/F9A3*	89

*ENGINE SYSTEM NOISE ONLY

The observations that we made from the results of this Task II preliminary design study are as follows:

1. The GE19 series of engines based on the F101 core can meet the noise and emissions objectives and are believed to be competitive commercial powerplants for the 1980 time period.

2. The variable pitch fan engines achieve low noise at better DOC than other under-the-wing EBF types. At the 1.25 fan pressure ratio of the GE19/F6D & E, they can meet the 95 EPNdB noise goal with flap impingement noise being the limiting constituent.

3. The reverse pitch feature has a significant advantage in weight compared to a conventional reverser at fan pressures below 1.30 provided that light weight blades can be developed to be acceptable for a commercial engine. It must be pointed out that uncertainty as to the level of reverse thrust and the mechanical operation of the fan in reverse mode exists which must be resolved by suitable experimental programs.

4. Both geared and direct drive designs can be used for a 1.25 variable pitch fan engine with the geared design having a small advantage in weight. Performance is essentially the same but the direct drive design is expected to provide lower maintenance costs. The direct drive engine has a higher design tip speed but the multiple pure tone noise (MPT's) is suppressed in the inlet so that there is no difference in system noise.

5. The 1.35 fan pressure ratio fixed pitch engine in an over-the-wing installation can meet 97 EPNdB at the 500' side line condition. Because of shielding effects, the noise footprint has the same area as an EBF aircraft with 95 EPNdB sideline noise.

6. The 1.35 fan p/p fixed pitch OTW installation shows up very well on a DOC basis compared to other EBF installations considering propulsion system effects only. Effects of aircraft design differences including whatever means are required to achieve flow attachment to the upper surface of the flaps for good lift performance must be added to arrive at the total DOC difference.

7. The under-the-wing installation of the fixed pitch engine has a higher noise and a poorer DOC considering propulsion system effects only relative to the OTW installation. Adding an external mixer or "decayer" to reduce noise results in a significant increase in DOC and does not appear to be a productive way of achieving low noise for a 1980 application.

8. The augmentor wing engine has a basic problem in that the noise in reverse thrust is excessive even if the engine is throttled back substantially. Reverse thrust noise does not appear to be limiting for either the fixed pitch or reverse pitch engines.

9. Emissions objectives established for this study are believed to be achievable without the use of water injection provided that adequate development effort is applied.

10. The translating plug inlet studied for the augmentor wing engine did not show a payoff relative to a fixed geometry suppressed inlet. The fixed geometry inlet with relatively high throat Mach nos. at take-off is an interesting approach which will require further evaluation.

11. The engines studied do not meet the transient response objectives set by NASA. The variable pitch engine comes closest if high fan speed is maintained at approach but this may be at the expense of approach noise. However, the response rates of all the engines are believed to be attractive for the STOL aircraft and further study of the requirements is recommended.

12. Growth of the variable and fixed pitch engines of 25% thrust can be accomplished within the same fan size utilizing reasonable projections of F101 core capability. State-of-the-art improvements in flap and engine noise or increased suppression thereof should prove possible for the time period when 25% growth would be required in order to meet acceptable aircraft noise levels.

I - SYSTEMS AND PERFORMANCE

REQUIREMENTS

The following series of figures summarizes the requirements placed upon the Task II engine and propulsion system design by NASA. Table I - 1 describes the sizing required and Table I - 2 the noise objectives. Specific installation requirements are shown on Table I - 3, Figures I - 1 and I - 2. Life and duty cycle requirements are shown on Figure I - 3, Tables I - 4 and I - 5. The aircraft characteristics to be used in the noise evaluation are shown on Table I - 6 and Figure I - 4.

PERFORMANCE

All performance data are predicated on application of specific QCSEE low pressure spool designs to the F101 core engine. Commercial type ratings have been applied as shown on Table I-7.

Overall cycle design parameters are shown on Table I - 8. T41 is defined as rotor inlet total temperature. The maximum T41 would be reached as takeoff power on a 90° (32.22°C) day with nominal bleed and horsepower extraction. The core duct exit velocity shown on the Table for the GE19/F2C is the mixed flow velocity. Mixer plane conditions were selected to provide near optimum performance, while separate flow cycles were designed to reduce core exit velocity consistent with reasonable fan turbine exit conditions. Component efficiency levels are given on Table I - 9.

Table I-1. Task II Requirements, General.

- ~1980 CERTIFICATION
- F101 CORE
- T/O THRUST FLAT RATED TO 90°F (32.2 °C)
  - 24,000 - 25,000 LB - EBF
    (106757.) - (111206. N)
  - 14,000 - 15,000 LB - AW
    (62275.) - (66723. N)
- T_4 ~ 2400°F (1310 °C)
- V.P. 1.25 FAN P/P
  - — DIRECT DRIVE EBF
  - — GEAR DRIVE EBF
- F.P. 1.35 FAN P/P
  - — EBF
  - — EBF WITH DECAYER
  - — UPPER SURFACE BLOWING
- AW 3.0 FAN P/P
  - — 2 FLOW SYSTEM

Table I-2. Task II Acoustic Goals.

- 500' SIDELINE
  (152.4)
- T/O POWER SETTING
- 80 KT @ 100' ALTITUDE
  (41.16 n/sec) (30.48 n)
- GRASS/GROUND ATTENUATION
- ENGINE + FLAP INTERACTION NOISE FOR EBF
- ENGINE SYSTEM NOISE ONLY FOR AW

		EPNdB
1.25 P/P VP EBF		~ 95
1.35 P/P FP EBF		~ 100
	EBF WITH DECAYER	~ 97
	UPPER SURFACE BLOWING	~ 97
3.0 P/P FP AW		~ 92

Table I-3. Task II Installation Requirements.

- ENGINE-MOUNTED REVERSER
- VERTICAL ENGINE REMOVAL
- BARE ENGINE SEPARABLE FROM NACELLE
- ACCESSORIES MOUNTED IN NACELLE
- BORESCOPE PORTS BETWEEN STAGES
- TWO-HOUR COMPONENT REPLACEMENT
  - NASA-SUPPLIED CURVES
    - ELECTRIC POWER
    - HYDRAULIC POWER

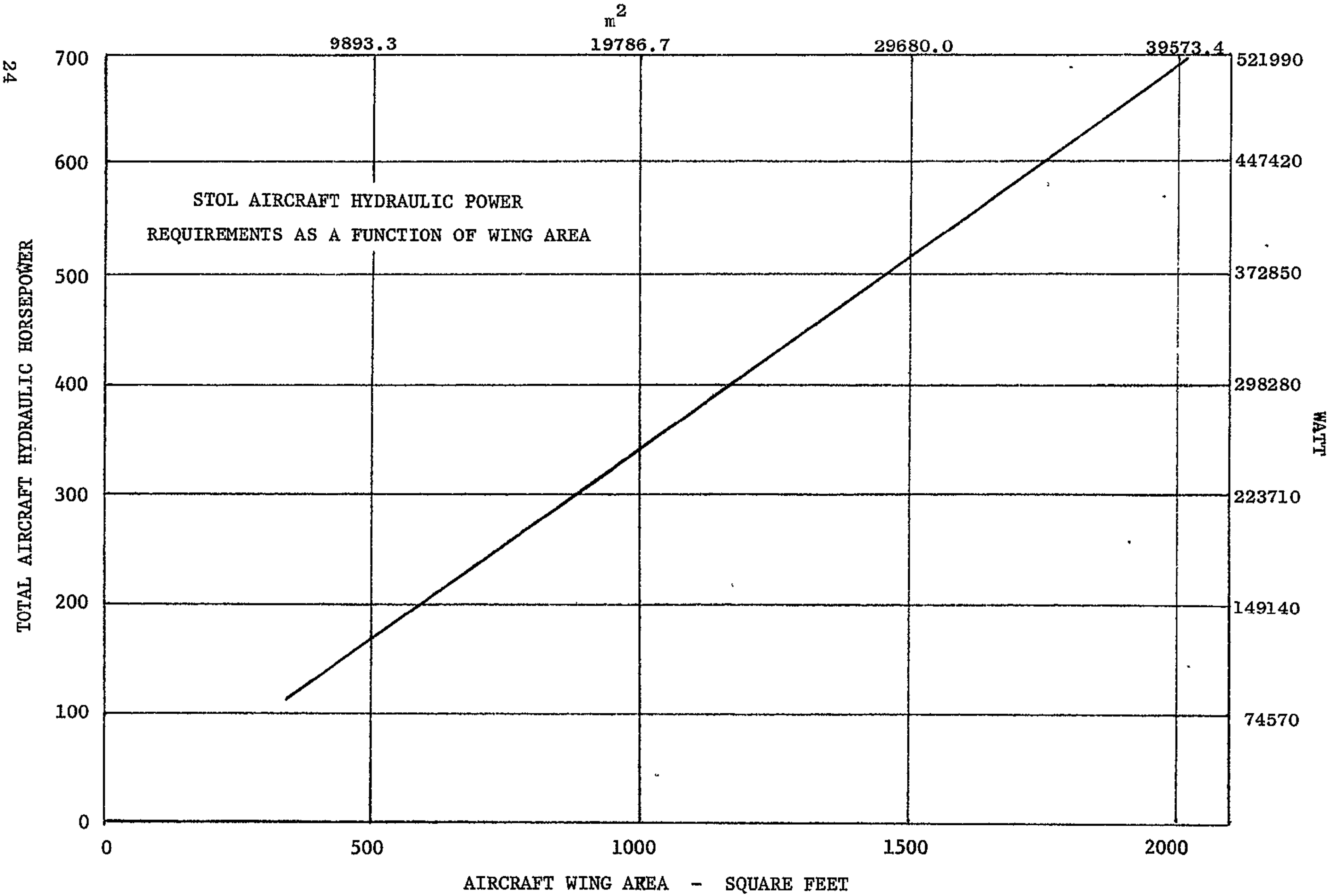

Figure I-1. Task II Requirements, Hydraulic Horsepower.

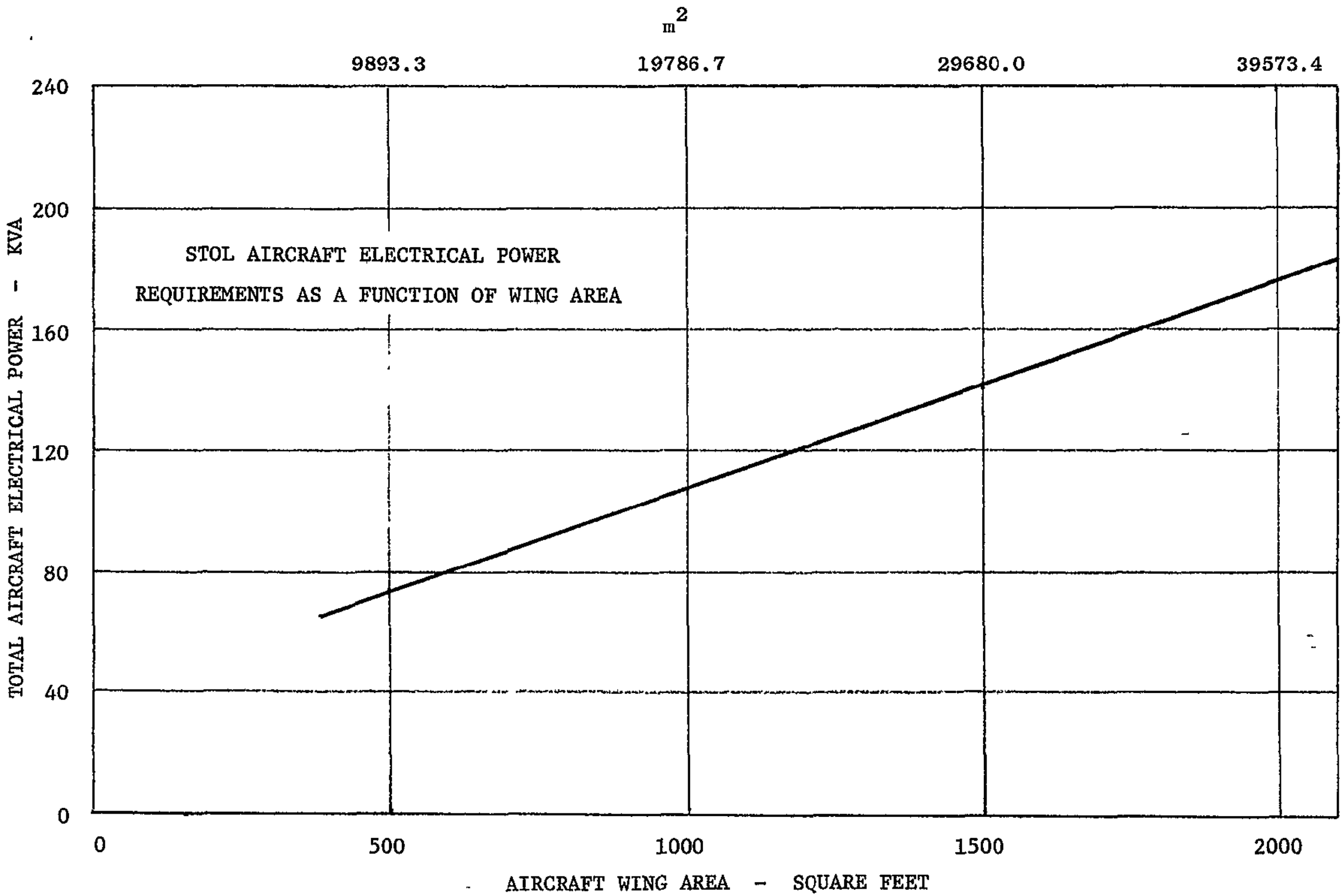

Figure I-2. Task II Requirements, Electrical Power.

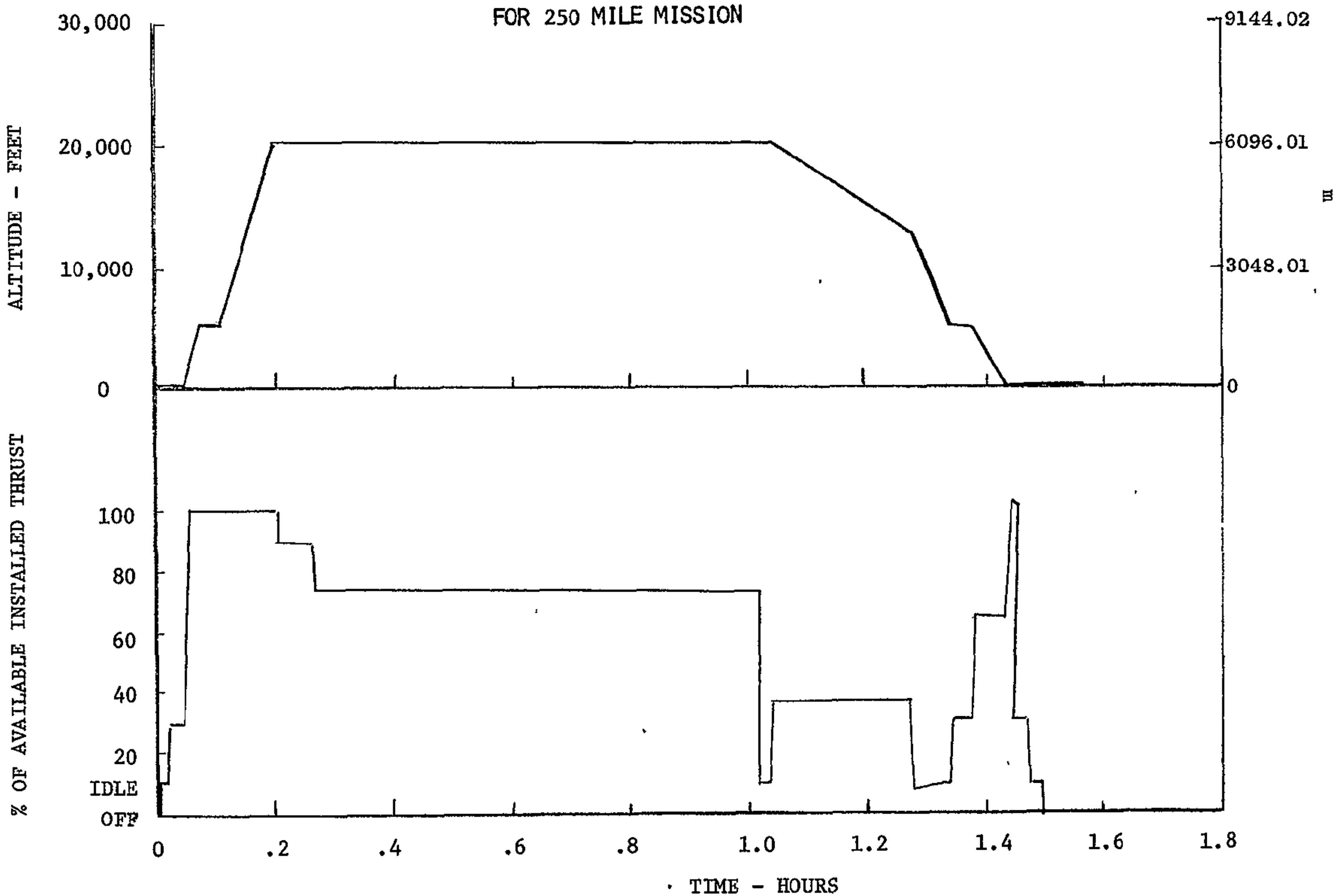

Figure I-3. Task II Requirements, Duty Cycle for 250-Mile Mission.

Table I-4. Task II Requirements, Typical STOL Mission.

Mission Segment	Altitude	Speed	% Power	Time (Min)	% Time
Start	0 (0 Kn)	0	-	.5	1
Idle - Taxi	0 (0 Kn)	0	4-20	7	12
Takeoff	0 (0 Kn)	0	T/O	1	2
Climb	0-30K (0 - 9.144 Kn)	.3-.8M	Max Climb	6	11
Cruise	30K 9.144 Kn)	.8	70% Max Cruise*	16	28
Descent	30K-5K (9.144 - 1.524 Kn)	.8-.3	Flt. Idle	14	25
Maneuver	5K (1.524 Kn)	.5	60	3	5
Landing	5K-0 (1.524 - 0 Kn)	.2-.15	35/55*	2	4
Thrust Reverse	0 (0 Kn)	.15-.02	T/O	.15	.3
Idle Taxi	0 (0 Kn)	0	4-20	7	12

* Max. Cruise for V. P. Cycles

Table I-5. Task II Requirements, Component Life.

Component	Service Life/Installation Hours	Service Life/Installation Flight Cycles	Total Service Life Hours	Total Service Life Flight Cycles
Combustor	9000	18000	18000	36000
HPT Blades & Vanes	9000	36000	18000	36000
LPT Blades & Vanes	9000	18000	27000	54000
Bearings & Seals	18000	36000	18000	36000
C & A Components*	18000	36000	36000	72000
Other Components	18000	36000	36000	72000

* Feedback cables, T/C and harness, bleed valves, and fuel nozzles are 1/2 this value.

Table I-6. Task II Requirements, Aircraft Characteristics.

- INSTALLED T/O THRUST / T/O GROSS WEIGHT
  - .615 EBF
  - .40 AW
- EBF APPROACH POWER SETTING 72% MAX F_N @ 80 KTS (41.16 n/sec)
- AW APPROACH POWER SETTING 55% MAX F_N @ 80 KTS (41.16 n/sec)
- .8 Mo 30,000' (9144.02 n) CRUISE CAPABILITY

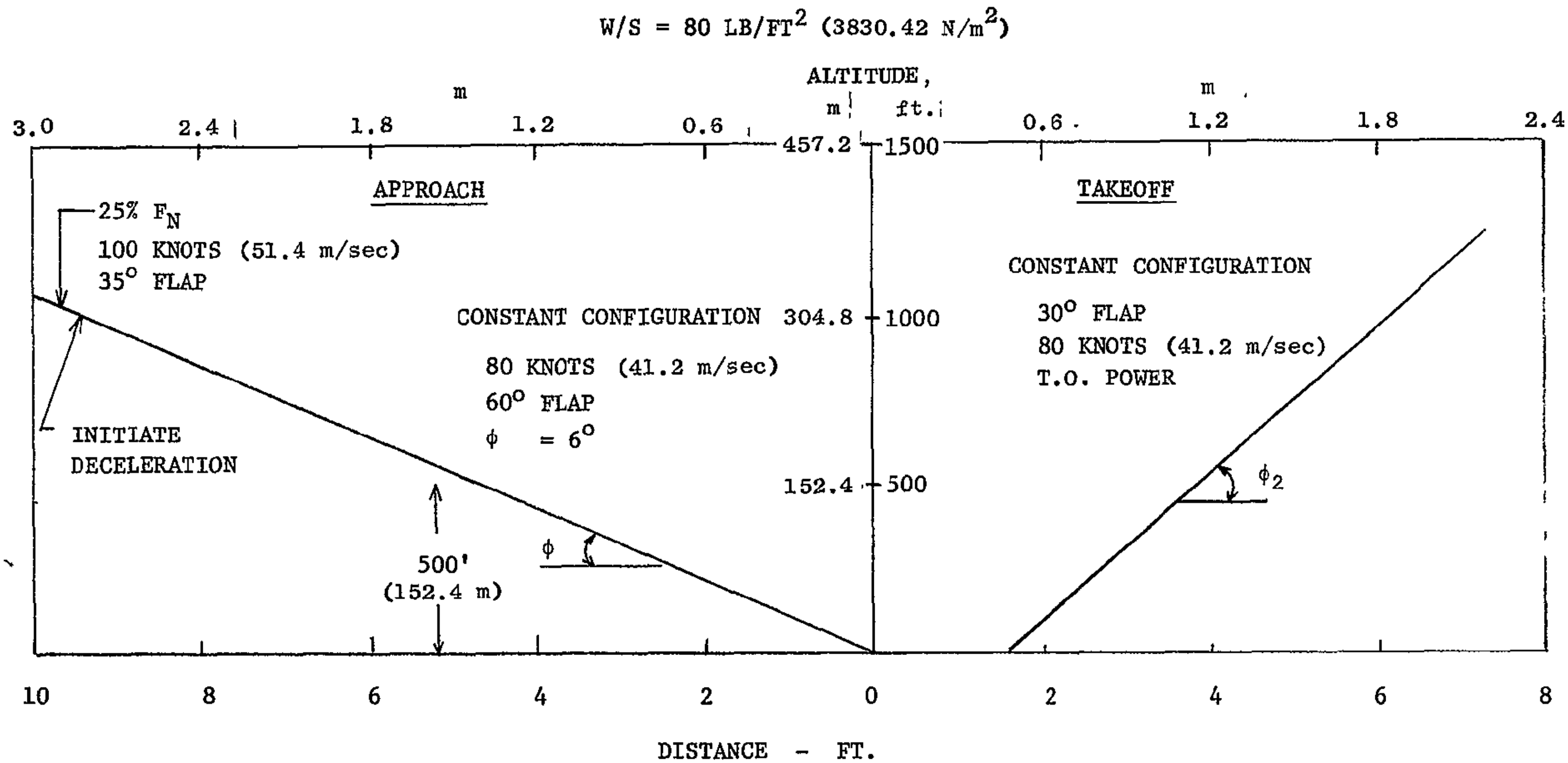

	Approach Power Setting	Takeoff Angle $\phi 2$	Installed T/W
EBF	72% of Installed Max Thrust at 80 Knots (41.2 m/sec)	12.5°	0.615 (6.0 N/kg)
OTW	72% of Installed Max Thrust at 80 Knots (41.2 m/sec)	12.5°	0.615 (6.0 N/kg)
AW	55% of Max Uninstalled Thrust at 80 Knots (41.2 m/sec)	8°	0.40 (3.9 N/kg)

Figure I-4. Task II Requirements, Flight Paths.

Table I-7. Task II Engine Ratings.

FLAT RATING

- T/O RATING TO 90°F DAY (32.22°C)
- CLIMB RATING TO +18°F DAY @ 30,000 FT (91440.02 n) (-7.78°C)
- CRUISE RATING TO +18°F DAY @ 30,000 FT (91440.02 n) (-7.78°C)

SUBJECT TO:

- FAN INLET CORRECTED AIRFLOW LIMIT

AIRFLOW LIMITS

- 100% OF SLS T/O CORRECTED AIRFLOW FOR FP + AW ENGINES
- 106% OF T/O CORRECTED AIRFLOW FOR VP ENGINES (1275 LB/SEC) (5671.48 n/sec)

Table I-8. Task II Cycle Design, SLS, +31°F (+17.2°C).

	GE19/F6D	GE19/F6E	GE19/F2C	GE19/F9A
FN/SFC T/O UNINSTALLED	24000 / .287 (10676. N)/.287	24000 / .291 (10676. N)/.291	24000 / .346 (10676. N)/.346	14900 / .589 (10676. N)/.589
P/P FAN	1.25	1.25	1.35	3.0
CORRECTED AIRFLOW	1200 (544.3 Kg)	1200 (544.3 Kg)	970 (440. Kg)	366 (166.0 Kg)
BYPASS RATIO	14.3	14.3	8.2	2.2
P/P OVERALL	15.5	16.2	22.7	24.9
P/P OVERALL (CRUISE)	17.4	18.2	25.0	24.5
T_{41} °F	2460 (1348.90°C)	2440 (1337.80°C)	2400 (1310.00°C)	2370 (1299.00°C)
FAN DUCT VELOCITY	652	653		
FAN RPM	2640	3120	4730	7910
CORE DUCT VELOCITY	780 (237.74 n/sec)	780 (237.74 n/sec)	823 (250.85 n/sec)	830 (252.98 n/sec)
CORE RPM	14080	14030	14580	14740

Table I-9. Task II Component Efficiency Levels, SLS, +31°F (+17.2°C).

	GE19/F6D	GE19/F6E	GE19/F2C1	GE19/F9A
FAN η_{TIP}	.879	.870	.820	.826
FAN η_{HUB}	.800	.788	.832	.848
LPT η	.897	.892	.899	.886
C_V FAN	.996	.996	.996	----
C_V CORE	.996	.996	.996	.996

Tables I - 10 and I-11 summarize the performance of the Task II engines at three flight conditions, on both uninstalled and installed bases. Detailed performance data for all engines have been provided in separate appendixes. issued 11/15/72 which include a description of the station numbering system. The installed data provided are based on the assumptions in Table I - 12. These levels of bleed and power extraction are consistent with a 125 PAX airplane and the requirements given in Figures I - 1 and I - 2. Typical installed throttle curves for three engines are shown in Figures I - 5, through I - 10. The interference drag estimates are based on NASA-supplied guidelines.

Fan speed is an acceptable power setting parameter for engines having higher fan pressure ratios such as the F2 and F9 series. In the case of the F6 series, however, thrust is more sensitive to installation and duct losses and blade angle derivations are an additional uncertainty. A second parameter should be measured in addition to fan speed: blade angle, fan duct Mach no., inlet throat Mach no., or perhaps shaft torque. Future work with airline and airframe customers will result in the ultimate choice of the power setting parameters to be used in the overall power management system.

Table I-10. Task II Performance Summary, F2C1, F2C2, and F2C3.

		F2C1		F2C2		F2C3	
		UNINSTALLED	INSTALLED	UNINSTALLED	INSTALLED	UNINSTALLED	INSTALLED
SEA LEVEL STATIC	F_N	24000 (106757. N)	22900 (101864. N)	24000 (106757. N)	22300 (99195. N)	24000 (106757. N)	23100 (102754. N)
STANDARD DAY	SFC	.333	.348	.333	.358	.333	.346
T/O POWER SETTING	BPR	8.2	8.2	8.2	8.2	8.2	8.2
	$W_{12}R$	970	970	970	970	970	970
	FAN P/P	1.35	1.35	1.35	1.35	1.35	1.35
SEA LEVEL, M_o = .10	F_N	20700 (92078. N)	19800 (88075. N)	20700 (92078. N)	19200 (85406. N)	20700 (92078. N)	20000 (8896. N)
STANDARD DAY	SFC	.383	.403	.383	.415	.383	.399
T/O POWER SETTING	BPR	8.3	8.3	8.3	8.3	8.3	8.3
	$W_{12}R$	970	970	970	970	970	970
	FAN P/P	1.35	1.35	1.35	1.35	1.35	1.35
30,000 FT, M = .75 (9144.02 n)	F_N	5800 (25800. N)	5400 (24020. N)	5800 (25800. N)	5300 (23576. N)	5800 (25800. N)	5400 (24020. N)
STANDARD DAY	SFC	.630	.663	.630	.682	.630	.660
MAX CRUISE POWER SETTING	BPR	7.9	8.0	7.9	8.0	7.9	8.0
	$W_{12}R$	965	965	965	965	965	965
	FAN P/P	1.42	1.42	1.42	1.42	1.42	1.42

ORIGINAL PAGE IS OF POOR QUALITY

Table I-11. Task II Performance Summary, F6D, F6E, F9A2, and F9A3.

		F6D		F6E		F9A2		F9A3	
		UNINST.	INST.	UNINST.	INST.	UNINST.	INST.	UNINST.	INST.
SEA LEVEL STATIC	F_N	24000 (106757. N)	23000 (102309.N)	24000 (106757.N)	23000 (102309.N)	14900 (66279.N)	14400 (64054.N)	14900 (66279.N)	14400 (64054.N)
STANDARD DAY	SFC	.275	.290	.275	.290	.563	.583	.563	.582
T/O POWER SETTING	BPR	14.3	14.4	14.3	14.4	2.2	2.2	2.2	2.2
	$W_{12}R$	1200	1200	1200	1200	365	365	365	365
	FAN P/P	1.25	1.25	1.25	1.25	3.0	3.0	3.0	3.0
SEA LEVEL, M_o = .10	F_N	20100 (89409.N)	19100 (84961.N)	20100 (89409.N)	19100 (84961.N)	13700 (60941.N)	13200 (58717.N)	13700 (60941.N)	13300 (59161.N)
STANDARD DAY	SFC	.326	.345	.326	.345	.613	.636	.613	.635
T/O POWER SETTING	BPR	14.4	14.4	14.4	14.4	2.2	2.2	2.2	2.2
	$W_{12}R$	1200	1200	1200	1200	365	365	365	365
	FAN P/P	1.25	1.25	1.25	1.25	3.0	3.0	3.0	3.0
30,000 FT, M = .75 (9144.02 m)	F_N	5000 (22241.N)	4700 (20907.N)	5000 (22241.N)	4700 (20907.N)	4300 (19127.N)	4000 (17793.N)	4300 (19127.N)	4000 (17793.N)
STANDARD DAY	SFC	.620	.670	.621	.671	.767	.809	.767	.809
MAX CRUISE POWER SETTING	BPR	14.0	14.0	14.0	14.0	2.2	2.2	2.2	2.2
	$W_{12}R$	1275	1275	1275	1275	365	365	365	365
	FAN P/P	1.33	1.33	1.33	1.33	3.0	3.0	3.0	3.0

ORIGINAL PAGE IS OF POOR QUALITY

Table I-12. Task II Performance Assumptions.

	UNINSTALLED	INSTALLED
RAM RECOVERY	1.0	WITH ACOUSTIC TREATMENT + INLET LOSSES
BLEED	0	.78 LB/SEC INTERSTAGE
HP EXTRACTION	0	200 HP TAKEOFF (149140 watt) 50 HP CRUISE (37285 watt)
DUCT LOSSES	WITHOUT ACOUSTIC TREATMENT REFERENCE LINES	WITH ACOUSTIC TREATMENT
NOZZLE C_V	REFERENCE NOZZLE	VARIABLE NOZZLE

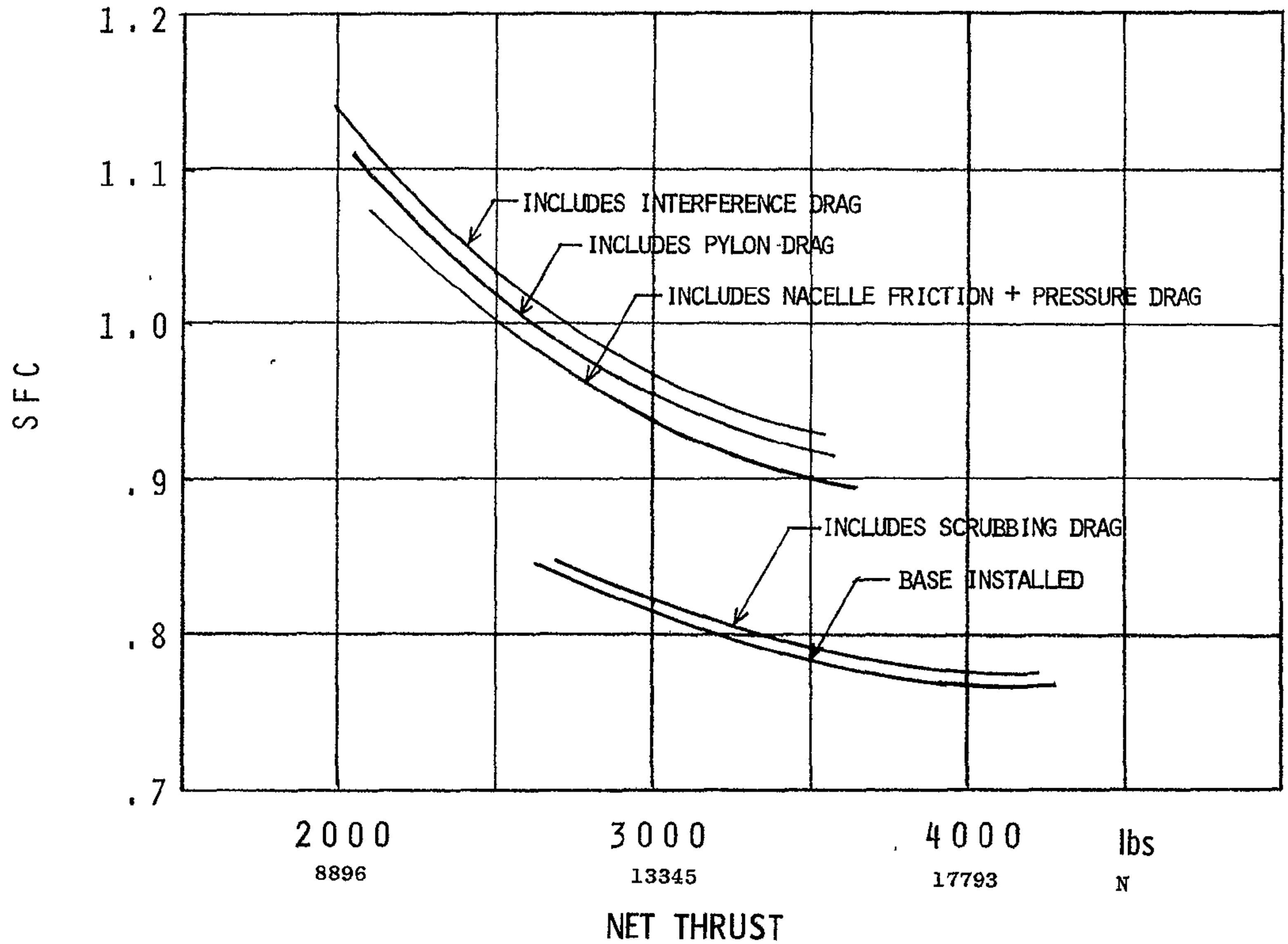

Figure I-5. Task II Summary, GE19/F6E1 30,000 Ft (9144.0m) 0.8 M.

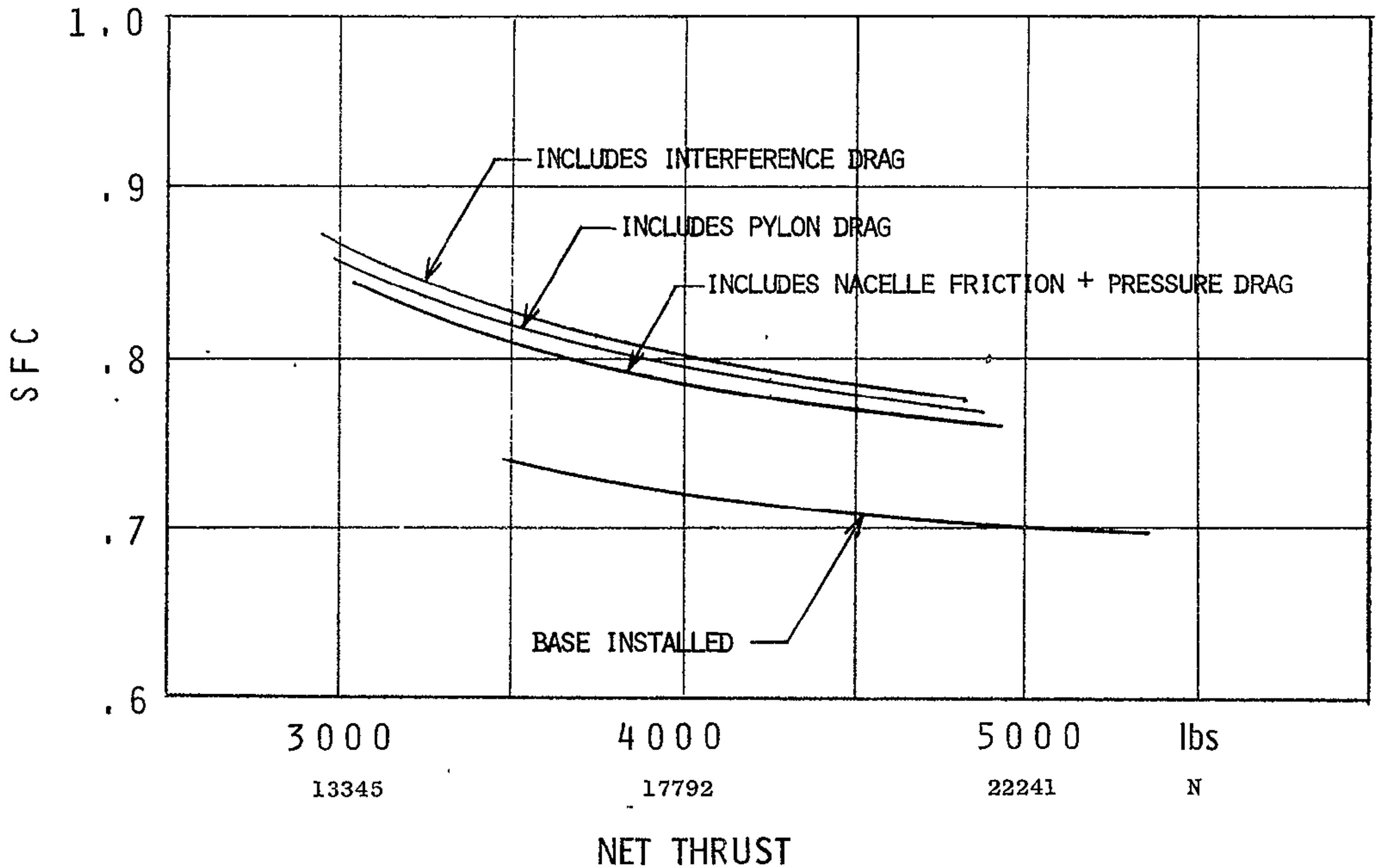

Figure I-6. Task II Summary, GE19/F2C1 30,000 Ft (9144.0m) 0.8 M.

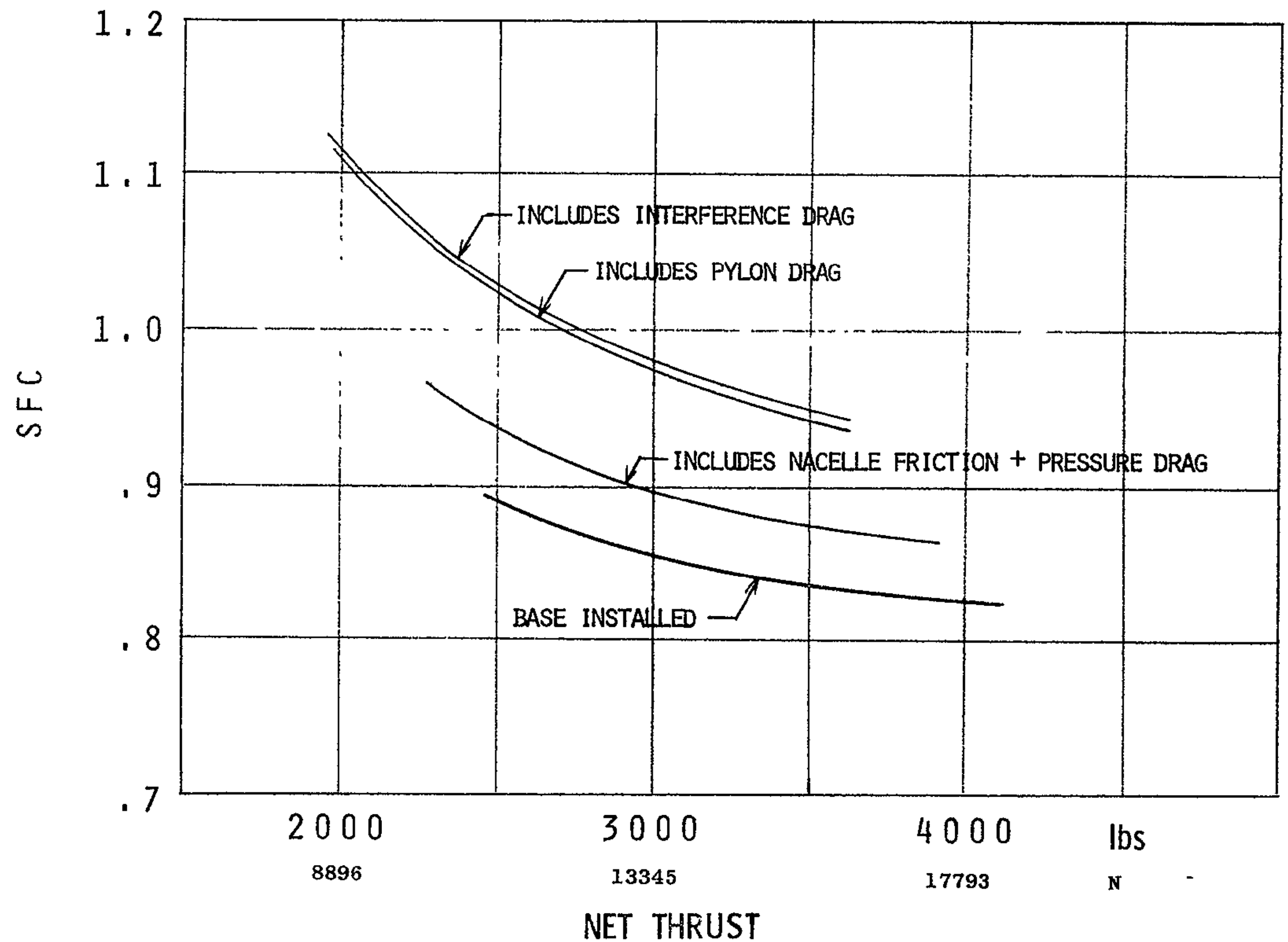

Figure I-7. Task II Summary, GE19/F9A2 30,000 Ft (9144.0m) 0.8 M.

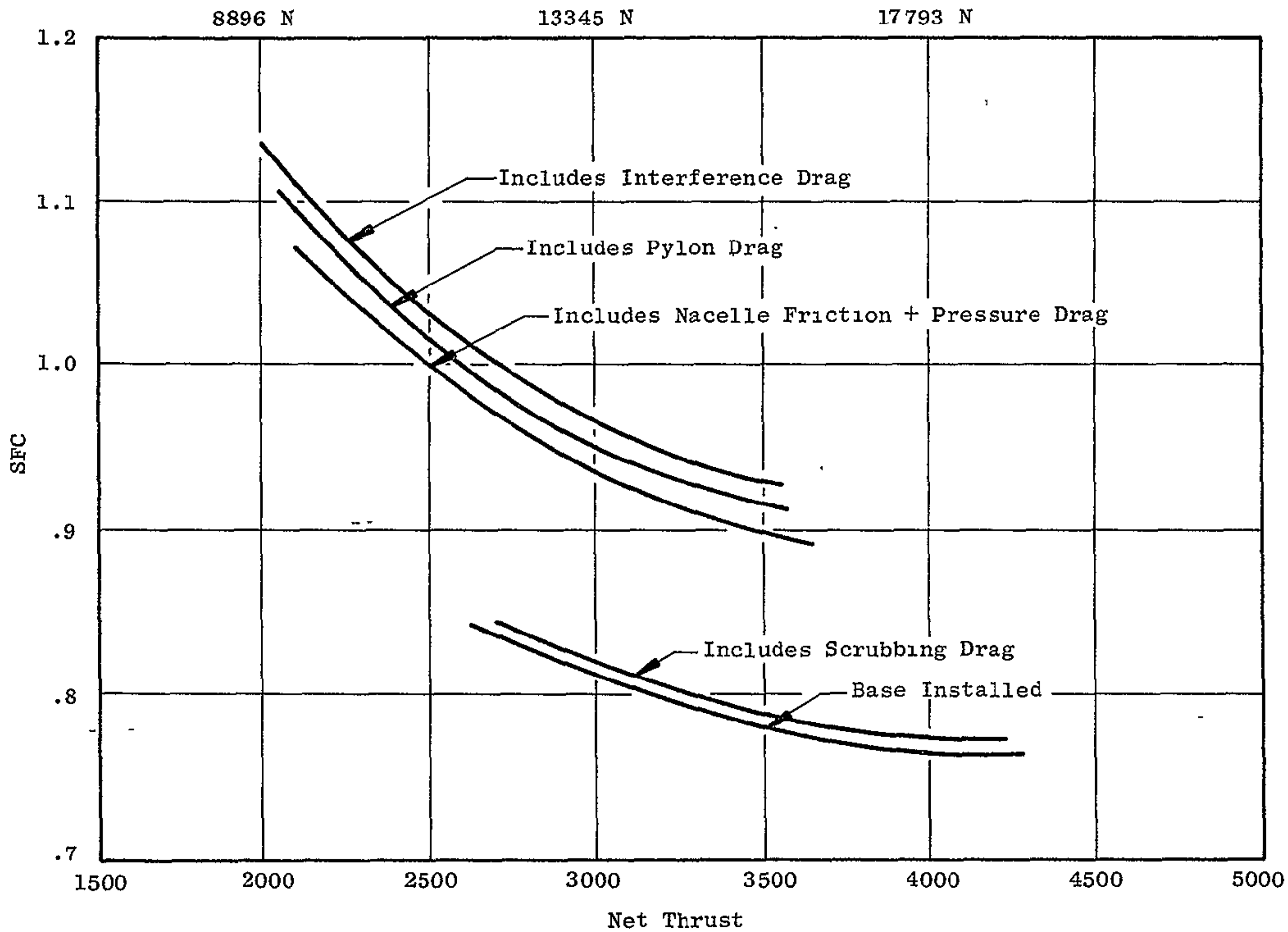

Figure I-8. Task II Summary, GE19/F6D1 30,000 Ft (9144.0m) 0.8 M.

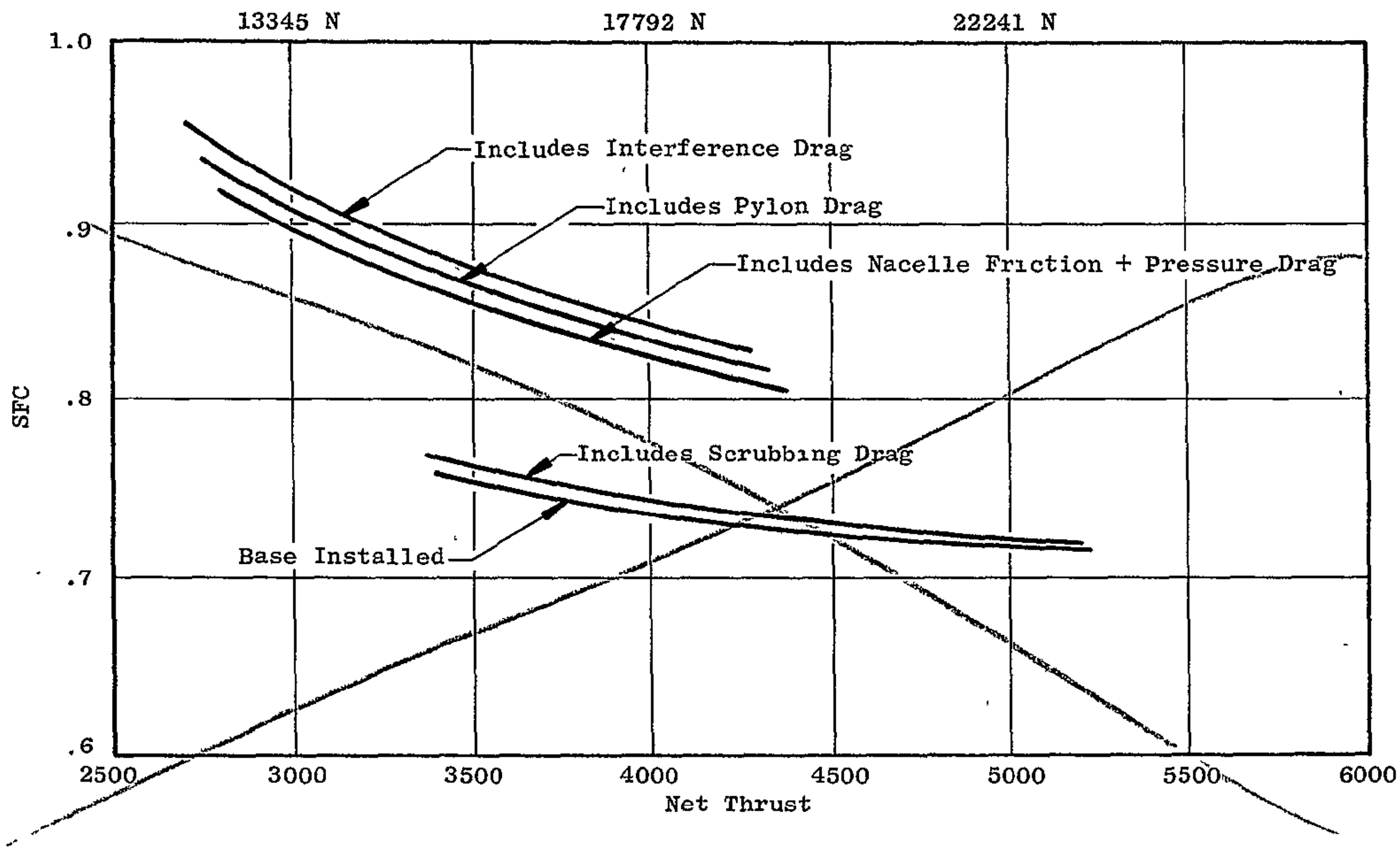

Figure I-9. Task II Summary, GE19/F2C2 30,000 Ft (91440.02 m) 0.8 M.

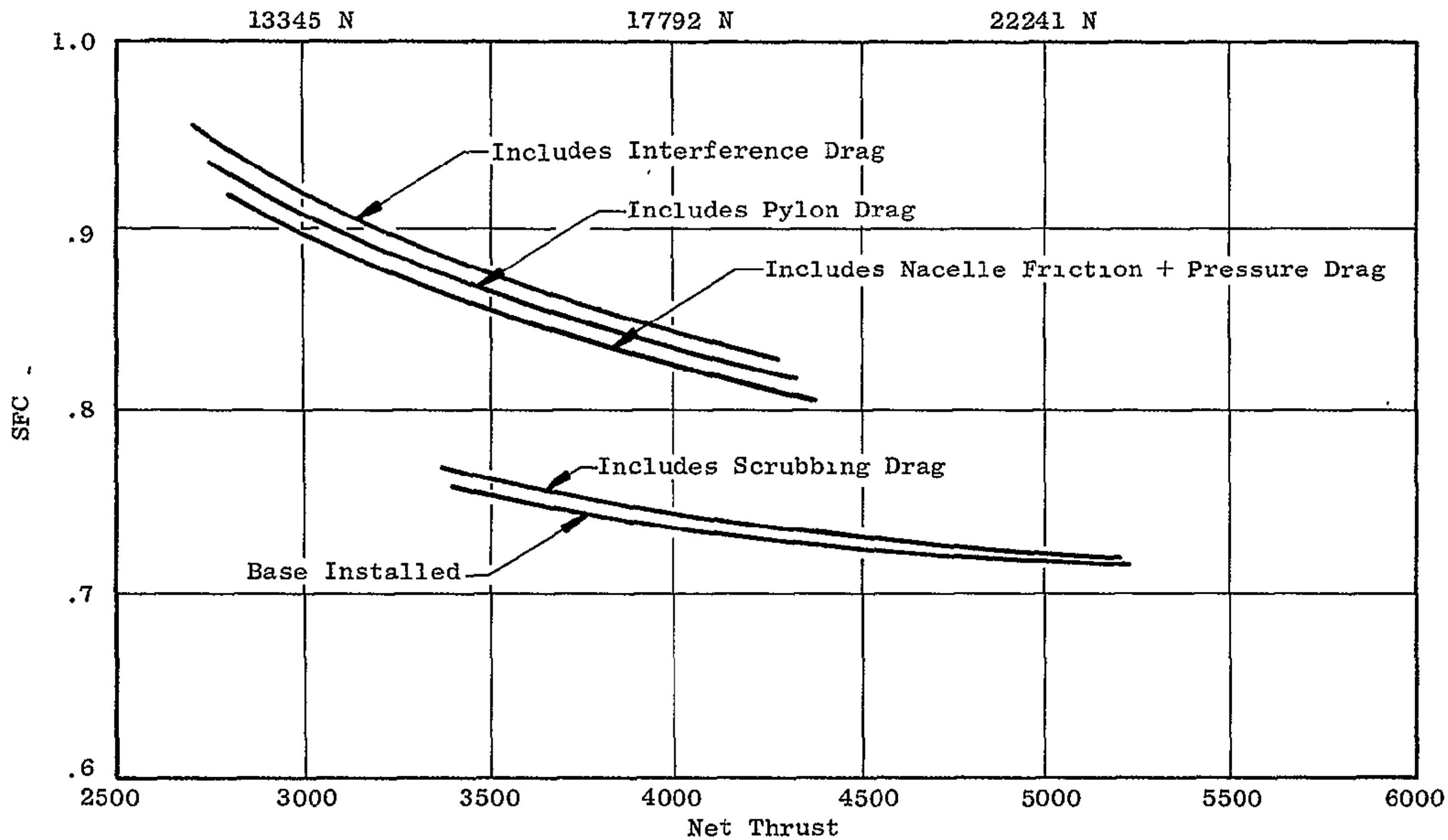

Figure I-9. Task II Summary, GE19/F2C2 30,000 Ft (9144.0m) 0.8 M.

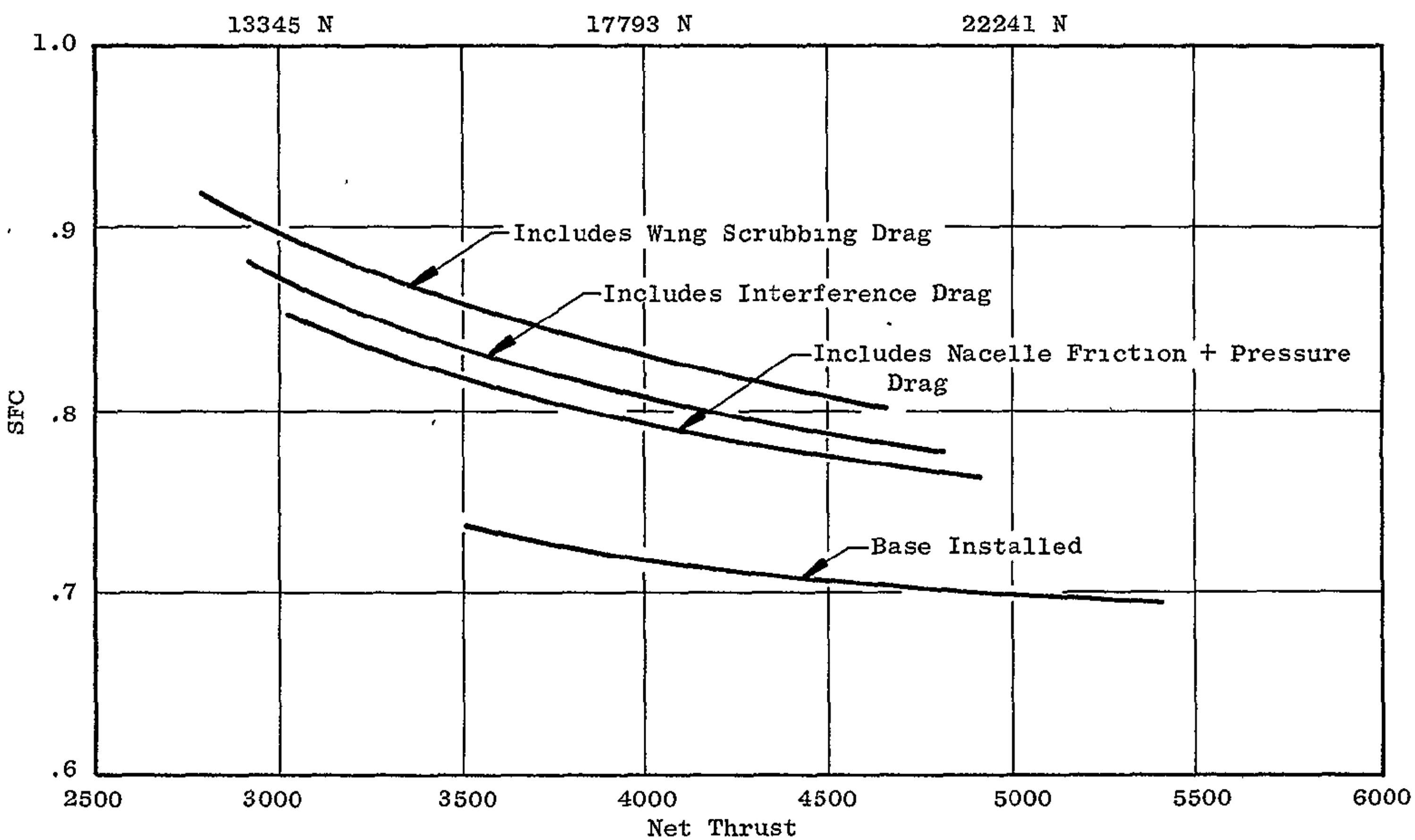

Figure I-10. Task II Summary, GE19/F2C3 30,000 Ft (9144.0m) 0.8 M.

FAN AND BOOSTER AERODYNAMIC DESIGN

Of paramount importance in the design of fans and boosters is the selection of required operating margins. In the case of STOL operations, it can be expected that levels of distortion may be higher than those encountered in CTOL. It is also the case that the distortions will be even greater as a percentage of the stage energy for the low pressure ratio fan involved. An evaluation of probable STOL engine fan operating margins is given on Table I - 13. Operating margin is defined as the percentage of combination pressure ratio increase and airflow reduction that can be tolerated along a constant corrected speed line above the normal operating point.

This definition is more logical for low pressure ratio fans having flat characteristics than for the more common pressure ratio/corrected airflow definition normally applied to higher pressure ratio fans.

Another way to look at it, is that this operating margin is the percentage that the fan duct nozzle could be closed without making fan operation impractical.

Mathematically:

$$\text{Operating margin} = \left\{ \frac{\left[(P/P \Big/ \frac{W\sqrt{\theta}}{\delta} \right]_{\text{limit}}}{\left[(P/P \Big/ \frac{W\sqrt{\theta}}{\delta} \right]_{\text{operating line}}} - 1 \right\}_{\frac{N}{\sqrt{\theta}} = \text{Const.}}$$

Table I-13. Task II Fan Operating Margin Requirements at Takeoff.

Engine	GE19/F2C 1.35 FP	GE19/F6D and E 1.25 VP	GE19/F9A 3.0 AW
Limit Line Effects			
Inlet Distortion (Cross Wind & Angle of Attack)	9%	10%	9%
Deterioration	2%	2%	2%
Variations (Incl. VP Position)	2%	3%	2%
Operating Line Effects			
Inlet Distortion/Recovery	2%	3%	2%
Variations (Incl. Jet Nozzle Area)	3%	3%	3%
Total	18%	21%	18%

* Operating Margin Defined As $$\frac{\left(\dfrac{P/P}{W\sqrt{\theta}/\delta}\right)_{\text{LIMIT}}}{\left(\dfrac{P/P}{W\sqrt{\theta}/\delta}\right)_{\text{O.P. LINE}}} - 1 \quad @ \text{ Const. } N/\sqrt{\theta}$$

A final selection of operating margin would evolve from airplane/engine studies in a normal development cycle, but the values shown are representative and would not be expected to be significantly different than shown. An important point is that, while low pressure ratio fans may not stall or surge in the classical sense, there is some line on the map beyond which the flow becomes distorted and the performance is so poor that operation is unreasonable.

The General Electric stall line and pressure rise predictions have been assembled from test data from dozens of stages and include consideration of the effects of blade speed, axial velocity, reaction, solidity, aspect ratio, clearance, and Reynolds number. The minimum tip speeds selected for our geared V.P. engine reflect the lowest value which, when combined with fan tip casing treatment, yields the required operating margin.

Details of fan tip speed selection for the 1.25 p/p fans are shown on Figure I - 11. The low solidity approach allows reversal in both directions (see Section VIII and Table VIII - 4). The direct drive 1100 ft/sec. (335.25 m/sec.) tip speed was chosen to provide a balance between fan noise and low pressure turbine size. The gear-driven fan tip speed of 930 ft/sec. (283.46 m/sec.), when combined with casing tip treatment, just provides what is considered to be minimum required operating margin. This determination is based on an empirical stall correlation procedure developed by General Electric, which relates solidity, aspect ratio, and vector diagram, and allows the designer to predict the peak pressure rise of a new design by relating to the demonstrated performance of similar existing machines.

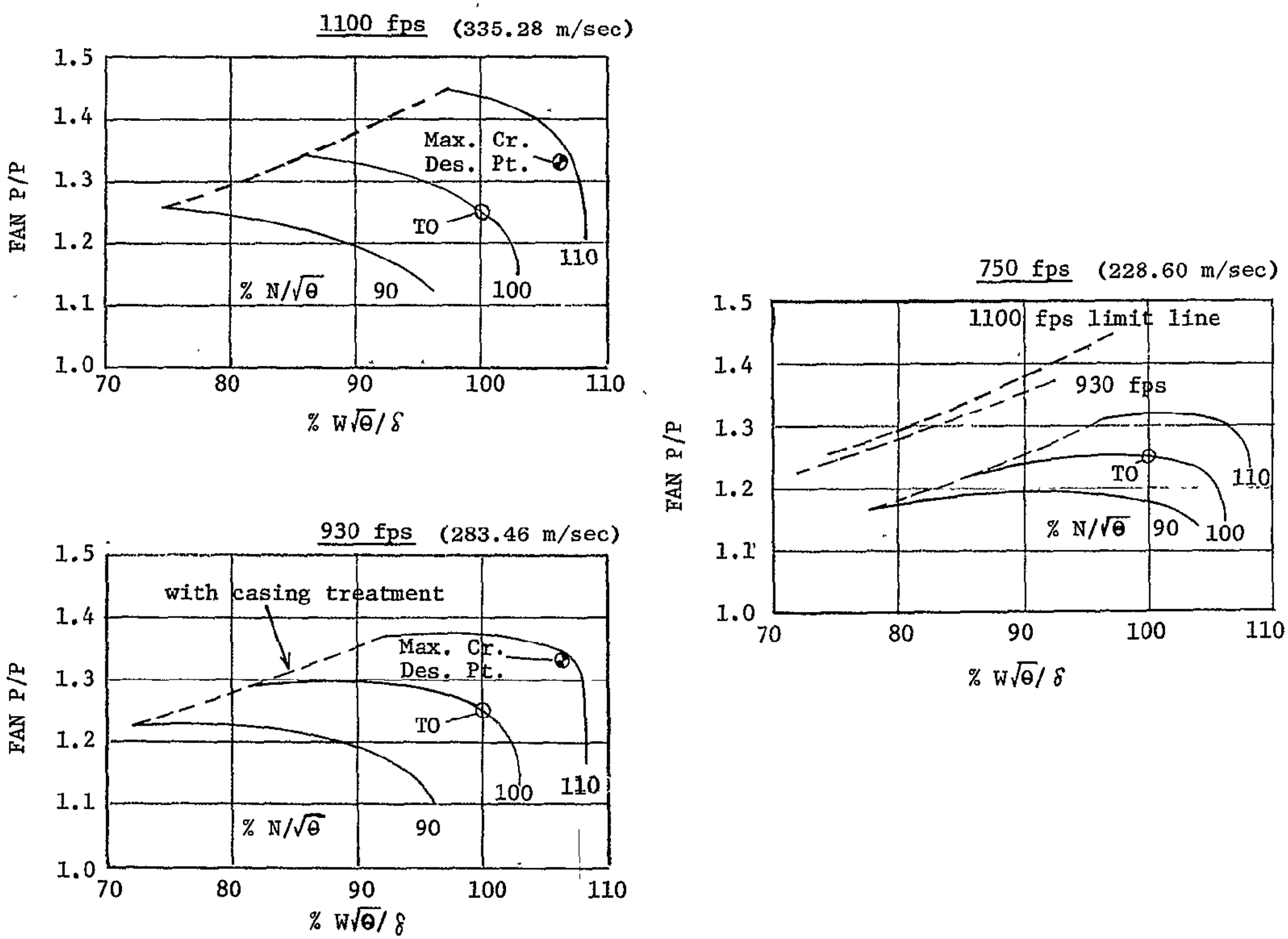

Figure I-11. Effect of Tip Speed on 1.25 P/P Fan Characteristics, Nominal Blade Position.

For example, minimum tip speed allowable for a given required operating margin can be determined given solidity, aspect ratio, and pressure rise characteristics. In contrast, a 750 ft/sec. (328.60 m/sec.) tip speed fan characteristic is shown on the right hand side of the figure. Its operating margin is considered to be unacceptable for STOL engine use and there is a question as to its ability to provide the desired pressure ratio at design speed with distorted inlet conditions.

The fan aerodynamic design characteristics are summarized on Table I - 14. Fan and booster detailed aerodynamic data are given on Tables I - 15 through I - 23. Except for the augmentor wing engine, the design points were located at higher pressure ratio points than the takeoff point. The takeoff operating conditions are also shown on Table I - 14.

The F9A augmentor wing fan is basically a modified F101 with a third stage added. The third stage is split with the outer portion of the stage supplying the full 3.0 fan pressure ratio and the inner portion supplying only 2.5 to keep within F101 core capability. This split stage arrangement has precedence in the TF39 stage 2 fan but the size of the F9A stage is much smaller.

Figures I - 12 and I - 13 show the distribution of fan rotor pressure ratio and diffusion factor for the four fans at design point conditions vs. stream function (a measure of flow). The three high bypass engines all have nonconstant work. The diffusion factor over the outer portion of the blade is highest for geared fan since its tip speed was selected on the basis of minimum stall margin. The areas near the hub of the two variable

Table I-14. Task II Fan Aero Design Summary.

Engine		GE19/F2C FP	GE19/F6D Geared VP	GE19/F6E Direct VP	GE19/F9A AW	
$U_T/\sqrt{\theta}$	Des./TO	1425/1400	995/930	1175/1100	1525	FPS
Fan P/P (Bypass)	Des./TO	1.42/1.35	1.33/1.25	1.33/1.25	3.0 in 3 stages 2.5 into core	
$\frac{W\sqrt{\theta}}{\delta A_A}$	Des./TO	41.8/41.8	42.1/39.7	42.1/39.7	42.0	LB/SEC FPS
$\frac{W\sqrt{\theta}}{\delta}$	Des./TO	969/969	1275/1200	1275/1200	362	LB/SEC
Tip Diam.		70 (177.8 cm)	83.0 (210.8 cm)	83.0 (210.8 cm)	45 (114.3 cm)	IN.
Radius Ratio		0.36	0.44	0.44	0.48	
Rotor Pitch Solidity		1.77	0.95 const.	0.95 const.	Modified F101 Fan & 3rd blade stage	
Rotor Aspect Ratio		3.7	2.0	1.7		
OGV Pitch Solidity		2.0	1.2	1.2		
OGV Aspect Ratio		4.5	1.8	1.8		
No. of Blades/OGV's		46/92	16/24	14/24		
Rotor-OGV Spacings (No. rotor chords)		2.0	1.25	1.25		

TABLE I - 15. QCSEE TASK II GE19/F2C FAN AND BOOSTER AERODYNAMIC PARAMETERS, Rotor 1, Stator 1, and Rotor 2.

PARAMETER	ROTOR 1			STATOR 1			ROTOR 2		
	HUB	PITCH	TIP	HUB	PITCH	TIP	HUB	PITCH	TIP
RADIUS RATIO	.36	.66	1.0	.418	.466	.514	.424	.466	.513
INLET RADIUS	12.58	23.04	34.93	14.61	16.27	17.97	14.8	16.28	17.93
ABSOLUTE INLET AIR ANGLE	0	0	0	44.59	41.99	39.97	11.22	16.52	23.9
RELATIVE INLET AIR ANGLE	38.23	53.43	65.46	-	-	-	37.91	36.95	41.24
ABSOLUTE INLET MACH NUMBER	.647	.654	.604	.754	.761	.716	.551	.578	.529
RELATIVE INLET MACH NUMBER	.805	1.094	1.453	-	-	-	.685	.693	.642
EXIT AIR ANGLE*	-2.309	44.34	67.74	11.16	16.95	23.24	3.48	20.19	24.19
ACCUMULATIVE PRESSURE RATIO	1.392	1.459	1.381	1.347	1.417	1.421	1.708	1.646	1.644
EFFICIENCY	.879	.946	.654	.790	.864	.866	.835	.886	.875
DIFFUSION FACTOR	.368	.403	.308	.428	.404	.361	.395	.278	.290
CAMBER	57.71	9.64	-2.12	46.83	32.70	24.61	49.48	21.33	23.35
STAGGER	7.16	44.63	64.52	21.46	26.10	29.56	16.25	26.63	30.42
SOLIDITY	2.70	1.817	1.40	1.508	1.396	1.270	1.469	1.352	1.240
ASPECT RATIO	-	3.687	-	-	1.745	-	-	1.881	-
MERIDIONAL MACH NUMBER	.647	.654	.604	.538	.566	.549	.541	.554	.484

* RELATIVE IN REFERENCE TO ROTOR AND ABSOLUTE IN RELATION TO STATOR

TABLE I - 16. QCSEE TASK II GE19/F2C FAN AND BOOSTER AERODYNAMIC PARAMETERS, Stator 2, Rotor 3, and Stator 3.

PARAMETER	STATOR 2			ROTOR 3			STATOR 3		
	HUB	PITCH	TIP	HUB	PITCH	TIP	HUB	PITCH	TIP
RADIUS RATIO	.423	.462	.508	.421	.459	.503	.418	.454	.496
INLET RADIUS	14.76	16.15	17.74	14.71	16.03	17.58	14.61	15.85	17.33
ABSOLUTE INLET AIR ANGLE	41.68	34.52	40.02	10.81	13.44	16.98	35.43	34.75	38.98
RELATIVE INLET AIR ANGLE	-	-	-	36.0	39.83	44.56	-	-	-
ABSOLUTE INLET MACH NUMBER	.732	.660	.636	.562	.535	.496	.699	.632	.598
RELATIVE INLET MACH NUMBER	-	-	-	.683	.677	.664	-	-	-
EXIT AIR ANGLE*	10.58	13.59	17.17	9.46	20.0	25.51	7.08	10.35	13.99
ACCUMULATIVE PRESSURE RATIO	1.663	1.636	1.623	1.990	1.925	1.909	1.957	1.913	1.885
EFFICIENCY	.790	.875	.850	.814	.891	.855	.793	.882	.837
DIFFUSION FACTOR	.378	.328	.389	.300	.313	.360	.365	.348	.378
CAMBER	45.45	30.50	35.36	37.46	25.04	26.64	45.30	35.89	37.87
STAGGER	21.45	22.36	26.53	18.99	27.48	32.34	18.34	20.81	24.29
SOLIDITY	1.465	1.357	1.246	1.463	1.359	1.252	1.468	1.360	1.257
ASPECT RATIO	-	2.440	-	-	1.824	-	-	2.704	-
MERIDIONAL MACH NUMBER	.547	.544	.488	.553	.520	.475	.570	.520	.467

* RELATIVE IN REFERENCE TO ROTOR AND ABSOLUTE IN RELATION TO STATOR

TABLE I - 17 QCSEE TASK II GE19/F2C FAN AND BOOSTER AERODYNAMIC PARAMETERS

PARAMETER	ROTOR 4			STATOR 4			BYPASS OGV		
	HUB	PITCH	TIP	HUB	PITCH	TIP	HUB	PITCH	TIP
RADIUS RATIO	.415	.449	.491	.410	.443	.484	.530	.761	1.0
INLET RADIUS	14.49	15.70	17.14	14.34	15.49	16.92	18.50	26.59	34.93
ABSOLUTE INLET AIR ANGLE	7.09	10.25	13.84	27.70	30.48	36.83	39.56	30.18	34.06
RELATIVE INLET AIR ANGLE	37.47	41.36	45.26	-	-	-	-	-	-
ABSOLUTE INLET MACH NUMBER	.551	.511	.477	.642	.567	.539	.701	.601	.493
RELATIVE INLET MACH NUMBER	.687	.668	.655	-	-	-	-	-	-
EXIT AIR ANGLE*	18.17	25.84	29.34	2.00	2.00	2.00	0	0	0
ACCUMULATIVE PRESSURE RATIO	2.222	2.171	2.164	2.189	2.161	2.138	1.427	1.437	1.365
EFFICIENCY	.802	.888	.839	.786	.882	.824	.877	.909	.631
DIFFUSION FACTOR	.247	.288	.361	.300	.354	.454	.453	.331	.395
CAMBER	23.50	17.25	22.96	41.50	42.99	49.82	43.50	37.63	47.45
STAGGER	23.66	30.84	34.70	14.71	14.69	16.22	15.71	12.67	14.73
SOLIDITY	14.74	1.367	1.261	1.489	1.393	1.274	1.955	1.484	1.188
ASPECT RATIO	-	1.845	-	-	3.004	-	-	4.50	-
MERIDIONAL MACH NUMBER	.547	.503	.463	.570	.490	.433	.540	.520	.409

* RELATIVE IN REFERENCE TO ROTOR AND ABSOLUTE IN RELATION TO STATOR

Table I-18 Task II GE19/F6D Fan and Booster Aerodynamic Parameters, Rotor 1 and Core Stator 1.

PARAMETER	ROTOR 1			CORE STATOR 1		
	HUB	PITCH	TIP	HUB	PITCH	TIP
RADIUS RATIO	.44	.724	1.0	.496	.520	.545
INLET RADIUS	18.25	30.057	41.50	20.60	21.60	22.60
ABSOLUTE INLET AIR ANGLE	0	0	0	36.17	36.47	34.67
RELATIVE INLET AIR ANGLE	34.82	46.65	53.28	-	-	-
ABSOLUTE INLET MACH NUMBER	.599	.637	.698	.669	.707	.768
RELATIVE INLET MACH NUMBER	.724	.926	1.166	-	-	-
EXIT AIR ANGLE*	4.44	28.148	44.30	-5.0	3.39	8.54
ACCUMULATIVE PRESSURE RATIO	1.22	1.354	1.350	1.166	1.224	1.254
EFFICIENCY	.844	.913	.789	.649	..794	.800
DIFFUSION FACTOR	.591	.513	.413	.411	.351	.353
CAMBER	47.86	29.28	13.30	54.40	42.20	29.04
STAGGER	14.63	31.57	45.52	10.17	15.54	18.11
SOLIDITY	.95	.95	.95	1.860	1.776	1.698
ASPECT RATIO	-	2.083	-	-	1.404	-
MERIDIONAL MACH NUMBER	.599	.637	.698	.540	.569	.632

* RELATIVE IN REFERENCE TO ROTOR AND ABSOLUTE IN RELATION TO STATOR

ORIGINAL PAGE IS OF POOR QUALITY

Table I-19. Task II GE19/F6D Fan and Booster Aerodynamic Parameters, Core Rotor 2, Core Stator 2, and Bypass OGV.

PARAMETER	CORE ROTOR 2			CORE STATOR 2			BYPASS OGV		
	HUB	PITCH	TIP	HUB	PITCH	TIP	HUB	PITCH	TIP
RADIUS RATIO	.496	.519	.542	.496	.517	.539	.595	.774	1.012
INLET RADIUS	20.60	21.55	22.50	20.57	21.475	22.38	24.70	32.106	42.00
ABSOLUTE INLET AIR ANGLE	-4.83	1.76	8.61	36.49	30.26	36.50	34.17	30.94	45.75
RELATIVE INLET AIR ANGLE	42.95	34.48	34.40	-	-	-	-	-	-
ABSOLUTE INLET MACH NUMBER	.521	.578	.581	.773	.645	.591	.705	.699	.644
RELATIVE INLET MACH NUMBER	.709	.727	.696	-	-	-	-	-	-
EXIT AIR ANGLE*	40.04	29.39	32.46	0	0	0	0	0	0
ACCUMULATIVE PRESSURE RATIO	1.505	1.445	1.451	1.467	1.425	1.427	1.247	1.339	1.324
EFFICIENCY	.776	.835	.825	.725	.807	.786	.781	.877	.735
DIFFUSION FACTOR	.438	.333	.298	.354	.339	.378	.493	.390	.397
CAMBER	56.02	26.30	28.99	52.21	43.19	51.01	41.88	45.36	50.34
STAGGER	12.54	21.40	19.29	14.14	13.08	14.13	13.13	13.03	12.94
SOLIDITY	1.666	1.594	1.529	1.405	1.345	1.290	1.546	1.189	.910
ASPECT RATIO	-	1.321	-	-	1.738	-	-	1.730	-
MERIDIONAL MACH NUMBER	.519	.578	.575	.623	.558	.475	.583	.599	.564

* RELATIVE IN REFERENCE TO ROTOR AND ABSOLUTE IN RELATION TO STATOR

Table I-20. Task II GE19/F6E Fan and Booster Aerodynamic Parameters, Core Rotor 2, Core Stator 2, and Bypass OGV.

PARAMETER	ROTOR 1			STATOR 1		
	HUB	PITCH	TIP	HUB	PITCH	TIP
RADIUS RADIUS	.44	.723	1.0	.496	.522	.547
INLET RADIUS	18.25	30.00	41.50	20.60	21.65	22.70
ABSOLUTE INLET AIR ANGLE	0	0	0	35.78	35.89	36.23
RELATIVE INLET AIR ANGLE	39.06	51.27	58.05	-	-	-
ABSOLUTE INLET MACH NUMBER	.607	.638	.688	.638	.669	.676
RELATIVE INLET MACH NUMBER	.773	1.016	1.298	-	-	-
EXIT AIR ANGLE*	14.87	41.18	53.99	-5.0	3.45	9.16
ACCUMULATIVE PRESSURE RATIO	1.25	1.35	1.35	1.199	1.260	1.292
EFFICIENCY	.846	.901	.768	.684	.810	.826
DIFFUSION FACTOR	.563	.449	.344	.414	.335	.260
CAMBER	48.35	18.13	6.93	53.92	40.93	29.73
STAGGER	18.83	41.70	53.46	10.02	15.46	19.06
SOLIDITY	.95	.95	.95	1.86	1.772	1.691
ASPECT RATIO	-	1.715	-	-	1.471	-
MERIDIONAL MACH NUMBER	.607	.638	.688	.518	.542	.545

* RELATIVE IN REFERENCE TO ROTOR AND ABSOLUTE IN RELATION TO STATOR

Table I-21. Task II GE19/F6E Fan and Booster Aerodynamic Parameters, Rotor 2, Stator 2, and Bypass OGV.

PARAMETER	ROTOR 2			STATOR 2			BYPASS OGV		
	HUB	PITCH	TIP	HUB	PITCH	TIP	HUB	PITCH	TIP
RADIUS RATIO	.496	.520	.545	.496	.518	.540	.595	.771	1.012
INLET RADIUS	20.60	21.60	22.60	20.60	21.50	22.40	24.70	31.998	42.00
ABSOLUTE INLET AIR ANGLE	-4.97	2.13	9.83	33.45	29.84	35.69	32.80	27.80	26.00
RELATIVE INLET AIR ANGLE	49.29	43.12	41.44	-	-	-	-	-	-
ABSOLUTE INLET MACH NUMBER	.481	.557	.544	.776	.645	.604	.68	.65	.61
RELATIVE INLET MACH NUMBER	.734	.763	.714	-	-	-	-	-	-
EXIT AIR ANGLE*	8.56	21.91	19.75	0	0	0	0	0	0
ACCUMULATIVE PRESSURE RATIO	1.585	1.526	1.531	1.545	1.505	1.504	1.282	1.337	1.326
EFFICIENCY	.792	.849	.847	.746	.823	.808	.800	.876	.720
DIFFUSION FACTOR	.385	.335	.274	.348	.333	.377	.419	.330	.339
CAMBER	51.54	23.55	27.99	47.92	42.47	50.02	40.14	41.29	46.49
STAGGER	20.97	28.39	26.56	12.88	12.77	13.86	12.61	11.94	12.02
SOLIDITY	1.664	1.591	1.523	1.404	1.344	1.289	1.546	1.193	.910
ASPECT RATIO	-	1.357	-	-	1.733	-	-	1.73	-
MERIDIONAL MACH NUMBER	.479	.556	.536	.650	.560	.492	.57	.577	.551

*RELATIVE IN REFERENCE TO ROTOR AND ABSOLUTE IN RELATION TO STATOR

Table I-22. Task II GE19/F9A Fan Aerodynamic Parameters, Rotor 1, Stator 1, Rotor 2, and Stator 2.

PARAMETER	ROTOR 1			STATOR 1			ROTOR 2			STATOR 2		
	HUB	PITCH	TIP	HUB	PITCH	TIP	HUB	PITCH	TIP	HUB	PITCH	TIP
RADIUS RATIO	.478	.732	1.000	.559	.740	.952	.579	.737	.934	.598	.766	.912
INLET RADIUS	10.865	16.657	22.748	22.720	16.847	21.666	13.175	16.777	21.250	13.596	17.434	20.748
ABSOLUTE INLET AIR ANGLE	0	0	0	43.92	31.98	32.04	2.33	5.40	7.10	40.81	36.23	40.03
RELATIVE INLET AIR ANGLE	50.47	56.52	69.53	-	-	-	50.16	53.34	63.61	-	-	-
ABSOLUTE INLET MACH NUMBER	.641	.694	.548	.835	.702	.669	.614	.685	.582	.773	.664	.617
RELATIVE INLET MACH NUMBER	.934	1.247	1.511	-	-	-	.955	1.142	1.278	-	-	-
EXIT AIR ANGLE*	11.9	47.9	56.2	2.1	6.1	7.1	20.4	44.9	51.7	-	-	-
ACCUMULATIVE PRESSURE RATIO	1.677	1.595	1.604	1.601	1.573	1.557	2.452	2.337	2.334	2.370	2.300	2.281
EFFICIENCY	.887	.896	.750	.802	.868	.700	.829	.884	.724	.794	.872	.702
DIFFUSION FACTOR	.419	.414	.312	.319	.280	.287	.377	.410	.342	.386	.317	.238
CAMBER	74.79	5.39	10.78	47.71	25.64	31.93	43.24	6.04	14.27	41.50	28.69	28.26
STAGGER	11.53	52.45	59.73	14.90	14.70	15.89	25.73	49.86	54.80	18.83	20.33	24.41
SOLIDITY	2.174	1.602	1.358	2.005	1.767	1.651	2.361	1.750	1.373	2.024	1.859	1.742
ASPECT RATIO		3.044			3.685			3.477			2.985	
MERIDIONAL MACH NUMBER	.641	.694	.548	.603	.617	.567	.613	.682	.578	.585	.536	.473

* RELATIVE IN REFERENCE TO ROTOR AND ABSOLUTE IN RELATION TO STATOR

Table I-23. Task II GE19/F9A Fan Aerodynamic Parameters, Core and Bypass Portions of Rotor 3 and Stator 3.

PARAMETER	ROTOR 3 (CORE PORTION)			STATOR 3 (CORE PORTION)			ROTOR 3 (BYPASS PORTION)			STATOR 3 (BYPASS PORTION)		
	HUB	PITCH	TIP	HUB	PITCH	TIP	HUB	PITCH	TIP	HUB	PITCH	TIP
RADIUS RATIO	.604	.639	.705	.602	.636	.704	.712	.798	.905	.727	.803	.901
INLET RADIUS	13.750	14.540	16.050	13.700	14.477	16.007	16.200	18.163	20.590	16.550	18.266	20.500
ABSOLUTE INLET AIR ANGLE	5.47	6.61	8.55	14.38	15.21	19.71	8.23	11.81	15.59	32.13	34.85	39.54
RELATIVE INLET AIR ANGLE	51.12	53.02	56.08	-	-	-	55.61	58.19	61.52	-	-	-
ABSOLUTE INLET MACH NUMBER	.551	.543	.535	.563	.537	.501	.568	.552	.531	.635	.597	.580
RELATIVE INLET MACH NUMBER	.874	.896	.948	-	-	-	.977	1.025	1.073	-	-	-
EXIT AIR ANGLE*	47.2	50.6	55.4	0	0	0	44.2	51.8	56.2	0	0	0
ACCUMULATIVE PRESSURE RATIO	2.532	2.518	2.521	2.500	2.500	2.500	3.049	3.022	3.021	3.0	3.0	3.0
EFFICIENCY	.789	.813	.850	.777	.806	.841	.858	.867	.723	.841	.859	.713
DIFFUSION FACTOR	.103	.106	.136	.097	.116	.160	.304	.303	.310	.376	.385	.440
CAMBER	3.67	0	0	14.72	16.03	22.77	18.62	6.73	5.69	37.82	42.82	51.54
STAGGER	45.29	49.94	54.32	4.66	4.94	6.61	43.92	52.34	56.59	12.48	13.71	15.77
SOLIDITY	1.850	1.807	1.723	1.495	1.414	1.277	1.384	1.321	1.24	1.834	1.661	1.483
ASPECT RATIO		.798			1.635			1.599			2.754	
MERIDIONAL MACH NUMBER	.549	.539	.529	.545	.519	.472	.563	.540	.512	.538	.490	.447

* RELATIVE IN REFERENCE TO ROTOR AND ABSOLUTE IN RELATION TO STATOR

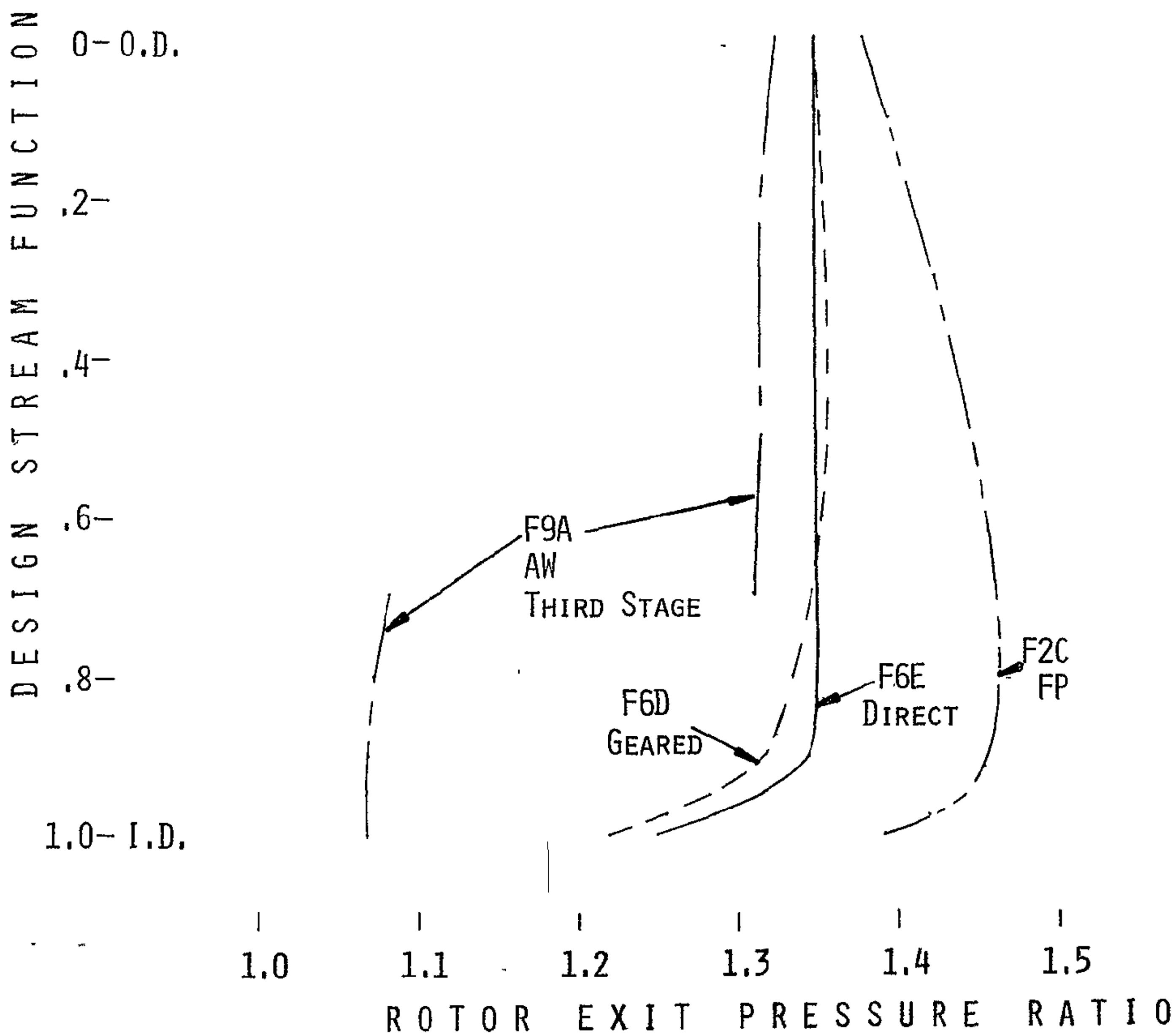

Figure I-12. Task II Radial Distribution of Rotor Total Pressure Ratio.

ORIGINAL PAGE IS OF POOR QUALITY

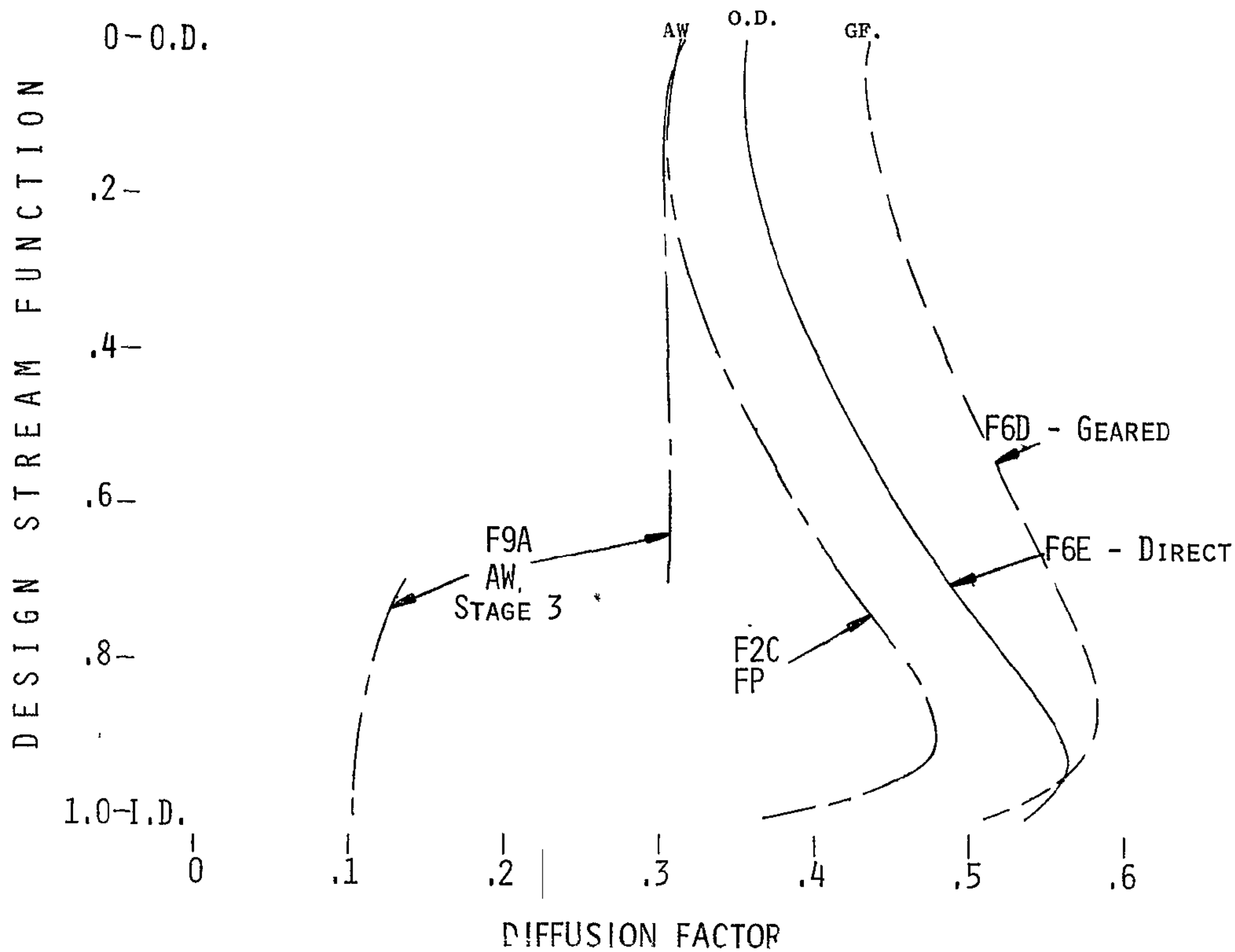

Figure I-13. Task II Radial Distribution of Rotor Diffusion Factor.

pitch fans were loaded about the same from the D factor standpoint which allowed a higher hub pressure ratio for the direct drive fan.

For the variable pitch engines, an integrated fan bypass OGV and frame strut arrangement was selected in order to reduce the fan rotor length while still retaining the design fan rotor - OGV spacing (1-1/4 tip chords). The implications of this design are indicated on Figure I - 14. This arrangement is very similar in concept to the OGV/frame treatment used in the TF39/C5A installation. The nominal OGV blade shape is shown solid but must be tailored adjacent to the top and bottom fairings as illustrated by the dotted lines. A 2" (5.08 cm) thickness is required for the power takeoff shaft. At the bottom of the engine, this is extended out to an island which might be 8" (20.32 cm) thick. At the top, this must be extended out to a structural pylon which might be on the order of 15" (38.1 cm) thick, depending on airframe company design.

The booster aerodynamic design characteristics are summarized on Table I - 24. The designs are patterned after the CF6-50 design. Bleed valves are required for booster stall control during engine deceleration. They will also be used for the VP engines to assure satisfactory booster operation with the disturbed inlet conditions which will be involved in the reverse mode.

Fan Turbine Aerodynamic Design

Table I - 25 summarizes the fan turbine design requirements and overall characteristics. High loadings were utilized where a distinct

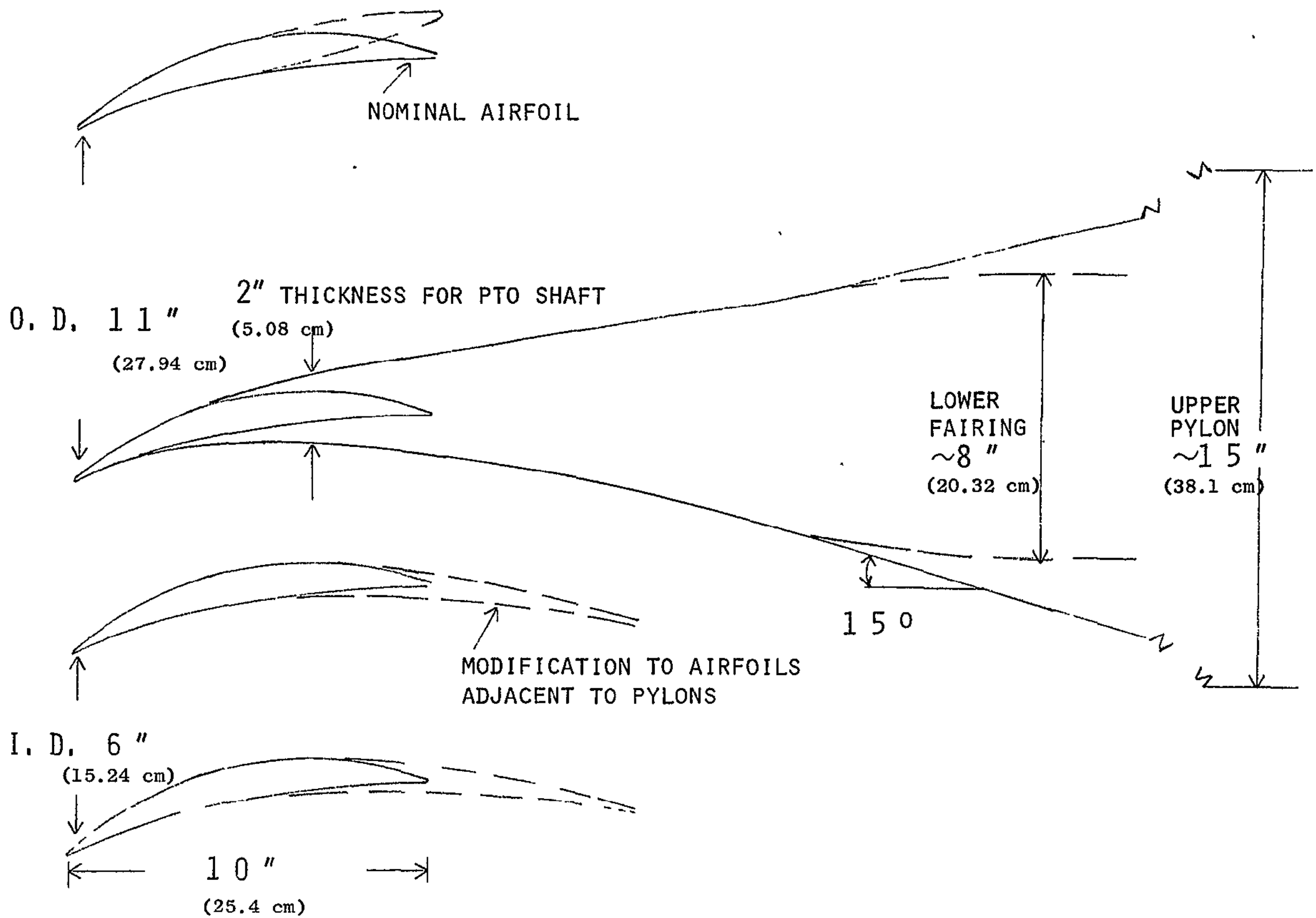

Figure I-14. Task II Vane-Frame for VP Fans.

Table I-24. Task II Booster Aero Design Summary, GE19/F2C, GE19/F6D, GE19/F6E, and CF6-50.

ENGINE	GE19/F2C	GE19/F6D	GE19/F6E	CF6-50	
NO. OF STGS.	3 + FAN HUB	1 + FAN HUB	1 + FAN HUB	3 + FAN HUB	
FAN HUB & BOOSTER P/P *	2.16	1.42	1.50	2.40	
$W\sqrt{\theta}/\delta A$ - 1ST BOOSTER INLET *	36.0	37.0	37.0	36.8	LB/SEC/FT^2
$UT/\sqrt{\theta}$ - " " " *	604	494	583	682	FPS
STALL MARGIN	20%	20%	20%	20%	
BOOSTER STALL PROTECTION	BLEED VALVES AND CONTROL AS IN CF6-50				
REVERSE PITCH OPERATION		BLEED OPEN TO RUN LOW BOOSTER OPERATING LINE			

* AT FAN DESIGN $N/\sqrt{\theta}$

Table I-25. Task II LP Turbine Characteristics.

	F6D	F6E	F2C	F9A
LP TURBINE CHARACTERISTICS - SLS + 31°F (+17.2°C) MATCH POINT				
STG 1 ROTOR INLET TEMPERATURE	1799 (976.1°C)	1775 (968.33°C)	1681 (1027.33°C)	1658 (903.33°C)
ENTHALPY DROP	163	161	156	175
LOADING PARAMETER - AVERAGE	.81	1.55	1.26	1.03
TIP SPEED - PHYSICAL - LAST STG	1390	607	784	1324
NO. OF STAGES	2	5	4	2
DISCHARGE MACH NO.	.35	.333	.395	.439

payoff existed such as in the GE19/F6E design which limits the number of stages to five for this high bypass ratio engine. Several recent NASA programs have provided valuable design information leading to highly loaded turbines having reasonable efficiency levels.

On Tables I - 26 to I - 29 are tabulated more detailed data on the fan turbine designs. The overall conditions at both the takeoff operating point and an off-design operation point are shown. There is a considerable migration of operating conditions for the variable pitch engines with fixed primary jet nozzles. This is due to the increase in turbine pressure ratio which results at flight conditions since the jet nozzle becomes effectively larger as ram pressure ratio and hence jet nozzle pressure ratio increases. For this reason, the exit swirl at the takeoff condition was set somewhat negative at takeoff so that it would not swing to too high a positive value at the maximum climb point. Fan turbine vector diagram data are tabulated on Tables I - 30 through I - 34.

The last stage is loaded relatively low in order to maintain swirl at a reasonable level. The first stage of both the two-stage designs (F6D and F9A) is then loaded quite heavily and the stage pressure ratio is also high. These stages are more closely related to high pressure turbine stages than to the usual LPT stages used on high bypass engines. An alternate three-stage LPT configuration has merit for both these engines.

Table I-26. Task II GE19/F2C Fan Turbine Design.

	(DESIGN POINT) SLTO	MX. CLIMB
$\frac{\Delta H}{T}$	.0724	.0786
$\frac{N}{\sqrt{T}}$	102.5	97.5
INLET $\frac{W\sqrt{T}}{P}$	59.3	60.1
ψ^*_{PAVE}	1.26	1.52
EXIT SWIRL	3.4°	13.8°

STAGE DATA (SLTO)

STAGE	1	2	3	4
ΔH = BTU/LB	43.5	43.5	43.5	23.3
PRESSURE RATIO	1.44	1.40	1.50	1.26
ROOT REACTION	.20	.20	.20	.06
EXIT AXIAL MACH NO.	.358	.347	.374	.395

$*\psi = \frac{gJ\Delta H}{2U^2}$

Table I-27. Task II GE19/F6D Fan Turbine Design.

	(Design Point) SLTO	Max. Climb
$\frac{\Delta H}{T}$	.0729	.0874
$\frac{N}{\sqrt{T}}$	181.4	192.4
Inlet $\frac{W\sqrt{T}}{P}$	53.8	53.9
ψ pave	.81	.866
Exit Swirl	-7.9°	13.6°

Stage Data (SLTO)

Stage	1	2
ΔH = BTU/LB	106.0	56.6
Pressure Ratio	2.37	1.68
Root Reaction	.20	.05
Exit axial Mach No.	.37	.35

$*\psi = \frac{GJ\Delta H}{2U^2}$

Table I-28. Task II GE19/F6E Fan Turbine Design.

	(Design Point) SLTO	Max. Climb
$\frac{\Delta H}{T}$	.0724	.0877
$\frac{N}{\sqrt{T}}$	66.3	70.3
Inlet $\frac{W\sqrt{T}}{P}$	54.8	54.6
Ψ* (pitch) ave.	1.55	1.67
Exit Swirl	-8.1°	4.4°

Stage Data (SLTO)

Stage	1	2	3	4	5
ΔH = BTU/LB	35.4	37.1	37.5	36.9	13.9
Pressure Ratio	1.33	1.36	1.38	1.41	1.15
Root Reaction	.2	.2	.2	.2	-.04
Exit Axial Mach No.	.340	.341	.345	.364	.333

$*\Psi = \frac{gJ\Delta H}{2U^2}$

Table I-29. Task II GE19/F9 Fan Turbine Design.

	(Design Point) SLTO
$\frac{\Delta H}{T}$	.0830
$\frac{N}{\sqrt{T}}$	168.4
Inlet $\frac{W\sqrt{T}}{P}$	58.4
Ψ^{*} (pitch) ave.	1.03
End Swirl	14.3

	Stage Data (SLTO)	
Stage	1	2
ΔH = BTU/LB	110	67.1
Pressure Ratio	2.60	1.96
Root Reaction	.05	.10
Exit Axial Mach No.	.364	.446

$$^{*}\Psi = \frac{gJ\Delta H}{2U^2}$$

Table I-30. Task II GE19/F2C Fan Turbine Vector Diagrams.

STAGE		ROOT (1)	PITCH (1)	TIP (1)	ROOT (2)	PITCH (2)	TIP (2)	ROOT (3)	PITCH (3)	TIP (3)	ROOT (4)	PITCH (4)	TIP (4)
VANE IN. MACH	Mo	.499	.489	.481	.498	.471	.450	.491	.455	.430	.513	.470	.443
VANE EX. MACH	M_I	.839	.778	.729	.818	.731	.667	.850	.732	.653	.692	.596	.538
VANE IN. ANGLE	α_0	26.1	24.2°	22.6	44.1	40.6°	37.5	44.9	40.2°	36.3	43.1	37.3°	32.7
VANE EX. ANGLE	α_1	59.0	56.5°	54.2	62.2	58.8°	55.7	63.2	58.9°	55.0	56.4	50.5°	45.5
VANE TURN ANGLE	$\Delta\alpha$	85.1	80.7	76.8	106.3	99.4°	93.2	108.1	99.1°	91.3	99.5	87.8°	78.2
NUMBER OF VANES			98			176			184			186	
ZWEIFEL NO. *	Ψ Z		.843			.818			.82			.911	
VANE SOLIDITY	C/B		1.568			1.792			1.768			1.815	
VANE ASPECT RATIO	AR		1.83			4.20			5.72			6.35	
BLADE IN. REL. MACH	M_{RI}	.608	.532	.474	.580	.474	.403	.605	.463	.383	.478	.388	.369
BLADE EX. REL. MACH	$M_R{}^2$	.718	.711	.710	.716	.709	.713	.741	.736	.748	.500	.542	.589
BLADE IN. ANGLE	$\beta 1$	50.5	43.8	36.4	52.8	42.9	31.2	53.7	40.3	23.7	38.6	17.4	-4.2
BLADE TURN ANGLE	$\Delta\beta$	107.2	100.2°	92.8	111.3	101.1°	89.7	111.2	97.7°	81.8	76.5	60.6°	43.7
NUMBER OF BLADES			186			171			168			173	
ZWEIFEL NO.	Ψ Z		1.028			1.021			1.009			.968	
BLADE EX. DIA.		25.180	28.240	31.300	25.300	29.550	33.800	25.300	30.830	36.360	25.300	31.650	38.000
BLADE SOLIDITY	C/T		1.553			1.493			1.512			1.755	
BLADE ASPECT RATIO	AR		4.13			5.25			6.34			6.30	
STAGE LOADING	Ψ	2.03	1.63	1.34	2.00	1.48	1.14	2.00	1.36	.99	1.07	.69	.48
STAGE EFFICIENCY	η_{TT}		.875			.893			.898			.910	

* $\Psi_Z = 2 \cos \beta_2 \,(\tan \beta_1 \cos \beta_2 + \sin \beta_2)\, \frac{T}{A_W}$

Table I-31. Task II GE19/F6D Fan Turbine Vector Diagrams.

STAGE		ROOT	PITCH 1	TIP	ROOT	PITCH 2	TIP
VANE IN. MACH	M_O	.336	.330	.325	.507	.475	.449
VANE EX. MACH	M_I	1.147	1.014	.913	.952	.784	.679
VANE IN. ANGLE	α_O	28.1	26.2°	24.6	43.1	38.7°	34.9
VANE EX. ANGLE	α_1	70.9	68.7°	66.6	68.1	63.7°	59.6
VANE TURN ANGLE	$\Delta\alpha_R$	99.0	94.9	91.2	111.2	102.4°	94.5
NUMBER OF VANES			76			85	
ZWEIFEL NO.	Ψ_Z		.608			.75	
VANE SOLIDITY	C/B		1.79			1.72	
VANE ASPECT RATIO	AR		1.51			2.96	
BLADE IN. REL. MACH	MRI_R	.701	.528	.409	.535	.346	.338
BLADE EX. REL. MACH	M_{R2+}	.923	.945	.979	.538	.651	.769
BLADE IN. ANGLE	β_{1R}	61.2	51.2°	37.0	51.7	20.5°	-18.7
BLADE TURN ANGLE	$\Delta\beta_R$	124.6	115.4°	102.1	100.4	77.5°	43.8
NUMBER OF BLADES			147			141	
ZWEIFEL NO.	Ψ_Z		.997			.995	
BLADE EX. DIA.		25.520	29.510	33.500	24.000	30.600	37.200
BLADE SOLIDITY	C/T		1.39			1.38	
BLADE ASPECT RATIO	AR		4.57			7.00	
STAGE LOADING	Ψ	1.45	1.11	.87	.87	.54	.37
STAGE EFFICIENCY	η		.886			.897	

Table I-32. Task II GE19/F6E Fan Turbine Vector Diagrams, Stages 1, 2, and 3.

		ROOT	PITCH	TIP	ROOT	PITCH	TIP	ROOT	PITCH	TIP
STAGE			1			2			3	
VANE IN. MACH	M_0	.373	.367	.361	.479	.464	.449	.485	.466	.449
VAN EX. MACH	M_I	.729	.693	.662	.754	.711	.674	.773	.717	.671
VANE IN. ANGLE	α_0	25.9	24.0°	22.4	44.7	42.8°	40.9	45.4	43.0°	40.8
VANE EX. ANGLE	α_1	60.4	58.9°	57.3	60.6	58.8°	57.0	61.5	59.2°	57.0
VANE TURN ANGLE	$\Delta\alpha$	86.3	82.9°	79.7	105.3	101.6°	97.9	106.9	102.2°	97.8
NUMBER OF VANES			146			240			246	
ZWEIFEL NO.	Ψ_Z		.820			.819			.815	
VANE SOLIDITY	C/B		1.561			1.780			1.807	
VANE ASPECT RATIO	AR		1.34			3.02			3.81	
BLADE IN. REL. MACH	M_{R1}	.543	.502	.467	.551	.506	.464	.568	.502	.449
BLADE EX. REL. MACH	M_{R2}	.657	.651	.646	.675	.667	.662	.686	.677	.674
BLADE IN. ANGLE	β_1	50.8	47.0°	43.0	51.1	46.4°	41.5	52.0	46.0°	39.5
BLADE TURN ANGLE	$\Delta\beta$	107.8	103.7°	99.4	108.8	103.8°	98.7	110.2	103.8°	97.2
NUMBER OF BLADES			262			244			214	
ZWEIFEL NO.	Ψ_Z		1.0			1.0			1.0	
BLADE EX. DIA.		33.120	35.400	37.680	33.880	36.750	39.620	34.060	37.770	41.480
BLADE SOLIDITY	C/T		1.644			1.600			1.583	
BLADE ASPECT RATIO	AR		3.26			3.79			4.23	
STAGE LOADING	Ψ	2.20	1.93	1.71	2.19	1.87	1.62	2.18	1.79	1.49
STAGE EFFICIENCY	η_{TT}		.868			.884			.888	

Table I-33. Task II GE19/F6E Fan Turbine Vector Diagrams, Stages 4 and 5.

		ROOT	PITCH	TIP	ROOT	PITCH	TIP
STAGE			4			5	
VANE IN. MACH	Mo	.492	.467	.447	.496	.468	.447
VANE EX. MACH	M_I	.813	.738	.681	.576	.525	.489
VANE IN. ANGLE	α_O	45.4	42.3°	39.6	42.7	38.9°	35.6
VANE EX. ANGLE	α_1	61.8	59.0°	56.3	53.0	48.9°	45.3
VANE TURN ANGLE	$\Delta\alpha$	107.2	101.3°	95.9	95.7	87.8°	80.9
NUMBER OF VANES			222			222	
ZWEIFEL NO.	Ψ Z		.820			.925	
VANE SOLIDITY	C/B		1.800			1.868	
VANE ASPECT RATIO	AR		4.32			5.15	
BLADE IN. REL. MACH	M_{RI}	.603	.514	.449	.407	.360	.340
BLADE EX. REL. MACH	M_{R2}	.689	.681	.681	.378	.403	.431
BLADE IN. ANGLE	$\beta 1$	52.7	45.2°	36.7	33.3	19.6°	5.9
BLADE TURN ANGLE	$\Delta\beta$	109.3	101.4°	92.9	61.7	54.1°	45.3
NUMBER OF BLADES			214			216	
ZWEIFEL NO.	Ψ Z		1.0			1.0	
BLADE EX. DIA.		33.760	38.460	43.160	33.300	38.900	44.500
BLADE SOLIDITY	C/T		1.622			1.623	
BLADE ASPECT RATIO	AR		5.14			6.11	
STAGE LOADING	Ψ	2.17	1.69	1.35	.84	.62	.48
STAGE EFFICIENCY	η_{TT}		.890			.913	

Table I-34. Task II GE19/F9 Fan Turbine Vector Diagrams.

		ROOT	PITCH	TIP	ROOT	PITCH	TIP
STAGE			1			2	
VANE IN. MACH	Mo	.367	.360	.355	.547	.499	.463
VANE EX. MACH	M_I	1.399	1.201	1.061	1.070	.850	.722
VANE IN. ANGLE	α_O	28.1	26.2°	24.6	48.4	43.3°	38.9
VANE EX. ANGLE	α_1	71.7	69.3°	66.9	68.7	63.6°	59.0
VANE TURN ANGLE	$\Delta\alpha$	99.8	95.5°	91.5	117.1	106.9°	97.9
NUMBER OF VANES			76			72	
ZWEIFEL NO.	Ψ Z		.624			.795	
VANE SOLIDITY	C/B		1.86			1.65	
VANE ASPECT RATIO	AR		1.39			2.96	
BLADE IN. REL. MACH	M_{R1}	.964	.715	.543	.665	.406	.356
BLADE EX. REL. MACH	M_{R2}	.948	.962	.993	.744	.830	.932
BLADE IN. ANGLE	$\beta 1$	65.9	57.9°	46.7	56.5	28.9°	-10.4
BLADE TURN ANGLE	$\Delta\beta_R$	130.6	123.1°	112.8	109.7	86.5°	51.1
NUMBER OF BLADES			100			118	
ZWEIFEL NO.	Ψ Z		1.01			.93	
BLADE EX. DIA.		25.200	30.075	34.950	23.920	31.460	39.000
BLADE SOLIDITY	C/T		1.36			1.50	
BLADE ASPECT RATIO	AR		4.02			5.80	
STAGE LOADING	Ψ	1.86	1.35	1.02	1.26	.74	.49
STAGE EFFICIENCY	η_{TT}		.863			.896	

SECTION II - CONTROLS AND TRANSIENTS

GENERAL REQUIREMENTS

The controls utilized in the QCSEE Task II are digital electronic supporting a hydromechanical main fuel control. The general requirements of the control system are given on Table II - 1. Table II - 2 further subdivides the specific function by engine series, pointing out those features unique to each engine. The F9 requires no booster bleed valve. The F2 and F9 require no variable pitch control. The F2 and F6 require no inlet control. The F6D is the only engine requiring fan turbine overspeed protection.

Overall control system characteristics are given in Table II - 3, while Table II - 4 defines probable control modes. In the case of modes which are integrated with the aircraft system, a great deal of flexibility is available in the digital control in deciding exactly what combination of aircraft inputs is optimum.

Mechanization of the various control elements is summarized on Table II - 5.

As shown on Table II - 6, one possible variable pitch control method would be to provide an additional control mode selector having three positions; normal, approach, and reverse. In the normal mode, control would be the same as a fixed pitch fan. In the approach mode, fan speed would be held at 100% by controlling pitch angle. This high fan speed improves response time for go-around maneuver.

Table II-1. Task II General Requirements.

- MODULATE THRUST
- MINIMIZE THRUST VARIATION
- PROVIDE TRANSIENT CAPABILITY
- SCHEDULE VARIABLE GEOMETRY
- PREVENT STALL
- PREVENT BLOWOUT
- MAINTAIN LIMITS - SPEED, TEMPERATURE, PRESSURE
- BLEED/HORSEPOWER EXTRACTION COMPENSATION
- INTEGRATE WITH A/C MANAGEMENT

Table II-2. Task II Specific Functions.

FUNCTION	F2	F6	F9
FUEL FLOW CONTROL	X	X	X
TURBINE TEMPERATURE LIMITING	X	X	X
BOOSTER BLEED SCHEDULING	X	X	-
CORE STATOR SCHEDULING	X	X	X
FAN PITCH ANGLE CONTROL	-	X	-
EXHAUST NOZZLE POSITIONING	X	X	X
SONIC INLET CONTROL	-	-	X
EMISSIONS CONTROL	X	X	X
LP TURBINE O/S PROTECTION	-	X	-
RAPID FORWARD F_N RESPONSE	X	X	X
RAPID F_N REVERSER DEPLOY	X	X	X

Table II-3. Task II System Characteristics.

ITEM	F2	F6	F9
FUEL FLOW (PPH)	9040	7880	8242
PUMP FLOW (PPH)	13400	12000	12600
CORE STATOR ACTUATION TIME (SEC)	1	1	1
BLEED DOOR ACTUATION TIME (SEC)	1	1	-
REVERSER ACTUATION TIME (SEC)	1	1	1
EXHAUST NOZZLE ACTUATION TIME (SEC)	5	1	5
A/C HYDRAULIC PUMP (GPM)	95	95	95
A/C GENERATOR (KVA)	45	45	45
HYDRAULIC PUMP (GPM)	20	20	20

Table II-4. Task II Probable Control Modes.

FUEL FLOW W_F	$= f(N_1, N_2, T_2, T_{4B})$
COMPRESSOR STATORS	$= f(N_2, T_{25})$
VARIABLE BLEED DOORS	$= f(N_1, N_2, T_{25})$
ACCEL FUEL FLOW	$= f(N_2, T_{25}, P_{S3})$
EXHAUST NOZZLE AREA	$= f(PLA, Mo)$
SONIC INLET	$= f(P_2, P_{25}, PLA)$
VARIABLE PITCH ANGLE	$= f(PLA, N_1, A/C\ MODE)$
EMISSION CONTROL	$= f(PLA)$
OVERSPEED S/D	$= f(N_1, \dot{N}_1)$
TURBINE TEMPERATURE LIMIT	$= f(T_{4B})$

Table II-5. Task II Mechanization: Pumps, Valves, and Actuators.

FUEL PUMP	- ENGINE DRIVEN - CONSTANT DISPLACEMENT - VANE - WITH INTEGRAL BOOST
FUEL VALVE	- HYDROMECHANICAL - BYPASSING - BACKUP CONTROL ON SPEED, ACCEL W_F
ENGINE CONTROL	- DIGITAL - ACCESS TO ALL VARIABLE GEOMETRY - FLY-BY-WIRE INPUTS
REV/NOZZLE ACTUATORS	- LINEAR ACTUATORS - OIL HYDRAULIC SERVO PUMP ELECTRICAL COMMAND
VSV/VBV ACTUATORS	- LINEAR - FUEL PRESSURE ELECTRICAL/ MECHANICAL DEMAND

Table II-6. Task II Variable Pitch Control.

- MODE SELECTOR
  - NORMAL
  - APPROACH
  - REVERSE

- NORMAL MODE
  - FAN SPEED SCHEDULED WITH PLA (LIMITED AUTHORITY)
  - CORE SPEED SCHEDULED WITH PLA

- APPROACH MODE
  - PITCH ANGLE VARIES TO HOLD FAN SPEED AT 100%
  - CORE FUEL FLOW ANTICIPATION PROVIDED FOR RESPONSE

GE19/F2C FUEL SYSTEM AND BASIC CONTROL LOGIC

The function of the fuel system is to control the engine manipulated variables - fuel, flow, core stators, and bypass doors - to maintain safe, efficient operation throughout the flight envelope. The fuel system is not influenced by the type of engine installation.

Control of fuel flow, core stators, and bypass doors is accomplished hydromechanically with electrical trim. The fuel pump is a centrifugally boosted vane pump with the fuel/oil cooler and fuel filter integrally mounted. It is sized for 32 gpm (.60546 m^3/min.) and 1000 psi (689.48 N/cm^2) operation at 6000 rpm. Pressurized fuel is supplied to the main fuel control which contains a core speed governor, fuel metering valve, core stator and bypass door servos, compressor inlet temperature servo, compressor discharge and bleed flow pressure sensors, hydromechanical computational devices, and a pressurizing valve with low pressure turbine overspeed solenoid shut-off valve. Following metering, fuel is supplied to the manifold and injected into the combustor through dual orifice valves and pigtails.

The stators and bypass doors are positioned by porting pressurized fuel to the head or rod end of the actuators, which are typical single-ended hydraulic actuators. A push-pull cable provides mechanical feedback to the control.

The compressor inlet temperature sensor (T_{25}) is a helium-filled coil and servo which indicates temperature by allowing the pressure in the bulb (function of temperature) to position a lever which varies an orifice across which the pressure drop is measured. This pressure drop is very nearly linear with T_{25}.

The ground idle permit signal entering the main fuel control operates on the landing gear; ground idle is allowed only when the landing gear are down. This is the method presently used on the CF6/DC-10. The signal supplied is a 28 VDC electrical signal to a solenoid which is energized to permit ground idle.

The digital trim control takes sensor inputs and feedback from the main fuel control to trim both engine fuel flow and the bypass doors. This allows the bypass doors to be biased with corrected fan speed and the core speed governor to be overriden for corrected fan speed governing or turbine blade temperature limiting.

The digital trim control uses power lever angle (PLA) to schedule corrected fan speed which is biased by P_2 to provide flat rating and by T_2 to prevent a scheduled T_4 overtemperature. The core speed (N_2) cam in the hydromechanical control and the corrected fan speed ($N1/\sqrt{\theta 2}$) schedule are designed so that, at some point just above idle, the core speed demand requests a larger fuel flow than the fan speed demand, and the smaller one overrules the larger at the selector and is satisifed. From this point up to maximum, corrected fan speed is governing unless limited by some other function. The other basic engine control function in the digital trim control is the T_{4B} limit to prevent over-temperature of the high pressure turbine rotor blades.

Control schematics for the F2C and F6 engines are given on Fig. II - 1 and the F9A on Fig. II - 2. Control block diagrams (hydromechanical and electrical) are shown on Figures II - 3, II - 4, II - 5, and II - 6.

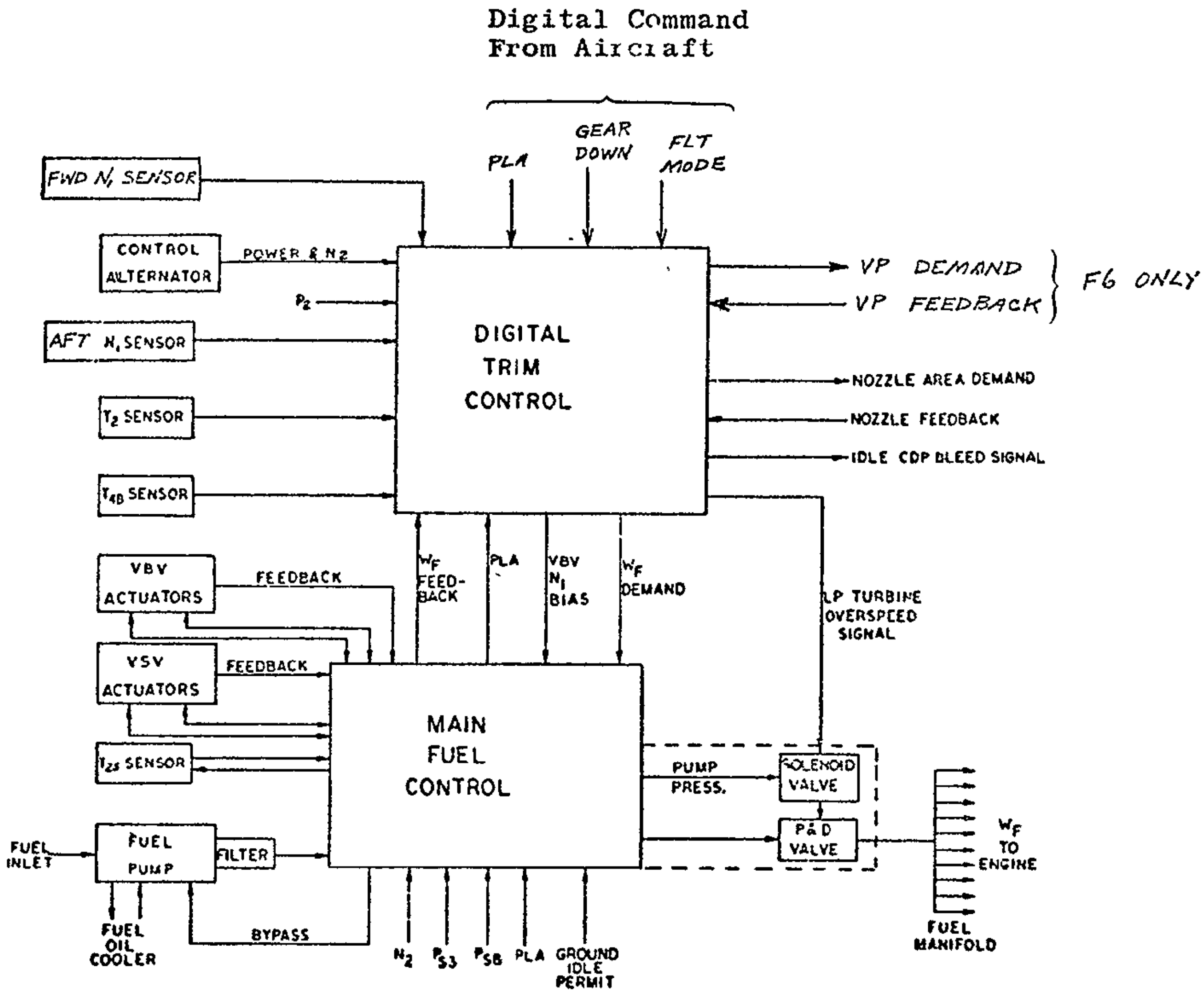

Figure II-1. Task II GE19/F2C and F6 Fuel System.

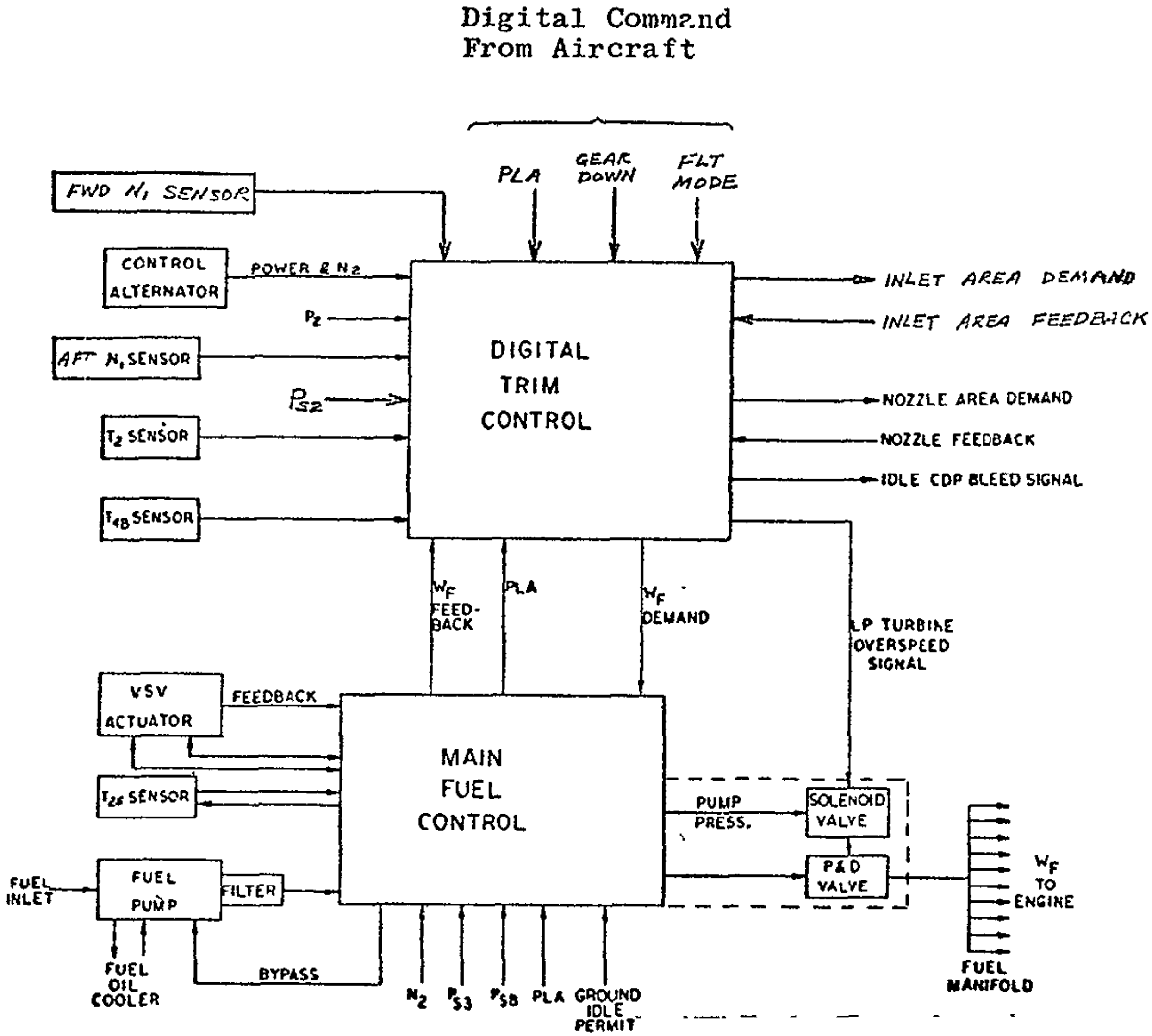

Figure II-2. Task II GE19/F9A Fuel System.

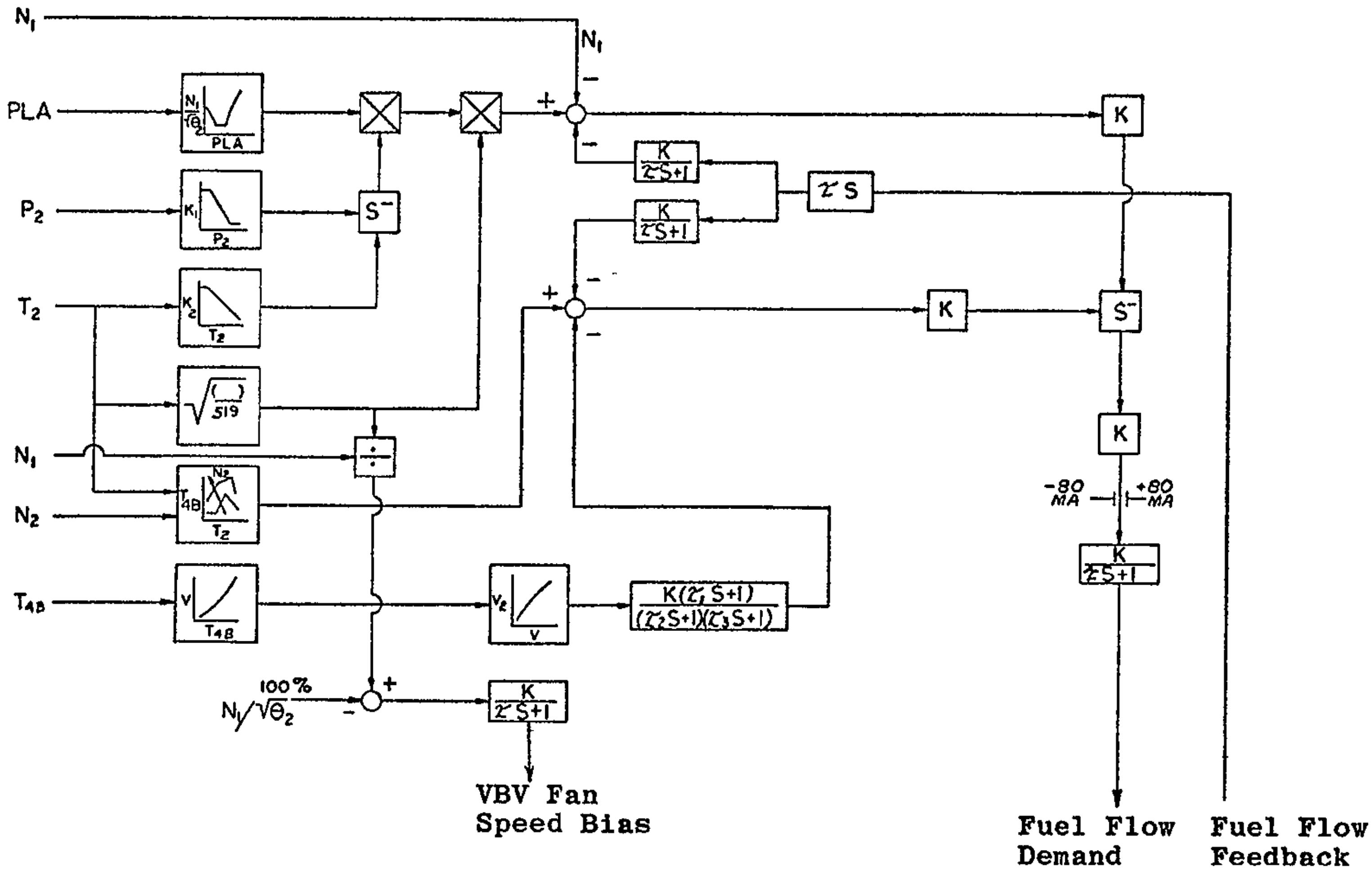

Figure II-3. Task II GE19/F2C and F6 Fuel System Block Diagram (Electrical Section).

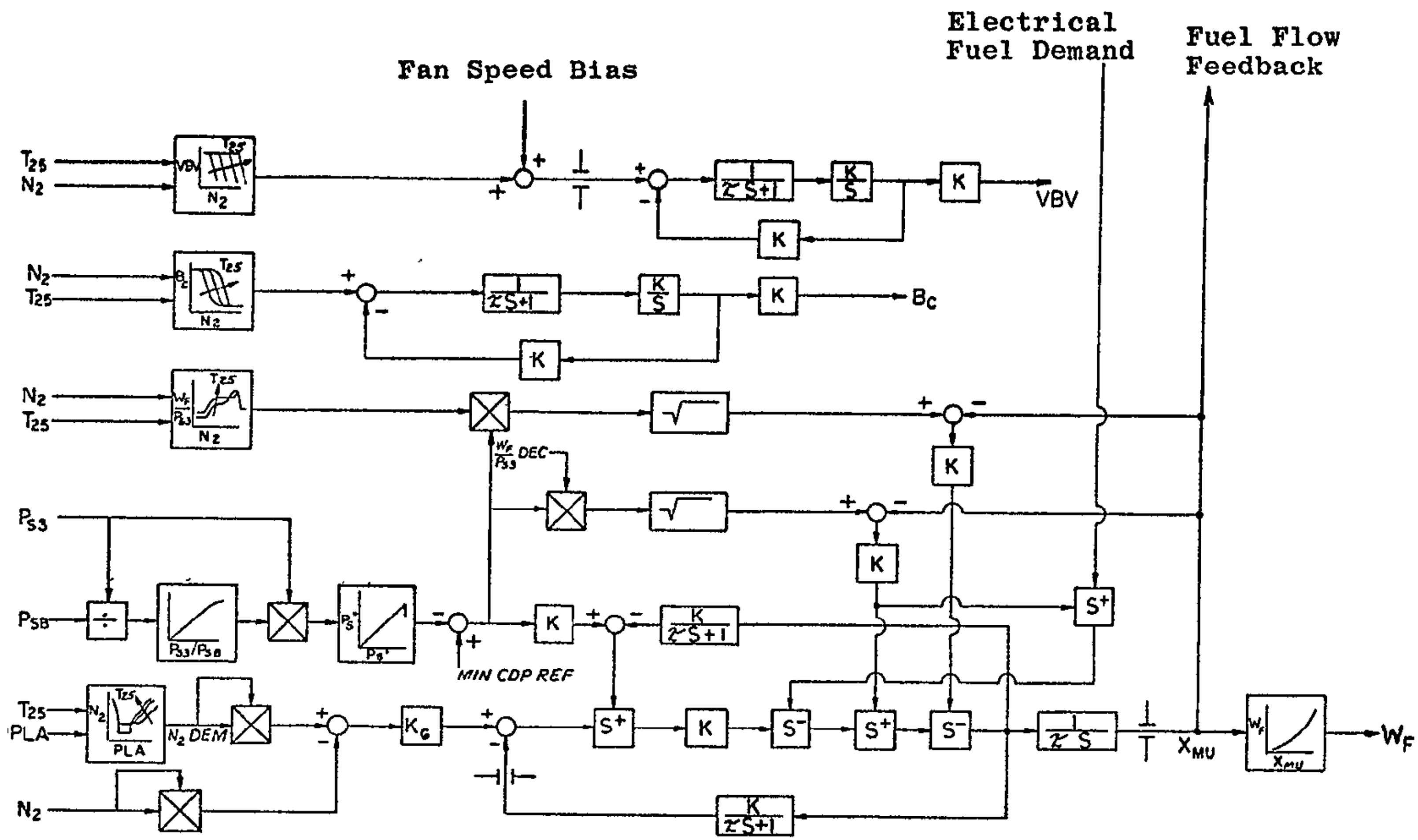

Figure II-4. Task II GE19/F2C and F6 Fuel System Block Diagram (Hydromechanical Section).

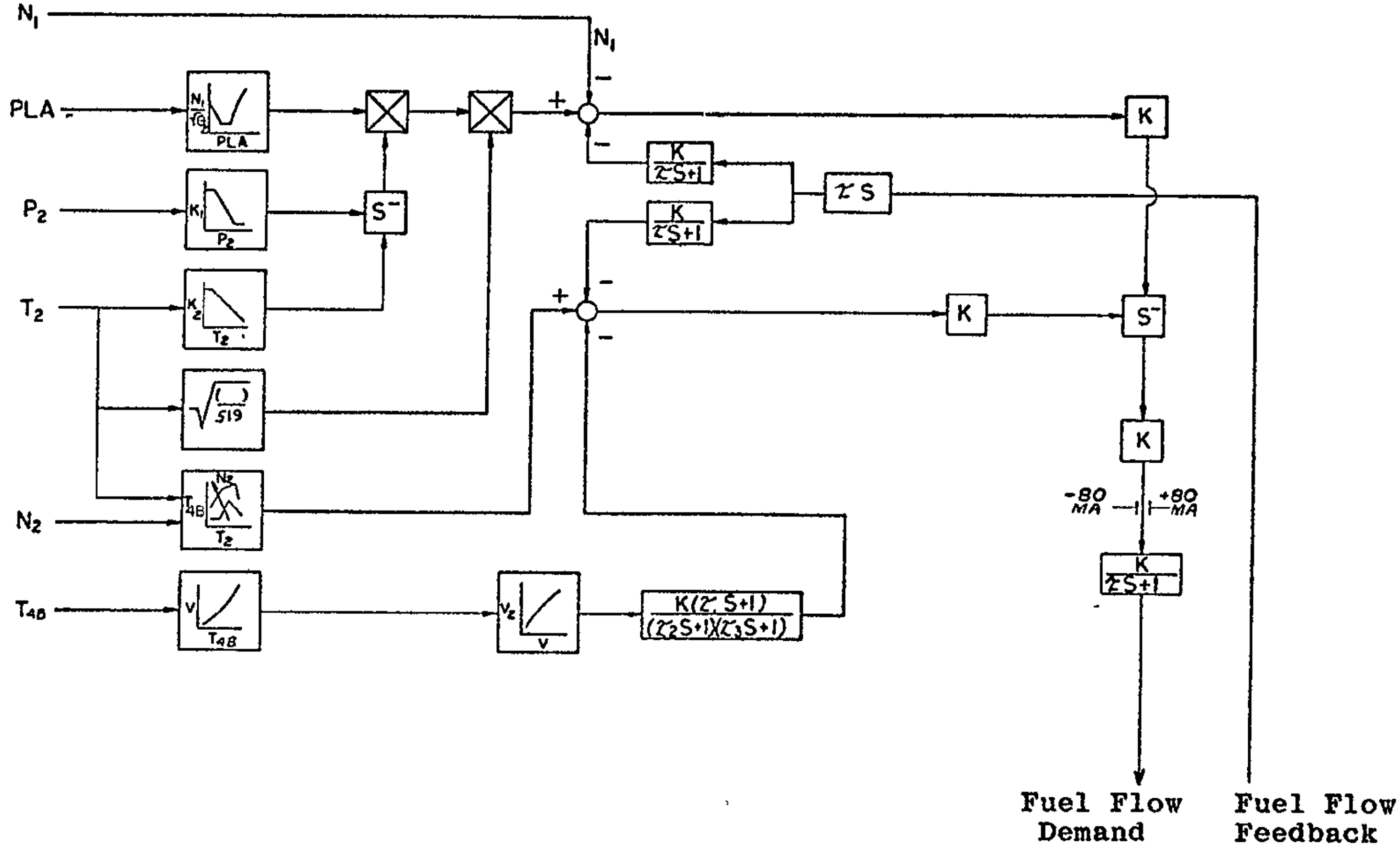

Figure II-5. Task II GE19/F9A Fuel System Block Diagram (Electrical Section).

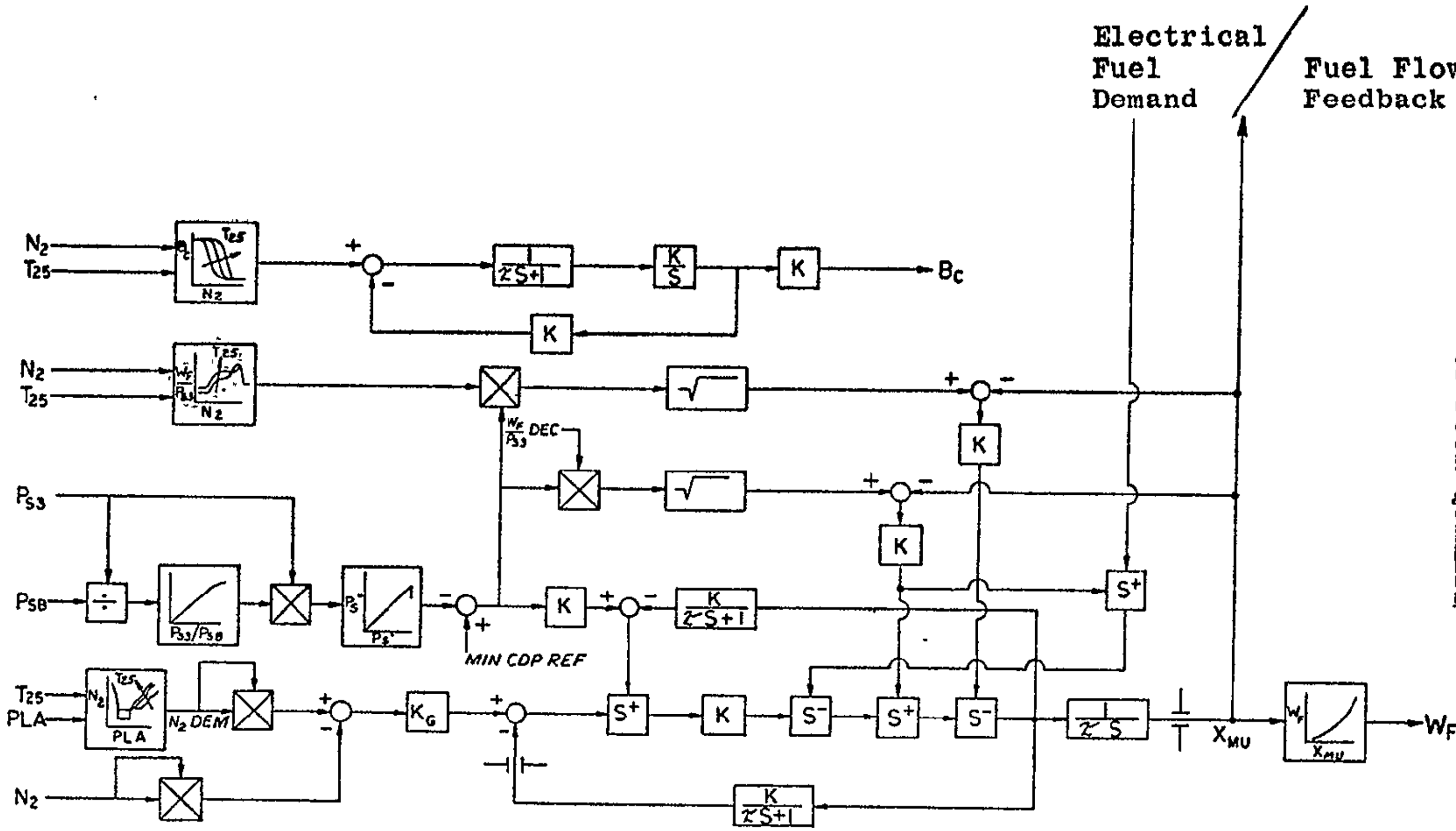

Figure II-6. Task II GE19/F9A Fuel System Block Diagram (Hydromechanical Section).

ORIGINAL PAGE IS OF POOR QUALITY

GE19/F2C NOZZLE ACTUATOR

Both the conventional pylon-mounted engine and the over-the-wing (OTW) engine require variable nozzle area. The conventional mount requires a two-position nozzle flap with thrust reverse accomplished by moving the plug aft. Thrust reverser actuation is handled mechanically while nozzle actuation is hydraulic. Oil from the tank is filtered and supplied to the pump which is a variable flow, piston pump commonly referred to as a servo pump. The pump piston stroke is variable so that only the required fluid is pumped - unnecessary heat is not generated. Fluid is then supplied directly to the actuator head or rod ends depending upon the direction of motion desired. A linear variable differential transformer (LVDT) provides position feedback to the trim control.

Logic for nozzle area changes (computed in the trim control) should be automatic, if possible. The nozzle must be open for takeoff and landing and closed for climb and cruise. A possible scheme for accomplishing this is shown in the following logic diagram:

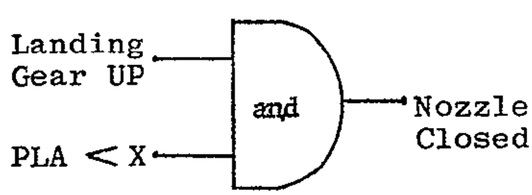

Landing Gear	PLA	Nozzle
U	$> X$	Open
U	$< X$	Closed
Down	$> X$	Open
Down	$< X$	Open

Where X = PLA between climb and takeoff power settings.

This indicates that the nozzle would be open unless the landing gear were up and the power lever angle was less than takeoff. The landing gear signal, as was explained earlier, is also used for ground idle permission.

The over-the-wing engine requires hydraulic nozzle actuation as well as hydraulic thrust reverser actuation. This is identical to the previous nozzle system except that a shuttle valve has been added to direct the fluid to the proper set of actuators. A schematic of the system is shown on Fig. II - 7.

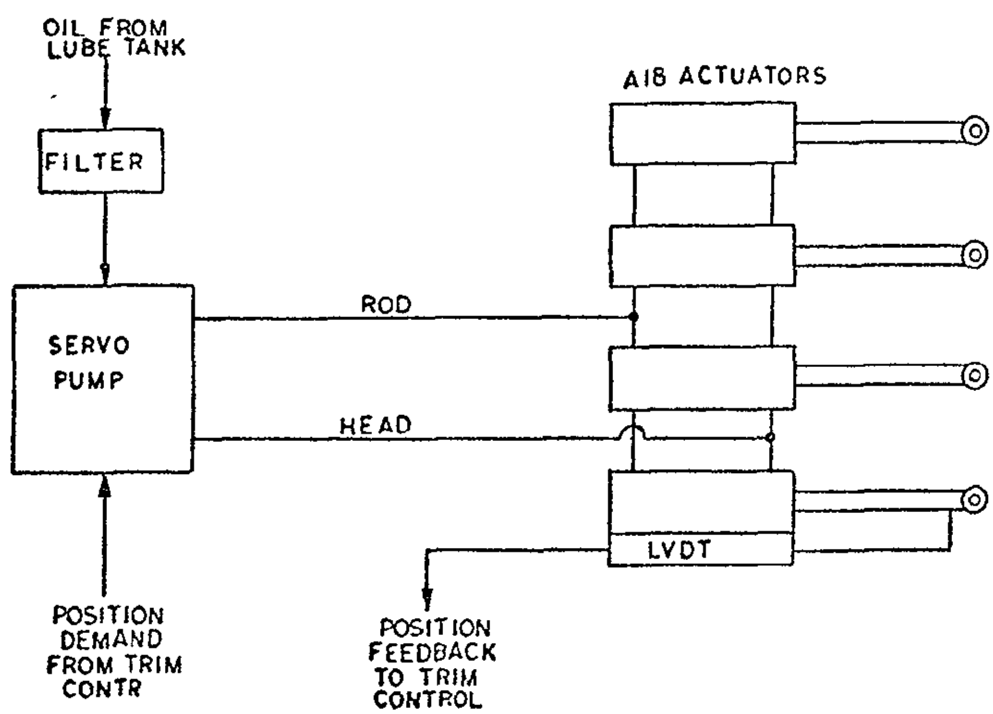

Figure II-7. Task II GE19/F2C and F6 Nozzle Actuation System.

GE19/F2C THRUST REVERSER ACTUATION

The conventional pylon-mounted, under-the-wing engine utilizes a plug actuator to deploy the thrust reverser. The plug actuation approach selected involves a pump, gearboxes, a clutchbrake package, and a ballscrew actuator. The input to the actuation package is directly coupled to the fan shaft. This input, through a gear reduction and an idler, then provides a two-directional output by proper hydraulic clutch actuation and braking. The pump requires a small amount of lube oil from the rear sump. A schematic is shown on Figure II - 8.

Pilot input is required to demand thrust reverser operation. Some advantages of this type of mechanical actuation are:

a. Only electrical signals need be transmitted from the outside to the engine centerline.

b. The weight is less than a pneumatic actuator or pneumatic motor plus ballscrew.

The over-the-wing engine installation requires an external actuation system. The combination of the nozzle and thrust reverser actuation systems requires that the pilot's thrust reverse command signal pass through the digital trim control so that shuttle valve position can be coordinated with both the nozzle and the thrust reverser. As is done on all thrust reverser actuation systems, the design must be such that no single failure will allow inadvertent deployment. This is accomplished on all QCSEE engines by using a latch actuator to lock the system in stow position. The electrically actuated shuttle valve on this combined nozzle and thrust reverser actuation system is designed to supply fluid to the nozzle actuators when unenergized and vice versa. This provides additional safety.

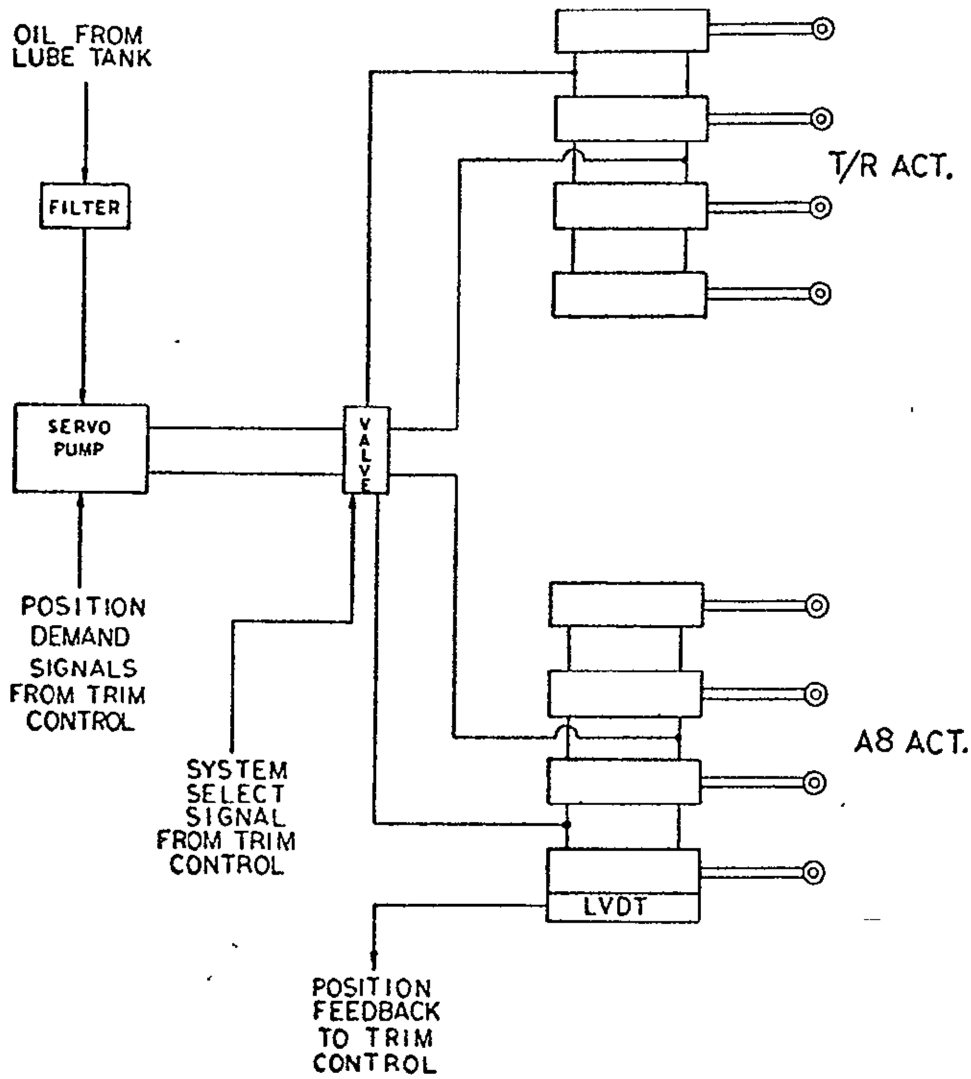

Figure II-8. Task II GE19/F2C (OTW) and F9A Nozzle and Thrust Reverser System.

GE19/F2C FUEL/OIL HEAT EXCHANGER

The fuel/oil cooler is an aluminum shell-and-tube type, with the oil and fuel flowing in parallel at the fuel inlet tube header. The heat exchanger mounts directly to the engine fuel pump to minimize weight and plumbing. In addition to serving as an oil cooler, it also is used as a cold fuel heater to avoid the possibility of fuel system ice blockage. The heat exchanger is located between the boost and main pump elements downstream of the bypass return for the following reasons:

a. To protect the filter from ice

b. To minimize weight (low pressure)

c. To maintain near constant thermal effectiveness

d. To take advantage of the largest available fuel flow

GE19/F6 FUEL SYSTEM AND BASIC CONTROL LOGIC

The function of the fuel system is identical to that described for the F2C except that fan variable pitch must be added. The system schematic is very similar to that for the F2C.

F6 V.P. FAN ENGINE CONTROL

The F6 engines have been used for investigating the ability - the control design to provide fast response for throttle bursts from 50 to 100% thrust by controlling the velocity of the variable pitch actuator as a function of fan speed derivative (see Figure II-9).

In this control design, the corrected fan speed reference is a constant size to produce 100% thrust. The core speed schedule is a "roof type" schedule, sized to take control of engine fuel flow in the event of core overspeeds or of a failure in the fan speed controller. The "fan speed kicker" circuit resets the fan speed reference high when a wave-off throttle burst is made; thus minimim

- A proposed control design for aircraft approach and fast wave-off thrust response.
- Functions shown are additions to F6 fuel control.

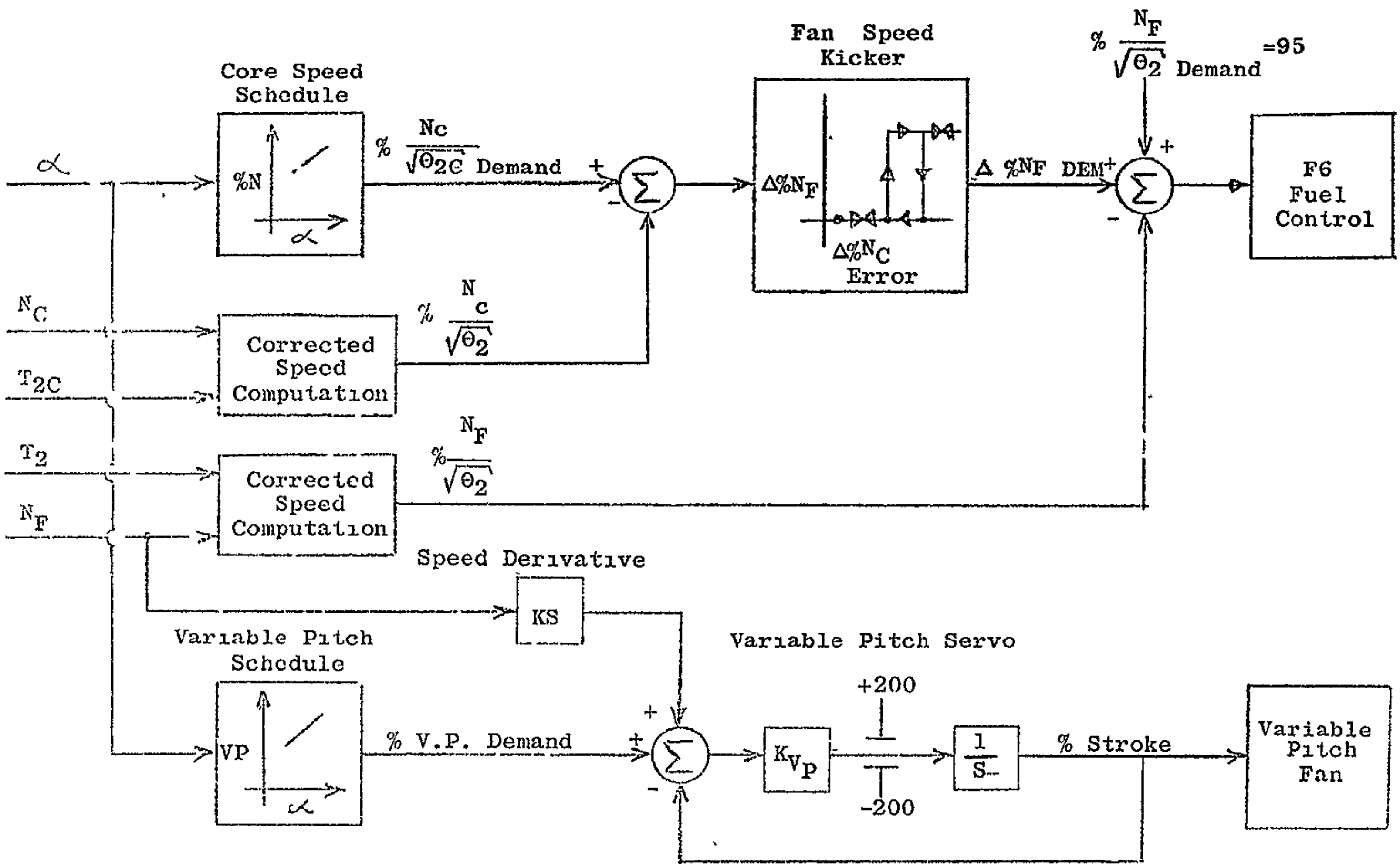

Figure II-9. GE19/F6 Variable Pitch Control.

time is used to change the fuel control from the steady-state fan speed to the core accel schedule mode of control.

In this design, variable pitch angle is scheduled as a function of power lever position; also, maximum velocity of the variable pitch actuator is sized to meet the requirement of slewing from the 100% forward thrust position to the 100% reverser thrust position in one second. An actuator servo loop gain of 2.5 is used, producing a closed loop servo time constant of 0.4 second. In this control, the fan speed derivative reset of variable pitch demand has been sized at 0.7% V.P. angle/% N_F/sec. In our opinion, future studies on variable pitch control design will indicate fan speed derivative to be quite effective in compensating for flight envelope and engine-to-engine variations and thus produce consistent thrust response.

F6D OVERSPEED PROTECTION

The F6D engine is protected from overspeed caused by a shaft failure by a solenoid-operated valve, which, upon receipt of a signal from the trim control, ports pump discharge pressure to the pressurizing valve to close it. Estimated time from failure to closed pressurizing valve is 0.04 second. This feature is required because of the aft bearing feature which prevents blade/vane interference at shaft failure which normally limits turbine overspeed in more conventional engine designs. Typical overspeed characteristics of the GE19/F6D are shown on Figure II-10. The shutdown system operates as shown on Figure II-11 to limit overspeed by shutting off fuel.

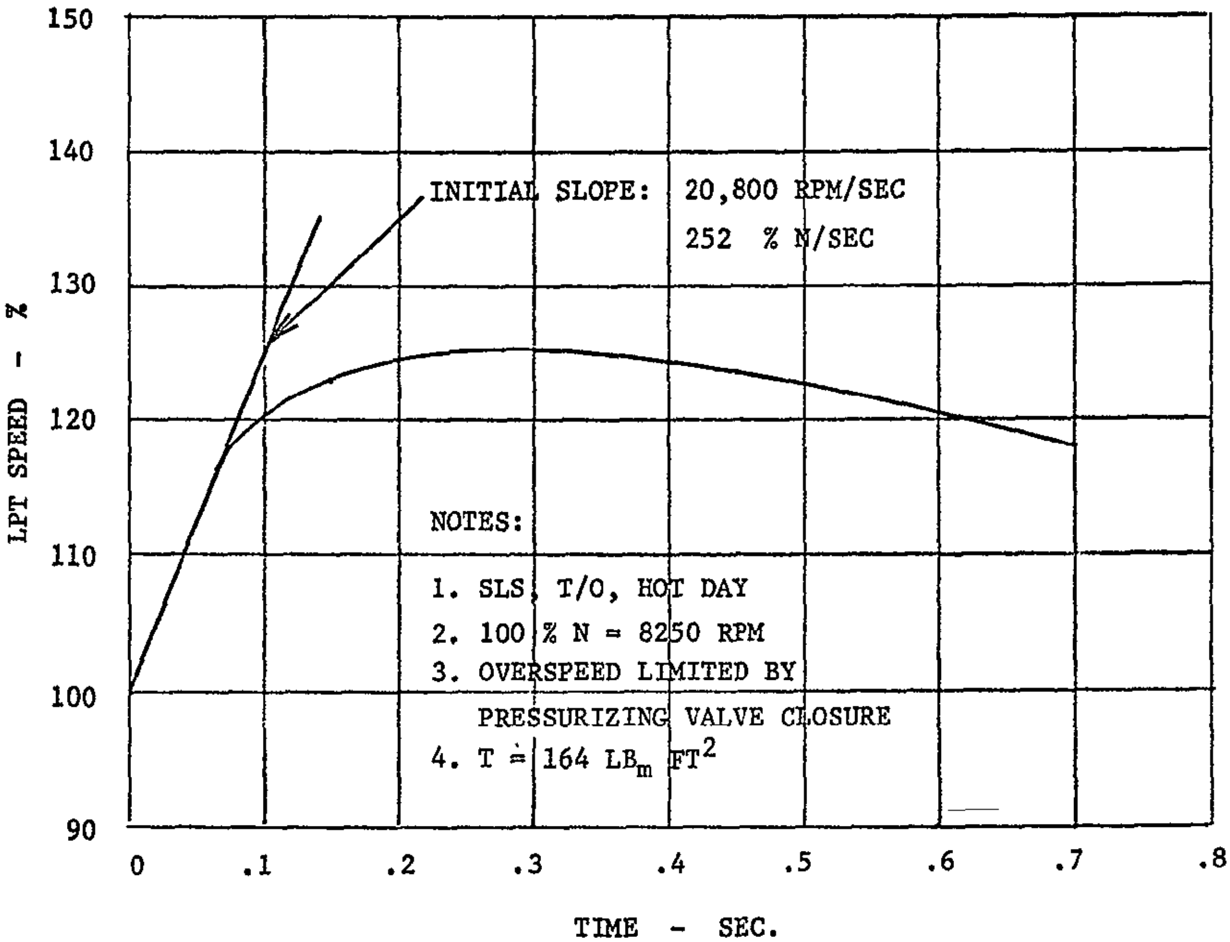

Figure II-10. Task II LPT Overspeed Study, GE19/F6D.

GE19/F9A FUEL SYSTEM AND BASIC CONTROL LOGIC

The fuel system is identical to that for the F2C with the exception of the bypass doors, which are removed. The high Mach no. inlet control schematic is shown on Figure II - 12.

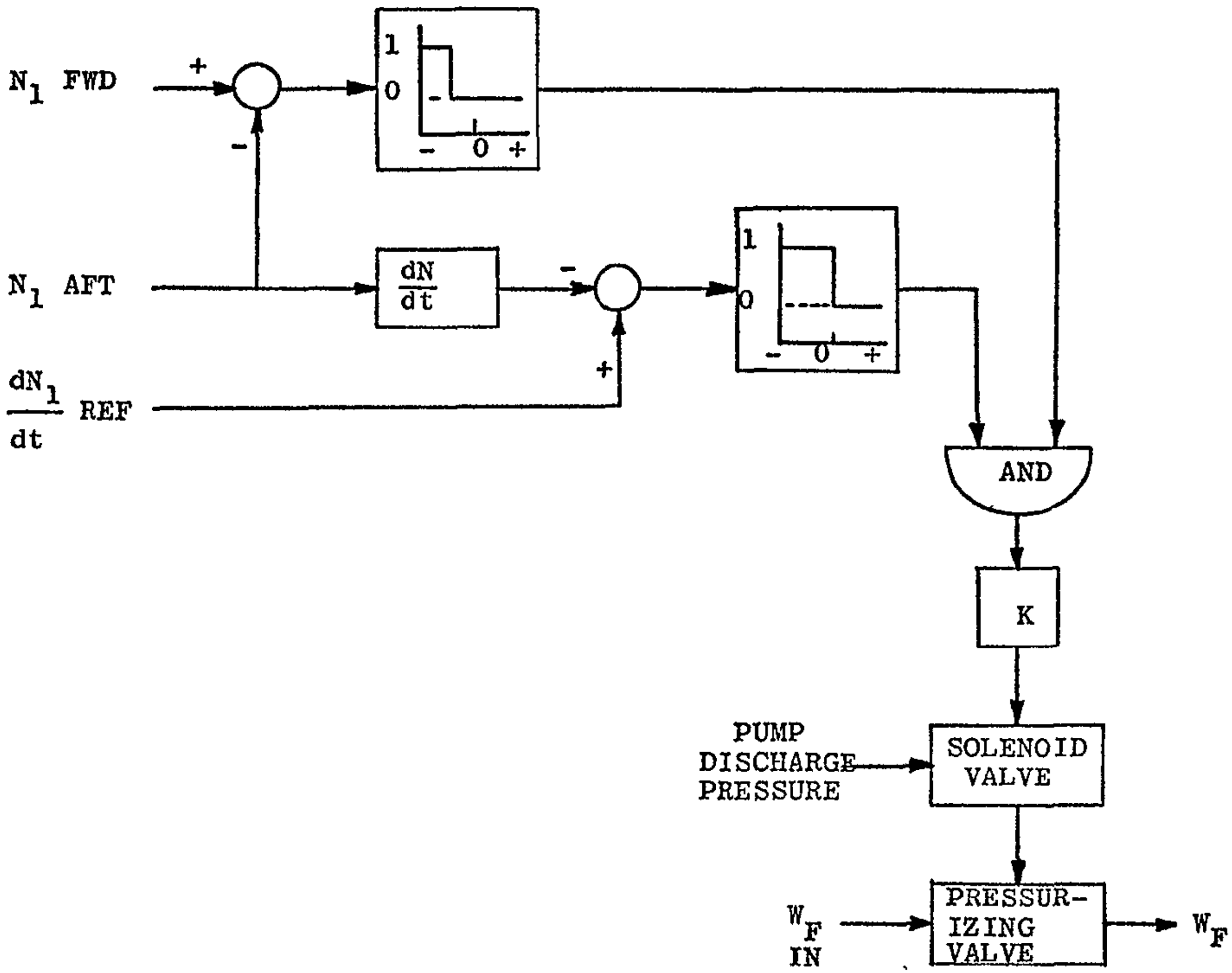

Figure II-11. Task II LPT Overspeed Shutdown System.

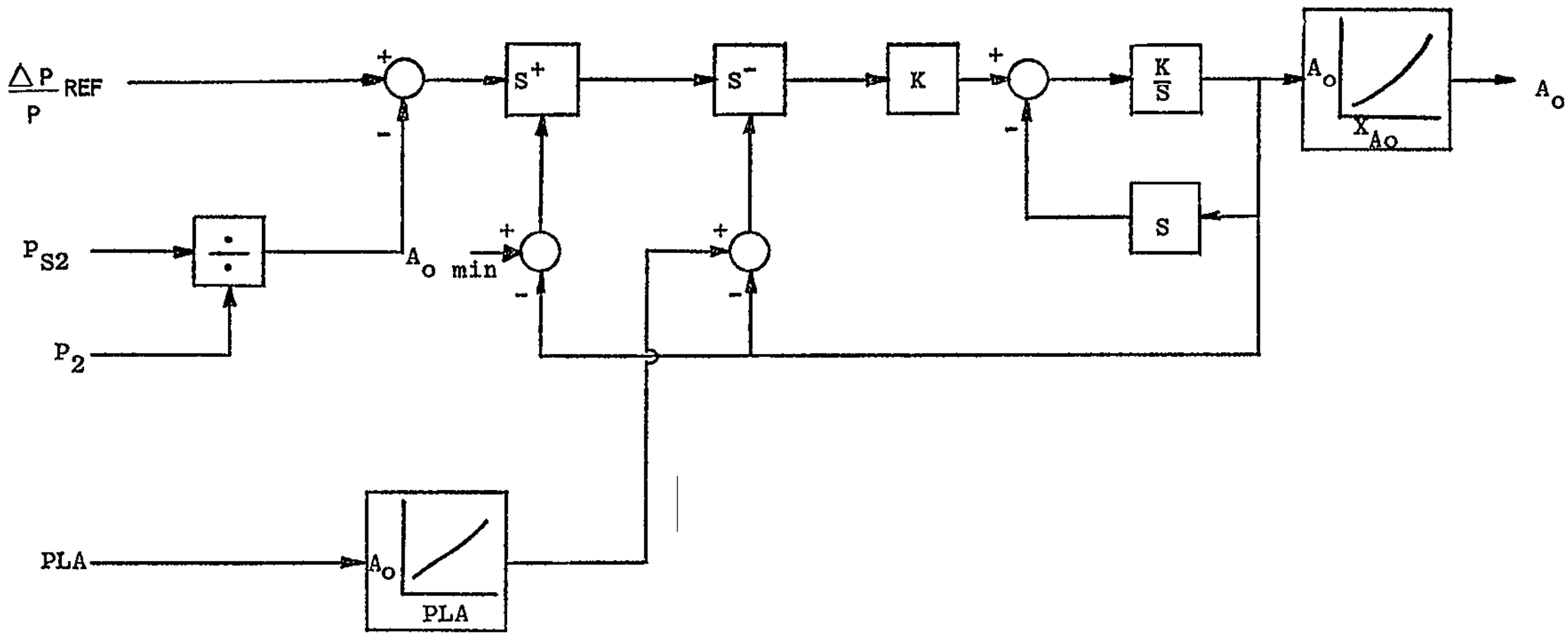

Figure II-12. Task II GE19/F9A Inlet Control System.

TRANSIENT RESPONSE

Dynamic models of the GE19/F6D, F6E, and F2C engine configurations have been simulated on the General Electric-Evendale hybrid computer. The thrust response data from the computer model are predictions for an average, uninstalled engine. Thrust response for the F9A augmentor wing engine has been estimated based on cycle and inertia comparisons with the F2C and the F101 engines.

The prime study objectives have been to assess whether these engines will meet the NASA thrust response goals for an approach wave-off and to determine how the F6D and F6E variable pitch fan engine controls should be designed. The key conclusions are:

- The GE19/F6D and F6E variable pitch fan engines will provide thrust increases faster than the F2C and F9A fixed pitch engines.
- To achieve the fast thrust increases with the variable pitch fan engine, fan speed must be maintained near 100%. Thus, approach thrust in the 50% range is achieved by scheduling variable pitch as a function of power lever. Thrust response profile and, thus, impulse to the aircraft is optimized by a control design which couples the variable pitch control to the fan rotor - using fan speed derivative to reset the variable pitch demand.
- Computer model results indicate that the currently proposed GE19 engines (both variable and fixed pitch fans) will not meet the NASA 50 to 100%

thrust response goal. However, results indicate that variable pitch engines with the above control design will meet the McDonnell Douglas goal at 0.4 second and beyond. A summary of response time results is given in Table II - 7 and Figure II - 13.

Information supplied from Ames airframe company contractors shown in Figure II - 14 and Table II - 8 indicates that response time achieved is adequate for intended STOL application. The difference between the NASA goal and current recommendations only results in a 5' (1.52 m) altitude loss on wave-off and a 15' (4.57 m) longer landing roll in reverse.

The current transient response levels as shown on Figure II - 13 use controlled T_{41} overshoot of 100° F, (55.5°C), a reasonable value. T_{41} overshoot is the incremental temperature transient above the final steady-state value which is encountered during a rapid throttle burst. The length of time is generally less than a few seconds, and design allowances are made in turbine configuration which result in no appreciable loss in life. As shown on Figures II - 15 and II - 16, improved response time for the F2C could be achieved without excessive stall margin loss by increasing Δ T overshoot or controlling to turbine temperature. Conventional control practice on existing engines dictates the use of a fixed acceleration fuel schedule which produces the characteristic turbine temperature-time relationship as shown on Figure II - 17. If desired for improved response time, fuel flow could be scheduled by turbine temperature, allowing a more rapid increase

Table II-7. Task II Response Time Summary.

STANDARD DAY - SEA LEVEL

50% ⟶ 95% MAX F_N

AVERAGE ENGINE UNINSTALLED

	RESPONSE TIME SECONDS
GOAL (NASA)	1.1
GE19/F6D	1.3
GE19/F6E	1.3
GE19/F2C	2.3/1.8*
GE19/F9A	1.9/1/5*

*TEMPERATURE LIMIT CONTROL

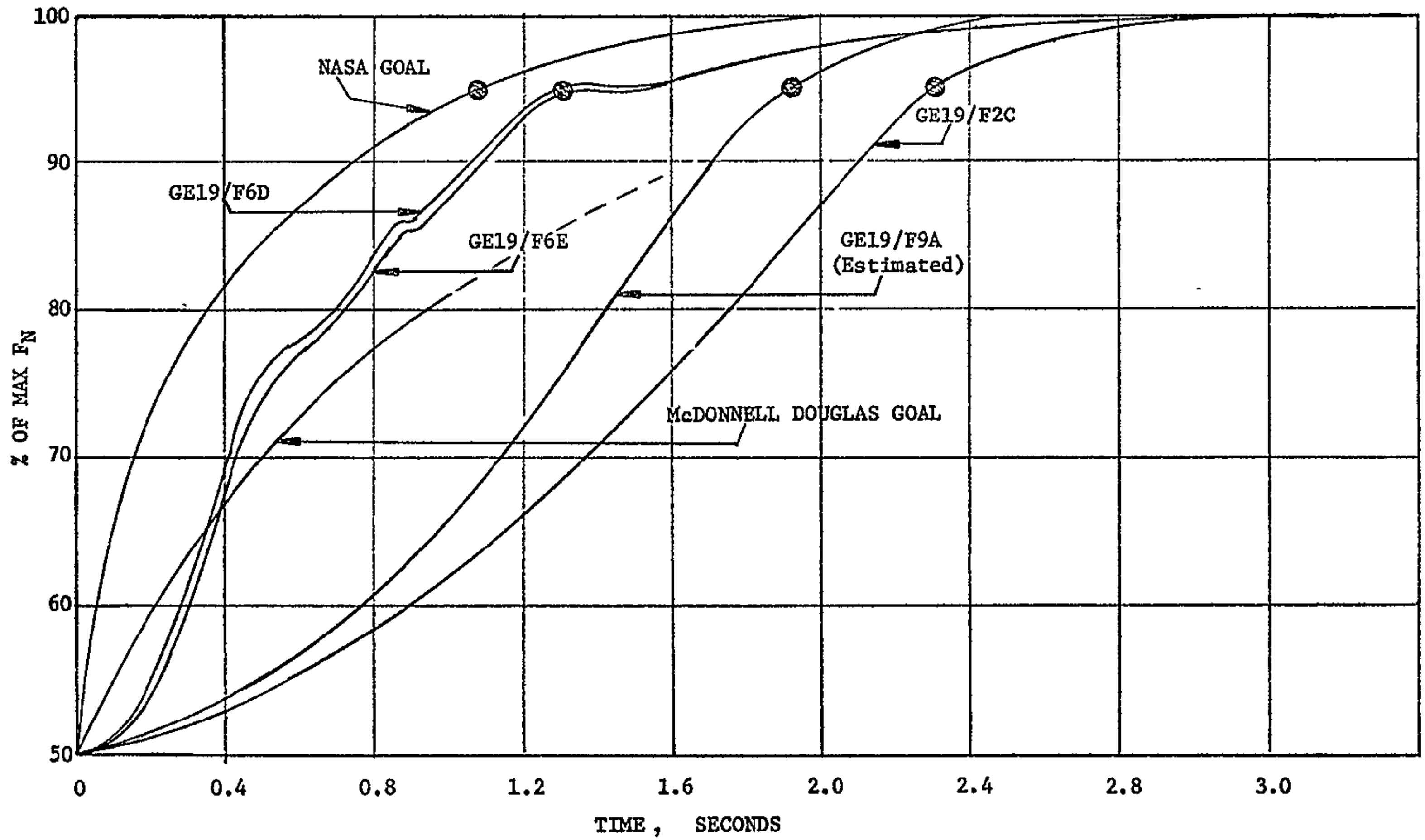

Figure II-13. Task II Transient Responce, Sea Level, 90° F, 100° F ΔT_{41} Overshoot.

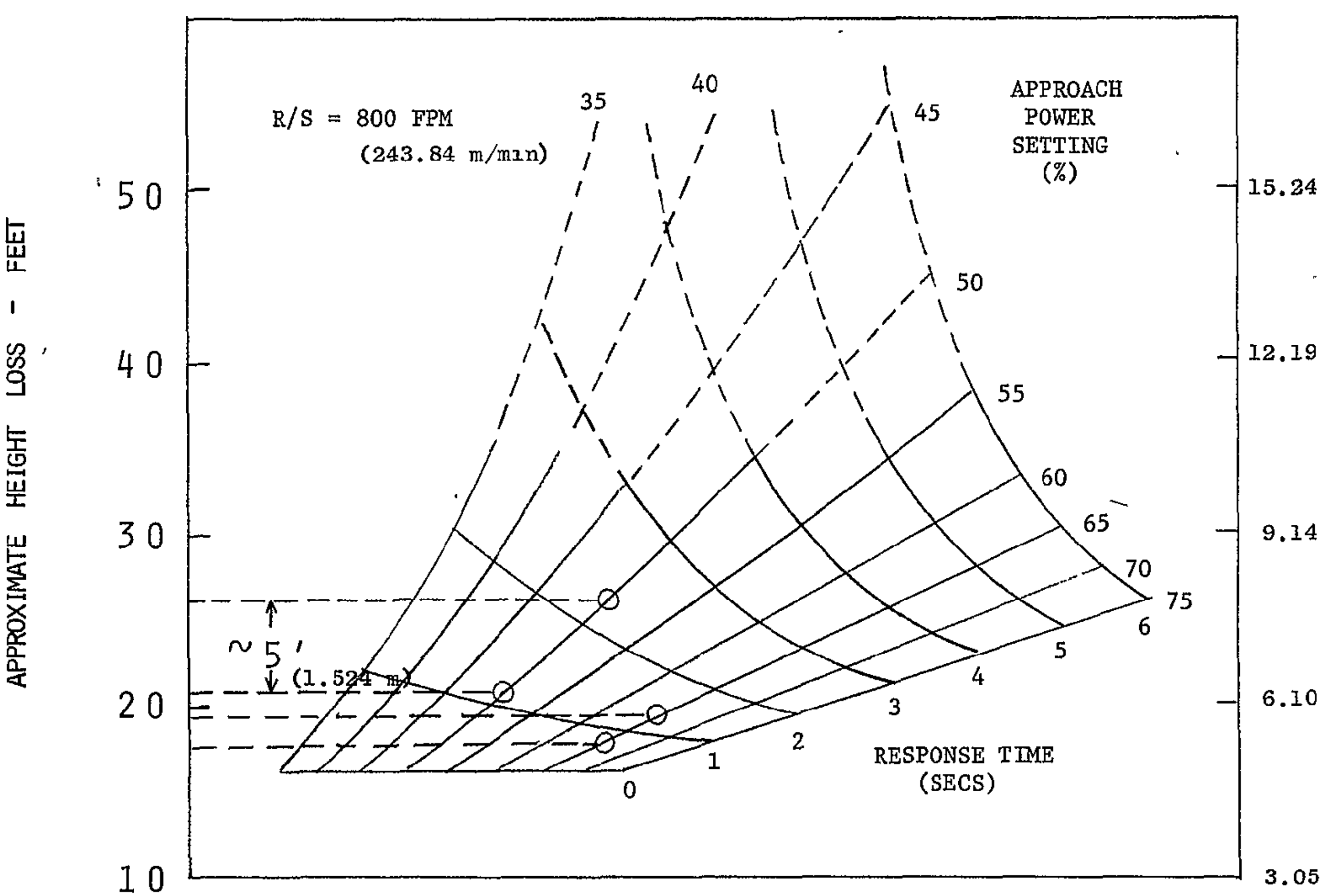

Figure II-14. Task II Effect of Response Time on Aircraft Altitude Loss for 4-Engine Go-Around Maneuver.

Table II-8. Task II Reverse Thrust Response.

- CONTROLS AND ACTUATION SIZED FOR

  <u>FIXED PITCH</u>

  1—SECOND DEPLOYMENT

  <u>VARIABLE PITCH</u>

  1—SECOND TO REVERSE PITCH

- Δ LANDING ROLL DISTANCE $\approx$ 15' (4.572 m) CORRESPONDS TO Δ.75 SECOND FP - VP ENGINE ACCELERATION TIME IN REVERSE FROM 65% F_N TO MAX F_N

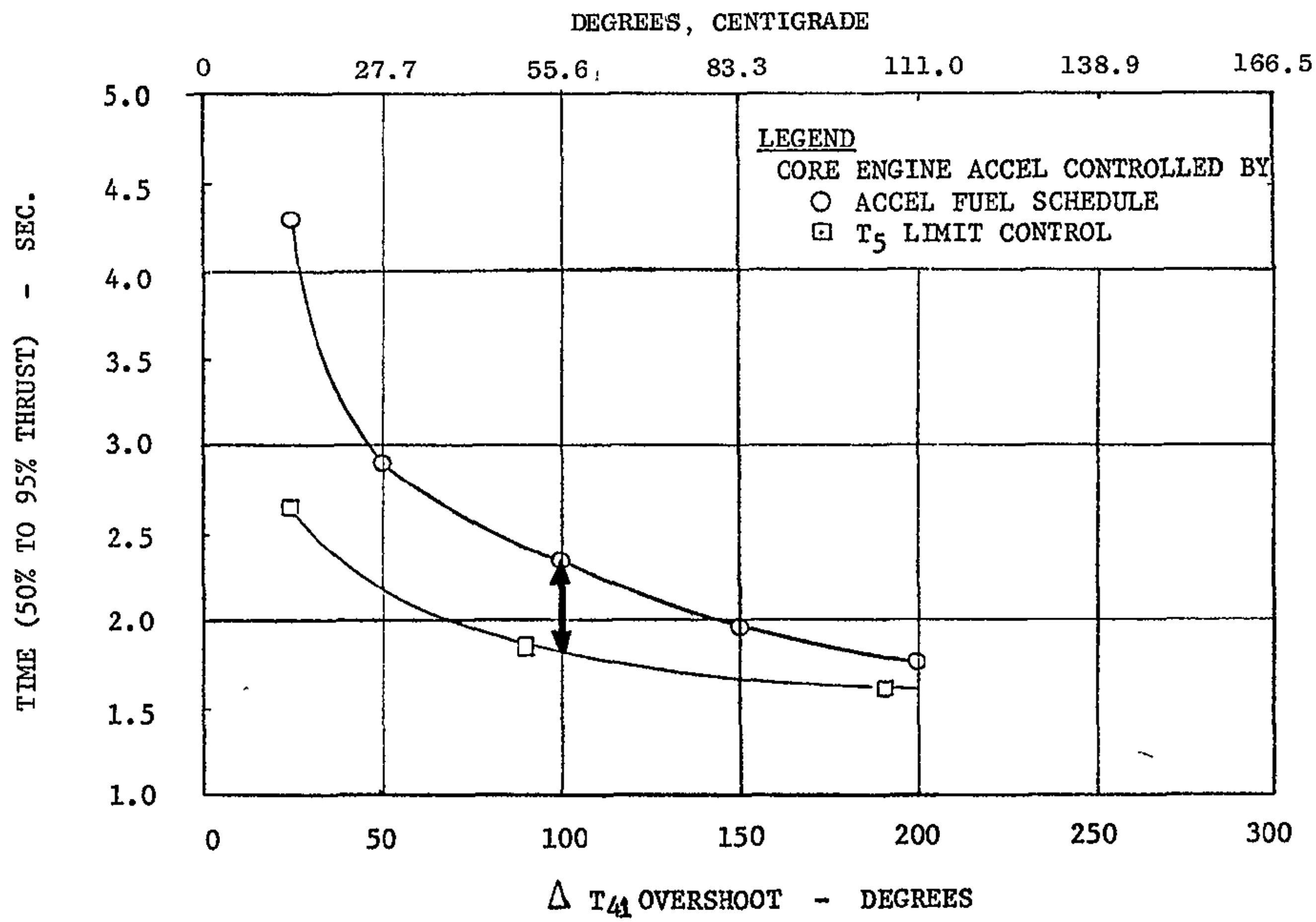

Figure II-15. Task II Effect of ΔT_{41} Overshoot on GE19/F2C Response Time (50% to 95% Thrust).

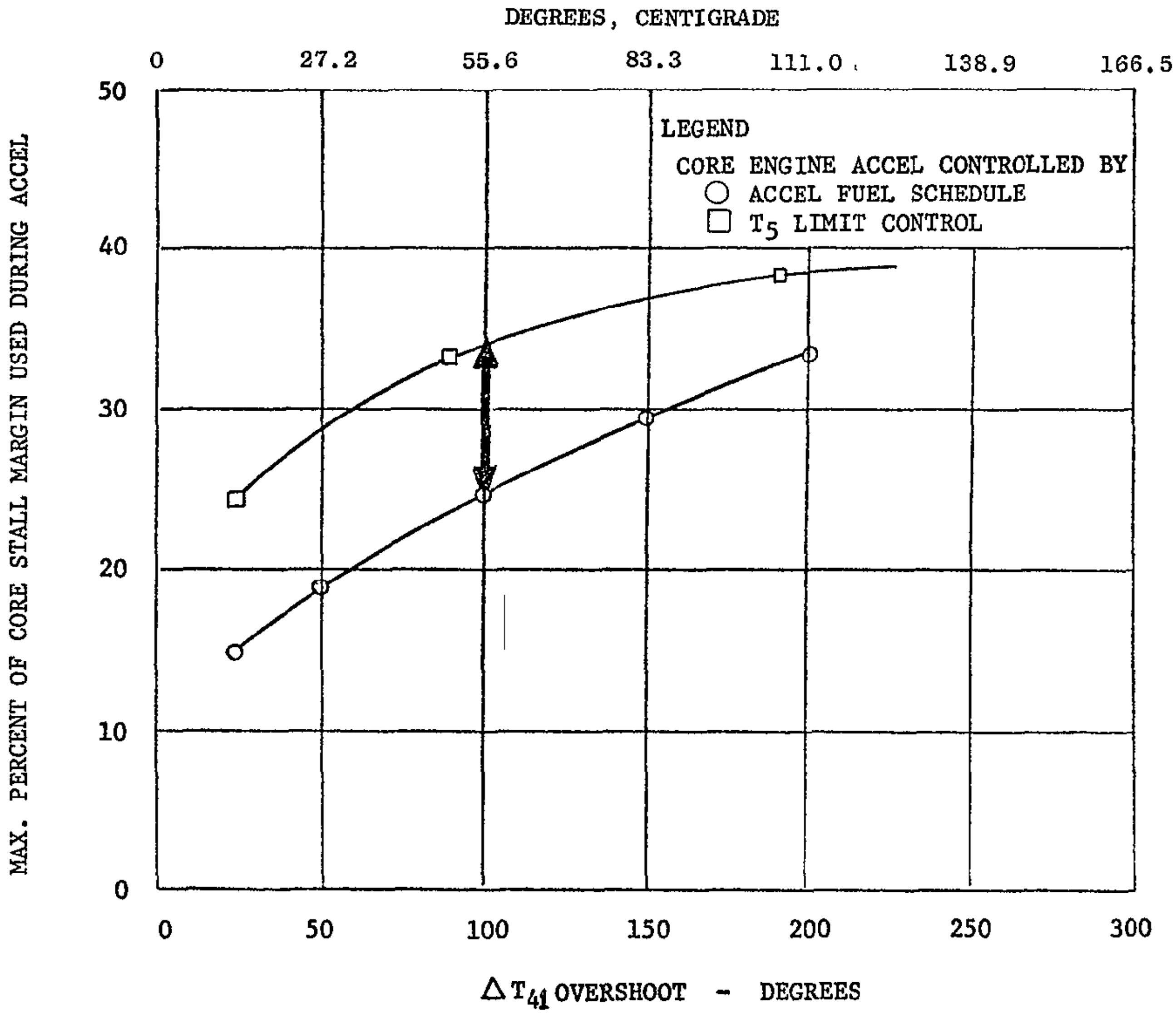

Figure II-16. Task II Effect of ΔT_{41} Overshoot on Compressor Stall Margin (50% to 95% Thrust).

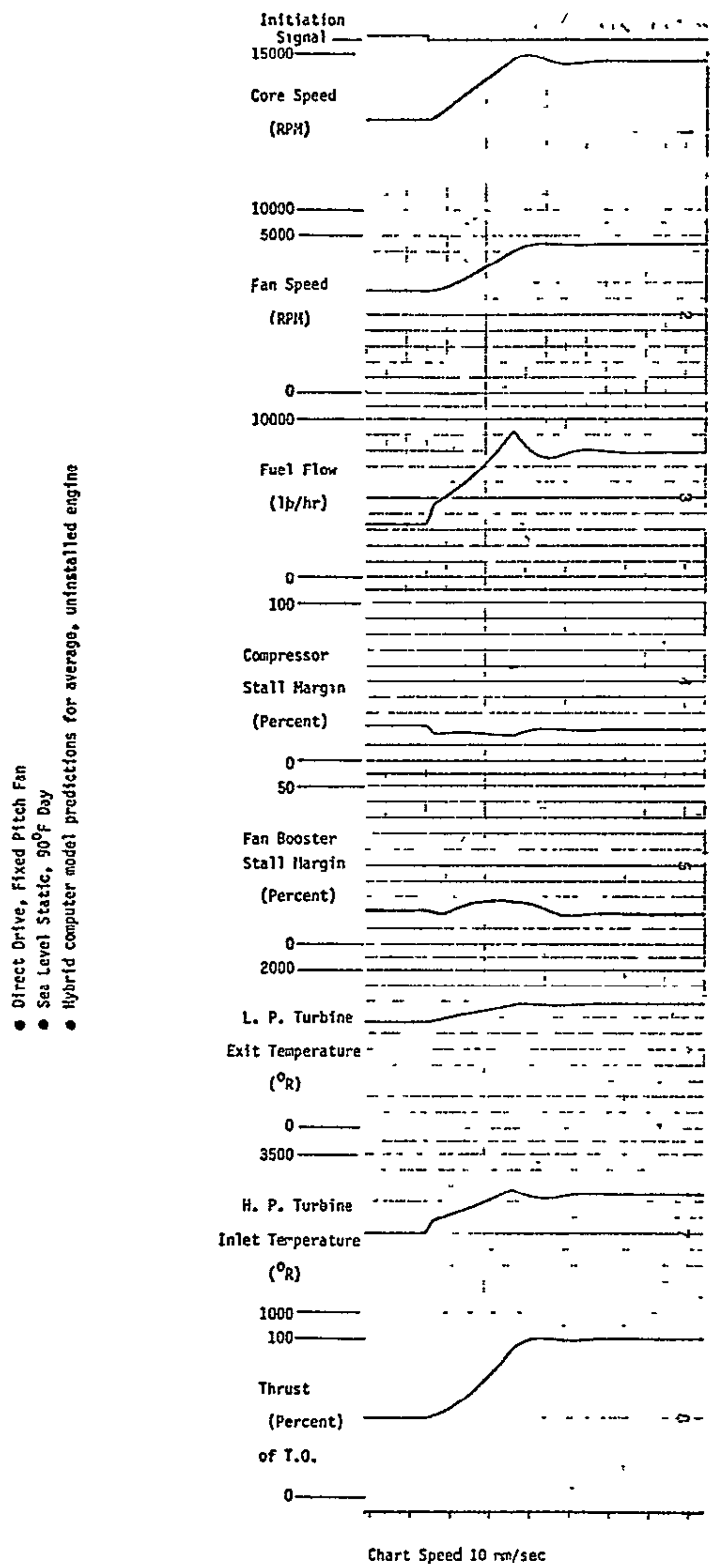

Figure II-17. Task II F2C Responce for 50% to 100% Thrust Change.

in initial fuel flow and a flatter overshoot characteristic. The lower curve on Figure II - 15 and the upper curve on Figure II - 16 represent an engine configuration with a temperature limit-control. The other two curves represent a more conventional control system. As previously stated, more study is required to confirm actual level of response required.

Transient characteristics were generated using the engine parameters shown on Table II - 9. Figures II - 17 and II - 18, give transient response of significant engine parameters.

Table II-9. Task II Engine Parameters, GE19/F6D, GE19/F6E, GE19/F2C, and GE19/F9A.

1. GE19/F6D*

   Separated Flow
   Variable Pitch, Gear-Driven Fan
   Fan Design Speed - 2800 RPM
   L.P. Turbine Design Speed - 8250 RPM
   Fan Spool Inertia - 992 LB-FT^2 (409.95 N-m^2)
   L.P. Turbine Spool Inertia - 164 LB-FT^2 (67.77 N-m^2)
   Total Inertia at Fan Shaft - 2415.8 LB-FT^2 (998.34 N-m^2)
   For Sea Level, Static, 90^{o}F (32.22°C, Uninstalled, T/O Power

2. GE19/F6E*

   Separated Flow
   Variable Pitch, Direct Driven Fan
   Fan Design Speed - 3200 RPM
   L.P. Spool Inertia - 1590 LB-FT^2 (657.08 N-m^2)
   For Sea Level, Static, 90^{o}F (32.22°C), Uninstalled T/O Power.

3. GE19/F2C*

   Mixed Flow
   Fixed Pitch, Direct Driven Fan
   Fan Design Speed - 4700 RPM
   L.P. Spool Inertia - 1565 LB-FT^2 (646.74 N-m^2)
   For Sea Level, Static, 90^{o}F (32.22°C), Uninstalled T/O Power

4. GE19/F9A*

   Separated Flow
   Fixed Pitch, Direct Driven Fan
   Fan Design Speed - 7444 RPM
   L.P. Spool Inertia - 668.1 LB-FT^2 (276.10 N-m^2)
   For Sea Level, Static, 90^{o}F (32.22°C), Uninstalled T/O Power

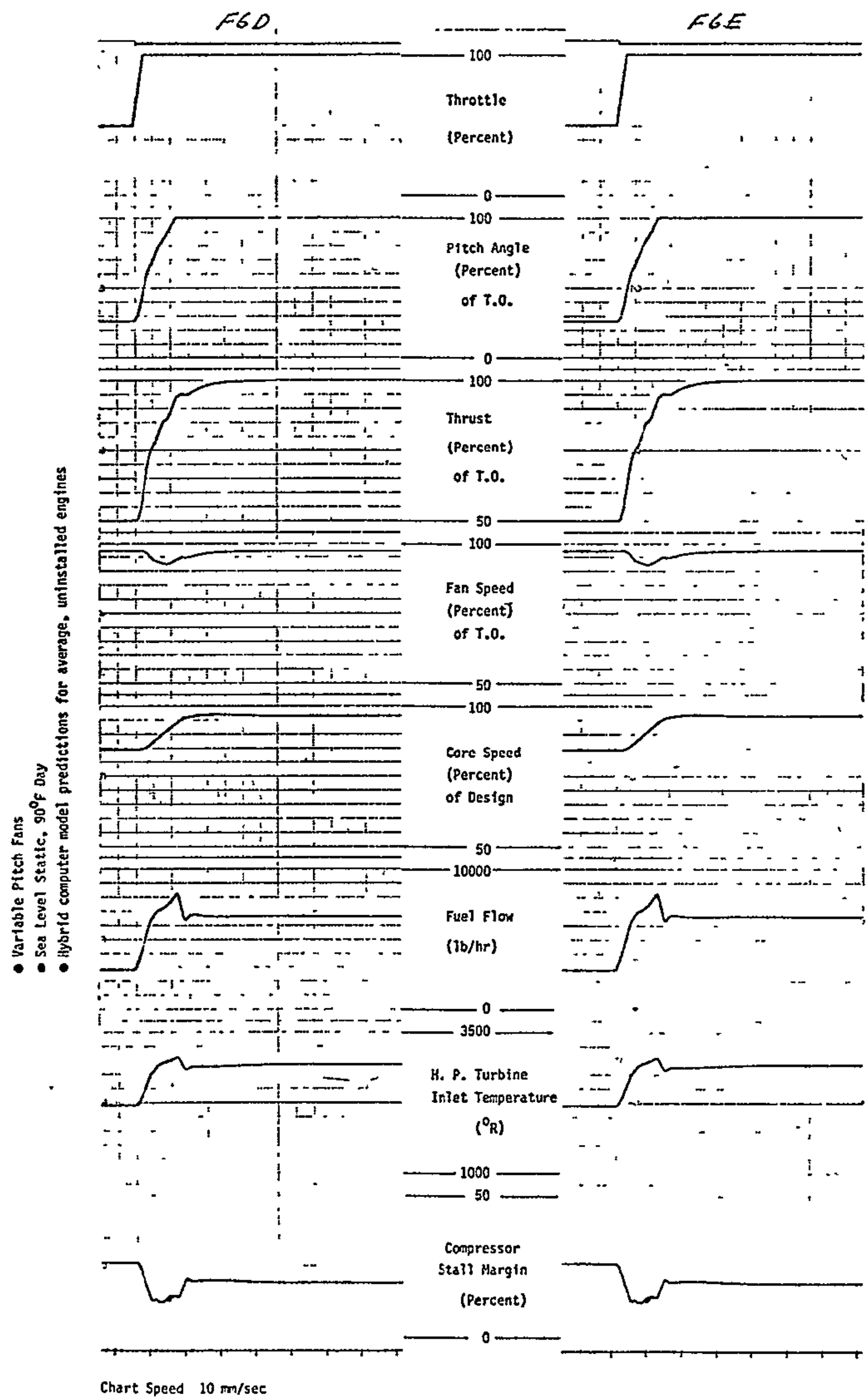

Figure II-18. Task II Transient Comparison of F6D (Gear-Driven Fan) and F6E (Direct-Drive Fan).

III - EMISSIONS

REQUIREMENTS

NASA-defined emission objectives for the four basic Task II engine cycles are given below:

	F2C	F6D	F6E	F9A
Smoke Level (SAE 1179)	15	15	15	15
T/O NO_2 (LB/1000 lbs fuel)	9	6	6	9
Idle CO (LB/1000 lbs fuel)	40	40	40	40
Idle HC (LB/1000 lbs fuel)	8	8	8	8

In addition, all engine drains are internal so that no pollutents are discharged under normal operation.

These objectives are reasonable for a 1980 time period STOL engine and could be demonstrated in the 1975 time period assuming that existing and planned technology programs proceed as anticipated.

The clean combustor which meets these goals will do so without the use of either idle bleed or water injection, except as backup designs.

Meeting the NO_x emissions goals proposed for 1980 is expected to involve significant advances in combustor design technology. Investigations conducted at General Electric have shown that significant NO_x emissions level reductions can be attained through the use of water injection into combustors. The reduced NO_x levels are due to the reduced flame temperatures that result from the injection of the water. While this approach does result in reduced NO_x emissions levels, its use does not appear to be an attractive and suitable means of obtaining the needed reductions in NO_x emissions levels, even during takeoff and climbout operations. Its use is clearly unacceptable at any other high power or cruise operating conditions. Even when limited to takeoff and climbout operations, the use of water injection in aircraft engines does involve some significant weight penalties and does require the addition of water tankage, pumping, valving and plumbing provisions to the engine. Also, the use of water injection can adversely affect the life characteristics of combustor parts due to thermal shocks and gradients resulting from the presence of the water. Further, the use of special treatment to obtain water with a low mineral content is required. Thus, the use of water injection has several significant drawbacks. Accordingly, means of reducing NO_x emissions levels by combustor design modifications, rather than by water injection, represent an important development need.

A more general approach for reducing flame temperatures and, thereby, minimizing the quantities of NO_x emissions formed in a given combustor is to minimize the quantities and residence times of combustion gas mixtures with near-stoichiometric fuel-air proportions. This general approach, which involves the difficult problems of precisely controlling the average and local fuel-air ratios within the primary combustion and dilution zones of combustors, is a potential means of reducing NO_x emissions levels by combustor design features rather than by the use of water injection. Exploratory investigations of some approaches of this kind have already been conducted at General Electric. Additional investigations are currently being conducted as a part of programs like the NASA Experimental Clean Combustor Programs. As in the case of the combustor design approaches required to provide very low CO and C_xH_y emissions levels, the implementation of approaches of this kind for reducing NO_x emissions levels is expected to involve considerably more advanced and complex combustor designs. For example, these approaches may involve the use of staged combustion processes or the use of variable geometry techniques to control the primary combustion zone fuel-air ratios by the modulation of the air flow into the primary zone. Another possible general approach is the use of modular combustor designs, comprised of many small combustor modules each equipped with fuel injection and fuel-air mixing provisions, with which staging of the combustion process may be obtained.

The final QCSEE clean combustor design is expected to evolve from these studies and programs. For the present, a weight allowance has been put into the Task II basic engine weight in anticipation of modification to the existing combustor design.

Smoke

Low smoke combustors have been demonstrated in commercial service (CF6 on DC10). All carbureting combustors under development by GE since 1966 are of the low smoke type, see Fig. III - 1. No problem is foreseen in meeting the SAE 15 smoke level objective for QCSEE.

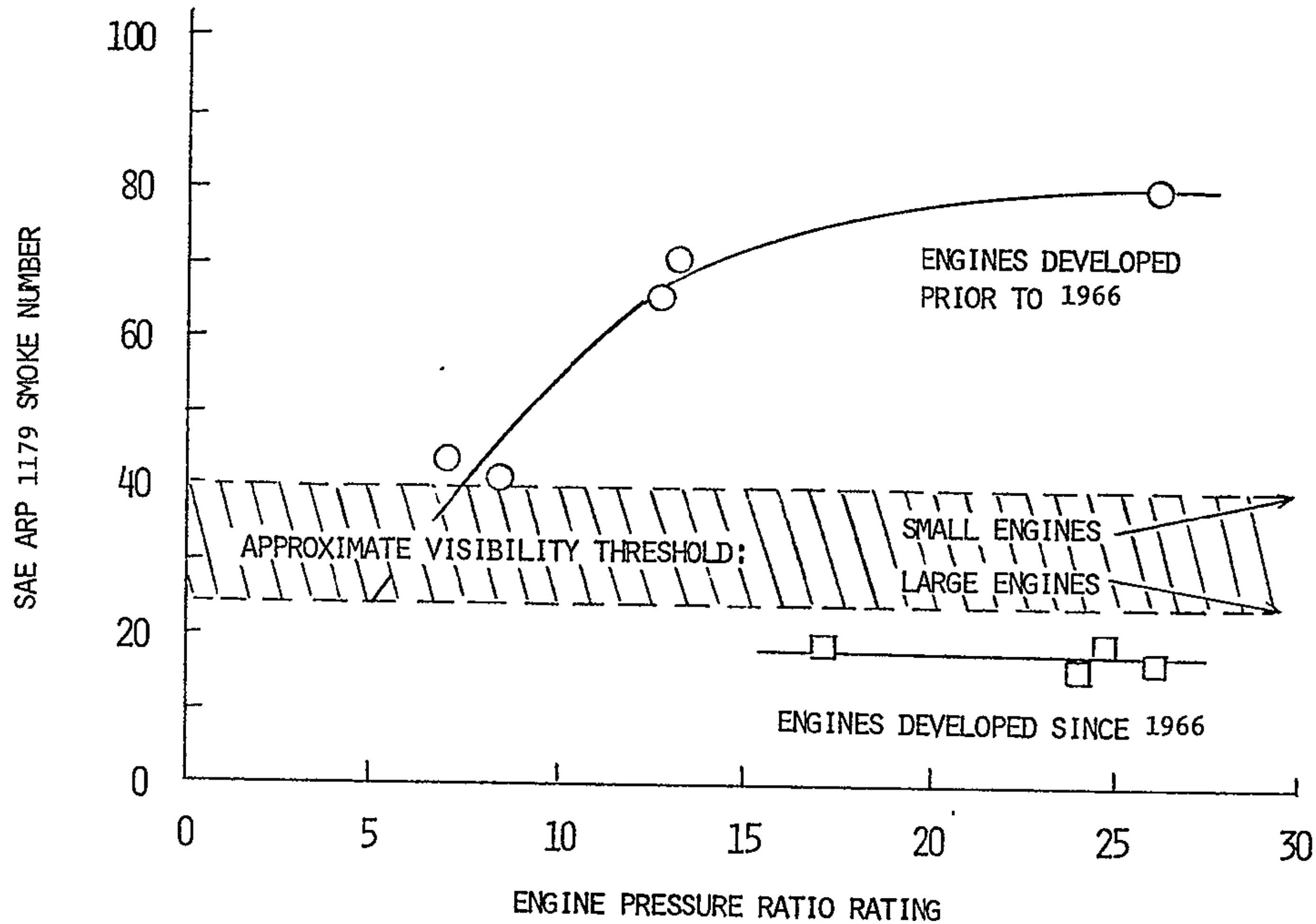

Figure III-1. Comparison of Peak Smoke Emission Characteristics.

Idle Emission (HC and CO)

High idle HC and CO emissions are caused by low engine cycle pressure ratios, which result in low combustion efficiency performance at idle, as shown in Figure III - 2. In a given engine cycle, the levels of these emissions are strongly dependent on the fuel-air ratio of the combustor primary zone. HC and CO emissions of QCSEE designs are controlled by use of fuel staging at idle, which increases local fuel-air ratio in the primary zone. One such method of reducing idle emissions in these designs is to supply fuel only to every second fuel tube, which doubles the fuel flows in the remaining tubes and provides locally higher fuel-air ratios.

NO Emissions at T/O

Combustion system design techniques are under development that have, as an objective, the reduction of NO_x emissions to acceptable levels without the need for water injection. The preferred overall approach is to operate the primary zone of the combustor with a very lean mixture (~ 0.6 ER) at full load conditions or to use fuel or air staging to accomplish the major portion of the reaction with lean mixtures. However, at light-off conditions, and for good efficiency at ground idle conditions, the burning zone must be relatively rich.

A specific combustor design has not been specified at this time, but a weight allowance has been made in the basic engine weight to cover the possibility of the combustor being heavier than the standard F101.

Design approaches to solve these problems will be investigated for the NASA Experimental Clean Combustor program.

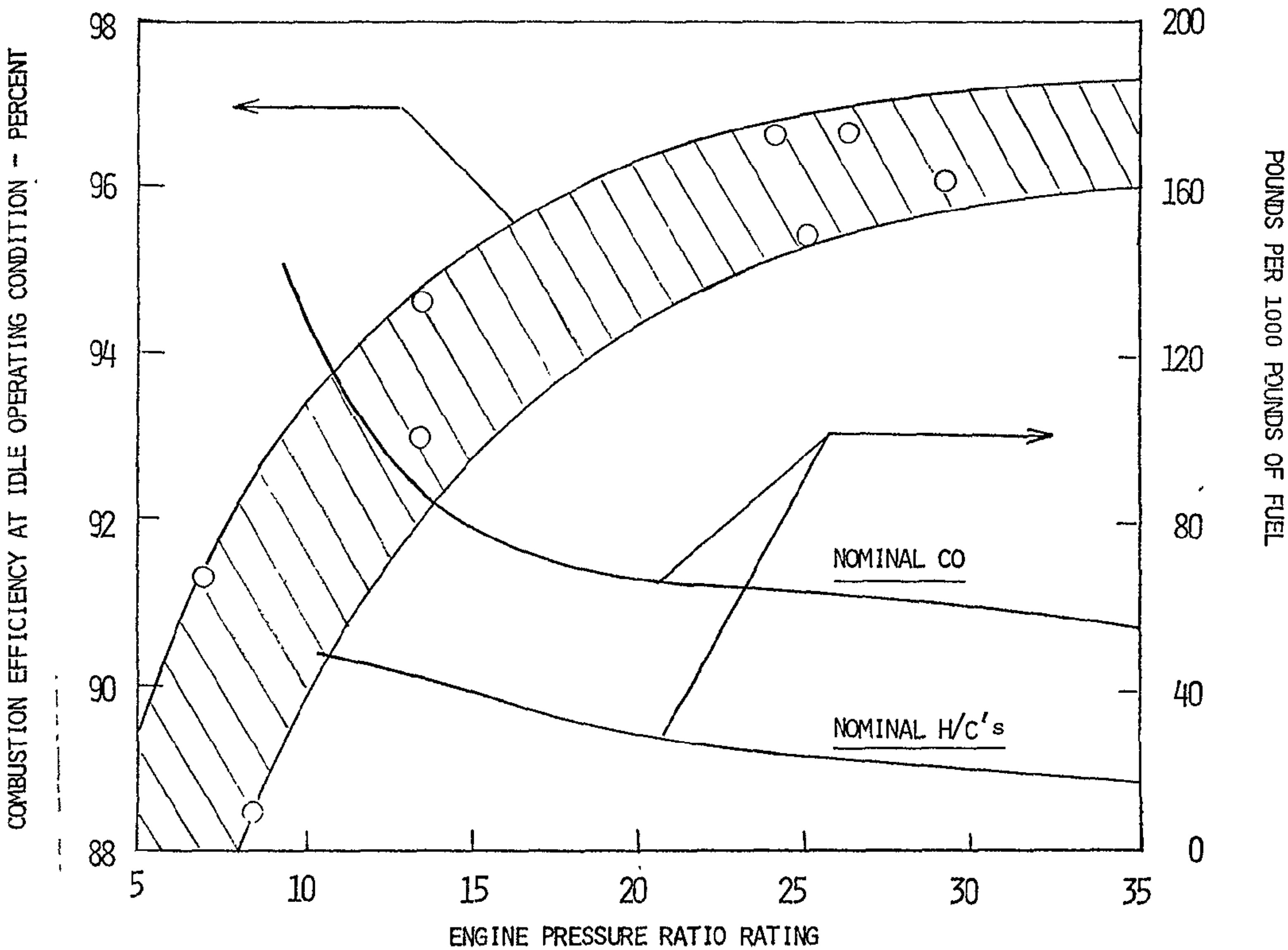

Figure III-2. Idle Combustion Efficiency Performance Trends, Existing General Electric Engines.

IV. - ACOUSTICS

SUMMARY

The objective of the acoustics study is to provide noise level estimates and to define noise reduction designs - both at the source and by nacelle suppression - necessary for the selected Task II engine systems to meet various NASA-specified noise goals in the range between 92 - 100 EPNdB at the nominal 500 ft sideline point. Seven engine systems are studied. Three of these are 1.35 fan pressure ratio EBF engines, two are 1.25 P/P variable pitch fan EBF engines, and two are 3.0 P/P two-flow augmentor wing engines.

Performance of the Task II study took approximately 11 weeks. Scope and depth of the preliminary acoustics design investigation are therefore necessarily limited. Emphasis of the effort was given to the analysis and application of the latest relevant test and design information in order to have the results reflect the latest state of the art in design and noise prediction. Comparatively less effort was spent in the development of design and calculation details which are deemed unessential at this stage of the development cycle.

Results of the study indicate that six of the seven study engines, when fully suppressed, can meet or better the specified NASA noise goals. The remaining one comes within 1 EPNdB of meeting the goal. Table IV-1 presents a summary of the suppressed engine systems noise levels in EPNdB. Takeoff, approach, and thrust reverser operation noise levels at the nominal 500 ft sideline point are included. For reference, NASA noise goal for each of the engines is also shown.

Table VI-1. Summary of Estimated Noise Levels, EPNdB.

- 500' SIDELINE
- STANDARD DAY
- 4 ENGINES

ENGINE	P/P	LIFT SYSTEM	SIDE-LINE GOAL T. O.	TAKE-OFF	APPROACH	REVERSE (70% P.S.)
F2C1	1.35	EBF, W/O DECAYER	100	100	99	99
F2C2	1.35	EBF, DECAYER	97	98	97	99
F2C3	1.35	OTW	97	97	96	96
F6D1	1.25 (GEARED)	EBF	95	95	93	99
F6E1	1.25	EBF	95	95	93	99
F9A2 *	3	AW	92	92	92	117
F9A3 *	3 (CHOKED INLET)	AW	92	89	90	117

* NOT INCLUDING WING JET NOISE

IMPORTANT FINDINGS AND CONCLUSIONS

Task II study yields the following important results and conclusions:

- 95 EPNdB (500 ft sideline) noise goal can be met by four 24,000 (106757 N) thrust 1.25 P/P variable pitch systems, either direct drive (GE19F6E1) or geared fans (GE19F6D1).

- 97 EPNdB (500 ft sideline) noise goal can be met by four 24,000 (106757 N) thrust 1.35 P/P systems when installed over-the-wing (GE19F2C3).

- 92 EPNdB (500 ft sideline) noise goal can be met by 4 14900 lb (66279 N) thrust 3.0 P/P two-flow augmenter wing engines (GE19/F9A2, A3), excluding wing jet noise.

- 1.25 P/P EBF and 1.35 OTW systems have about equal noise exposure "footprint" areas even though the sideline maximum noise levels are two EPNdB apart.

- Use of operational procedures at approach and takeoff can have substantial benefit in reducing noise exposure "footprint" areas. Further investigation of this concept is indicated.

- Inlet fan noise control, by combining high Mach fixed inlet with extended wall treatment and treated centerbody, shows considerable promise for STOL engine application.

- 1.25 P/P system without the use of inlet splitters is feasible in meeting noise goal of 95 EPNdB.

- Lift augmentation related flap noise is the most critical noise constituent. Advanced technology in this area promises the most payoff in further reducing the systems noise or in relaxing the nacelle and core suppression requirements to meet current noise goals. Early flap retraction at takeoff to minimize noise exposure area should be further investigated.

- Reverser jet noise problem without jet noise suppression is extremely serious for AW engines.

- Low frequency core noise suppression appears essential for STOL engines. Special development effort is indicated in view of the present lack of suppression design know-how for this type of noise source.

- Flow noise in the fan duct and other possible secondary noise sources cannot be accurately accounted for in the present study due to lack of comprehensive and definitive full-scale engine data. Special and continuing attention must be given to them in future development programs.

- Considering the limited scope of this study and the state of the art in noise prediction, the probable accuracy of the systems EPNdB estimates is not believed to be better than ± 3dB.

NOISE CONSTITUENT LEVELS

Tables IV-2 to IV-8 contain estimated noise constituent PNdB levels for all the study engines. Five operating conditions are considered.

Fn	A/C Speed, kts	Flap	Observer Positions
TO	0	30^{o}	500 ft sideline
TO	80	30^{o}	500 ft sideline (A/C at 200' (60.96 m) alt.)
TO	130	30^{o}	500 ft sideline (A/C at 200' (60.96 m) alt.)
72%	80	60^{o}	500 ft sideline (A/C at 500' (152.4 m) alt.)*
25%	100	35^{o}	500 ft sideline (A/C at 500' (152.4 m) alt.)*

In addition to the 500 ft sideline point data, constituent levels are also shown for an observer position directly beneath the flight path with the airplane at 500 ft (152.4 m) altitude for takeoff, 72% and 25% Fn. STOL systems noise sources are not axi-symmetric relative to the engine centerline, due mainly to the complex directivity characteristics of the flap noise. Underneath-the-airplane noise estimates are carried out in order to permit footprint area calculation. In estimating the noise levels at a point directly below the aircraft, extra ground attenuation and fuselage shielding effects are not included.

In summing the constituent PNdB levels to obtain total PNdB, consideration is given to the fact that PNdB levels do not in general add logarithmically. The approxi-

* By NASA direction

Table IV-2. GE19/F2C1 Estimated Noise Levels.

- 4 engines, 500 ft. sideline, dirt/grass ground
- Standard day, installed, Fn(80 kts) (41.16 m/sec) = 18900 lbs (84071.39 N)
- 1.35 p/p EBF w/o decayer, suppressed nacelle and core

	Max Front~60°, PNdB				Max Aft~110°, PNdB				
	Fan	Core	Jet + Flap	Total	Fan	Core	Jet + Flap	Total	EPNdB
TAKEOFF, 30° FLAP									
• 500' S.L., on the ground, static	92.3	80.3	94.5	97.3	91.5	86.3	97.5	99.4	-
• 500' S.L., after lift-off, 200' (60.96 m) Alt., 80 knots (41.16 m/sec)	95.0	83.1	97.7	100.3	94.1	89.1	100.7	102.4	100.0
• 500' S.L., after lift-off, 200' (60.96 m) Alt., 130 knots (66.88 m/sec)	95	83.1	97.7	100.3	94.1	89.1	100.7	102.4	97.9
• Directly overhead, 500' (152.4 m) Alt., 80 knots (41.16 m/sec)	98.1	85.3	105.4	106.8	97.2	91.3	108.4	109.3	106.8
APPROACH POWER, 72% F_N, 80 KNOTS (41.16 m/sec), 60° FLAP									
• 500' S.L., 500' (152.4 m) Alt., 80 knots (41.16 m/sec)	95.6	82.1	96.2	99.7	88.1	88.1	99.2	100.3	99.1
• Directly overhead, 500' (152.4 m) Alt., 80 knots (41.16 m/sec)	98.7	84.3	103.9	105.7	91.2	90.3	106.9	107.2	105.0
APPROACH POWER, 25% F_N, 100 KNOTS (51.44 m/sec) 35° FLAP									
• 500' S.L. 500' (152.4 M) Alt., 100 knots (51.44 m/sec)	89.4	83.7	nil	91.1	82.1	89.7	nil	91.0	89.0
• Directly overhead, 500' (152.4 m) Alt., 100 knots (51.44 m/sec)	92.5	85.9	nil	94.0	85.2	91.9	nil	93.4	91.1

Table IV-3. GE19/F2C2 Estimated Noise Levels.

- 4 engines, 500 ft. sideline, dirt/grass ground
- Standard day, installed, Fn(80 kts) (41.16 m/sec) = 18400 lbs (81847.28 N)
- 1.35 p/p, EBF with decayer, suppressed nacelle and core

Condition	Max Front ~60°, PNdB: Fan	Core	Jet + Flap	Total	Max Aft ~110°, PNdB: Fan	Core	Jet + Flap	Total	EPNdB
TAKEOFF, 30° FLAP									
• 500' S.L., on the ground, static	92.3	80.3	91.3	95 7	91 5	86.3	94.3	97.2	-
• 500' S.L., after lift-off, 200' (60.96 m) Alt., 80 knots (41.16 m/sec)	95.0	83.1	94.4	98.5	94.1	89.1	97.4	100.1	97.8
• 500' S.L., after lift-off, 200' (60.96 m) Alt., 130 knots (66.88 m/sec)	95.0	83.1	94.4	98.5	94.1	89.1	97.4	100.1	95.7
• Directly overhead, 500' (152.4 m) Alt., 80 knots (41.16 m/sec)	98.1	85 3	102.1	104.3	97.2	91.3	105.1	106.5	104.1
APPROACH POWER, 72% F_N, 80 KNOTS (41.16 m/sec), 60° FLAP									
• 500' (152.4 m) S.L., 500' Alt., 80 knots (41.16 m/sec)	95.6	82.1	92.1	98.0	88.1	88.1	95.1	97.2	96.9
• Directly overhead, 500' (152.4 m) Alt., 80 knots (41.16 m/sec)	98.7	84.3	99.8	103.0	91.2	90.3	102.8	103 8	101 8
APPROACH POWER, 25% F_N, 100 KNOTS (51.44 m/sec), 35° FLAP									
• 500' S.L., 500' (152.4 m) Alt., 100 knots (51.44 m/sec)	89.4	83.7	nil	91.1	82.1	89.7	nil	91.0	89.0
• Directly overhead, 500' (152.4 m) Alt., 100 knots (51.44 m/sec)	92.5	85.9	nil	94.0	85.2	91.9	nil	93.4	91.1

Table IV-4. GE19/F2C3 Estimated Noise Levels.

- 4 engines, 500 ft sideline, dirt/grass ground
- Standard day, installed, Fn 80 knots (41.16 m/sec) = 19000 lbs (84516.21 N)
- 1.35 P/P, over-the-wing, suppressed nacelle and core

Condition	Max Front ~60°, PNdB				Max Aft ~110°, PNdB				EPNdB
	Fan	Core	Jet + Flap	Total	Fan	Core	Jet + Flap	Total	
TAKEOFF, 30° FLAP									
• 500' S.L., on the ground, static	94.1	83.6	91.9	97.0	95 3	89.6	94 9	99 4	-
• 500' S.L., after lift-off, 200' (60.96 m) Alt., 80 knots (41.16 m/sec)	95.0	81. 6	93.3	98.0	93.1	87.6	96.3	99 0	96.9
• 500' S.L., after lift-off, 200' (60.96 m) Alt., 130 knots (66.88 m/sec)	95 0	81. 6	93.3	98.0	93.1	87 6	96.3	99 0	94.8
• Directly overhead, 500' (152.4 m) Alt., 80 knots (41.16 m/sec)	98 1	76. 8	98.0	101.7	87.2	82.8	101.0	101 5	99.9
APPROACH POWER, 72% F_N, 80 KNOTS (41.16 m/sec), 60° FLAP									
• 500' S.L., 500' (152.4 m) Alt., 80 knots (41.16 m/sec)	95.6	80 6	88.9	97.2	87 1	86.6	91 9	94 6	95.8
• Directly overhead, 500' (152.4 m) Alt., 80 knots (41.16 m/sec)	98 7	75.8	93 6	100.5	81.2	81.8	96.6	97 0	98.1
APPROACH POWER, 25% F_N, 100 KNOTS (51.44 m/sec), 35° FLAP									
• 500' S.L., 500' (152.4 m) Alt., 100 knots (51.44 m/sec)	89.4	80.7	nil	90.5	81.1	86.7	nil	88.4	88.2
• Directly overhead, 500' (152.4 m) Alt., 100 knots (51.44 m/sec)	92.5	75.9	nil	92.6	75.2	81.9	nil	83.4	89.0

Table IV-5. GE19/F6E1 Estimated Noise Levels.

- 4 engines, 500 ft. sideline, dirt/grass ground
- Standard day, installed, Fn (80 kts) (41.15 m/sec) = 18600 lbs (82736.5 N)
- 1.25 p/p direct drive, EBF w/o decayer, suppressed nacelle and core

	Max Front ~60°, PNdB				Max Aft ~110°, PNdB				
	Fan	Core	Jet + Flap	Total	Fan	Core	Jet + Flap	Total	EPNdB
TAKEOFF, 30° FLAP									
• 500' S.L., on the ground, static	89.9	77.6	88.0	92.9	90.7	83.6	91.0	94.9	–
• 500' S.L., after lift-off, 200' (68.96 m) Alt., 80 knots (41.16 m/sec)	92.7	80.4	91.2	95.8	93.4	86.4	94.2	97.8	95.4
• 500' S.L., after lift-off, 200' (60.96 m) Alt., 130 knots (66.88 m/sec)	92.7	80.4	91.2	95.8	93.4	86.4	94.2	97.8	93.3
• Directly overhead, 500' (152.4 m) Alt., 80 knots (41.16 m/sec)	95.8	82.6	98.9	101.4	96.5	88.6	101.9	103.8	101.3
APPROACH POWER, 55% F_N, 80 KNOTS (41.16 m/sec), 60° FLAP									
• 500' S.L., 500' (152.4 m) Alt., 80 knots (41.16 m/sec)	91.2	80.2	88.7	94.0	87.8	86.2	91.7	94.6	93.4
• Directly overhead, 500' (152.4) Alt., 80 knots (41.16 m/sec)	94.3	82.4	96.4	99.3	90.9	88.4	99.4	100.8	98.6
APPROACH POWER, 25% F_N, 100 KNOTS (51.44 m/sec), 35° FLAP									
• 500' S.L., 500' (152.4 m) Alt., 100 knots (51.44 m/sec)	91.0	80.0	nil	91.8	85.6	86.0	nil	89.5	89.4
• Directly overhead, 500' (152.4 m) Alt., 100 knots (51.44 m/sec)	94.1	82.2	nil	94.8	88.7	88.2	nil	92.1	91.6

Table IV-6. GE19/F6D1 Estimated Noise Levels.

- 4 engines, 500 ft. sideline, dirt/grass ground
- Standard day, installed Fn (80 kts) (41.16 m/sec) = 18500 lbs (82291.7 N)
- 1.25 p/p geared, EBF w/o decayer, suppressed nacelle and core

	Max Front~60°, PNdB				Max Aft~110°, PNdB				
	Fan	Core	Jet + Flap	Total	Fan	Core	Jet + Flap	Total	EPNdB
TAKEOFF, 30° FLAP									
• 500' S.L., on the ground, static	89.6	76 3	88.0	92.7	90 7	82 3	91 0	94.8	-
• 500' S.L., after lift-off, 200' (68.96 m) Alt., 80 knots (41.16 m/sec)	92.4	79.1	91.2	95.6	93.4	85.1	94 2	97 8	95.4
• 500' S.L., after lift-off, 200' (60.96 m) Alt., 130 knots (66.88 m/sec)	92.4	79.1	91.2	95.6	93.4	85.1	94.2	97 8	93.3
• Directly overhead, 500 (152.4 m) Alt., 80 knots (41.16 m/sec)	95.7	81.3	98.9	101.3	96 5	87.3	101.9	103.8	101.3
APPROACH POWER, 55% F_N, 80 KNOTS (41.16 m/sec), 60° FLAP									
• 500' S.L., 500' (152.4 m) Alt., 80 knots (41.16 m/sec)	91.0	79.6	88.7	93.9	87.8	84.6	91 7	94 4	93.2
• Directly overhead, 500' (152.4 m) Alt., 80 knots (41.16 m/sec)	94.1	80 8	96 4	99.1	90.9	86.8	99 4	100 8	98.5
APPROACH POWER, 25% F_N, 100 KNOTS (51.44 m/sec), 35° FLAP									
• 500' S.L., 500' (152.4 m) Alt., 100 knots (51.44 m/sec)	90 7	79 2	nil	91 5	85 6	85 2	nil	89.1	89.1
• Directly overhead, 500' (152.4 m) Alt., 100 knots (51.44 m/sec)	93 8	81 4	nil	94.5	88 7	87.4	nil	91.8	91.3

Table IV-7. GE19/F9A2 Estimated Noise Levels.

- 4 engines, 500 ft. sideline, dirt/grass ground
- Standard day, installed, Fn (80 kts) (41.16 m/sec) = 13000 lbs (57826.6 N)
- 3.0 p/p, 2 flow A.W., suppressed nacelle and core

	Max Front ~60°, PNdB				Max Aft ~110°, PNdB				
	Fan	Core	Jet + Flap	Total	Fan	Core	Jet + Flap	Total	EPNdB
TAKEOFF, 30° FLAP									
• 500' S.L., on the ground, static	90.5	81.5	82.8	92.3	-	87.5	88.8	91.2	-
• 500' S.L., after lift-off, 200' (68.96 m) Alt., 80 knots (41.16 m/sec)	93.2	84.3	80.6	94.5	-	90.3	86.6	91.8	92.3
• 500' S.L., after lift-off, 200' (60.96 m) Alt., 130 knots (66.88 m/sec)	93.2	84.3	74.9	94.4	-	90.3	80.9	90.8	89.9
• Directly overhead, 500' (152.4 m) Alt., 80 knots (41.16 m/sec)	96.3	86.5	82.8	97.5	-	92.5	88.8	94.0	95.1
APPROACH POWER, 55% F_N, 80 KNOTS (41.16 m/sec), 60° FLAP									
• 500' S.L., 500' (152.4 m) Alt., 80 knots	92.8	84.3	56.5	94.0	-	90.3	62.5	90.2	92.4
• Directly overhead, 500' (152.4 m) Alt., 80 knots (41.16 m/sec)	95.9	86.5	58.7	97.0	-	92.5	64.7	92.5	94.5
APPROACH POWER, 25% F_N, 100 knots (51.44 m/sec), 35° FLAP									
• 500' S.L., 500' (152.4 m) Alt., 100 knots (51.44 m/sec)	91.2	84.2	nil	92.6	-	90.2	nil	90.2	90.2
• Directly overhead, 500' (152.4 m) Alt., 100 knots (51.44 m/sec)	94.3	86.2	nil	95.5	-	92.2	nil	92.2	92.2

Table IV-8. GE19/F9A3 Estimated Noise Levels.

- 4 engines, 500 ft. sideline, dirt/grass ground
- Standard day, installed, Fn(80 kts) (41.16 m/sec)
- 3.0 p/p, 2 flow, choked inlet, A.W., suppressed nacelle and core

	Max Front~60°, PNdB				Max Aft~110°, PNdB				
	Fan	Core	Jet + Flap	Total	Fan	Core	Jet + Flap	Total	EPNdB
TAKEOFF, 30° FLAP									
• 500' S.L., on the ground, static	80.6	81.5	82.8	87.2	-	87.5	88.8	91.2	-
• 500' S.L., after lift-off, 200' (60.96 m) Alt., 80 knots (41.16 m/sec)	83.3	84.3	80.6	88.4	-	90.3	86.6	91.8	89.0
• 500' S.L., after lift-off, 200' (60.96 m) Alt., 130 knots (66.88 m/sec)	83.3	84.3	74.9	87.8	-	90.3	80.9	90.8	86.1
• Directly overhead, 500' (152.4 m) Alt., 80 knots (41.16 m/sec)	86.4	86.5	82.8	91.0	-	92.4	88.8	94.0	91.4
APPROACH POWER, 55% F_N, 80 KNOTS (41.16 m/sec), 60° FLAP									
• 500' S.L., 500' (152.4 m) Alt., 80 knots (41.16 m/sec)	88.5	84.3	56.5	90.6	-	90.3	62.5	90.3	89.6
• Directly overhead, 500' (152.4 m) Alt., 80 knots (41.16 m/sec)	91.6	86.5	58.7	93.4	-	92.5	64.7	92.5	91.5
APPROACH POWER, 25% F_N, 100 KNOTS (51.44 m/sec), 35° FLAP									
• 500' S.L., 500' (152.4 m) Alt., 100 knots (51.44 m/sec)	89.8	84.2	nil	91.5	-	90.2	nil	90.2	89.3
• Directly overhead, 500' (152.4 m) Alt., 100 knots (51.44 m/sec)	92.9	86.2	nil	94.4	-	92.2	nil	92.2	91.2

mate procedure, consistent with addition of typical dissimilar spectra (by adding an extra 0.4 - 0.8 PNdB on top of the logarithmic sum), is used.

Conversion from maximum systems noise PNdB to EPNdB for the study engines is based on an approximate generalized procedure (see Figure IV-1) which is established from detailed computer results of various typical highly suppressed engine systems where detailed spectral and directivity factors are accounted for. Tone correction for all the highly suppressed and broad band flap noise dominated Task II engines is assumed to be zero at the maximum sideline angle.

NOISE PREDICTION METHODS, GROUND RULES AND ASSUMPTIONS

This section will give a general discussion of the source noise prediction methods used in the Task II study. An exact accounting is also given on how the final constituent PNdB levels are computed, including the delta values assigned for distance attenuation, grass/soft ground correction, and fuselage shielding corrections. It is not, however, the burden of this limited design study to provide comprehensive background data and analysis to substantiate all the design practices that are used. The basic approach is adopted in this study that source noise levels shall be predicted based on applicable empirical data. Full-scale engine data are to be preferred over scale model data where a choice is available. Where empirical data are not at hand, assumptions consistent with past empirical trends and theoretical reasoning are used and stated.

A General-Electric-developed procedure is used in predicting the fan source noise. It is evolved from test data from various General Electric engines and fans

- A/C velocity = 80 knots
- For A/C Mach different from 80 knots; correct by $\Delta dB = 10 \ LOG$ (speed ratio)
- Tone correction = 0

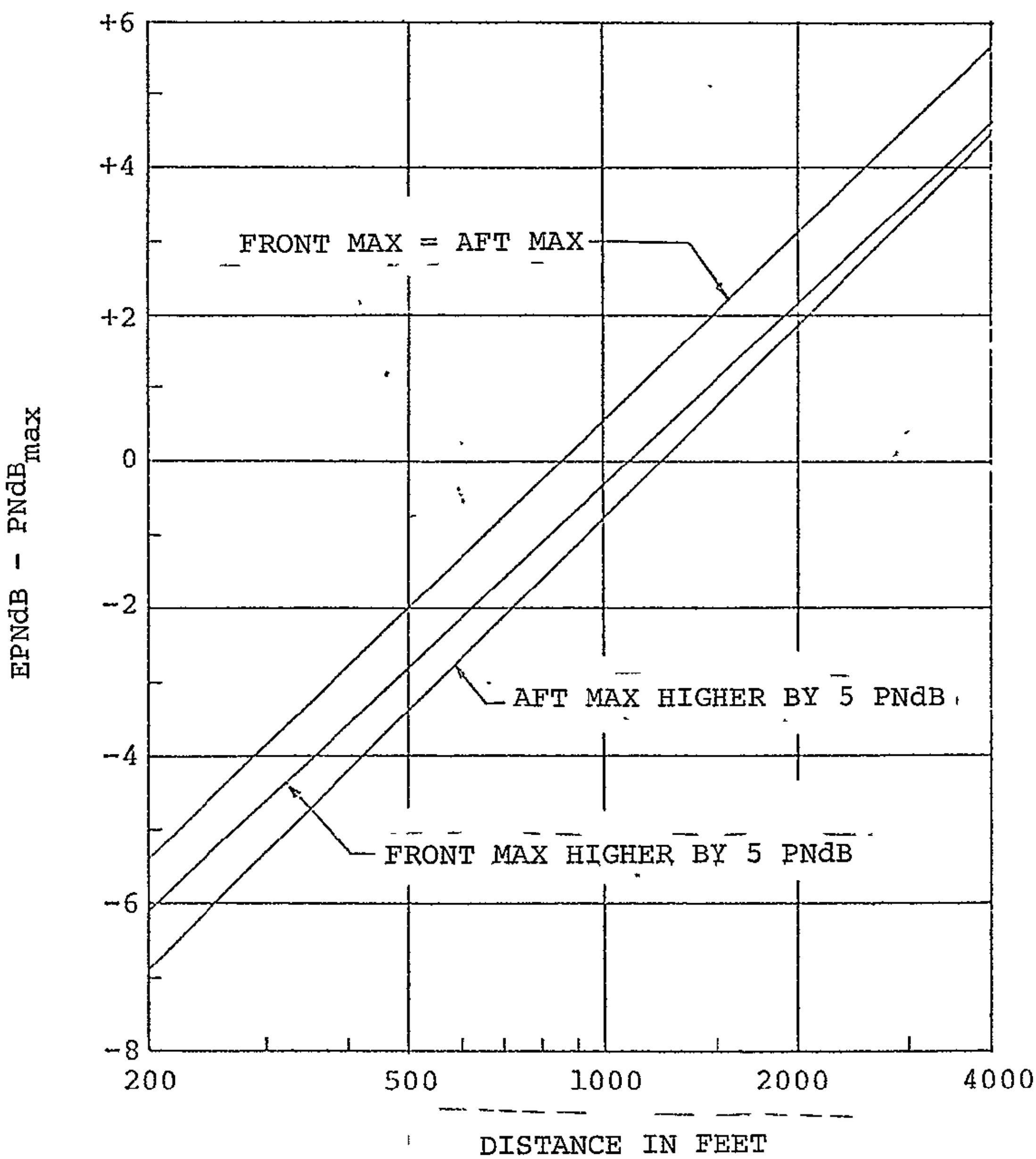

Figure IV-1. Approximate PNdB to EPNdB Conversion for Highly Suppressed Engines.

(CF6/6, CF6/50, TF34, TF39, NASA QEP fans A, B, and C). It was found that, within an accuracy of about ± 1.5 PNdB, front-radiated fan noise can best be correlated on the basis of flow and fan tip speed, and aft-radiated fan noise on the basis of flow and pressure ratio. Other important factors are blade/vane spacing, number of stages, and salient frequency characteristics. All these are taken into consideration in defining the study engine fan source level. Although test experience on low pressure low tip speed fan is limited, it was found that the procedure predicts within 1.5 PNdB the noise level of a full-scale 1.20 P/P 700 ft per second fan recently run by NASA-Lewis.

Core noise in the context of this study is taken to include both turbine noise and low frequency internally generated noise that propagates through the core exhaust. The low frequency noise source is believed to be associated with the combustion process. Core noise does not include exhaust jet noise which is taken to be generated outside the core exit plane and whose amplitude is believed to follow the classic 8th power law with velocity. Empirically, for a given set of full-scale engine noise data, low frequency core noise was arrived at simply by subtracting out the predicted jet noise from the total measured level. The low frequency core noise derived in this manner from several engines was found to correlate with the compressor discharge pressure and the temperature rise across the combustor. Figure IV-2 shows this correlation. Spectral shape of the combustion noise is taken to be broad band, similar to that of jet noise, and has a general peak in the vicinity of 200-400 Hz.

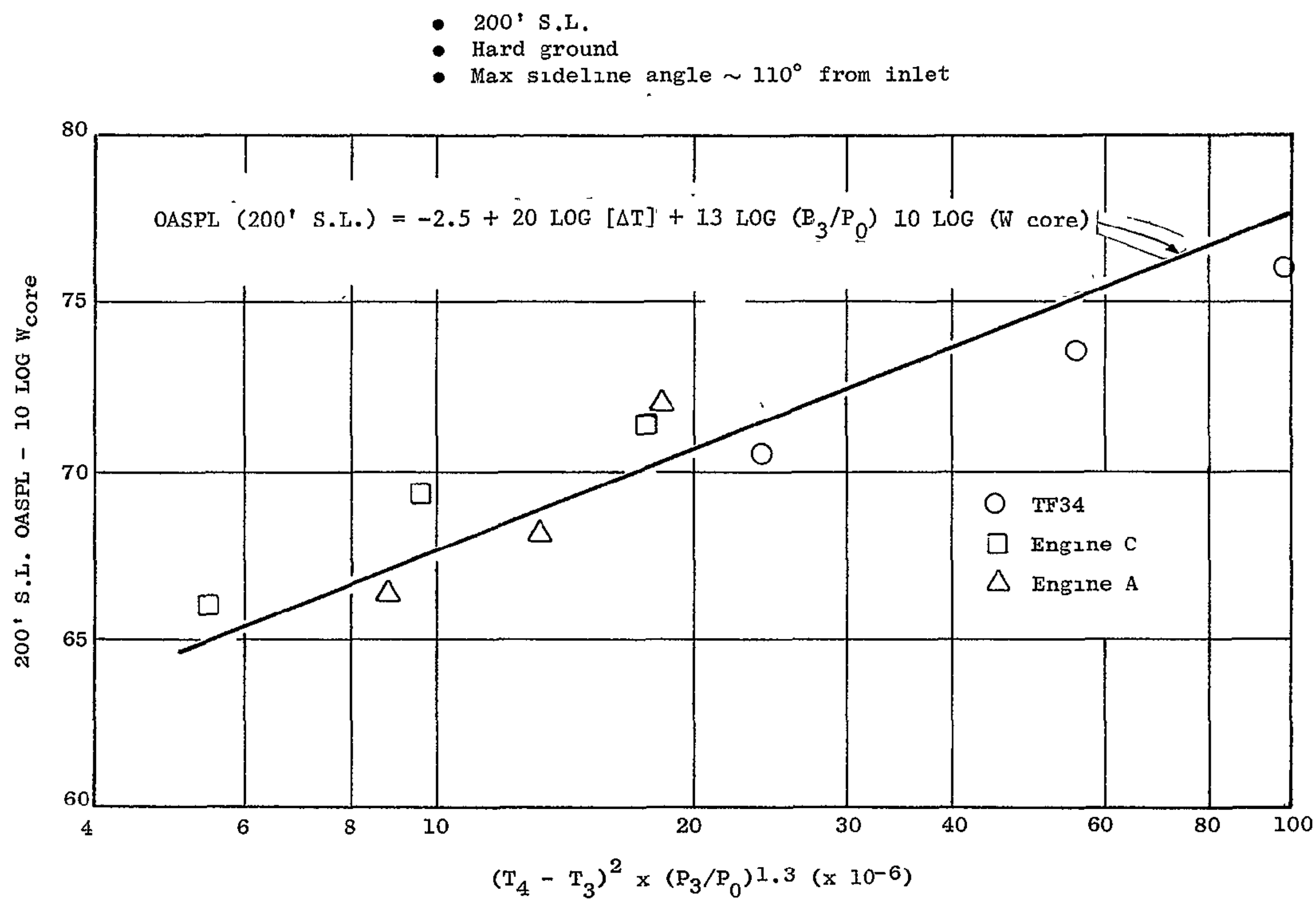

Figure IV-2. Low Frequency Core Noise Prediction Procedure.

Turbine noise is separately estimated based on the General Electric turbine noise prediction computer program. Both interaction tone noise and broad band noise are taken into consideration. Turbine noise and low frequency combustion noise are then combined spectrally to yield the PNdB constituent estimates.

Flap noise for under-the-wing EBF systems is predicted based on recent NASA-sponsored tests at Edwards, California on the TF34 and the CF700 with appropriate wing and flap arrangements. The empirical prediction curve used is shown in Figure IV-3. These test results are generally consistent with scale model test data obtained previously by NASA-Lewis. Most of the Edwards test data are obtained simulating an observer position underneath the airplane. For sideline noise estimate, an approximate view factor correction of -5.5 PNdB based on NASA-Lewis scale model test results is used. Unambiguous full-scale engine data verifying this are not available. The effect of flap angle on flap noise underneath the wing is given in Figure IV-4, based on interpretation of available data from the TF34 and scale models.

Over-the-wing scrubbing noise prediction is based on interpretation of scale model results reported recently by NASA-Lewis. It is assumed that the proposed nozzle/deflector design used in the F2C3 OTW exhaust system to achieve flow attachment will cause a noise increase of about 2 PNdB relative to the scrubbing noise without flow attachment. This assumption is not inconsistent with a very limited amount of scale model data by NASA-Lewis where the flow attachment was achieved by a simple deflector plate. It was found that, while the deflector plate

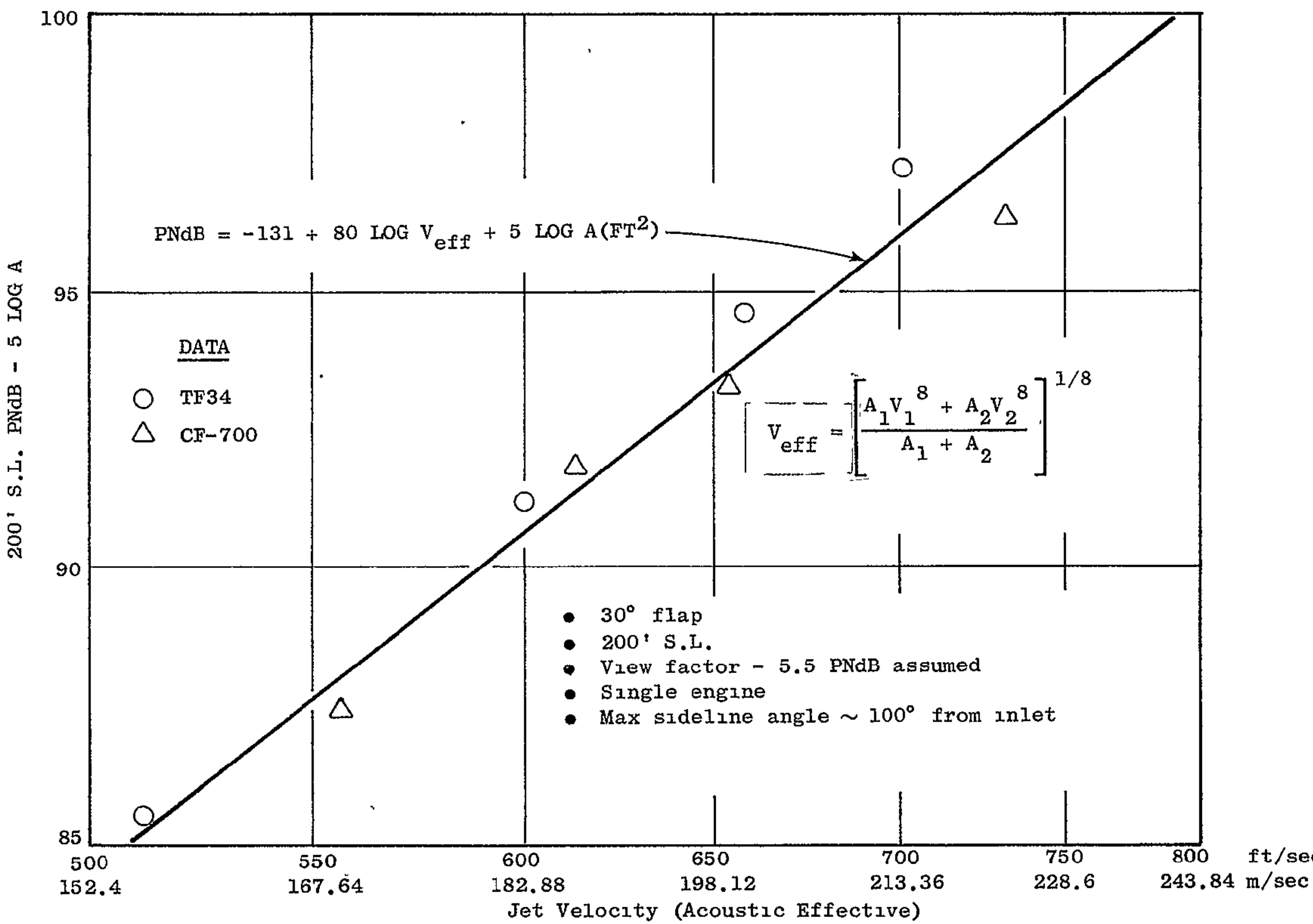

Figure IV-3. EBF Under-the-Wing Flap + Jet Noise Prediction.

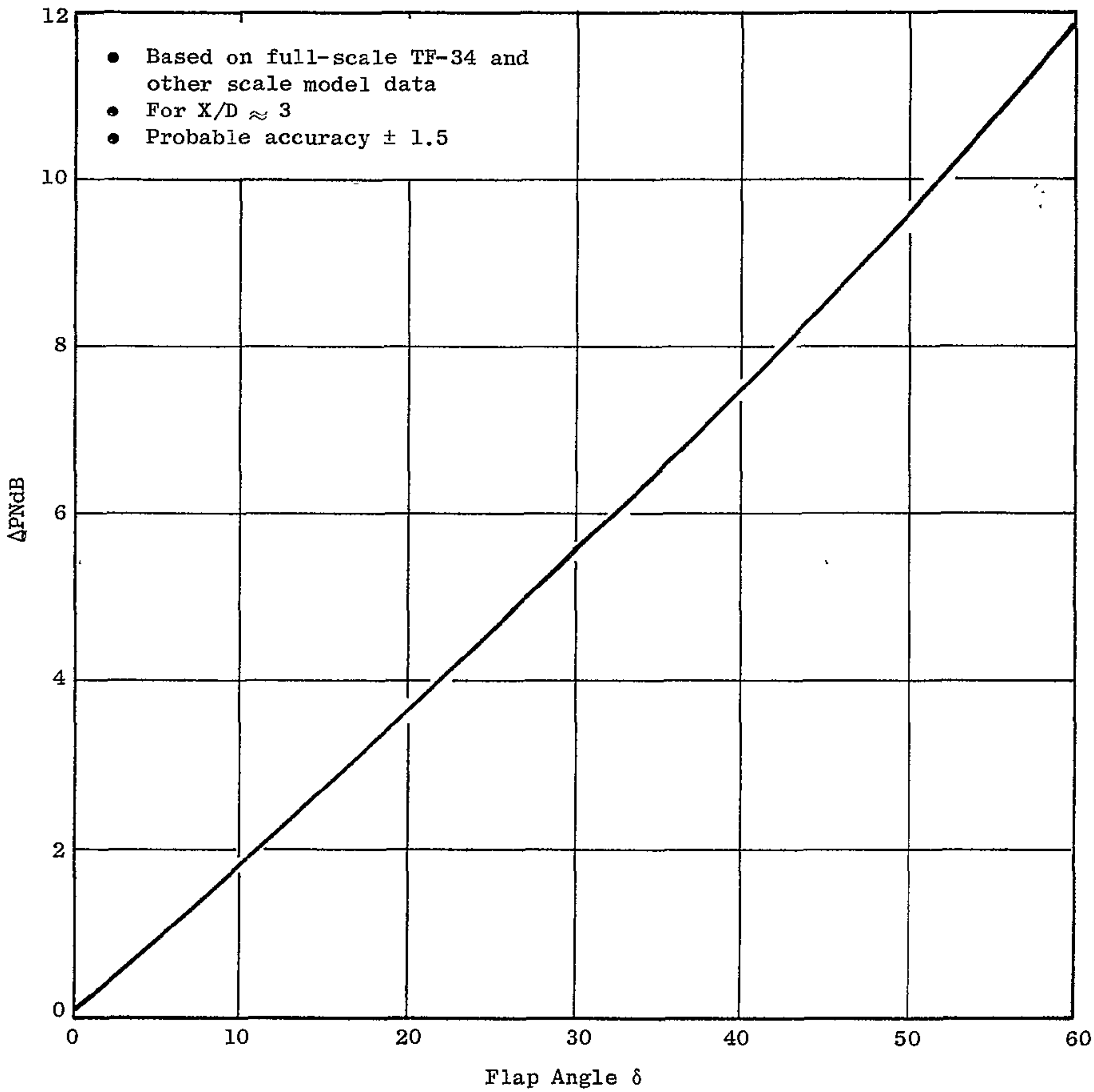

Note: Flap angle refers to the last flap, relative to horizontal.

Figure IV-4. Generalized ΔPNdB Vs. Flap Angle (Under-the-Wing).

caused a large amount of low frequency noise increase, its effect on high frequency noise and on PNdB was relatively minor. It is believed that the proposed Task II (F2C3) nozzle/deflector design is superior, noise-wise, to the simple flat deflector plate used in the NASA-Lewis experiment. The appropriate prediction curve used is shown in Figure IV-5.

Estimates of the wing shielding effects on aft-radiated fan and core noise for over-the-wing installation are based also on the interpretation of a limited amount of scale model test results reported by NASA-Lewis. These estimates must be considered as very tentative, in view of the fact that the data base is very scathy and that the exact amount of shielding must depend strongly on the actual airplane wing-fuselage geometry which is not yet defined.

For both over-the-wing and under-the-wing EBF systems, there is no separate accounting for the exhaust jet noise. Original static noise data taken in flap and jet test arrangements, upon which current estimates are based, were made up of combined flap and jet noise sources. In the present study it is assumed that there is no flight velocity effects on the combined flap and jet noise on over- and under-wing EBF systems. This assumption is probably conservative, but not unjustified, since there exists no test data supporting this phenomena operating on the flap noise.

For AW engines, jet noise from the core engine is calculated by a procedure prescribed by NASA; namely:

$$200 \text{ S. L. OASPL} = -145 + 80 \log U_R + 10 \log A$$

where U_R is relative jet velocity in feet per second and A is the exhaust nozzle area

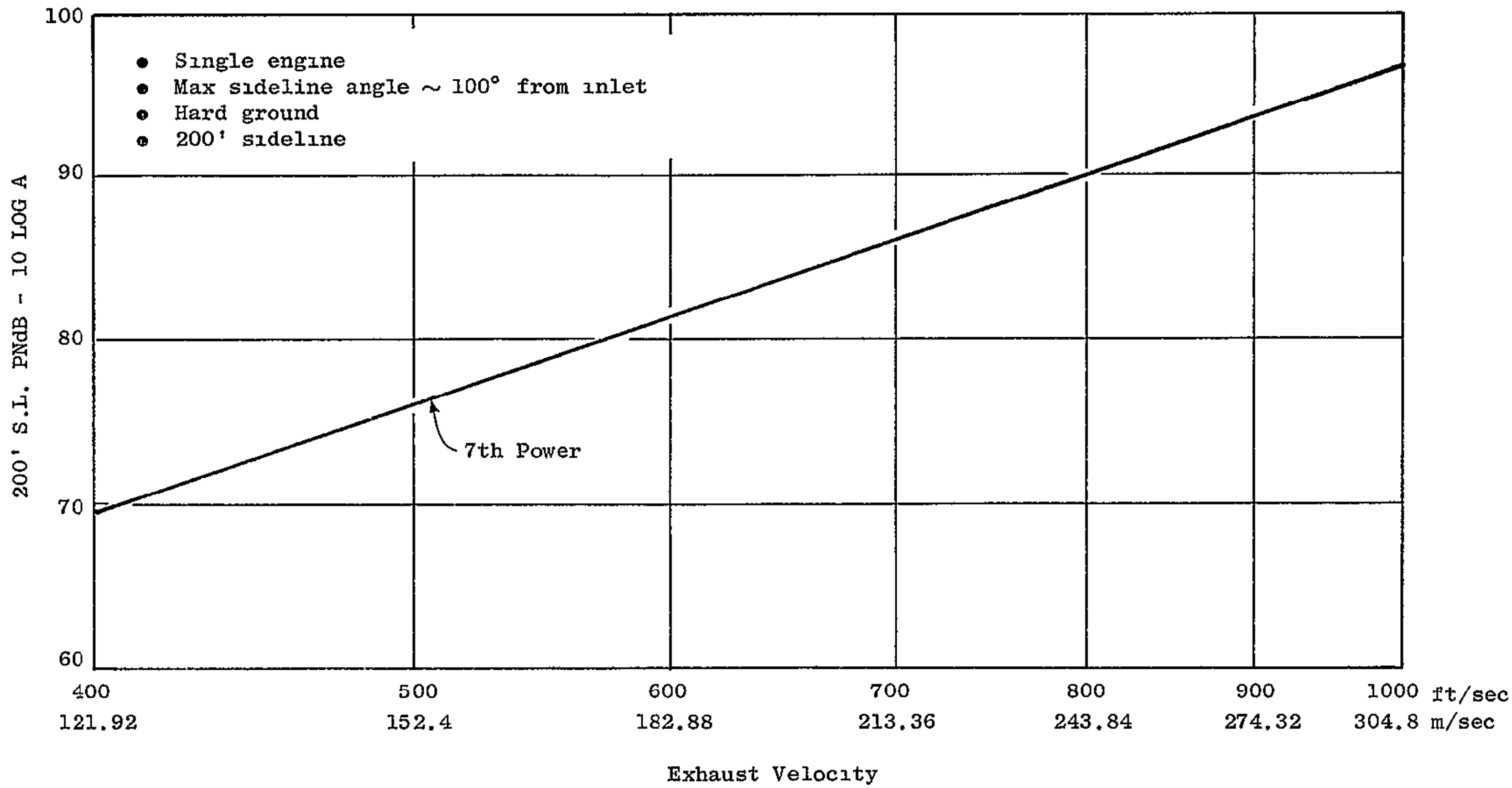

Figure IV-5. Over-The-Wing Flap + Jet Noise Estimate.

in sq ft. Conversion from OASPL to PNdB is based on a modified SAE flight spectrum shape.

In estimating the 500 ft sideline noise, extra ground attenuation, fuselage shielding and grass/soft ground effects are taken into consideration. They are estimated based on General Electric procedures that are consistent with actual flight test experience including FAA certification testing. Typical corrections are shown below:

	Delta PNdB
- Grass/soft ground	1.5 (fan), 0.5 (others)
- Extra ground attenuation [200' SL/0 altitude to 500' SL/200'(60.96 m) alt.]	1 to 2
- Fuselage shielding (20° elevation angle)	1.2

Tables IV-9 to IV-20 show an accounting of how the constituent PNdB levels are obtained. In each case, the particular source noise level in PNdB for a reference design at a reference 200' S. L. distance on hard ground is estimated using prediction procedures just described. Appropriate corrections in terms of Δ PNdB are then applied, and itemized.

These corrections included:

- distance attenuation including EGA
- number of engines
- grass/soft ground
- fuselage and/or wing shielding
- location of peak frequency and spectrum shape effects on relative PNdB (e.g. typical fan spectrum with peak at 3.2 KC band is about 2 PNdB higher than that whose peak is at 1.6 KC, assuming same OASPL for both)
- blade/vane spacing
- multistage effect
- inlet Mach number effect

To show the link between the unsuppressed and suppressed constituent levels, Tables IV-9 to IV-20 also show the amount of suppression for each constituent.

Table IV-9. Fan Inlet Noise Calculation Procedure, Static, Take-off Power.

Engine:	F2C1	F2C2	F2C3	F6D1	F6E1	F9A2	F9A3
200' S.L., reference PNdB *	121.8	121.8	121.8	111.5	115.9	117.9	117.9
Correction:							
200' to 500' S.L. Attenuation (0 Altitude)	-11.8	-11.8	-11.8	-11.5	-11.5	-12.8	-12.8
No. of Engines (4)	+ 6.0	+ 6.0	+ 6.0	+ 6.0	+ 6.0	+ 6.0	+ 6.0
Booster plus Fan/OGV Spacing	0	0	0	+ 1.0	+ 1.0	0	0
No. of Fan Stages	0	0	0	0	0	+ 2.5	+ 2.5
Blade Passing Freq. Location	0	0	0	- 2.5	- 2.5	+ 1.0	± 1.0
Wing/Fuselage Shielding	- 3.0	- 3.0	- 1.2	- 3.0	- 3.0	- 3.0	- 3.0
Dirt/Grass Ground	- 1.5	- 1.5	- 1.5	- 1.5	- 1.5	- 1.5	- 1.5
Inlet Mach No. Effects	- 6.2	- 6.2	- 6.2	- 2.2	- 4.5	- 6.0	-15.0
Unsuppressed PNdB	105.3	105.3	107.1	97.8	99.9	104.1	95.1
Acoustic Treatment Suppression	-13.0	-13.0	-13.0	- 8.2	-10.0	-13.6	-14.5
Suppressed PNdB (4 engine, 500' S.L.)	92.3	92.3	94.1	89.6	89.9	90.5	80.6

*Refers to reference design: 200' sideline hard ground single IGV-less fan, 2 chord b/v spacing, 3200 Hz BPF, fan noise only.

Table IV-10. Fan Inlet Noise Calculation Procedure, Takeoff, 80 Knots (41.16 m/sec).

Engine:	F2C1	F2C2	F2C3	F6D1	F6E1	F9A2	F9A3
200' S.L., reference PNdB*	121.8	121.8	121.8	111.5	115.9	117.9	117.9
Correction:							
200' to 500' S.L. Attenuation[200' Alt. (60.96 m)]	-10.9	-10.9	-10.9	-10.5	-10.5	-11.9	-11.9
No. of Engines (4)	+ 6.0	+ 6.0	+ 6.0	+ 6.0	+ 6.0	+ 6.0	+ 6.0
Booster plus Fan/OGV Spacing	0	0	0	+ 1.0	+ 1.0	0	0
No. of Fan Stages	0	0	0	0	0	+ 2.5	+ 2.5
Blade Passing Freq. Location	0	0	0	- 2.5	- 2.5	+ 1.0	+ 1.0
Wing/Fuselage Shielding	- 1.2	- 1.2	- 1.2	- 1.2	- 1.2	- 1.2	- 1.2
Dirt/Grass Ground	- 1.5	- 1.5	- 1.5	- 1.5	- 1.5	- 1.5	- 1.5
Inlet Mach No. Effect	- 6.2	- 6.2	- 6.2	- 2.2	- 4.5	- 6.0	-15.0
Unsuppressed PNdB	108.0	108.0	108.0	100.6	102.7	106.8	97.8
Acoustic Treatment Suppression	-13.0	-13.0	-13.0	- 8.2	-10.0	-13.6	-14.5
Suppressed PNdB (4 engine, 500' S.L.)	95.0	95.0	95.0	92.4	92.7	93.2	83.3

*Refers to reference design: 200' sideline, hard ground, single IGV-less fan, 2 chord b/v spacing, 3200 Hz BPF, fan noise only.

Table IV-11. Fan Inlet Noise Calculation Procedure, 72% Fn, 80 Knots (41.16 m/sec).

Engine:	F2C1	F2C2	F2C3	F6D1	F6E1	F9A2	F9A3
200' S.L., reference PNdB*	119.2	119.2	119.2	109.5	111.4	115.0	115.0
Correction:							
200' to 500' S.L. Attenuation [500' Alt.] (152.4 m)	-13.7	-13.7	-13.7	-13.3	-13.3	-14.7	-14.7
No. of Engines (4)	+ 6.0	+ 6.0	+ 6.0	+ 6.0	+ 6.0	+ 6.0	+ 6.0
Booster plus Fan/OGV Spacing	+ 1.0	+ 1.0	+ 1.0	+ 1.5	+ 1.5	0	0
No. of Fan Stages	0	0	0	0	0	+ 2.5	+ 2.5
Blade Passing Freq. Location	0	0	0	- 2.5	- 2.5	0	0
Wing/Fuselage Shielding	- 1.2	- 1.2	- 1.2	- 1.2	- 1.2	- 1.2	- 1.2
Dirt/Grass Ground	- 1.5	- 1.5	- 1.5	- 1.5	- 1.5	- 1.5	- 1.5
Inlet Mach No. Effect	- 1.2	- 1.2	- 1.2	0	0	0	- 6.0
Unsuppressed PNdB	108.6	108.6	108.6	98.5	100.4	106.1	100.1
Acoustic Treatment Suppression	-13.0	-13.0	-13.0	- 7.5	- 9.2	-12.3	-11.6
Suppressed PNdB (4 engine, 500' S.L.)	95.6	95.6	95.6	91.0	91.2	93.8	88.5

*Refers to reference design: 200' sideline, hard ground, single IGV-less fan, 2 chord b/v spacing, 3200 Hz, BPF, fan noise only.

** Except for F9A2 and F9A3 at 55% Fn.

ORIGINAL PAGE IS OF POOR QUALITY

Table IV-12. Fan Exhaust Noise Calculation Procedure, Static, Takeoff.

Engine:	F2C1/F2C2	F2C3	F6D1/F6E1
200' S.L., reference PNdB *	117.4	117.4	115.7
Correction:			
200' to 500' S.L., Attenuation (0 Altitude)	-12.4	-12.4	-11.5
No. of Engines (4)	+ 6.0	+ 6.0	+ 6.0
Booster	+ 0.5	+ 0.5	+ 0.5
Fan/OGV Spacing	0	0	+ 2.0
Blade Passing Freq. Location	0	0	- 3.0
Wing/Fuselage Shielding	- 3.0	- 4.2	- 3.0
Dirt/Grass Ground	- 1.5	- 1.5	- 1.5
Unsuppressed PNdB	107.0	105.8	105.2
Acoustic Treatment Suppression	-15.5	-10.5	-14.5
Suppressed PNdB (4 engine, 500' S.L.)	91.5	95.3	90.7

*Refers to reference design: 200' S.L., hard ground, single IGV-less fan, 2 chord b/v spacing, 3200 Hz BPF, fan noise only (via fan duct)

Table IV-13. Fan Exhaust Noise Calculation Procedure, Takeoff, 80 Knots (41.16 m/sec).

Engine:	F2C1/F2C2	F2C3	F6D1/F6E1
200' S.L., reference PNdB *	117.4	117.4	115.7
Correction:			
200' to 500' S.L., Attenuation [200' Alt.] (60.96 m)	-11.6	-11.6	-10.6
No. of Engines (4)	+ 6.0	+ 6.0	+ 6.0
Booster	+ 0.5	+0.5	+ 0.5
Fan/OGV Spacing	0	0	+ 2.0
Blade Passing Freq. Location	0	0	- 3.0
Wing/Fuselage Shielding	- 1.2	- 7.2	- 1.2
Dirt/Grass Ground	- 1.5	- 1.5	- 1.5
Unsuppressed PNdB	109.6	103.6	107.9
Acoustic Treatment Suppression	-15.5	-10.5	-14.5
Suppressed PNdB (4 engine, 500' S.L.)	94.1	93.1	93.4

*Refers to reference design: 200' S.L. hard ground, single IGV-less fan, 2 chord b/v spacing, fan noise only (via fan duct), 3200 Hz BPF.

Table IV-14. Fan Exhaust Noise Calculation Procedure, 72% Fn Approach, 80 Knots (41.16 m/sec).

Engine:	F2C1/F2C2	F2C3	F6D1/F6E1
200' S.L., reference PNdB *	114.2	114.2	112.4
Correction:			
200' to 500' S.L., Attenuation [500' Alt] (152.4 m)	-14.4	-14.4	-13.4
No. of Engines (4)	+ 6.0	+ 6.0	+ 6.0
Booster	+ 1.0	+ 1.0	+ 1.0
Fan/OGV Spacing	0	0	+ 2.0
Blade Passing Freq. Location	0	0	- 3.0
Wing/Fuselage Shielding	- 1.2	- 7.2	- 1.2
Dirt/Grass Ground	- 1.5	- 1.5	- 1.5
Unsuppressed PNdB	104.1	98.1	102.3
Acoustic Treatment Suppression	-16.0	-11.0	-14.5
Suppressed PNdB (4 engine, 500' S.L.)	88.1	87.1	87.8

*Refers to reference design: 200' S.L. hard ground, single IGV-less fan, 2 chord b/v spacing, 3200 Hz BPF, fan noise only (via fan duct)

Table IV-15. Core Noise Calculation Procedure, Static, Takeoff.

Engine:	F2C1/F2C2	F2C3	F6D1	F6E1	F9A2/F9A3
200' S.L. reference PNdB	103.3	103.3	99.8	101.1	104.0
Correction:					
200' to 500' S.L. Attenuation	-11.5	-11.5	-11.5	-11.5	-11.5
No. of Engines (4)	+ 6.0	+ 6.0	+ 6.0	+ 6.0	+ 6.0
Wing Fuselage Shielding	- 3.0	- 3.2	- 3.0	- 3.0	- 3.0
Dirt/Grass Ground	- .5	- .5	- .5	- .5	- .5
Unsuppressed PNdB	94.3	94.3	90.8	92.1	95.0
Suppression	- 8.0	- 4.5	- 8.5	- 8.5	- 7.5
Suppressed PNdB (4 engines, 500' S.L.)	86.3	89.6	82.3	83.6	87.5

*Aft-radiated noise level. Maximum front PNdB assumed 6 PNdB less.

Table IV-16. Core Noise Calculation Procedure, Takeoff, 80 Knots (41.16 m/sec).

Engine:	F2C1/F2C2	F2C3	F6D1	F6E1	F9A2/F9A3
200' S.L. reference PNdB	103.3	103.3	99.8	101.1	104.0
Correction:					
200' to 500' S.L. Attenuation	-10.5	-10.5	-10.5	-10.5	-10.5
No. of Engines (4)	+ 6.0	+ 6.0	+ 6.0	+ 6.0	+ 6.0
Wing Fuselage Shielding	- 1.2	- 6.2	- 1.2	- 1.2	- 1.2
Dirt/Grass Ground	- .5	- .5	- .5	- .5	- .5
Unsuppressed PNdB	97.1	92.1	93.6	94.9	97.8
Suppression	- 8.0	- 4.5	- 8.5	- 8.5	- 7.5
Suppressed PNdB (4 engine, 500' S.L.)	89.1	87.6	85.1	86.4	90.3

*Aft-radiated noise. Maximum front PNdB, assumed 6 PNdB less.

Table IV-17. Core Noise Calculation Procedure, 72% Fn, 80 Knots (41.16 m/sec).

Engine:	F2C1/F2C2	F2C3	F6D1	F6E1	F9A2/F9A3
200' S.L. reference PNdB	103.1	103.1	100.1	101.7	104.8
Correction:					
200' to 500' S.L. Attenuation	-13.3	-13.3	-13.3	-13.3	-13.3
No. of Engines (4)	+ 6.0	+ 6.0	+ 6.0	+ 6.0	+ 6.0
Wing Fuselage Shielding	- 1.2	- 6.2	- 1.2	- 1.2	- 1.2
Dirt/Grass Ground	- .5	- .5	- .5	- .5	- .5
Unsuppressed PNdB	94.1	89.1	91.1	92.7	95.8
Suppression	- 6.0	- 2.5	- 6.5	- 6.5	- 5.5
Suppressed PNdB (4 engine, 500' S.L.)	88.1	86.6	84.6	86.2	90.3

*Aft-radiated noise. Front max PNdB assumed 6 PNdB less.

** Except for F9A3 and F9A2 at 55% Fn.

Table IV-18. Flap + Jet Noise Calculation Procedure, Static, Takeoff.

Engine:	F2C1	F2C2	F2C3	F6D1	F6E1	F9A2/F9A3***
200' S.L., reference PNdB**	106.5	105.8	102.1	101.0	101.0	97.8
Corrections:						
200' to 500' S.L. attenuation	-11.5	-11.5	-11.5	-11.5	-11.5	-11.5
No. of Engines (4)	+ 6.0	+ 6.0	+ 6.0	+ 6.0	+ 6.0	+ 6.0
Peak Freq. Location	0	0	0	- 1.0	- 1.0	0
Wing/Fuselage Shielding	- 3.0	- 3.0	- 1.2	- 3.0	- 3.0	- 3.0
Decayer	0	- 2.5	0	0	0	0
Flap Angle Correction	0	0	0	0	0	0
Dirt/Grass Ground	- .5	- .5	- .5	- .5	- .5	- .5
Unsuppressed PNdB (4 engine, 500' S.L.)	97.5	94.3	94.9	91.0	91.0	88.8

*Max aft noise (~110°). Max front PNdB, 3 PNdB less.

**Reference design; 200' S.L., 30° flap, single engine.

*** No flap noise, no wing jet noise, core jet only.

Table IV-19. Flap + Jet Noise Calculation Procedure, Takeoff, 80 Knots (41.16 m/sec).

Engine:	F2C1	F2C2	F2C3	F6D1	F6E1	F9A2/F9A3***
200' S.L., reference PNdB**	106.9	106.1	102.5	101.4	101.4	92.8
Corrections:						
200' to 500' S.L. attenuation	-10.5	-10.5	-10.5	-10.5	-10.5	-10.5
No. of Engines (4)	+ 6.0	+ 6.0	+ 6.0	+ 6.0	+ 6.0	+ 6.0
Peak Freq. Location	0	0	0	- 1.0	- 1.0	0
Wing/Fuselage Shielding	- 1.2	- 1.2	- 1.2	- 1.2	- 1.2	- 1.2
Decayer	0	- 2.5	0	0	0	0
Flap Angle correction'	0	0	0	0	0	0
Dirt/Grass Ground	- .5	- .5	- .5	- .5	- .5	- .5
Unsuppressed PNdB (4 engine, 500' S.L.)	100.7	97.4	96.3	94.2	94.2	86.6

---

*Max aft noise (~110°). Front max noise, 3 PNdB less.

**Refers to reference design, 200' S.L., 30° flap.

*** No flap noise, no wing jet noise, core jet only.

Table IV-20. Flap + Jet Noise Calculation Procedure, 72% Fn Approach,** 80 Knots (41.16 m/sec).*

Engine:	F2C1	F2C2	F2C3	F6D1	F6E1	F9A2/F9A3****
200' S.L., reference PNdB***	102.2	101.0	97.9	95.7	95.7	71.5
Corrections:						
200' to 500' S.L. attenuation (500' Alt)	-13.3	-13.3	-13.3	-13.3	-13.3	-13.3
No. of Engines (4)	+ 6.0	+ 6.0	+ 6.0	+ 6.0	+ 6.0	+ 6.0
Peak Freq. Location	0	0	0	- 1.0	- 1.0	0
Wing/Fuselage Shielding	- 1.2	- 1.2	- 1.2	- 1.2	- 1.2	- 1.2
Decayer	0	- 2.9	0	0	0	0
Flap Angle correction (60° flap)	+ 6.0	+ 6.0	+ 3.0	+ 6.0	+ 6.0	0
Dirt/Grass Ground	- .5	- .5	- .5	- .5	- .5	- .5
Unsuppressed PNdB (4 engine, 500' S.L.)	99.2	95.1	91.9	91.7	91.7	62.5

*Max aft noise (~110°). Max front noise, 3 PNdB less.

**Except F9A, F9A3 at 55% Fn.

***Reference design at 200' S.L., 30° flap.

**** No flap noise, no wing jet noise, core jet only.

DESIGN APPROACHES AND FEATURES

Inlet

To avoid IGV-rotor interaction noise, all the fans will be IGV-less designs. Control of inlet-radiated fan noise is achieved by the combined means of high throat Mach number and suppression treatment. No variable geometry inlet design is required except the F9A3 which is to be a variable geometry design by NASA direction. An important design objective is to avoid or minimize the use of inlet splitters.

Recent and previous research work at NASA, Boeing, GE and elsewhere has shown that considerable inlet noise attenuation can be realized even through the throat Mach number is short of full choke condition. For fan systems of moderately high tip speed design where multiple pure tones are strong, the attenuation associated with moderately high Mach numbers is significant. Based on previous data, it is estimated that an attenuation between 4 to 6 PNdB can be obtained using the high Mach fixed inlet design.

To fully meet the noise goals, additional inlet noise reduction beyond that provided by the inlet inflow velocity effect is required. For the 1.25 P/P system (F6D1, F6E1), this is accomplished by treatment of the inlet wall surfaces, and by deployment of a treated centerbody. 9-10 PNdB suppression may be achieved by such a design. For the other EBF and AW engines with a somewhat higher level of fan inlet source noise, a single treated inlet splitter is added. A suppression of approximately 13 PNdB at takeoff power is estimated. Combined high Mach inlet and wall treatment plus a single splitter are expected to yield a total inlet noise reduction of about 18-19 PNdB.

F9A3 Choked Inlet

For the AW F9A3 engine, a translating-centerbody choked inlet design is provided. Takeoff and approach throat Mach numbers are selected at 0.92 and 0.84, respectively. Inlet wall is acoustically treated. Attenuation due to partial choke and suppression are 15 and 14.5 PNdB, respectively, at takeoff, and 6 and 11.5 PNdB, respectively, at approach. The attenuation due to partial choke is estimated based on interpretation of recent Boeing and NASA-Lewis data. Some offsetting noise effect due to inlet angle of attack being different from zero is taken into consideration in arriving at the estimated noise levels.

Blade/Vane Spacing

To minimize rotor stator interaction noise, it is desirable to set the spacing at two true rotor tip chords or greater. This design criteria is well recognized. On the other hand, some compromise must be made in the event that adherence to this criterion would lead to engine length and weight increase for certain designs. In the case of the 1.35 P/P systems (F2C1, F2C2, and F2C3), 2-chord spacing criterion was followed, and without significant adverse impact on the engine system. For the variable pitch 1.25 P/P systems, it was necessary to limit the B/V spacing to about 1.25 true chords. Although a fan source noise penalty of 2 PNdB is assigned, sufficient fan duct acoustical treatment is provided such that the fan component noise goal and the 500' S.L. systems noise goal are met.

Acoustic Treatment Design

The object of the acoustic treatment design effort was to provide the Task II engines with acoustic suppression consistent with the program goal of 92 to 100 EPNdB at 500' S.L., but also reasonable in terms of weight, cost, and performance.

Inlet suppression designs are based on the latest QEP test results. The basic procedure is to assume that wall treatment suppression scales with the ratio of treated length to fan tip diameter. Corrections are made to account for source spectrum, additional suppression due to splitters and the treated centerbody. With the additional Mach number effects taken into account, the single splitter F2C and F9A2 inlet suppression results are generally consistent with scale model Fan C results. Multiphase treatment (three design frequencies) is used on all of the designs, based on recent full-scale Quiet Engine C tests which demonstrated a significant benefit for such a desig approach. Low frequency treatment is placed nearest the fan on the outer wall to optimize the suppression of multiple pure tones. Higher frequency suppression is obtained with the two remaining phases which are also used on the splitters. Allowable splitter thicknesses served as a constraint in the selection of these frequencies. To maximize their effectiveness, similar treatments on the splitter and wall are placed directly opposite each other. Treatment on the inlet centerbody is designed to the two higher frequencies.

As in the inlet, multiphase treatment designs are also used in the fan duct exhaust to maximize the suppression. The treatment is designed by GE procedures involving determination of a suitable spectrum shape based on QEP experience, and peak suppressions with corresponding suppression bandwidths based on QEP and extensive duct testing experience. With the use of a computer program, design frequency and treatment length are optimized subject to thickness and nacelle length restrictions. Low frequency treatment is generally placed nearest to the fan with high frequency and, hence, thinner treatment making up the splitter.

Design study shows that, to meet aft suppression goals, full fan duct wall treatment plus a single long splitter is adequate for the 1.25 P/P F6D1 and F6E1 engines. 14 PNdB suppression is achieved. General dimension of the treatment design may be found in the installation drawings in Section VI. The 1.35 P/P F2C1 and F2C2 under-the-wing EBF engine fan duct suppressor designs are identical - consisting of full wall treatment plus a single splitter below the OGV section and then followed by a double splitter set (as shown in Figure VI - 1). The estimated amount of aft suppression is 16 PNdB. The F2C3 over-the-wing system requires less suppression than the F2C1/C2 engines because of the wing shielding advantage associated with over-the-wing installations. Wall treatment plus a single 45 inch (114.3 cm) long splitter is sufficient to yield the required 10 PNdB suppression. Tables IV - 21 to 26 show the details of the nacelle wall and splitter designs for the various Task II engines.

All the inlet and fan duct treatment suppressions are initially estimated using current single-degree-of-freedom peak suppression and bandwidth design curves. A modest advance in technology of 10-15% (equivalent to 1-2 PNdB) suppression effectiveness improvement is further assumed. Currently available multiple-degree-of-freedom treatment design can be used to achieve the quoted suppression without assuming advanced technology in suppression effectiveness - but at a somewhat higher cost per unit treatment area. Therefore, two approaches toward advanced technology may be taken: improve the SDOF treatment design without cost increase or lower the cost of the basic currently available MDOF designs.

It is recognized in principle that a relatively low fan duct Mach number may be necessary in order to keep the flow-related noise generation in the duct to a level substantially below the absolute suppressed fan noise. Such flow noise may have several origins: boundary layer flow over wall and splitter surfaces, wakes from support struts and pylons, surface discontinuities, and trailing edge effects associated with the fan nozzle. At the present time, no sufficient definitive test data from engine and duct testing are available to permit establishment of verifiable design criteria relating duct Mach number and the different flow related "noise floors." Task II engine fan duct Mach number design point is set at about 0.45 which is assumed to be adequate. Designing

Table IV-21. GE19/F2C1, F2C2, and F2C3 Inlet Treatment Details.

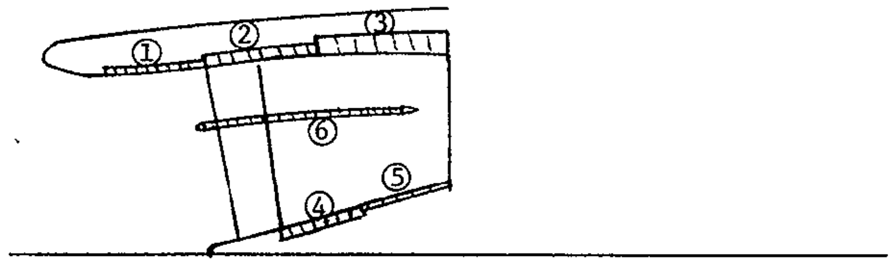

Region	Treated Length		Treated Thickness		Splitter Thickness		Design Frequency
	in.	cm	in.	cm	in.	cm	
1	20	50.8	0.3	0.756	-	-	3150
2	20	50.8	0.6	1.512	-	-	1600
3	24	60.96	2.0	5.08	-	-	800
4	15	38.1	0.6	1.512	-	-	1600
5	15	38.1	0.3	0.756	-	-	3150
6(Splitter)	32	81.28	0.3/0.6 mixed	0.756/1.512 mixed	0.9	2.286	3150/1600

Table IV-22. GE19/F6D1 and F6E1 Inlet Treatment Details.

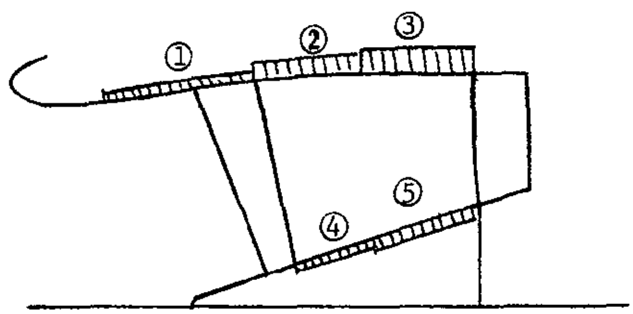

Region	Treated Length				Treated Thickness		Design Frequency
	F6D1		F6E1				
	In.	cm	In.	cm	In.	cm	
1	20	(50.8)	22	(55.9)	0.4	(1.02)	2500
2	20	(50.8)	22	(55.9)	0.7	(1.78)	1300
3	20	(50.8)	22	(55.9)	2.3	(5.84)	700
4	15	(38.1)	19	(48.3)	0.4	(1.02)	2500
5	15	(38.1)	19	(48.3)	0.7	(1.78)	1300

Table IV-23. GE19/F9A Inlet Treatment Details.

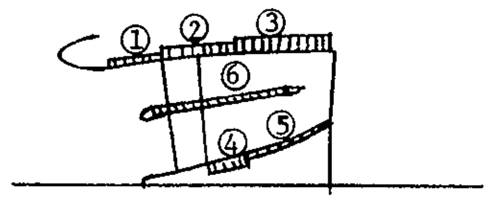

Region	Treated Length		Treatment Thickness		Splitter Thickness		Design Frequency
	In.	cm	In.	cm	In.	cm	
1	11	(27.94)	0.25	(0.635)	—	—	4000
2	14	(35.56)	0.5	(1.27)	—	—	2000
3	14	(35.56)	1.5	(3.81)	—	—	900
4	8	(20.32)	0.5	(1.27)	—	—	2000
5	14	(35.56)	0.25	(0.635)	—	—	4000
6 (Spl)	22	(55.88)	0.25/0.5 mixed	(0.635/1.27 mixed)	0.75	(1.90)	2000/4000

Table IV-24. GE19/F2C1 and F2C2 Exhaust Treatment Details.

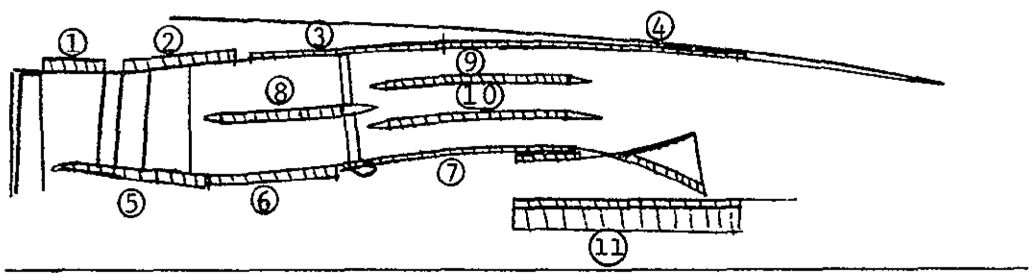

Region	Treatment Length		Treatment Thickness		Splitter Thickness		Design Frequency
	In.	cm	In.	cm	In.	cm	
1	12	(30.48)	2.2	(5.59)	-	-	1000
2	22.4	(56.9)	2.2	(5.59)	-	-	1000
3*	18.8	(47.75)	0.95	(2.41)	-	-	2500
4	69	(175.3)	0.6	(1.52)	-	-	4000
5	14.8	(37.59)	2.2	(5.59)	-	-	1000
6	25.6	(65.02)	0.95	(2.41)	-	-	2500
7	30.4	(77.21)	0.6	(1.52)	-	-	4000
8(Spl)	22.8	(57.91)	0.95	(2.41)	1.9	(4.83)	2500
9(Spl)	32	(81.28)	0.6	(1.52)	1.2	(3.05)	4000
10(Spl)	32	(81.28)	0.6	(1.52)	1.2	(3.05)	4000
11	25	(63.5)	2.5	(6.35)	-	-	300

* Reverser door

ORIGINAL PAGE IS
OF POOR QUALITY

Table IV-25. GE19/F2C3 Exhaust Treatment Details.

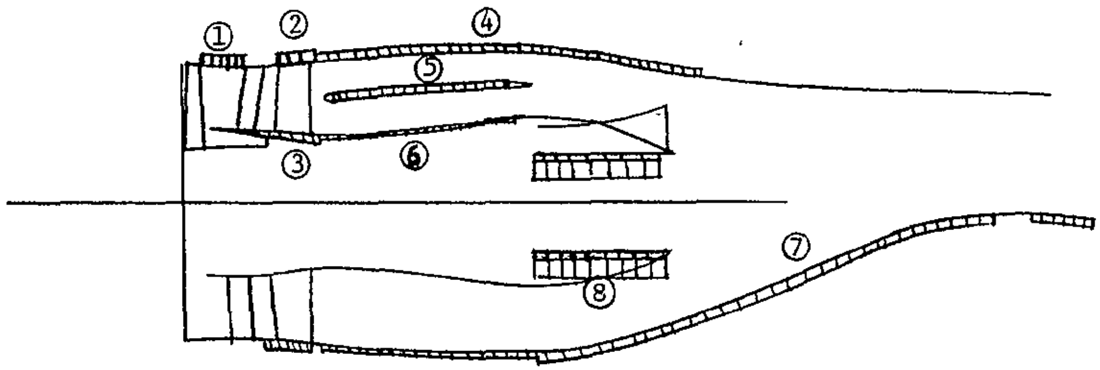

Region	Treatment Length		Treatment Thickness		Splitter Thickness		Design Frequency
	In.	cm	In.	cm	In.	cm	
1	12	(30.48)	2.0	(5.08)	-	-	1000
2	12.8	(32.51)	2.0	(5.08)	-	-	1000
3	10	(25.4)	2.0	(5.08)	-	-	1000
4	80	(203.2)	0.66	(1.68)	-	-	3150
5 (Spl)	45	(114.3)	0.66	(1.68)	1.32	(3.35)	3150
6	45	(114.3)	0.66	(1.68)	-	-	3150
7	129	(327.66)	2.0/0.66 mixed	(5.08/1.68 mixed)	-	-	1000/3150
8	15	(38.1)	2.5	(6.35)	-	-	300

Table IV-26. GE19/F6D1 and F6E1 Exhaust Treatment Details.

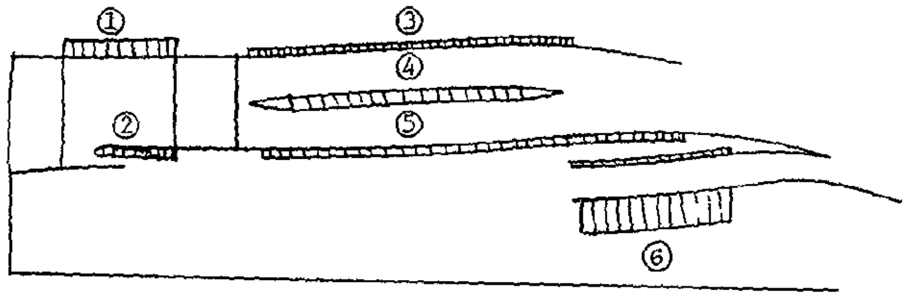

Region	Treatment Length		Treatment Thickness		Splitter Thickness		Design Frequency
	In.	cm	In.	cm	In.	cm	
1	22	(55.88)	2.4	(6.1)	-	-	800
2	15	(38.1)	2.4	(6.1)	-	-	800
3	71	(180.3)	1.25	(3.18)	-	-	2000
4(Spl)	40	(101.6)	1.25	(3.18)	2.5	(6.35)	2000
5	71	(180.3)	1.25	(3.18)	-	-	2000
6	30	(76.2)	2.5	(6.35)	-	-	300

for a rotor-stator set to have a lower exit Mach number and then diffusing the flow to an even lower Mach number than 0.45 by area and length increase is fully recognized. Such drastic design commitment with all the attendant disadvantages at a time before definitive design data become available is deemed to be premature. Clearly, considerable additional development effort and design refinement in this area is indicated.

Core Noise Control

Two approaches are taken to control the core noise. Blade row interaction pure tone noise from the turbine for all the study engines is kept low by deliberately selecting high blade numbers such that the tones are located in the inaudible or near-inaudible frequency range. Selection of high turbine blade numbers, fortunately, is also consistent with aeromechanical design criteria.

Remaining high frequency broad band noise from the turbine and low frequency combustion related noise are suppressed by acoustical treatment of the core exhaust duct passage. Treatment on the center plug consists of two "stacked" layers. The outer layer is thin and tuned to higher frequency turbine noise. The inner thick layer aims at the suppression of low frequency combustion noise. Thick treatment design is tuned to frequencies as low as 400 Hz, and is based on extrapolation of design practices applicable to fan duct treatment. The technology of low frequency suppression of engine core noise is extremely limited. The current proposed design must be considered as tentative. Special development effort in this area is needed in any follow-on experimental engine program.

THRUST REVERSER NOISE

Operation of the thrust reverser during landing is expected to significantly increase the noise level for a relatively short time duration. Based on NASA-Lewis scale model reverser (target type) data and a limited amount of CF6-6 data, jet noise at reverse is assumed to be 10 PNdB higher than that at normal operation for the same power setting. This amount of increase should be considered as approximate since acoustics information on cascade type reversers is very limited.

During reverser operation, flap noise which is a major noise constituent at takeoff is eliminated. On the other hand, the aft fan noise level is raised since that part of the duct/splitter treatment located downstream of the thrust reverser is essentially inactive so far as suppression is concerned.

For the variable pitch fan operating at reverse mode, inlet flow to the fan will be extremely distorted and turbulent. The associated increase in fan source noise is assumed to be 4.5 PNdB.

Using the above ground rules, the systems noise EPNdB for the several study engines is estimated for several power settings, and the results are presented in Figure IV-6. The augmenter wing engines as a group have 500' S.L. noise level far in excess of the 95 EPNdB goal. This is primarily due to the high fan pressure ratio implicit to the AW engine cycle, and the high level of resulting jet noise. The need toward control of the reverser jet noise on AW engines is clearly indicated. Relocating the reverser to the pylon area and having the exhaust jet issuing from a well-defined nozzle or jet suppressor arrangement (instead of the extra jet noise producing cascade reverser at the engine) may be one approach.

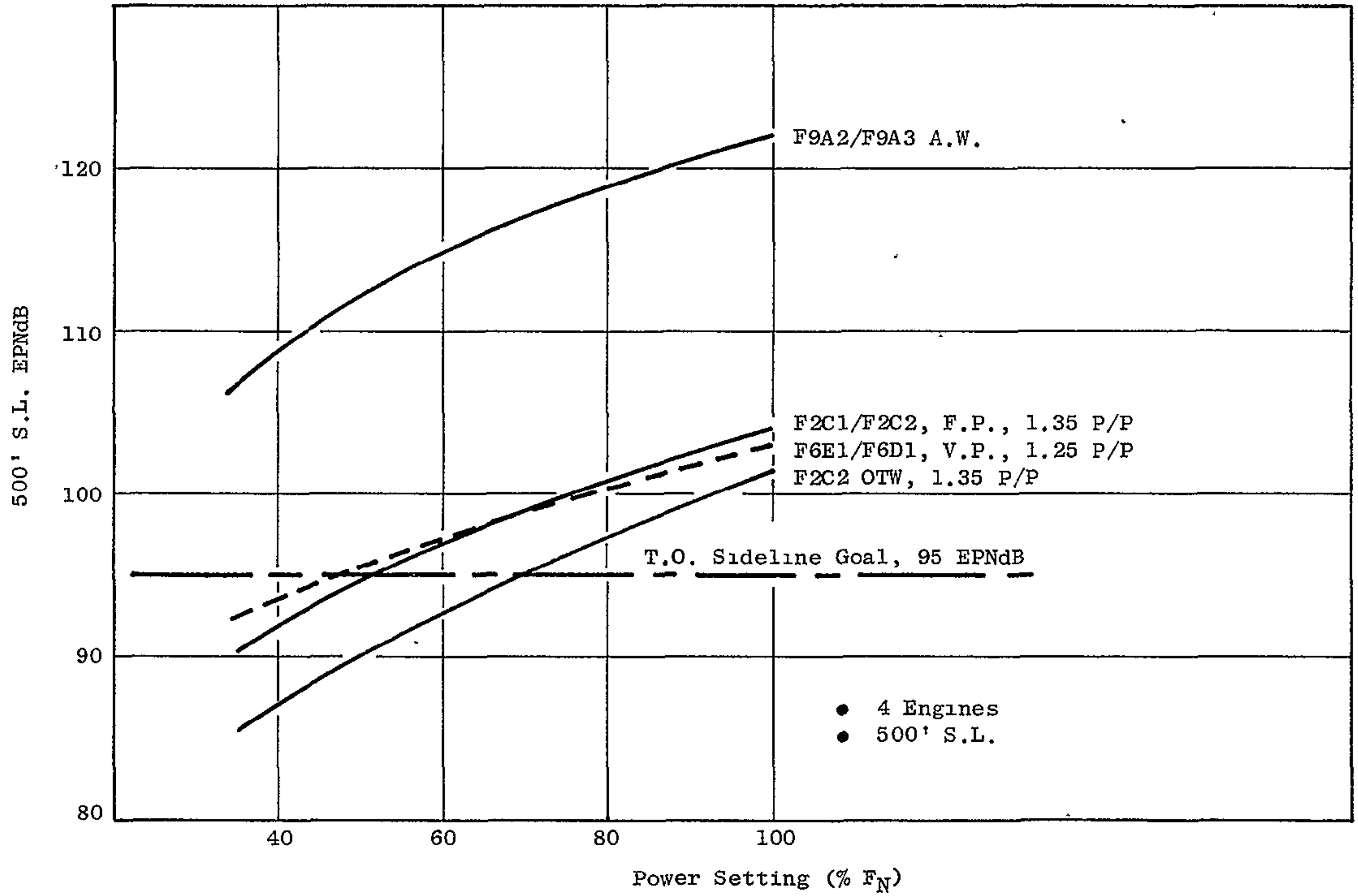

Figure IV-6. Thrust Reverser Noise Level Comparison.

For the EBF engines, to meet the 95 EPNdB noise goal will require the thrust reverser to be operated at about 50% power setting and, hence, permitting the brakes to perform part of the work for stopping. This is separately discussed in Section VI. It is noted that F2C2 (OTW) engine produces the minimum noise at reverse compared to the other systems. The reason lies in the location of the reverser at the end of the fan stream and that the fan noise is fully suppressed by the duct splitter treatments before it is escaped to the open.

At the reverse mode, the dominant noise sources for the F9A2/F9A3 AW engines are clearly due to the jet, as already indicated. For the fixed pitch 1.35 P/P under-the-wing systems, fan noise and jet noise contribute about equally at reverse. For the V.P. 1.25 P/P system, the fan noise appears to dominate. For the 1.35 P/P fixed pitch OTW system, the dominant noise source at reverse is the jet.

FOOTPRINT COMPARISON

Consistent with the noise levels shown in Tables IV -2 to -9, take-off and approach noise footprints are calculated for the four EBF engine systems. The flight path, flap setting, airplane speed and engine thrust characteristics at takeoff and approach followed the Task II NASA Guidelines. The airplane takeoff is at 12.5° climb angle, 80 knots (41.16 m/sec) and 30° flap. No operational procedure at takeoff is considered.* A two-phase approach is exercised. The initial phase is 25% Fn, 35° flap, 100 knots (51.44 m/sec) and a 6° glide slope. At 500' (152.40 m) altitude, the airplane is decelerated to 80 knots (41.16 m/sec), 72% Fn, 60° flap, and at a 6° glide slope.* This configuration is maintained until near touchdown.

---

*As directed by NASA

Exact footprint calculations cannot be performed in this study mainly because of the lack of complete data on the complex directivity characteristics of the nonaxisymmetric flap noise source. Noise levels directly under the wing are higher than those seen on a sideline. This difference in noise is commonly referred to as the view angle effect. In order to approximate the footprint of this nonaxisymmetric noise, two separate footprints were calculated representing the louder under-the-wing levels and the quieter sideline levels. These two footprints were then put together to represent the final footprints shown in Figures IV-7 and IV-8. The separate footprints are represented by a simple half-ellipse whose minor axis half-distance is equal to the lateral distance for which the noise source will provide the specified EPNdB level (e.g. sideline distances for 85 and 95 EPNdB), and whose major axis half-distance corresponds to that lateral distance divided by the sine of the climb angle of the airplane. The center of the ellipse is the point of airplane rotation. The lateral distance for the specified EPNdB level is calculated based on the 500' SL reference point EPNdB given in Tables IV-2 to -8, and on the approximation that EPNdB level varies inversely as the square of distance. These calculations are carried out using a computer program. The two half-ellipses are plotted. The final contour is drawn by "eye" by connecting the initial portion of the first half-ellipse (which is based on the sideline level) to the final portion of the second half-ellipse which is referenced to the overhead noise level. The static initial point of the contour is then estimated, set lateral to the airplane brake release point, and connected to the initial half-ellipse. This procedure, though inexact, is believed to be adequate when one considers the relative ignorance with regard to the complex directionality of the various noise sources involved. The footprint area is then estimated by using a planimeter traced over the drawn contour. One important aspect

- Constant Configuration T.O., Climb Angle = 12.5°, 80 Kts.
- Two Phase Approach: 1) 25% FN, 100 Kts., 35° Flaps
  2) @ 500' Alt, 72% FN, 80 Kts., 60° Flaps

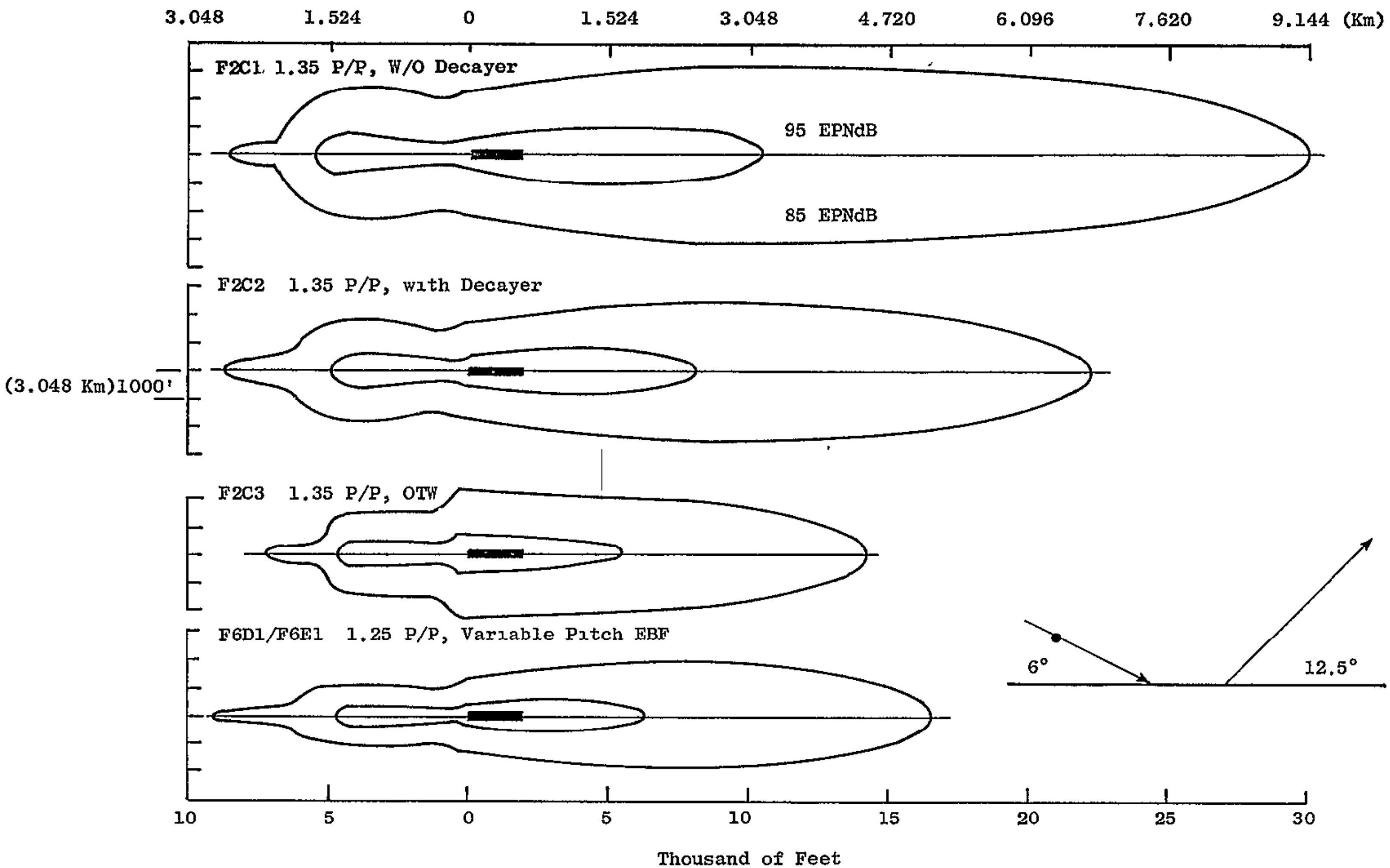

Figure IV-7. Footprint Comparisons (F2C1, F2C2, F2C3, and F6D1/F6E1).

- Constant configuration T.O., climb angle = 12.5°, 80 knots
- Two phase approach:
  1) 25% Fn, 100 knots, 35° flaps, 6° glide slope
  2) @ 500' alt., 55% Fn, 80 knots, 60° flaps, 6° g.s.
- 4 engines, including wing jet noise

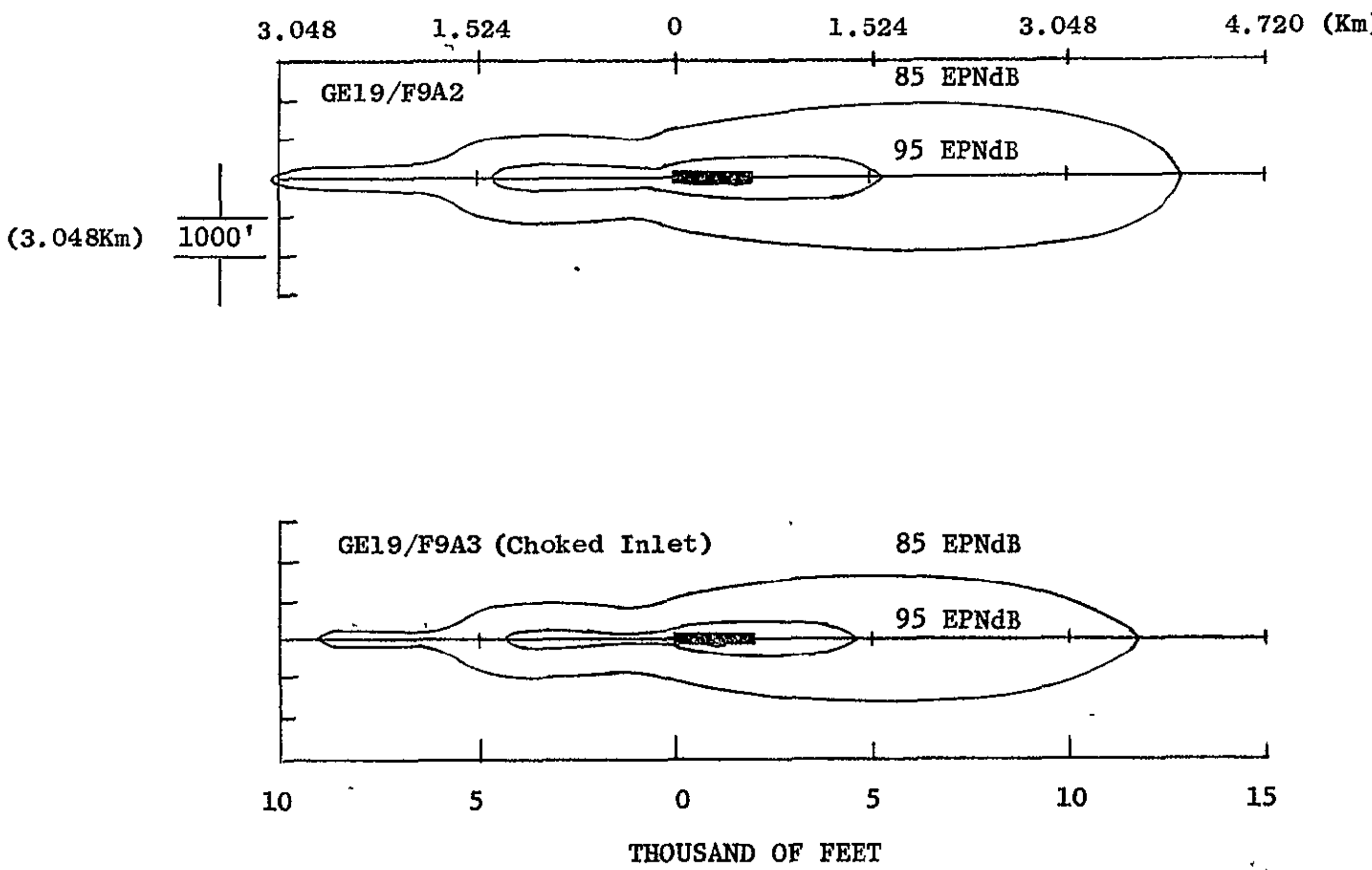

Figure IV-8. Footprint Comparisons (GE19/F9A2 and GE19/F9A3).

of this procedure involves the estimate that EPNdB level varies inversely as the distance squared. This approximate estimate is based on data from previous calculations of very highly suppressed engines; but may be subject to future modification based on more exact analysis when detailed spectral data for all noise sources at all directions associated with the engine-airplane system become available or can be estimated more accurately than the present state of the art permits.

85 and 95 EPNdB equal noise contours are shown in Figures IV-7 and IV-8 for the four EBF systems. Table IV-27 tabulates the areas enclosed by the contours. Inspection of the contours leads to several observations:

- The approach footprint area is considerably less extensive than that of takeoff. This is due to the use of operational procedure at approach where the initial approach phase is characterized by low thrust, low flap setting and higher speed, all of which means low noise. The ground rule adopted in the present study precludes the consideration of operational procedure at takeoff. It is anticipated that such operational procedure in early power cutback and/or early flap retraction to minimize flap noise can have significant impact in reducing the takeoff portion of the footprint area.

- For the same basic engine and cycle, and the same sideline noise, difference in installation (one over-the-wing and the other under-the-wing) has a significant difference in footprint area. Over-the-wing (F2C3) installation footprint area is about 30% less than that for under-the-wing EBF system (F2C2). The primary reason is that directly underneath the aircraft the flap noise in under-the-wing (decayer) system is nearly 5-6 PNdB higher than the scrubbing noise associated with over-the-wing installation.

- Comparing the F2C3 (OTW, 1.35 P/P) with the F6D1 (or F6E1) 1.25 P/P EBF under-the-wing system, it is seen that, in spite of the apparent sideline noise advantage of the lower P/P system (95 EPNdB vs. 97 EPNdB), the footprint areas between the two systems are nearly the same, again suggesting the noise directivity advantage of the OTW installation.

Table IV-27. Footprint Area Comparison in Acres.

ENGINE	LIFT	500' S.L. T/O EPNdB	85 EPNdB	95 EPNdB
F2C1	EBF	100	4260 (17239608 m^2)	540 (2185302 m^2)
F2C2	EBF	98	2550 (10319483 m^2)	340 (1375931 m^2)
F2C3	OTW	97	1540 (6232159 m^2)	250 (1011714 m^2)
F6D1/F6E1	EBF	95	1520 (6151222 m^2)	220 (890308 m^2)
F9A2	AW	92	1330 (5382319 m^2)	180 (728434 m^2)
F9A3	AW (CHOKED INLET)	89	960 (3884982 m^2)	120 (485623 m^2)

* T.O. GROUND ROLL, TAKEOFF AND APPROACH BUT NOT INCLUDING AREA DURING REVERSER OPERATION

UNCERTAINTIES AND LIMITATIONS OF THE PRESENT STUDY

The foregoing study and noise estimates have made use of certain assumptions and prediction procedures which are deemed to be appropriate based on today's knowledge, but nevertheless have not been substantiated by full-scale engine testing. These include:

- Over-the-wing scrubbing noise based on scale model results.
- Over-the-wing shielding effects.
- View factor (-5.5dB) assigned to EBF under-the-wing flap noise based on scale model results.
- Design method for low frequency core noise suppression.
- Prediction method for turbine noise.
- Fan noise prediction for low speed, low pressure ratio, variable pitch fans.
- Assumption that high Mach inlet and treatment suppression effects are approximately additive, and that broad band noise may not be significantly increased with higher inlet Mach number.
- Suppression effects assigned to treated inlet centerbody.
- Amount of noise increases (jet and fan) associated with thrust reverser operation.

The probable accuracy for noise and noise suppression prediction on each of the above items is believed to be not better than $\pm$ 2 PNdB. While the possible errors introduced on different noise components will not be cumulative on the total systems noise estimate*, it is easy to see that there is considerable room for possible discrepancies between predicted systems noise and actual final engine test levels.

---

* In order to increase the systems noise, by say 1 EPNdB, all the constituents must be raised by 1 PNdB.

There are several possible noise sources which have not been taken into consideration in the present study but which may surface into prominence when the major noise sources, as we understand them now, are reduced. These are:

- Flow noise in the fan duct associated with boundary layer flow over the splitters, wakes from support struts, surface discontinuities, and minor flow separations. (The current design criterion of fan duct Mach number of 0.45 in not being noise-floor critical is subject to review awaiting more comprehensive engine test results and analysis.)

- Casing radiation of the fan or core noise through the nacelle and core engine wall via structure-borne paths. Possible one-per-rev related acoustical signal has not been considered.

- Engine control and accessory noise, including pumps, gears and other mechanical vibration-related noise radiation.

GENERAL DISCUSSION OF RESULTS

1.35 P/P Under-The-Wing EBF Systems

Four baseline 1.35 P/P GE19/F2C1 EBF engines with fully suppressed nacelles but without velocity decayers are successful in meeting the NASA 100 EPNdB (500' S.L.) noise goal. The very significant improvement in noise design of this engine relative to today's engines may be seen by comparing their 95 EPNdB noise exposure footprint areas.

95 EPNdB Footprint Areas

Systems	Estimated Area, Acres
4 GE19/F2C1/STOL	540 (2185302 m^2)
New Wide-Body Trijet (e.g. DC-10-10)	1500 (6070285 m^2)
Current 707/DC8	9700 (39254507 m^2)

With operational procedures applied at takeoff, the STOL noise footprint area is expected to be further reduced.

The dominant noise constituent on the F2C1 engine is the flap plus jet - being 6 PNdB higher than the next highest constituent. Effectiveness of installing a modest 9-lobe velocity decayer (F2C2 engine) is only marginal. A 3.5 PNdB reduction in the flap noise component yields a net systems reduction of about 2 EPNdB. The noise exposure area is reduced by approximately 35%. The impact on Δ DOC due to the use of the velocity decayer is, however, fairly substantial (see Section V111).

Over-The-Wing Vs. Under-The-Wing Installation

Based on currently available test data, which are not extensive nor necessarily conclusive, generalized prediction methods devised to estimate the flap noise of the two installation systems indicate the following tentative flap noise comparisons:

		Δ PNdB (Flap & Jet)	
		UTW	OTW
	Flap Setting	F2C1 (no decayer)	F2C3
500' S.L. T.O.	30^{o}	Base	- 4.5
500' Overhead T.O.	30^{o}	Base	- 7.5
500" S.L. Approach	60^{o}	Base	- 7.0
500' Overhead Approach	60^{o}	Base	- 10.0

It is seen that the flap noise is significantly lower for the OTW systems. This is particularly true for overhead positions, and at large flap settings. OTW systems have an added noise advantage; namely, a shielding effect on aft-radiated fan and core noise. Current estimates show a reduction due to wing shielding of about 5-6 PNdB at the sideline position (elevation angle ~ 20^{o}) and 9-10 PNdB at the overhead position. Because of this advantage, the amount of aft nacelle suppression requirement may be greatly reduced.

Footprint comparison between the F2C1 (UTW without decayer) and the F2C3 (OTW) shows a reduction in footprint area by a factor of about 2.5. The aft nacelle suppression on the OTW installation is also less extensive (single splitter vs. 1 + 2 splitter). The noise advantages are again directly due to the OTW installation feature. It should be cautioned again that the above tentative conclusions are subject to revision when additional information and full scale test data (especially on the OTW systems) become available.

Advance Technology on Flap Noise Reduction

For all the EBF systems, the flap noise constituent is always the strongest constituent. Advance technology in flap noise reduction will have a strong impact on the final systems EPNdB level. Table IV-28 shows the possible approaches toward reducing the flap noise. The effect on the systems EPNdB level with a 3 PNdB reduction of the flap noise constituent for the five Task II EBF engines is also shown.

1.35 P/P OTW Versus 1.25 P/P UTW Systems

Comparison of these two systems is shown below:

	Four Engine EPNdB	
	1.35 P/P OTW (F2C3)	1.25 P/P UTW (F6D1/E1)
500' S.L. T.O.	96.9	95.4
500' Overhead T.O.	99.9	101.3
500' S.L. Approach	95.8	93.4
500' Overhead Approach	98.1	98.6
95 EPNdB Footprint, Acres	250	200
85 EPNdB Footprint, Acres	1540	1520

The sideline noise levels on the 1.35 OTW system are higher by about 1.5 - 2.5 EPNdB, but the overhead noise levels are lower by about 0.5 - 1.5 EPNdB. The footprint areas between the two systems are nearly the same. The conclusion may be drawn that , with OTW installations, a somewhat higher fan P/P engine cycle may be utilized in achieving about the same noise exposure area.

Table IV-28. Impact of Advanced Technology on Flap Noise Reduction.

- FLAP SURFACE TREATMENT
- TRAILING EDGE BLOWING
- OPTIMUM NOZZLE - FLAP ARRANGEMENT
- FLIGHT EFFECT (NO ADVANTAGE CLAIMED IN CURRENT STUDY)

Engine System		Systems EPNdB (4 Engines) Current Estimate	Adv. Technology**	△EPNdB
F2C1	1.35P/P, EBF	100	98	-2
F2C2	1.35P/P, EBF (DECAYER)	98	96	-2
F2C3	1.35P/P OTW	97	95	-2
F6D-1/F6E1	1.25P/P, EBF	95	94	-1

* ALL NUMBERS REFER TO 500' SL T.O. 80/KTS, (41.16 M/SEC), 4 ENGINES, EPNdB

**BASED ON 3 PNdB REDUCTION OF FLAP + JET NOISE; OTHER SOURCES REMAINED UNCHANGED

V - BASIC ENGINE DESIGN

The four engines laid out for Task II all used the F101 core. No design changes are required to the basic core components except for emissions reduction. A brief description of the mechanical features of each Task II engine follows. Key stresses are listed on Table V - 1. A weight breakdown is given in Table V - 2. A summary of materials utilized is presented in Table V-3.

GE19/F2C

The F2C utilizes a fixed-pitch blade, tip-shrouded titanium fan. This design is patterned after a series of higher fan pressure designs laid out for other engines including the quiet engine program tip shroud fan A and F101 multistage fan plus study single stage fans. The tip speed of the F2C fan is somewhat higher than fan A and somewhat lower than that of these other fans, and the stress levels are corresponding different. A separate OGV with two chord spacing and 2:1 vane-blade ratio is utilized in this design.

Three booster stages of Ti, similar to those utilized in the CF6-50, are employed in the F2C. Booster bleed valves are located in the inner portion of the fan frame. The fan frame is designed to support the inlet and to handle fan gyro and blade-out loads. The fan frame itself is titanium construction. This does not necessarily represent a final choice for the 1980 engine. On the one hand, a steel frame is cheaper but heavier. But composite technology may advance such that at least part of the fan frame and other cold structure could be composite construction.

Table V-1. Task II Study, Key Stress Data.

	GE19/F2C	GE19/F6D	GE19/F6E	GE19/F9A
Fan Blade Root Stress	39000	10600	14700	45700, 31800, 32600
Fan Disc Stress (max rim)	72000	72000	72000	72000, 70000, 68000
LPT - Blade Root Stress				
Stage 1	4950	22100	2070	22060
Stage 2	7150	37200	2660	36800
Stage 3	9650	---	3520	---
Stage 4	11660	---	4560	---
Stage 5	---	---	5590	---

Table V-2. Task II Study, GE19 Weight Breakdown.

		F2C3	F6D1	F6E1	F9A2
Fan Section					
Rotating Parts,	LBS	550	820	680	440
	KG	249.5	372.0	308.4	199.6
Static Parts,	LBS	980	1150	1300	550
	KG	444.5	521.6	589.7	249.5
Low Pressure Turbine Section					
Rotating Parts,	LBS	230	240	250	220
	KG	104.3	108.9	113.4	99.8
Static Parts,	LBS	430	280	500	390
	KG	195.0	127.0	226.8	176.9
Core Components,	LBS	940	940	940	940
	KG	426.4	426.4	426.4	426.4
Controls & Accessory Drive,	LBS	310	290	290	310
	KG	140.6	131.5	131.5	140.6
Bearings, Seals, Sumps, Lube System,	LBS	160	330	240	150
	KG	72.6	149.7	108.9	68.0
Total,	LBS	3600	4050	4200	3000
	KG	1632.9	1837.1	1905.1	1360.8

C-3

Table V-3. Task II Study, Materials List.

COMPONENT	GE19/F2C	GE19/F6D	GE19/F6E	GE19/F9A
Fan Blading				
Rotor	Titanium	Ti Spar - E/G Shell	Ti Spar - E/G Shell	Titanium
Stator	Aluminum	Titanium	Titanium	Titanium
Fan Rotor	Titanium	Titanium	Titanium	Titanium
Fan Shaft	Maraged 250 Steel	Maraged 250 Steel	Maraged 250 Steel	Maraged 250 Steel
Booster Blading				
Rotor	Titanium	Titanium	Titanium	Titanium
Stator	Titanium	Titanium	Titanium	Titanium
Booster Rotor	Titanium	Titanium	Titanium	Titanium
Fan Frame	Titanium	Titanium	Titanium	Titanium
Fan Casing	Aluminum	Aluminum	Aluminum	Aluminum
LPT Blading				
Rotor	René 80 *	1st Stage - René 120	René 80	René 80
Stator	René 80	2nd Stage - René 80	René 80	René 80
LPT Rotor	A286 **	Inco 718	A286	A286
Turbine Frame	Inco 718 *	Inco 718	Inco 718	Inco 718

* High Temperature Nickel Alloys

** High Temperature Iron Bond Alloy

The fan turbine is a moderately loaded four-stage design constructed in a manner similar to other recent GE designs. The fan turbine is supported by a rear frame in a manner similar to that employed on the F101 and TF34 engines. Cooling is required for the first stage vanes only plus the usual wheel space cooling.

GE19/F6D

The F6D utilized a 16-blade variable pitch fan of spar shell construction. A solid titanium spar and blade support trunnion is used. The shell material is graphite-epoxy with an expand polyurethane foam filler between shell and spar. It must be pointed out that satisfactory bird strike capability of composite fan blades for commercial aircraft has not been proved. For this reason, weight estimates were made if hollow Ti blades were used in place of the composite blades, the penalty being on the order of 500 lbs (2221.1 N).

The blades are suspended from tapered roller thrust bearings. Actuation is through a mechanical system consisting of a harmonic gear set, an actuation hydraulic motor coupled through a shaft and differential to the harmonic drive. The actuation system was laid out for reverse through fine pitch but the approach could be adapted for variation through feather at a weight penalty. Table V - 4 indicates some of the factors involved in the actuation. Again, the specific design selected for Task II does not represent a final choice for the 1980 engine. Other methods including

Table V-4. Task II Study, Variable Pitch Acuation System Description.

	GE19/F6D1	GE19/F6E1
ACTUATOR TYPE	HARMONIC GEAR / DIFFERENTIAL	SAME
BLADE ROTATION	BLADE SECTOR GEAR UNISON GEAR	SAME
DESIGN BLADE SLEW RATE	100°/SEC	SAME
SECTOR-TO-UNISON GEAR RATIO	.27 : 1	.33 : 1
HARMONIC GEAR RATIO	110 : 1	SAME

hydraulic are under study with emphasis being given to failure modes involved in the various approaches.

The fan bypass OGV's are integrated with the outer portion of the fan frame as previously described in Section I. The blade OGV spacing was set at 1-1/4 chords. The intent of these features was to reduce the overhang of the fan rotor from the fan frame to a practical magnitude. The fan frame is based on Ti construction. A single booster stage titanium construction is used and a bleed valve located in the inner portion of the fan frame.

The design of the main reduction gear is summarized on Table V - 5. The design is a lightweight sun-star gear set with a 3.24 reduction. A titanium carrier serves to suspend and retain the star gears while absorbing fan rotor loads through main rotor bearings. Oil is used as a coolant to absorb the less than 1% loss at design conditions. The lube system and cooling are described in a following section. The designs of the gear teeth and bearings are consistent with a long-life commercial application. The main fan rotor bearings are large, preloaded, thrust bearings selected to prevent axial motion of the fan rotor. These bearings must be designed to take both the forward and reverse loads as well as the large overturning moments generated by gyro loads and blade-out loads.

The low pressure turbine is two stages and, because of the high wheel speed and energy output, is closer to a core turbine than a high bypass

Table V-5. Task II Study, GE19/F6D1 Lightweight Main Drive Gear Description.

TYPE	- STAR - SUN (SPUR TEETH - INVOLUTE PROFILE)
WEIGHT	≃ 240 LBS (108.91KG)
GEAR RATIO	- 3.24 : 1
NR OF STAR GEARS	- 5
HORSEPOWER	- 17,000(12676897WATTS)
OUTPUT TORQUE	- 34,000 FT-LBS(496060N-M)
OUTPUT RPM	- 2,640
EFFICIENCY ESTIMATE	- 99+%
GEAR AND BEARING MATERIAL	- 9310 STEEL
GEAR SET SUPPORT MATERIAL	- TITANIUM
LOCATION	- AFT OF FAN
GEAR COOLANT	- ENGINE OIL

LPT in its mechanical design. This is most noticeable in comparing the LPT blade root stresses of the /F6D and /F6E. Since the geared turbine turns at nearly 3 times higher rpm than the direct drive /F6E and the radius ratio is much lower, there is a factor of approximately 10 in the blade stress. Airfoil cooling is required on the first stage vanes only. A rear frame arrangement similar to the F101 is employed. One difference in rotor construction is that turbine thrust is taken out by an aft thrust bearing. This requires that an overspeed trip to prevent turbine runaway be employed to account for breakage in the fan shaft, gear set or LPT shaft systems. Note that for other engines, the thrust bearing can be located such that a shaft failure will allow the LPT rotor to move rearward and interfere with static parts although it may still be desirable to have additional overspeed protection.

GE19/F6E

The F6E design is similar to that of the F6D in most respects. It utilizes 14 spar shell blades. The blade support and actuation systems are larger and heavier than that of the F6D to accommodate the higher loads, but the design approach is the same. The fan vane-frame and booster designs are similar to those of the F6D. The fan rotor and shaft arrangement must differ of course since no reduction gear is involved. Low speed rotor thrust is taken by the main fan rotor bearing rather than in separate fan and LPT turbine bearings in the case of the F6D.

The fan turbine is a five-stage design like the CF6-6 in DC10-10 but loaded more highly from the aerodynamic standpoint. However, the wheel speed and stresses are very low, and it turns out that the fan turbine rotor is only moderately heavier than that of the other GE19 designs. Because of its low wheel speed and moderate weight, the LPT rotor can be supported from a rear frame in a manner similar to the 2-stage F101 and 4-stage TF34 designs. Airfoil cooling is required on the first stage vanes of the LPT only.

Table V - 6 compares the physical differences of the geared and nongeared GE19 variable pitch engine designs. Both designs are feasible. The final choice for the product engines in the 1980 time period will depend largely on the airlines' experience with wide body jets using 4 - 5 stage turbines in high bypass turbofans in the decade of the 70's; i.e., will there be incentive to switch to geared drive.

GE19/F9A

This engine is close to the basic F101 engine in its general configuration. The first two stages of the fan are tip-shrouded titanium stages which are essentially a no-IGV version of the F101. The third stage is unique in that the inner and outer portions are divided by a platform which acts as a mid-span shroud in addition to its aerodynamic function of providing a higher bypass stream pressure than core inlet pressure. This construction has precedence in the second stage of the TF39 fan.

Table V-6. Task II Study, Direct Drive (F6E1) Vs. Geared (F6D1) Physical Differences.

Geared	Direct Drive
1. ~240 LB. (108.9 KG) 17000 HP (12,676,898 WATTS) LIGHT WT. GEARSET (3.24:1) CONSISTING OF:	1. 3 ADDITIONAL TURBINE STAGES CONSISTING OF THESE ADDITIONAL PARTS:
A) SUN GEAR	A) 3 TURBINE DISKS
B) 5 STAR GEARS	B) 1 ROTOR SHAFT CONE
C) RING GEAR	C) ~1200 BLADES AND VANES
D) 10 ROLLER BRG. SETS	D) 3 EXTRA SETS INTERSTAGE SEALS AND SHROUDS
E) GEAR SET SUPPORT STRUCTURE	
F) COOLING OIL JET SYSTEM	
2. TURBINE THRUST BRG. IN TURBINE	2. LONGER, LARGER DIAMETER TURBINE
3. 34" x 5" x 5-1/2" (86.36 CM x 12.7 CM x 13.97 CM) AIR-OIL COOLER AND ASSOCIATED VALVES AND PLUMBING	3. ADDITIONAL MAIN SHAFT PARTS
4. 19 GPM (0.0719226 M^3/MIN) ADDITIONAL ENGINE OIL FLOW RATE	
5. 50 GPM (1.89270 M^3/MIN) ADDITIONAL ENGINE SCAVENGE CAPACITY	
6. LP TURBINE OVERSPEED PROTECTION	

A titanium fan frame to support the entire fan rotor is utilized. IGV's and a front frame as in the F101 are not a part of this design. The fan turbine is a two-stage design larger in size than the F101 but similar in construction. Only the first stage vanes require cooling.

HAMILTON STANDARD STUDIES

As part of the General Electric QCSEE studies, two subcontracts were let to Hamilton Standard. The first of these was carried out during Task I and involved a specific gear set design and parametric trends on gear sets. Results were provided in a letter report which was made available to NASA. A summary of the design is shown on Table V - 7.

The specific gear set design and structural arrangement worked out between GE and Hamilton Standard during Task I was then adapted to the slightly larger Task II F6D design. The weight estimate of 240 lbs. (1067.6 N) for the gear assembly was made utilizing the data provided by Hamilton Standard.

The second of these subcontracts involved the designs of the entire fan rotor system. Hamilton Standard proposed they use their own aerodynamic and mechanical design approach to fan design and this was agreed to by General Electric. The results were documented in Hamilton Standard Report SF10A 72 and included the items listed in Table V - 8.

A brief summary of the design results is shown on Table V - 9. The engine size selected for the study was slightly larger than that of GE

Table V-7. Task II Study, Brief Review of Hamilton-Standard Gear Study Results.

<u>SPECIFIC DESIGN</u>	[GE TASK I CYCLE	- F_N = 21900 LBS (9933.8 KG)]
GEAR TYPE/RATIO	-	SUN - STAR / 2.98:1
DESIGN HORSEPOWER/OUTPUT TORUQE	-	16800/31800 FT-LBS (245112/463962 N-M)
OUTPUT RPM	-	2780
NR OF STAR GEARS	-	5
GEAR SET SUPPORT	-	TITANIUM CONE
GEAR AND BEARING MATERIAL	-	9310 STEEL
ESTIMATED GEAR SET WEIGHT	-	206 LBS (93.44 KG)

Table V-8. Task II Study, Major Items Supplied in H-S Fan Design Report No. SP10A72.

FAN AERO DEFINITION (BLADE AND DUCT)
ACOUSTIC ESTIMATES (FORWARD AND REVERSE THRUST)
MECHANICAL DESIGN (INCOMING CONTROL SYSTEM)
RELIABILITY ESTIMATES
WEIGHT ESTIMATES
COST ESTIMATES
GROUND TEST DEMONSTRATOR PROGRAM SUGGESTIONS

Table V-9. Task II Study, Brief Review of Hamilton-Standard Fan Design Study Results.

FAN PRESSURE RATIO	- 1.25
FAN FLOW/FN	- 1255 LB/SEC (569.3 KG/SEC)/25000 LBS (111205.0 N)
CORRECTED TIP SPEED	- 750 FT/SEC (228.6 M/SEC) (H-S AERO DESIGN)
TIP DIAMETER	- 85.5 INCHES (217.2 CM)
NR BLADES/TYPE	- 17/TI SPAR - BORON - EPOXY SHELL
DRIVE	- GEARED (3.89:1 SUN - STAR)
HORSEPOWER/TORQUE	- 15500/44000 FT-LBS (226, 45/641,960 N-M)
ACTUATION SYSTEM	- HARMONIC DRIVE THROUGH DIFFERENTIAL
GEAR LOCATION	- FORWARD OF FAN
BLADE BEARING AND GEAR LUBRICATION	- ALL WET SUMP
TOTAL SYSTEM WEIGHT	- 1060 LB (480.81 KG)

Task II design. The primary difference, however, was that the Hamilton Standard design involved a low tip speed fan involving reverse through feather. The gearbox was located forward of the fan and ahead of the variable pitch actuation system which is the opposite of the GE19/F6D approach. The harmonic drive actuation approach proposed by Hamilton Standard was utilized in the GE variable designs but details differed considerably.

LUBRICATION SYSTEM

The lubrication and sump requirements, as shown in Table V - 10, for the three direct drive engines are very conventional in terms of heat rejection, number, and purpose. Table V - 11 lists the principal system components and functions of all the engine designs. Key features of the systems used are listed in Table V - 12.

Typical of the three direct drive engine lubrication system schematics is the one shown in Figure V - 1 denoting oil flow rates, circuits and major components. However, the addition of a fan gearbox and variable pitch introduces another lubrication complexity not normally encountered.

A schematic of the lubrication system for the GE19/F6D, gear-drive engine is shown in Figure V - 2. The principal difference in this system as opposed to the typical direct-drive engine is the provisions for lubricating, cooling, scavenging and rejecting the heat from the gearbox. To accomplish this requires the addition of a strategically placed set of oil jets, a scavenge pump, a scavenge filter and the plumbing associated with an external cooler.

Figure V - 3 depicts one type of auxilliary air-oil cooler installation.

Table V-10. Task II Study, Lube System Functions.

- SUPPLY REQUIRED LUBRICATION AND COMPONENT COOLING
- REJECT GENERATED HEAT
- MINIMIZE OIL CONSUMPTION
- STORE MISSION OIL
- VENT PRESSURIZED CAVITIES

Table V-11. Task II Study, Lube System Description.

- SUPPLY - TANK, PUMP, FILTER
  DISTRIBUTION NOZZLES
- SCAVENGE - PUMPS, FILTER
  COOLER, DEAERATOR
- SEAL PRESSURIZATION - OIL
  CONSUMPTION LIMIT
- SUMP VENT - LIMITS TRANSIENT
  OIL CONSUMPTION

Table V-12. Task II Study, Lube System Key Features.

- FILTERED SUPPLY + SCAVENGE
- MAGNETIC CHIP COLLECTORS
- DRY SUMPS
- CENTER VENT
- STATIC LEAK C/V
- COLD START PRESSURE LIMIT

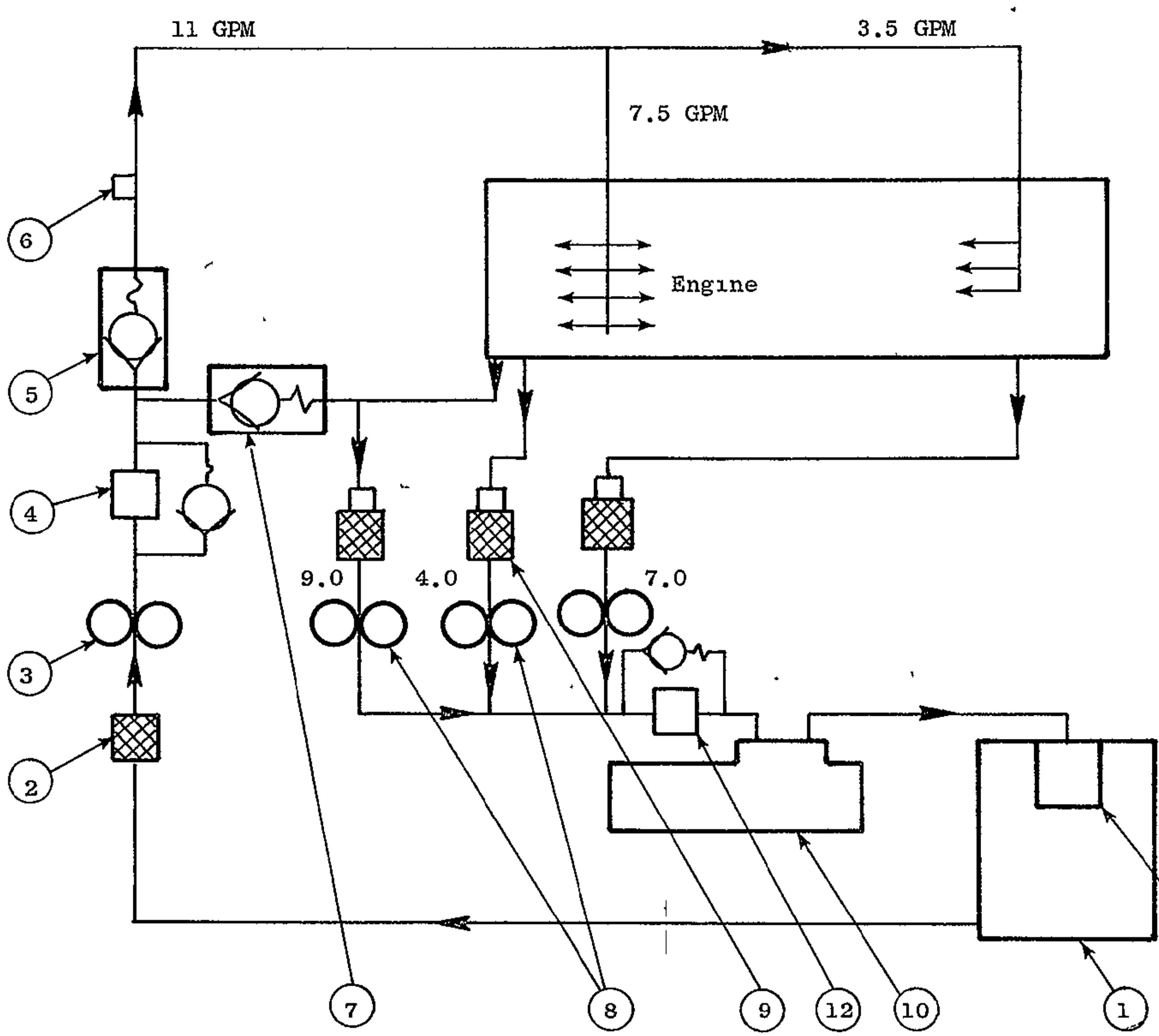

1. Oil Tank
2. Inlet Screen
3. Oil Supply Pump
4. Oil Supply Filter
5. Static Leak Check Valve
6. Oil Pressure Tap
7. Cold Start Bypass Valve
8. Scavenge Pumps
9. Inlet Screen with Magnetic Chip Collector
10. Oil Cooler
11. Scavenge Oil Deaerator
12. Oil Scavenge Filter

Figure V-1. Task II Direct-Drive Lube System.

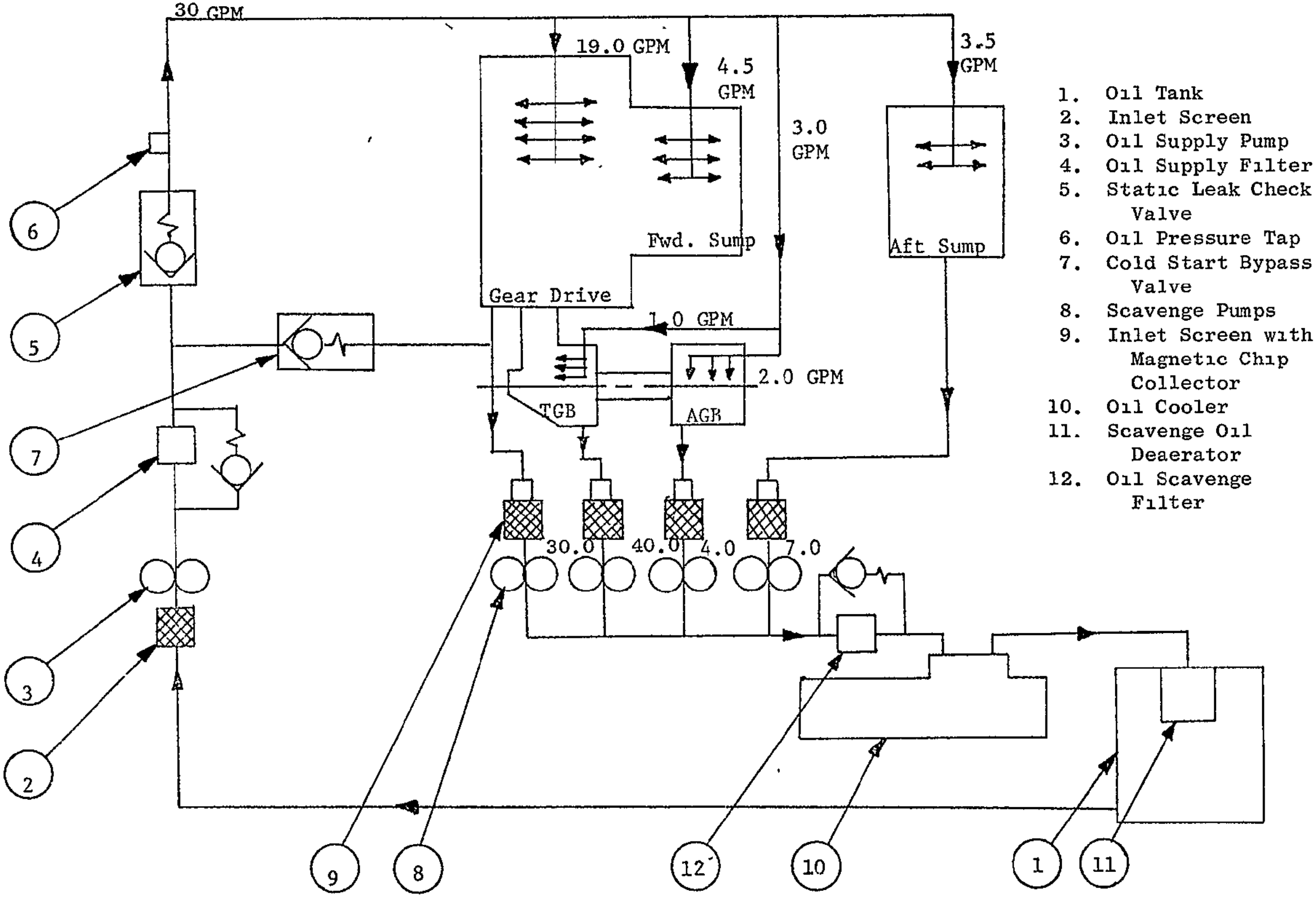

Figure V-2. Task II Geared Fan Lube System.

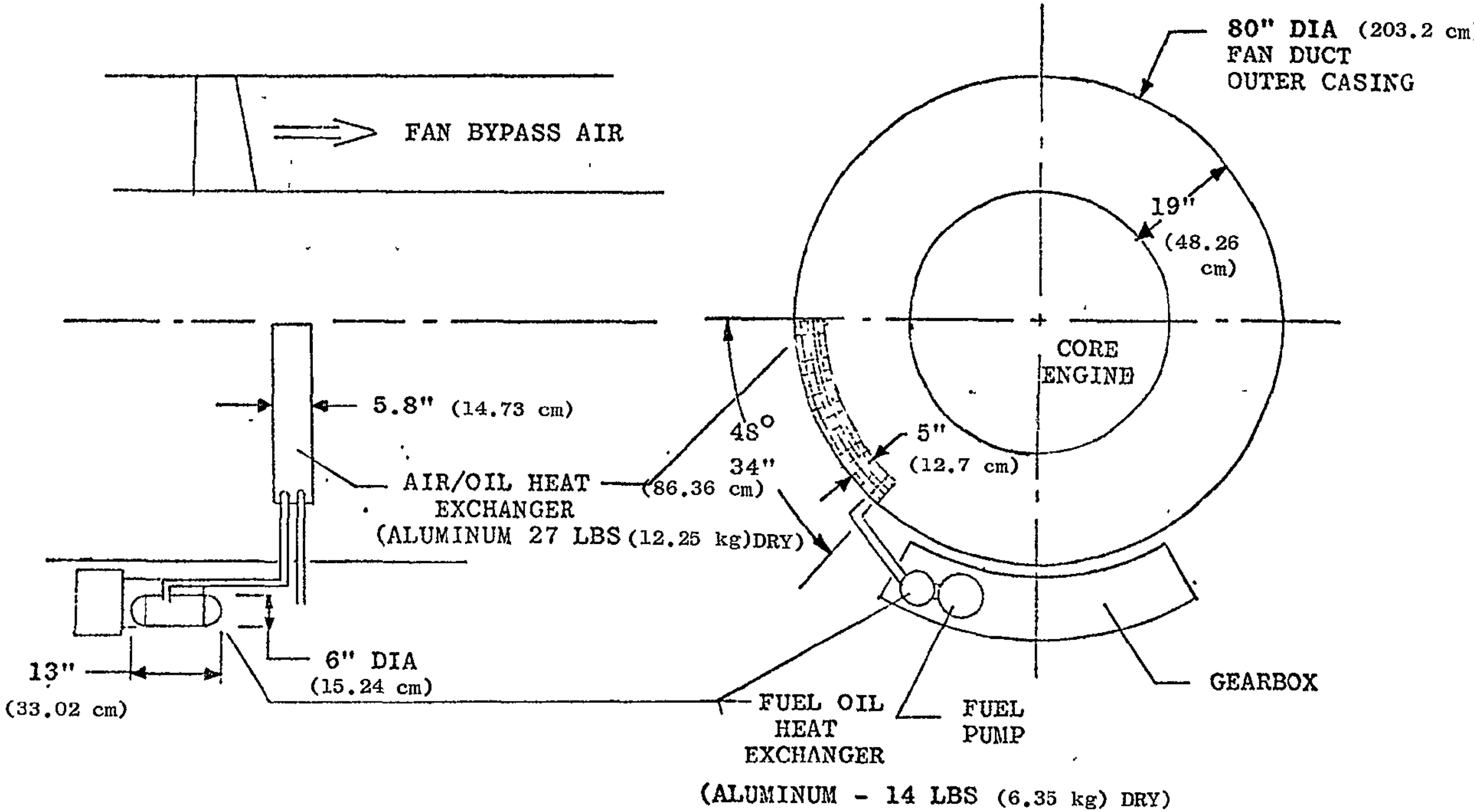

Figure V-3. Task II GE19/F6D Preliminary Size and Installation of Duct Ram Air/Oil Heat Exchanger and Fuel/Oil Heat Exchanger.

Fan duct air passes through the cooler to carry off the major portion of gearbox-generated heat. Some approximate weight and dimension values for major cooler components are also shown.

Although the typical fuel-oil cooler is adequate for most engines and flight conditions, the large amount of heat rejected by the gearbox requires another cooler, in this case an air-oil cooler mounted so as to have fan air ducted through the cooler. Scavenge oil temperature limits are lower than usual since the 9310 steel employed in the main gears begins to lose hardness when subjected to temperatures much above 325°F (162.78°C). For this reason, the scavenge exit oil temperature was limited to 275°F (135°C) as shown in Table V - 13. Although this penalizes the air-oil cooler size somewhat the only alternative would be to use a higher temperature gear material like 4340 steel in which GE does not have extensive experience.

The heat rejection requirements have introduced differences into oil flows and tank sizes, as shown in Tables V - 13 through V - 16 between the direct and gear drive engines. Heat rejection for the GE19/F6D gear-drive engine for 4 operating conditions is given in Table V - 17.

A chart showing main bearing size and approximate capacity is given in Table V - 18 comparing the direct drive and geared drive variable pitch engine. Conventional CEVM M50 steel is assumed in the designs with silver plated AMS6414 cage material. None of the engine designs created any unusual or vigorous bearing requirements on the main shaft (see Table V - 18).

Table V-13. Task II Study, Heat Exchanger Operating Requirements.

- ENGINE FUEL AND OIL SELF-COOLING LIMITS OF:

MAIN FUEL CONTROL INLET	300° F (148.9° C)	SHORT TIME
	275° F (135.0° C)	CONTINUOUS
LUBE OIL	275°F MAX (135.0° C)	
SCAVENGE OIL		

- HEAT EXCHANGER OIL PRESSURE DROP LESS THAN 50 PSID. (34.47 N)

- FUEL HEATING (ANTI-ICE) CAPABILITY OF 35°F (1.67° C) WITH ENGINE FUEL SUPPLY TEMPERATURES TO -40°F (-40° C)

Table V-14. Task II Study, Comparison of Direct (F6E1) and Geared (F6D1) Variable Pitch Engine Lubrication System.

	Direct	Geared
Oil Tank Capacity	7.2 gals (0.027255 m^3)	10.2 gals (0.0386112 m^3)
Total Engine Oil Flow	11 gpm (0.0416395 m^3)	30 gpm (0.1135624 m^3)
Engine Heat Rejection	2310 BTU/min (2,439,060 joules/min)	10964 BTU/min (11,576,559 joules/min)
Oil Heat Exchange	Fuel-Oil Cooler	Fuel-Oil and Air-Cool Cooler
Nr of scavenged sumps	3	4

Table V-15. Task II Study, Major Lube System Components, Lube and Scavenge Pumps.

- LUBE + SCAVENGE PUMPS

FEATURES - ENGINE DRIVEN, INTEGRATED ELEMENTS, SELF-CONTAINED FILTERS, AND COLD START VALVE

CAPACITY

	DIRECT DRIVE OIL FLOW		GEARED FAN OIL FLOW		INLET PRESSURE	
	GPM	M^3/MIN	GPM	M^3/MIN	PSIG	N/CM^2
A. LUBE SUPPLY	11.0	0.041635	30.0	0.113550	12 - 14	8.274 - 9.653
B. FORWARD SCAVENGE	---	---	30.0	0.113550	12 - 14	8.274 - 9.653
C. AFT SCAVENGE	7.0	0.026495	7.0	0.026495	12 - 14	8.274 - 9.653
D. TGB SCAVENGE	9.0	0.034065	40.0	0.151400	12 - 14	8.274 - 9.653
E. AGB SCAVENGE	4.0	0.015140	4.0	0.015140	12 - 14	8.274 - 9.653

SIZING CRITERIA - HEAT REJECTION

MINIMUM NOZZLE SIZE

Table V-16. Task II Study, Major Lube System Components, Oil Tank.

- OIL TANK

  FEATURES - ENGINE-MOUNTED, PROVIDES STORAGE, VOLUME ACCUMULATOR, DEAERATOR

  CAPACITY

		DIRECT DRIVE		GEARED FAN	
GULPING	USABLE	1.5 GAL.	(0.0056775 M^3)	4.0 GAL.	(0.0151400 M^3)
MISSION OIL	USABLE	3.0 GAL.	(0.0113550 M^3)	3.0 GAL.	(0.0113550 M^3)
RESERVE OIL	USABLE	1.25 GAL.	(0.0047313 M^3)	1.25 GAL.	(0.0047313 M^3)
UNUSABLE OIL		0.25 GAL.	(0.0009463 M^3)	0.25 GAL.	(0.0009463 M^3)
TOTAL OIL		6.0 GAL.	(0.022710 M^3)	8.5 GAL.	(0.0321725 M^3)
EXPANSION SPACE		1.2 GAL.	(0.0045420 M^3)	1.7 GAL.	(0.0064345 M^3)
TOTAL TANK CAPACITY		7.2 GAL.	(0.0272520 M^3)	10.2 GAL.	(0.0386070 M^3)

Table V-17. Task II Study, Cooling Summary.

Item	Flight Condition				
	Takeoff Max.	Ground Idle	Max. Climb	Max. Cruise	Flight Idle
Case No.	1	4	7	8	9
PCNH	95.4	68.2	96.0	92.4	75.0
PCNL	96.9	27.6	96.2	100.4	61.6
<u>Heat Rejection</u>					
Basic Engine - Btu/min	1930	728	2154	1646	866
- joule/sec	33963.8	12811.2	37905.7	28966	15239.7
Thrust Bearing Adder -					
Btu/min	460	65	454	489	174
joule/sec	8095	1143.9	7989.4	8605.3	3062
Lube & Scav. Pump -					
Btu/min	682	348	691	640	422
joule/sec	12001.7	6124.0	12160	11262.6	7426.3
Planetary Gearbox -					
Btu/min	7892	839	7783	8481	3194
joule/sec	138882	14764.6	136963	149247	56207
Total Btu/min	10964	1980	11082	11256	4656
joule/sec	192943	34844	195019	198081	81936

Note: $PCNH = \frac{\text{Core Engine Speed x 100}}{14460}$

$PCNL = \frac{\text{Fan Speed x 100}}{2780}$

GE19/F6D

ORIGINAL PAGE IS OF POOR QUALITY

Table V-18. Task II Study, Bearing Summary.

MAIN SHAFT BEARINGS - VP ENGINES

FEATURES - MATERIAL CEVM-M50

CAGE MATERIAL - SILVER PLATED AMS6414

DESIGN BASED ON PROVEN PRACTICE

SUBSTANTIATED BY LAB TEST.

BEARING DATA

	POSITION	BORE MM	DN	CAPACITY #
DIRECT DRIVE	FAN THRUST BRG.	420	1.31×10^6	55700 (247766 N)
DIRECT DRIVE	LP ROLLER BRG.	119	$.37 \times 10^6$	17600 (78299 N)
DIRECT DRIVE & GEARED FAN	HP THRUST BRG.	133	2.0×10^6	21600 (96082 N)
DIRECT DRIVE & GEARED FAN	INTERSHAFT	119	1.4×10^6	15700 (69837 N)
GEARED FAN	FAN THRUST BRG.	420	1.11×10^6	55700 (247766 N)
GEARED FAN	LP TURB. THRUST BRG.	102	$.92 \times 10^6$	22400 (99640 N)

Actuation lubrication requirements are unusual in that grease, dry lubricants, and lubricant metal platings all have their place. Although the differential and all associated bearings require oil-mist lubrication, the main harmonic gear generator bearing, the spline teeth, the sector-unison gear mesh, the sector thrust bearing, and the counterweight system will all have various forms of dry lubricant. The ability to do this depends on the fact that all actuation speeds are very low (2 - 4 rpm) and very short (approximately 1 second). Some limited highly loaded thrust bearing testing has been done with grease lubrication and results are very encouraging.

VI - INSTALLATION AERODYNAMICS

SUMMARY

For Task II, the internal and external aerodynamic design of the three basic installations plus their four variations was made in much greater depth than in Task I. The broad categories of aerodynamic design are:

- inlet - fixed and variable geometry
- fan exhaust duct
- core exhaust duct
- reverser - conventional and variable pitch fan types
- variable nozzles
- external aerodynamics

Figures VI - 1 through 7 show all seven installations.

F2C1/F2C2/F2C3 Engine Installation Features

The reverse thrust configuration is shown below the centerline on Figures VI - 1 and 2. Key features for the 1.35 fan pressure ratio installations are listed in Table VI - 1. Detail discussion of each installation is given later in this Section.

Single Splitter Inlet

Acoustic attenuation is achieved by a combination of throat Mach number and treated walls, centerbody and splitter. The internal flowpath is designed for optimum axial Mach number distribution by appropriate area progression and wall slope design.

Partial Arc, Highly Skewed Cascade Thrust Reverser

For STOL, the reverser must be usable down to much lower runway speed than for CTOL. This means that reingestion from the same or from another engine and foreign objects or dust kicked up from the ground must all be prevented or minimized in the design. As a result, a combination of partial arc and skewing of the reverse flow efflux must be used. For the F2C1 and 2 engines, the arc is 190°, for the F2C3, 160° (see Figure VI - 3). Skewing serves to further confine the efflux to safe regions.

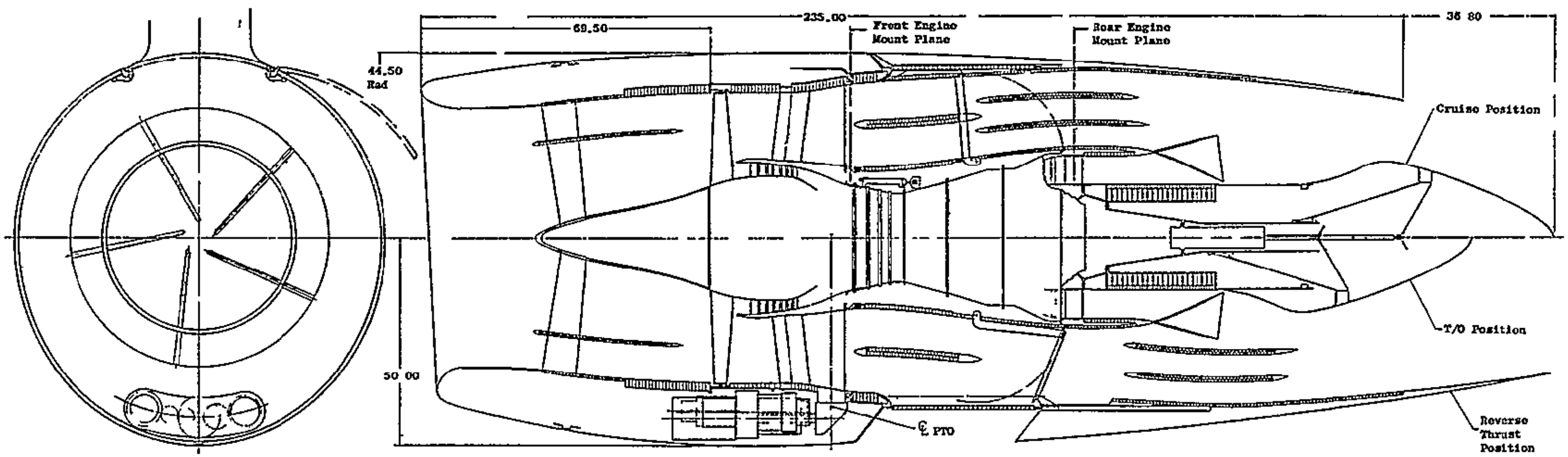

Figure VI-1. Task II GE19/F2C1 Installation.

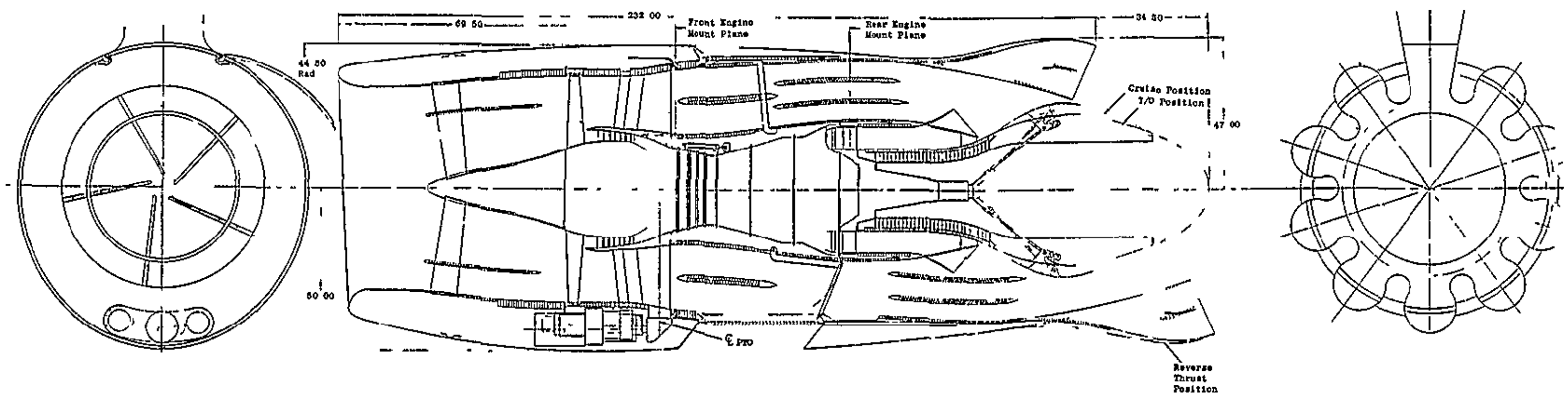

Figure VI-2. Task II GE19/F2C2 Installation.

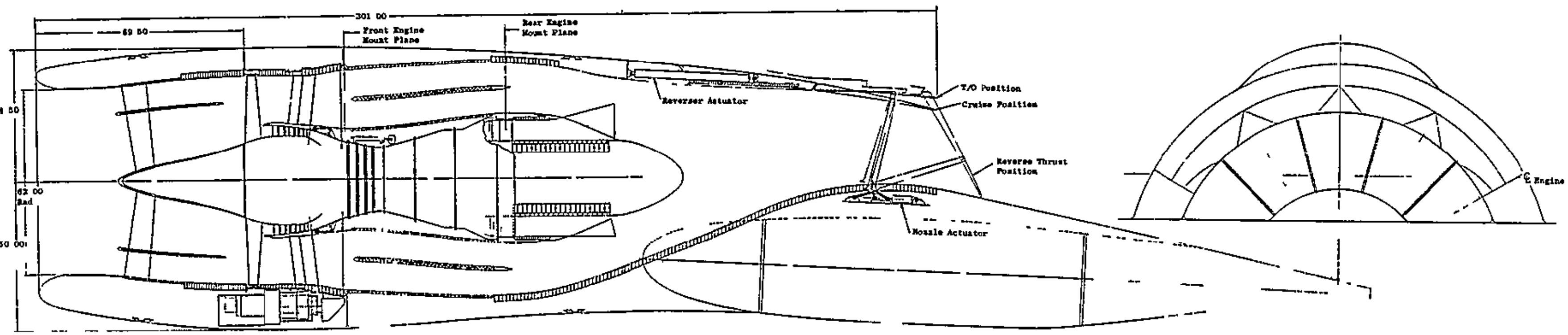

Figure VI-3. Task II GE19/F2C3 Installation.

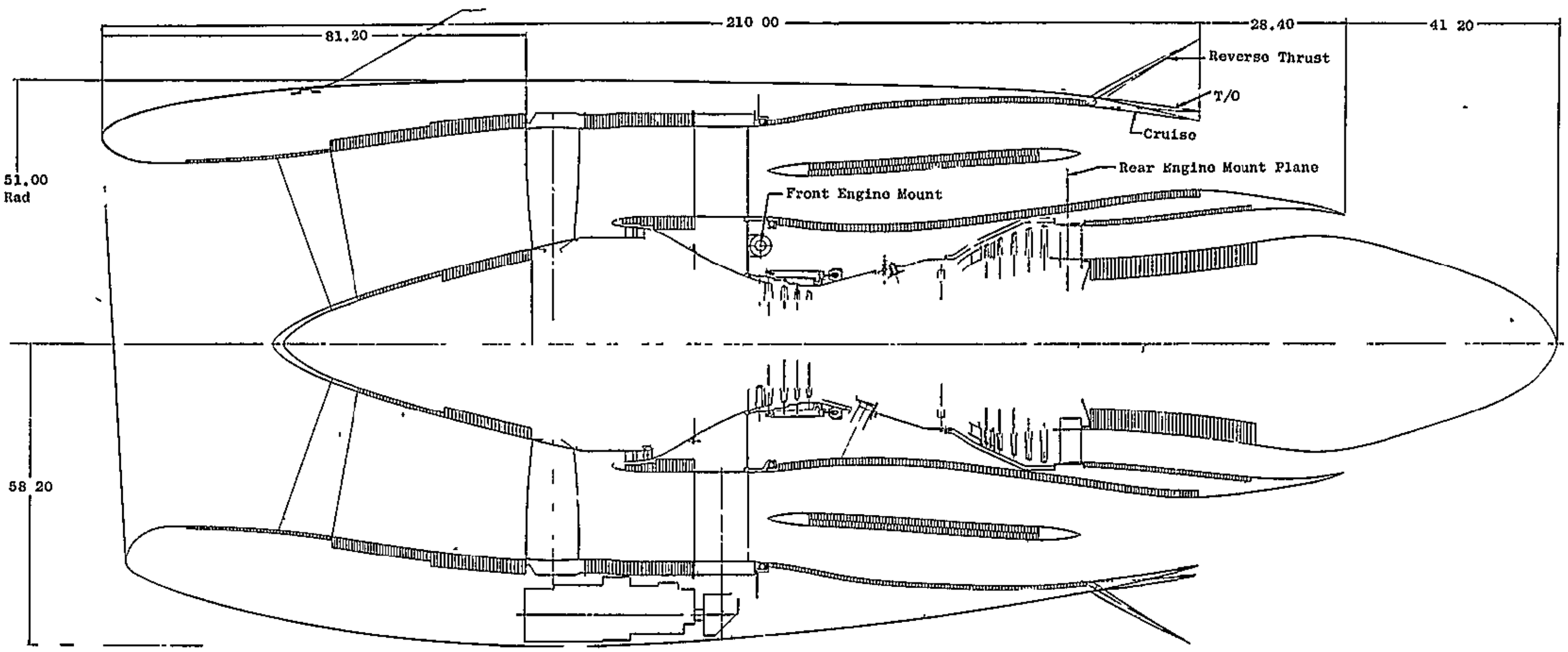

Figure VI-4. Task II GE19/F6E Installation.

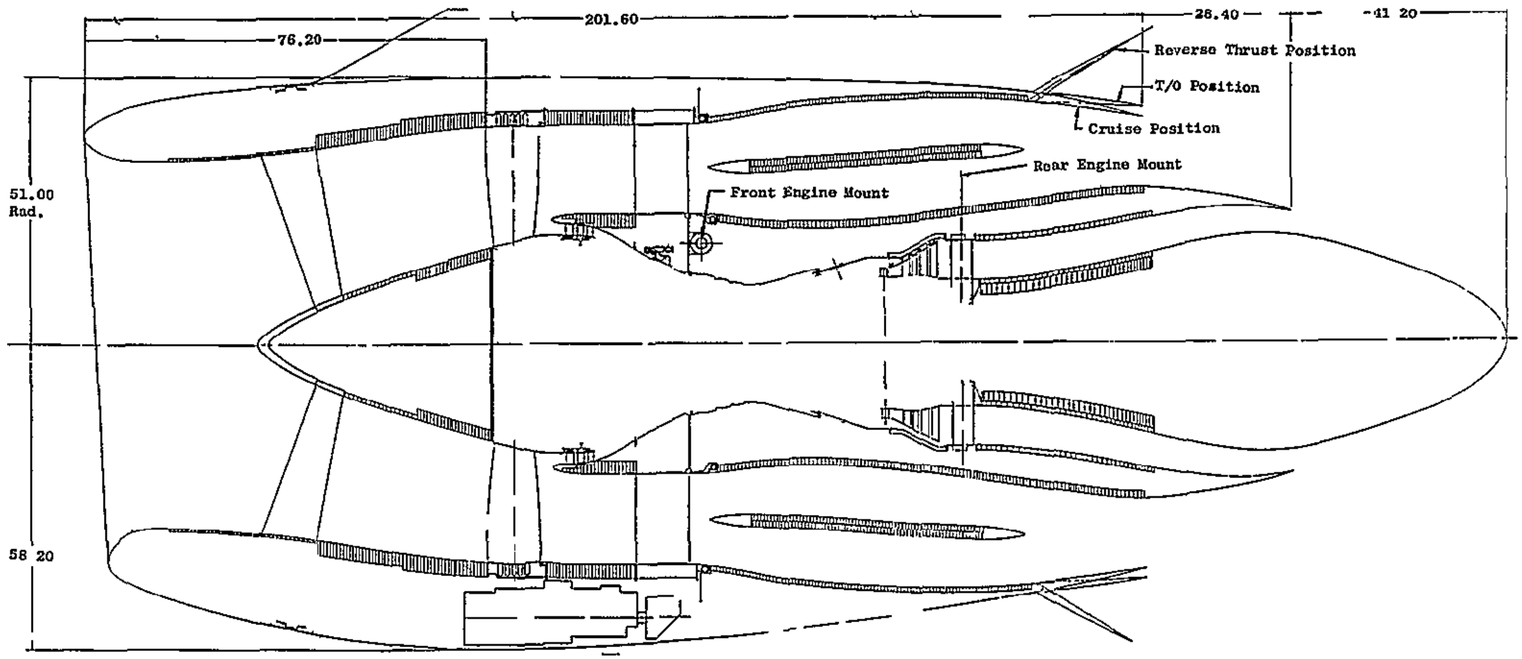

Figure VI-5. Task II GE19/F6D Installation.

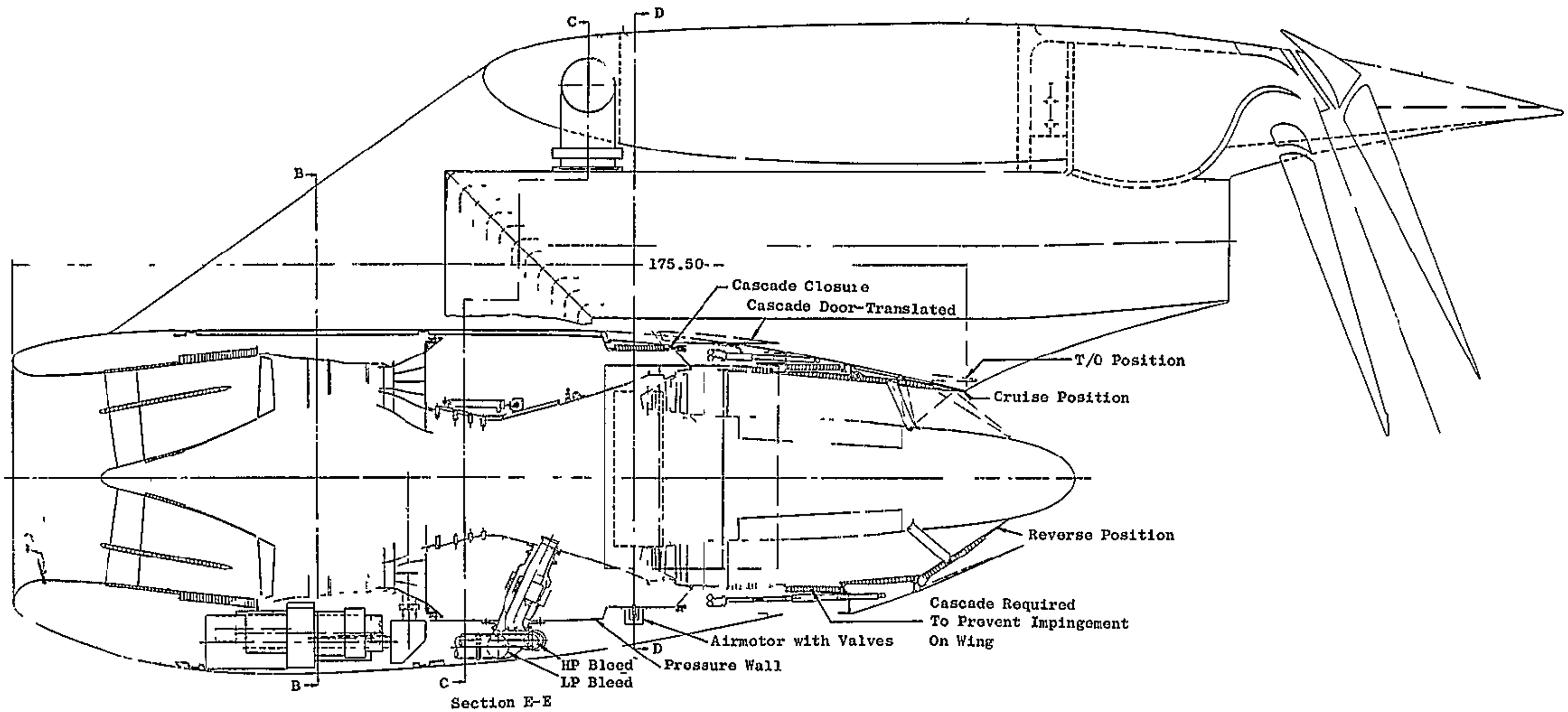

Figure VI-6. Task II GE19/F9A2 Installation.

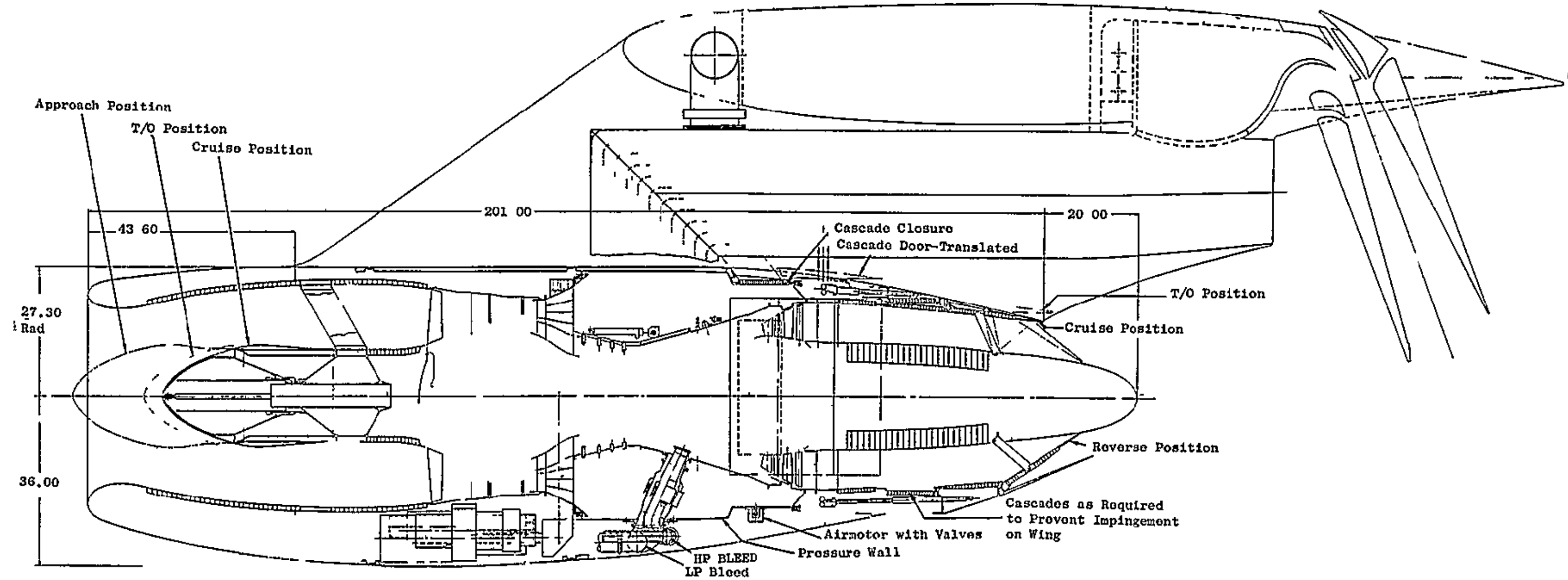

Figure VI-7. Task II GE19/F9A3 Installation.

Table VI-1. Task II Study, Key F2 Engine 1.35 P/P Aero/Acoustic Installation Features.

- INTEGRATED HIGH THROAT MACH AND SINGLE SPLITTER INLET
- PARTIAL ARC, HIGHLY SKEWED CASCADE THRUST REVERSER
- INTEGRATED T/R AND FAN EXHAUST SPLITTER DESIGN
- COMBINATION INTERNAL MIXER & CORE REVERSE THRUST SPOILER
- 2-POSITION EXHAUST NOZZLE
  - TRANSLATING PLUG (C - 1)
  - 9-LOBE EXTERNAL MIXER & EXPANDING PLUG (C - 2)
  - HINGED FLAP & T/R BLOCKER "D" NOZZLE (C - 3)

Integrated Thrust Reverser and Fan Exhaust Splitter Design

With fixed splitters in the exhaust, the flow in the inner part of the annulus would be prevented from reaching the cascades (F2C1 and 2 nacelles). The splitters have been grouped as shown, with the rear pair connected to the rearward sliding part of the nacelle (see the lower halves of the F2C1 and 2 drawings). Thus the flow to the cascades is not restricted.

Combination Internal Mixer and Core Reverse Thrust Spoiler

On the F2C1 and 2, where the fan stream only is reversed, the core nozzle area is greatly enlarged during reverse because of the absence of the 8:1 bypass flow. This area is only effective in spoiling thrust if the flow can fill it despite the short distance. The internal mixer provides the mixing capability.

Two-Position Exhaust Nozzle

On the F2C1 this is via a simple translating plug. On the decayer nozzle and expanding plug is used, to integrate with the geometry set by the lobes. On the F2C3 the blocker doors have conventional swinging links, as in the CF6/DC10 reverser, which are also actuated radially from the I.D. to provide variable exhaust area.

F6E/F6D Engine Installation Features

Table VI - 2 shows the key features of the 1.25 VP pressure ratio fan installations. The F6E1 and F6D1 installation drawings are shown in Figures VI - 4 and VI - 5, respectively. The only significant differences between the two nacelles are approximately 8" (20.32 cm) longer overall length for the direct drive engine and a slightly different core exhaust duct.

Inlet with Increased Throat Mach, Treated Wall and Fixed Centerbody Surfaces

This is similar to the F2 inlets, but requires no splitter because the fan source noise level is less.

Table VI-2. Task II Study, Key F6 Engine 1.25 P/P Aero/Acoustic Installation Features.

- INLET WITH INCREASED THROAT MACH, TREATED WALL AND FIXED CENTERBODY SURFACES
- COMBINATION 2 POSITION FAN EXHAUST NOZZLE AND REVERSE PITCH INLET
- SIMPLE FIXED GEOMETRY CORE INLET (ROUNDED LIP) FOR REVERSE PITCH OPERATION
- SIMILAR NACELLES (EXCEPT FOR CORE EXHAUST DUCT) FOR BOTH DIRECT (F6E) AND GEAR DRIVE (F6D)

Combination Two-Position Fan Exhaust and Reverse Pitch Inlet

For reverse flow, the exhaust flaps are opened as shown to provide a large area for the fan air inlet. It should be noted that the reverse flow is lower than normal flow because of blade geometry in negative pitch, and reduced core supercharge.

Simple Fixed Geometry Core Inlet for Reverse Pitch Operation

The flow to the core turns through 180° during reverse operation. The fan/core flow splitter has a large radius which results in a high contraction ratio, during reverse, similar to that of a bellmouth. This, combined with the ample axial spacing to the fan, and the essentially flat pitch of the blades near the hub, is designed to ensure good core inlet flow conditions with reverse pitch.

F9A2/F9A3 Engine Installation Features

Table VI - 3 lists the key features of the 3.0 fan pressure ratio augmenter wing engine installations. Figure VI - 6 shows the F9A2 engine installation and Figure VI - 7 shows the F9A3 engine installation.

Single Splitter Inlet

This inlet is similar to the F2 series inlets.

Alternate Translating Plug High Throat Mach Inlet

This inlet achieves the same attenuation as that on the F9A2 by high axial MN and wall treatment. The MN is maintained at a value of 0.82 at approach power settings by reduced throat area with the centerbody translated forward. For takeoff the MN is increased to 0.92 to attenuate the higher source noise level.

Table VI-3. Task II Study, Key F9 AW Engine Aero/Acoustic Installation Features.

- INTEGRATED HIGH THROAT MACH AND 1-SPLITTER INLET
- ALTERNATE TRANSLATING PLUG HIGH THROAT MACH INLET
- FAN EXHAUST (WING FLOW) COLLECTOR AND DIFFUSER DUCT WITH SELF-CONTAINED PISTON FORCE
- PARTIAL ARC HIGHLY SKEWED FAN EXHAUST THRUST REVERSER
- COMBINATION 2-POSITION CORE EXHAUST NOZZLE AND CORE THRUST SPOILER

Fan Exhaust Collector and Diffuser Duct with Self-Contained Piston Force

The fan flow is collected in a constant-area annulus pressure vessel formed by the core engine casing and the nacelle skin. The air is ducted circumferentially to a flange on top of the nacelle to which the wing flow duct is bolted, thus avoiding development of a large piston force. Horizontal piston forces are also avoided by suitable choice of annular areas of the connections between engine and nacelle.

Partial Arc Highly Skewed Fan Exhaust Thrust Reverser

Similar to the F2 reverser.

Combination Two-Position Core Exhaust Nozzle and Thrust Spoiler

An adaptation of the system used on the F2C3 is provided. It is necessary to spoil the core thrust for the low bypass ratio F9 engine to get adequate reverse thrust. The arrangement is similar to that on the CF6/DC10.

Tables VI - 4 through VI - 11 show various summarized data for all seven installations. Tables VI - 6 through 9 are self-explanatory; however, further details on Table VI - 4 and VI - 5 will be found later in this Section. Table VI - 10 summarizes the estimated reverser performance. The second line shows the various amounts of core thrust for the different systems. On the F2C1 and 2 the -0.28 value represents the residual forward thrust from the dumping effect of the large increase in nozzle area. On the F2C3 both streams are reversed so that the core and fan have the same value. On the F6 the core has full available forward thrust (less than normal, because of reduced supercharge), while on the F9 the thrust is assumed to be fully spoiled. The range of values quoted for the F6 reverse thrust stems from the uncertainty of reverse pitch performance, including the effect of blade camber which is different depending on the direction of blade movement from forward to reverse pitch. The last line shows the additional force from ram drag. Table VI - 11 presents a representative set of reverse mode noise levels. The amount of

Table VI-4. Task II Study, "Internal" Installation Losses.

Typical EBF Engine

Over-The-Wing

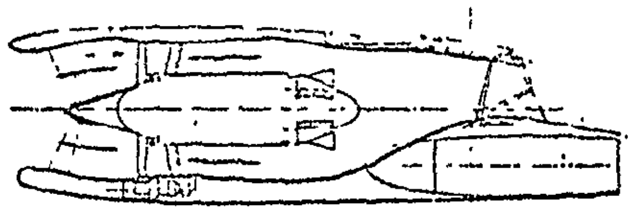

Inlet

- Lip & wall surfaces treated & non-treated
- Splitter surfaces
- Splitter profile drag
- Splitter support strut drag
- Splitter/strut interference drag

Fan Exhaust

- Wall & pylon surfaces, treated and non-treated
- Splitter surfaces
- Splitter profile drag
- Frame & tip & support strut & interference drag
- T/R mechanism & leakage
- Mixer
- Non-symmetric duct shapes
- Exhaust nozzle

Core Exhaust

- Wall and centerbody plug surfaces (treated & non-treated)
- Frame & support strut drag
- Mixer

Table VI-5. Task II Study, Installation Losses, Inlet, Fan Exhaust, and Core Exhaust.

$\Delta P_T/P_T$ @ T/O POWER

	INLET	FAN EXHAUST	CORE EXHAUST
• F2C1 EBF	1.00	2.11	0.79
• F2C2 EBF & DECAYER	1.00	3.61	0.79
• F2C3 OTW	1.00	1.64	0.64
• F6E1 DIRECT DRIVE	0.67	1.06	1.68
• F6D1 GEARED DRIVE	0.65	1.06	1.68
• F9A2	1.3	4.0*	1.03
• F9A3 ALTERNATE INLET	1.27	4.0*	1.03

* SELECTED DUCT LOSSES FROM EXHAUST GUIDE VANE EXIT INTO PYLON

Table VI-6. Task II Study, Nacelle Drag - Maximum Cruise, % of Max. Cruise Thrust @ 0.8 Mach, 30,000 ft (9.1440 km).

	$D_{FRICTION}$	$D_{PRESSURE}$	D_{SCRUB}	NET DRAG
• F2C1 - EBF	5.2	3.0	0.8	9.0%
• F2C2 - EBF & DECAYER	6.7	3.0	1.0	10.0%
• F2C3 - OTW	6.6	2.3	0/4.0*	8.9/12.9%
• F6E1 - EBF - O.D.	7.7	5.6	2.8	16.1%
• F6D1 - EBF - O.D.	7.4	5.8	2.8	16.0%
• F9A2 - A/W	0.7	1.0	1.7	3.4%
• F9A3 - A/W & ALT. INLET	0.8	1.0	1.7	3.5%

* ESTIMATED WING SCRUBBING DRAG

Table VI-7. Task II Study, Major Nacelle Dimensions.

(INCHES)

	INLET LENGTH	MAX DIA.	ACCESSORY BULGE	COWL LENGTH	O.A. LENGTH
F2C1 - EBF	69.5 (176.93 cm)	89 (226.06 cm)	5.5 (13.97 cm)	235 (596.9 cm)	251.8 (639.6 cm)
F2C2 - EBF & DECAYER		89/94 (226.06 cm/238.76 cm)		232 (589.3 cm)	266.5 (676.9 cm)
F2C3 - OTW				301 (764.5 cm)	301 (764.5 cm)
F6E1 - EBF (DD)	81.2 (206.2 cm)	102 (259.1 cm)	7.2 (18.3 cm)	210 (533.4 cm)	279.6 (710.2 cm)
F6D1 - EBF (GD)	76.2 (193.5 cm)			201.6 (512.1 cm)	271.2 (688.8 cm)
F9A2 - A/W	41.8 (106.2 cm)	54.6 (138.7 cm)	8.7 (22.1 cm)	174.6 (189.5 cm)	194.6 (494.3 cm)
F9A3 - A/W & ALT INLET	71.2 (180.8 cm)			201 (510.5 cm)	221 (561.3 cm)

Table VI-8. Task II Study, Inlet Design Features.

	$\frac{D_{Highlight}}{D_{Throat}}$	$\frac{D_{Highlight}}{D_{Max}}$	Lip Shape	Ave. Throat Mach @ T/O	Ave. Throat Mach @ MxCr	$\frac{L_{Spinner}}{D_{Fan}}$	Splitter Length/L_{treat}/thickness
F2C1 - EBF	1.14	0.80	2.2 Elipse	0.75	0.75	0.6	36"/32"/0.87" (91.4cm/81.3cm/2.2cm)
F2C2 - EBF & DECAYER	↓	↓	↓	↓	↓	↓	↓
F2C3 - OTW	↓	↓	↓	↓	↓	↓	↓
F6E1 - EBF (DD)	↓	0.78	↓	0.70	0.825	↓	—
F6D1 - EBF (GD)	↓	↓	↓	0.68	0.785	0.525	—
F9A2 - A/W	↓	↓	↓	0.775	0.775	0.65	24.8"/21.75"/0.7" (63.0cm/55.2cm/1.8cm)
F9A3 - A/W & ALT INLET	↓	↓	↓	0.92	0.92	—	—

Table VI-9. Task II Study, Fan and Core Exhaust Design Features.

	Aft Fan Suppression Design	Ave. Duct Mach No.	Exhaust Nozzle Design	Boattail* Chordal/ Trailing Edge	Comments
F2C1 - EBF	Wall treatment + one 1.9" (4.8 cm) thick (22.8") (57.9 cm) long splitter + two (32") (81.3 cm) 1.2" (3.0 cm) thick splitters	0.45	Mixed flow, 2-pos. translating plug	6°/12°	Cowl length set by internal mixing length req (60%)
F2C2 - EBF & DECAYER	"	"	Mixed flow, 2-pos. expanding plug	18° Max. (between lubes)	"
F2C3 - OTW	Wall treatment + one 1.32" (3.4 cm) thick 45" (114.3 cm) long splitter	"	Mixed flow "D" nozzle, 2-position cowl nozzle & T/R blocker door	6°/12°	Cowl length set by boattail angle and nozzle reverser mechanical design
F6E1 - EBF (DD)	Wall treatment + one 2.5" (6.4 cm) thick 40" (101.6 cm) long splitter	"	2-position fan nozzle, auxiliary inlet design + fixed core nozzle	4°/12°	Cowl length set by splitter & fan nozzle design
F6D1 - EBF (GD)	"	"	"	" "	"
F9A2 - A/W	Wall treatment	0.35	Translating cowl 2-position core plug nozzle & core thrust spoiler	5°/12°	Cowl length set by core treatment and thrust spoiler design
F9A3 - A/W & ALT INLET	"	0.35	"	5°/12°	"

* Chordal boattail angle refers to the angle formed by a straight line drawn from the nacelle max. dia. point to the nozzle trailing edge. Trailing edge boattail angle refers to the angle at the trailing edge of the nacelle cowling.

ORIGINAL PAGE IS OF POOR QUALITY

Table VI-10. Task II Study, Thrust Reverser Design Features.

	F2C1 & C2 (EBF)	F2C3 (OTW)	F6D1 & E1 (EBF)	F9A2 & A3 (A/W)
Fan Stream Reverse Thrust Coeff.*	0.46	0.35	0.25 - 0.6	0.44
Core Stream Reverse Thrust Coeff.*	-0.28 (Thrust Spoiling)	0.35	-0.85 - 0.75 (No T/R or Spoiler)	0.0 (Spoiler)
Net Engine Reverse Thrust/Static Thrust				
- Static (W/O Reingestion)	35%	35%	19 - 52%	35%
- 40 Kts (Relative to Static Thrust)	39%	39%	24 - 57%	39%

* Actual reverse gross thrust/normal ideal thrust.

Table VI-11. Task II Study, Reverse Thrust Operation.

	F2C1 & C2 (EBF)	F2C3 (OTW)	F6D1 & E1 (EBF)	F9A2 & A3 (A/W)
REVERSE THRUST NOISE - 500 FT S.L.	100	97	95	120
ENGINE REVERSE POWER SETTING	75%	85	55%	90%
AIRCRAFT POWER LOADING	0.615	0.5	0.615	0.4
NET ENGINE REVERSE THRUST	0.21g	0.20g	0.21g	0.15g
AIRCRAFT BRAKE & DRAG DECEL. FORCE FOR 0.35G	0.14g	0.15g	0.14g	0.20g
RUNWAY FRICTION FACTOR	.12 - .14 (WET)	.13 - .15 (WET)	.12 - .14 (WET)	.18 - .2 (DRY)
% MAX. BRAKE FORCE FOR NORMAL FRICTION FACTOR	40	40	50	60

reverse thrust shown requires no more braking than that obtainable from a wet runway, when the reverse noise is nearly the same as the forward noise at 500 ft. sideline, except for the F9 engine. Here the noise level is much higher despite the use of more braking. This is, of course, a result of the 3.0 fan pressure ratio and correspondingly high jet velocity.

Figure VI - 8 shows a typical time history of a ground roll with reverser deployed fully, 1 second after touchdown. It is assumed that the reverser would be retracted by the time a taxi speed of 15 knots (7.72 m/sec.) has been reached. It is seen that a typical noise duration, consistent with 2000° (609.6 m) STOL, for reverse thrust is 8 seconds.

Additional noise during reverse thrust operation has frequently been identified as a potential problem. Since reverse thrust operational requirements, such as: (1) engine power setting during reverse thrust, (2) duration of reverse thrust, (3) aircraft ground speed during reverse thrust can influence the level of reverse thrust noise, an attempt was made to explore the influence of some of these effects. Figure VI - 9 shows how reducing engine power setting during reverse thrust reduces reverse thrust noise at the 500 ft. (152.4 m) sideline location. In this exercise the airplane deceleration rate was kept constant at 0.35 g by assuming an increase in airplane wheel braking force. Since braking force is also a function of runway conditions, two scales have been included in this figure. The first scale assumes full braking force on a variety of runway surfaces, extending from an icy surface with a friction factor of ~ 0.05 out to a dry runway with a friction factor of 0.35. Note that to maintain a 0.35 deceleration rate on an icy surface requires maximum engine power and therefore maximum reverse thrust noise. However, in the case of a dry runway, the 0.35 acceleration g

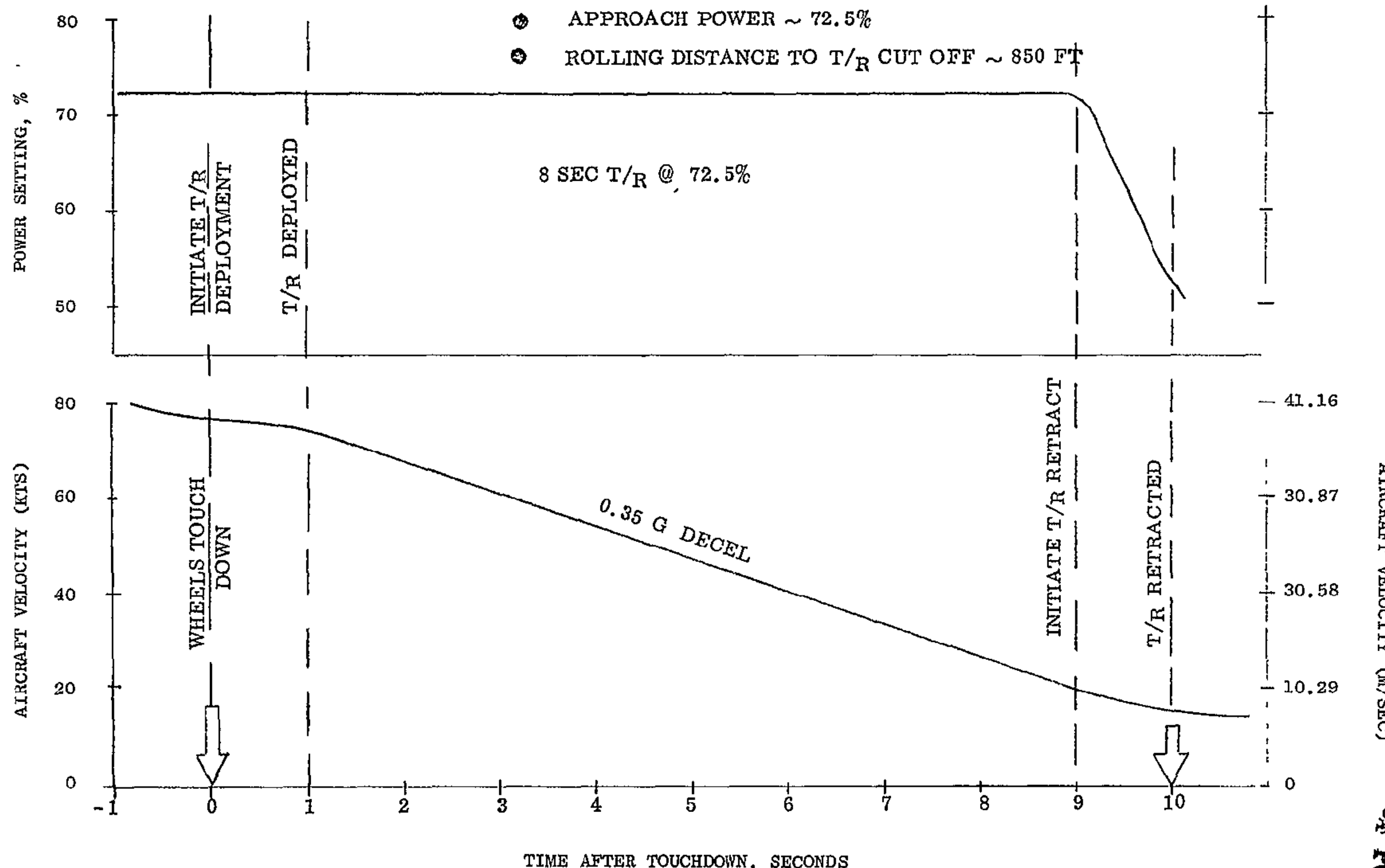

Figure VI-8. Task II Representative F2C1 & C2 Reverse Thrust Transient Characteristics.

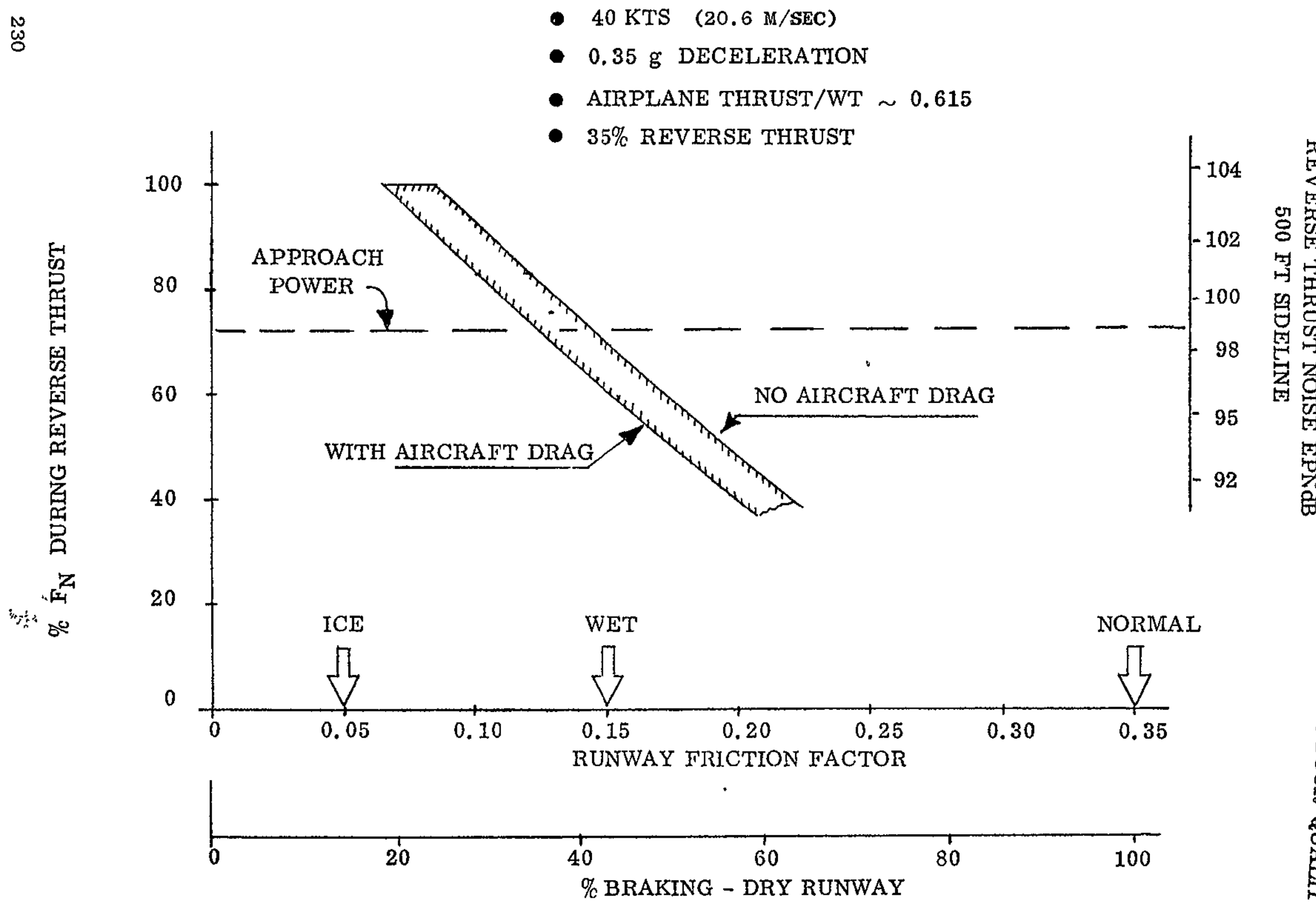

ORIGINAL PAGE IS OF POOR QUALITY

Figure VI-9. Task II F2C1 & C2 (EBF) Reverse Thrust, Noise, and Aircraft Brake Trades.

rate can be exceeded with no reverse thrust. The second scale indicates the fraction of the dry runway braking force required to maintain the 0.35 g deceleration rate.

Reverse thrust noise need not be a problem unless an icy runway condition is encountered. On this figure use of approach power during reverse results in 99 PNdB noise, a braking coefficient of about 0.13 corresponding to 37% of maximum braking (taken as 0.35) which means that this performance could be achieved on a dry or wet runway, but not on an icy runway. The shaded area is for constant 0.35 g deceleration, representative of a passenger comfort limit. The "aircraft drag" line is for a 0.25 C_D corresponding to a D/W of 0.017 and is thus a small effect.

Reverse thrust trend curves of the type shown in Figure VI - 9 were generated for each QCSEE engine to serve as a guide in selecting a representative reverse thrust engine power setting.

DESIGN DETAILS

This more detailed technical discussion reviews the major aerodynamic and performance factors considered in the definition of these seven QCSEE Task II nacelle design concepts.

F2C1

The cross section shown in Figure VI - 1 illustrates all of the major aerodynamic and acoustic design features of this EBF engine nacelle.

The inlet concept selected utilizes a combination of throat region Mach number and acoustic treatment to provide the required suppression of forward-radiated fan noise at takeoff. The acoustic treatment surface areas provided by the single splitter and fixed treated centerbody provides adequate suppression of the approach fan noise.

In addition to satisfying these inlet noise suppression requirements, this single splitter and treated centerbody combination was found to be an excellent compromise between inlet flowpath and recovery considerations, as well as mechanical design and weight considerations.

In formulating this inlet design concept, considerable attention was given to the promising aerodynamic and acoustic results published in (1) Monthly Reports from NASA Contract No. NAS3-15574 "Investigation of Noise Suppression by Sonic Inlets for Turbofan Engines" and (2) NASA Preliminary Data Report "Low Speed Wind Tunnel Investigation of the Aerodynamic and Acoustic Performance of a Translating Centerbody Choked Flow Inlet," by Brent Miller, et al.

The five struts shown supporting the centerbody and the splitter are positioned so as to minimize unfavorable acoustic and aerodynamic interference with the fan. The untreated portion of the centerbody, the leading edge of the splitter and the struts all have provisions for withstanding nominal bird strikes and anti-icing.

Because of the relatively high inlet throat region Mach numbers called for at T/O, attention was given tailoring the inlet wall contours and flowpath. The area distribution shown in Figure VI-10 shows modest wall angles and relatively gradual diffusion from the throat to the fan face. An effort was made to keep the average Mach number over the splitter in the 0.6-->0.65 range and to limit the average Mach number over the support struts to the 0.65-->0.68 range. The inlet lip shapes shown are larger than used in today's CTOL aircraft like the DC-10, in order to accommodate the more extreme inlet incidence angles anticipated for STOL aircraft. The inlet lip sizes (indicated by the ratio of highlight to throat diameter $\sim D_{hl}/D_t$) shown are 1.14 on the top and 1.2 on the bottom (where the local inflow incidence angles are expected to be the greatest).

The estimated inlet recovery characteristics are shown in Figure VI-11. It is anticipated that the relatively generous inlet lip shapes proposed will provide fully developed inlet flow at the relatively low flight speed of 80 knots (41.16 m/sec.). Therefore, inlet recovery at flight speeds of 80 knots (41.16 m/sec.) or greater will be primarily a function of corrected flow as indicated. Since the lower Reynolds numbers expected at 30,000 ft. (9144 m) alt. cruise will result in a slightly higher loss. An equation has been included to relate T/O and cruise inlet recoveries.

Considerable attention was given to formulating a fan exhaust duct splitter arrangement that would satisfy aft-radiated fan noise suppression requirements and thrust reverser design requirements while retaining a

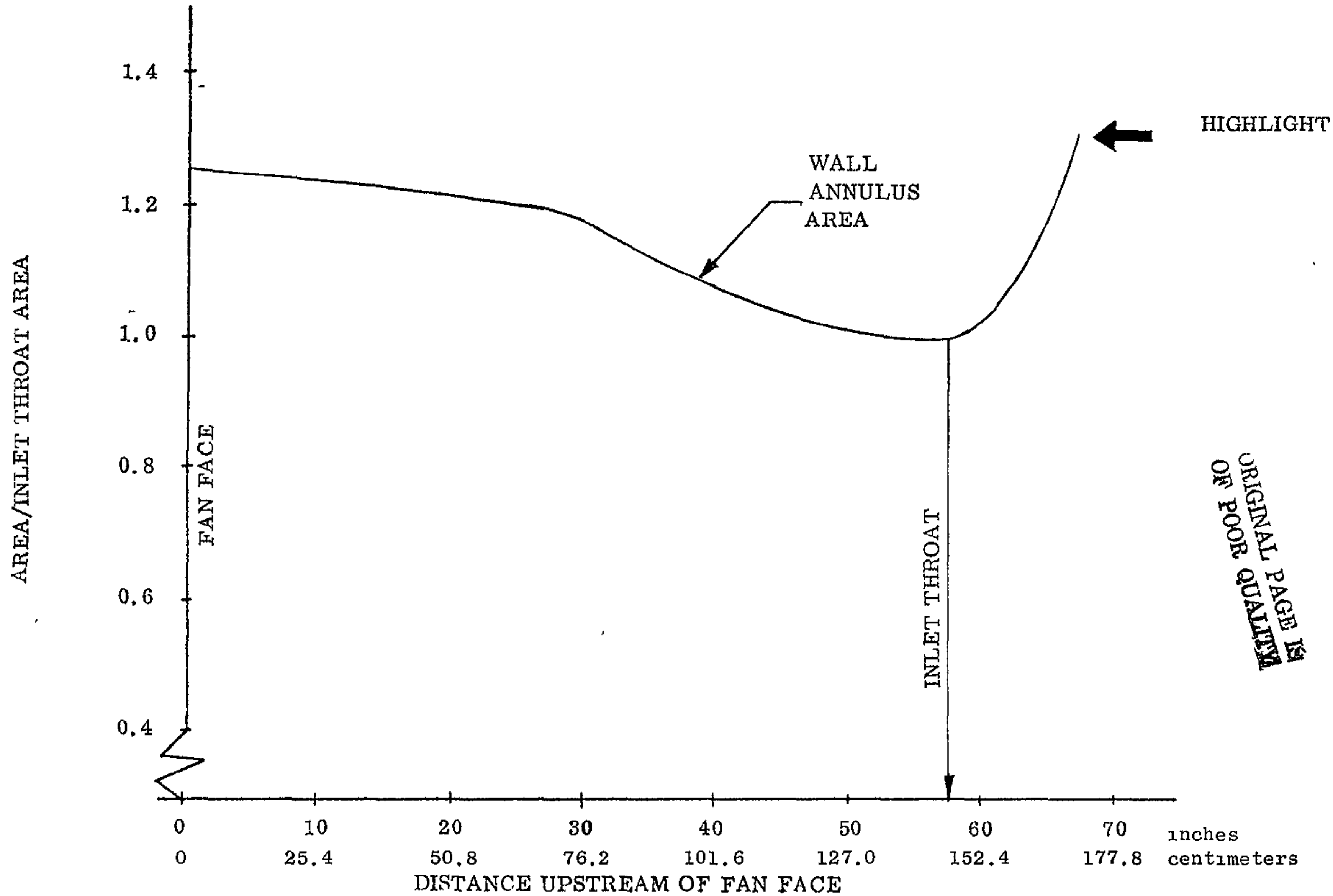

Figure VI-10. Task II F2C Inlet Area Distribution, Throat Area = 3005 inch^2 (3011.5 cm^2).

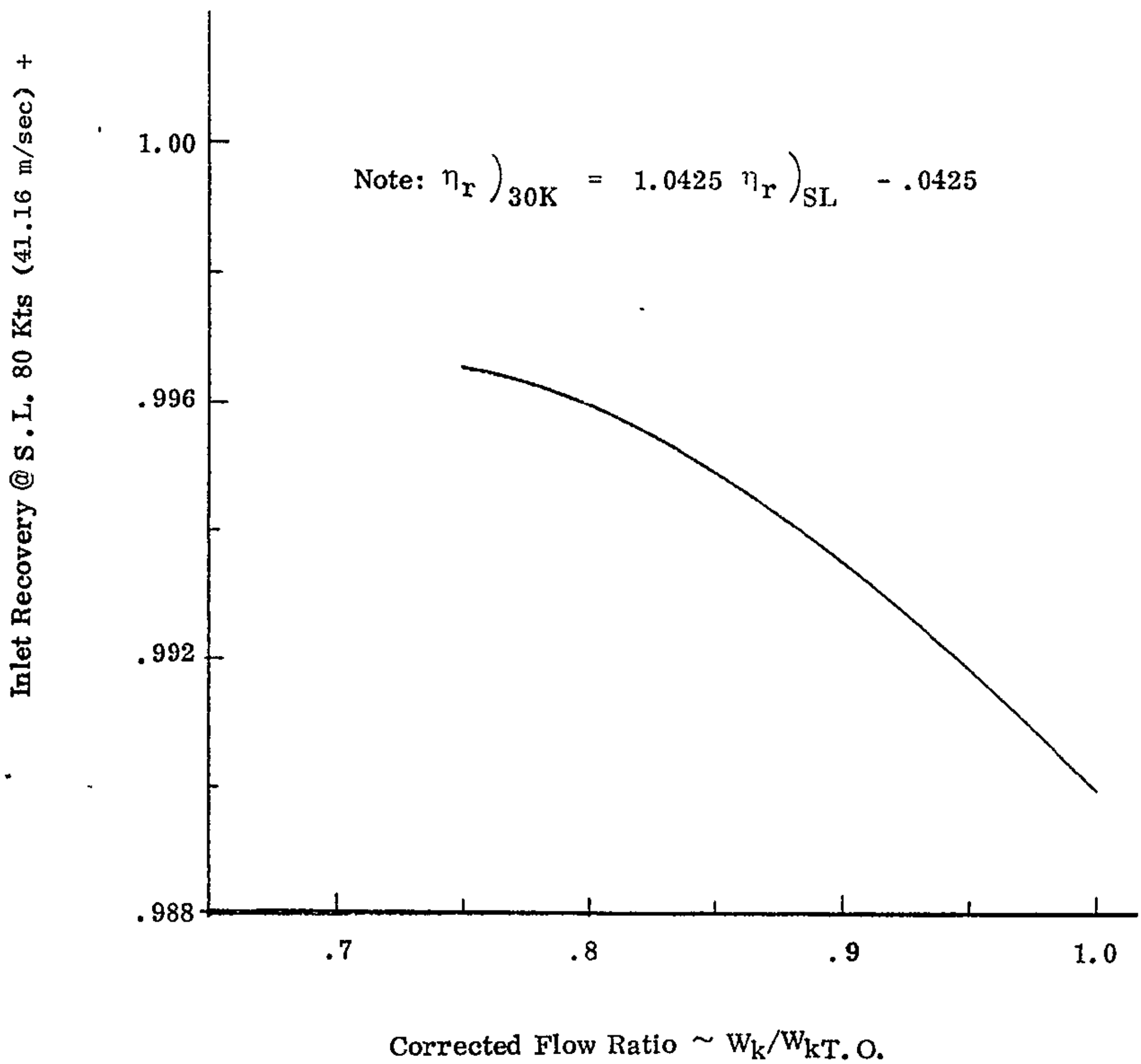

Figure VI-11. Task II GE19/F2C Inlet Recovery Vs. Corrected Flow.

reasonably low loss aerodynamic flowpath. The combination single and double splitter arrangement, with the 2 aft splitters mounted on the translating cowl section was found to be an effective solution.

Previous fan exhaust duct aero/acoustic design experience on systems like the TF-34 Quiet Engine Program have shown that satisfactory aft suppression levels could be achieved with duct designs having average Mach numbers in the 0.35 to 0.5 range. The lower Mach portion of this range tends to provide more effective acoustic suppression providing uniform flow properties are maintained. However, the combined influence of the following factors (1) fan exhaust guide vane exhaust Mach number of ~0.5 (2) the large portion of the duct annulus area blocked by the acoustically treated splitters (3) the duct flow area blockage of the pylon, (4) the space required to accommodate the fan stream thrust reverser, all make it impossible to diffuse the flow down to the lower Mach number region without resorting to excessively high wall angles or increasing nacelle duct diameter and length. The area distribution shown in Figure VI - 12 and the resulting average one dimension Mach number distribution shown in Figure VI - 13 represent what is believed to be a good "systems" balance between all these design considerations. To help illustrate the duct flow area blockage considerations, Figure VI-12 shows a breakdown of the splitter and pylon blockage areas along the length of the fan exhaust duct. The 0.45 duct Mach number indicated in Figure VI - 13 was selected as a target value to be used as a guide in configuring this duct design.

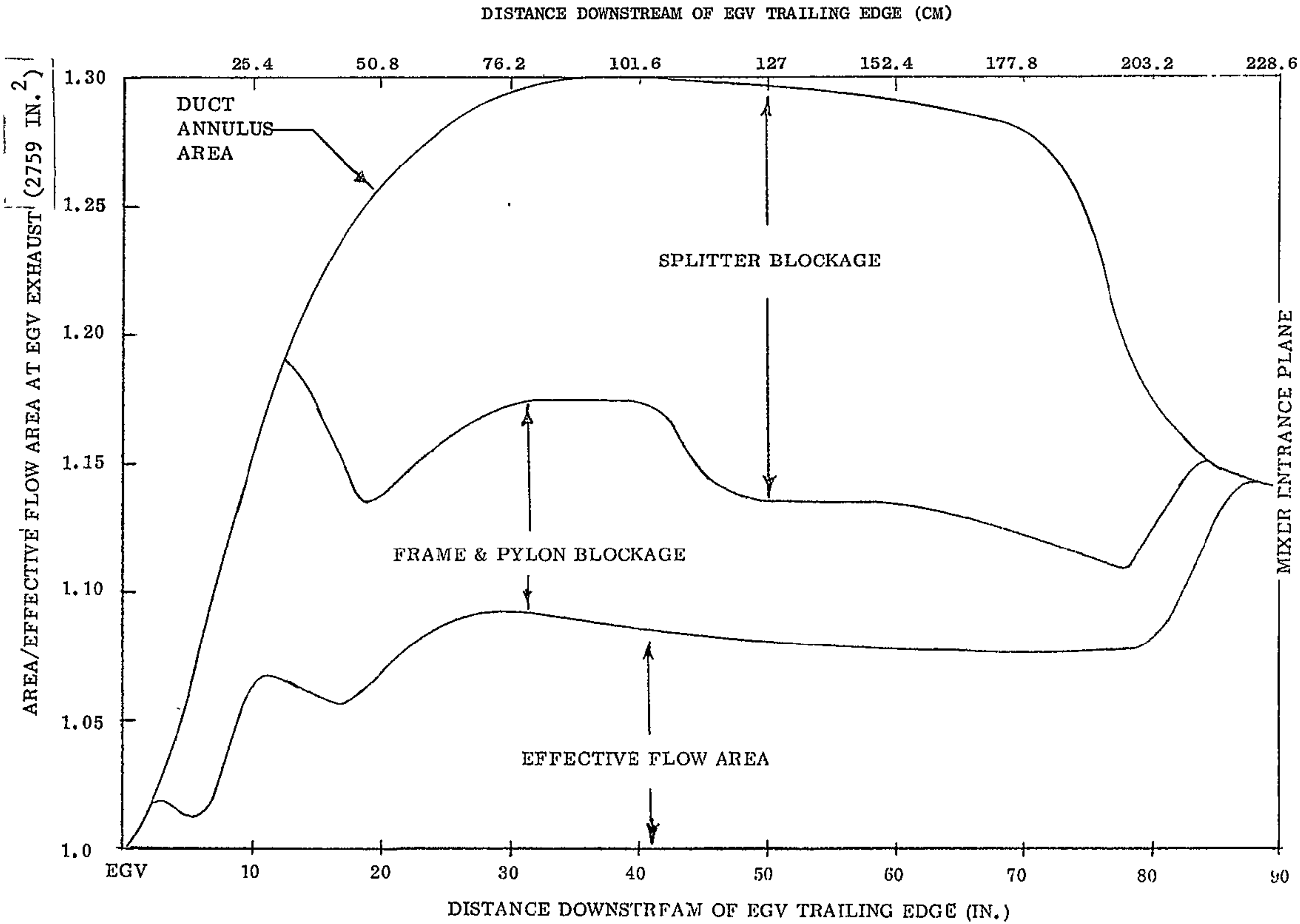

Figure VI-12. Task II GE19/F2C1 & C2 Fan Exhaust Area Distribution.

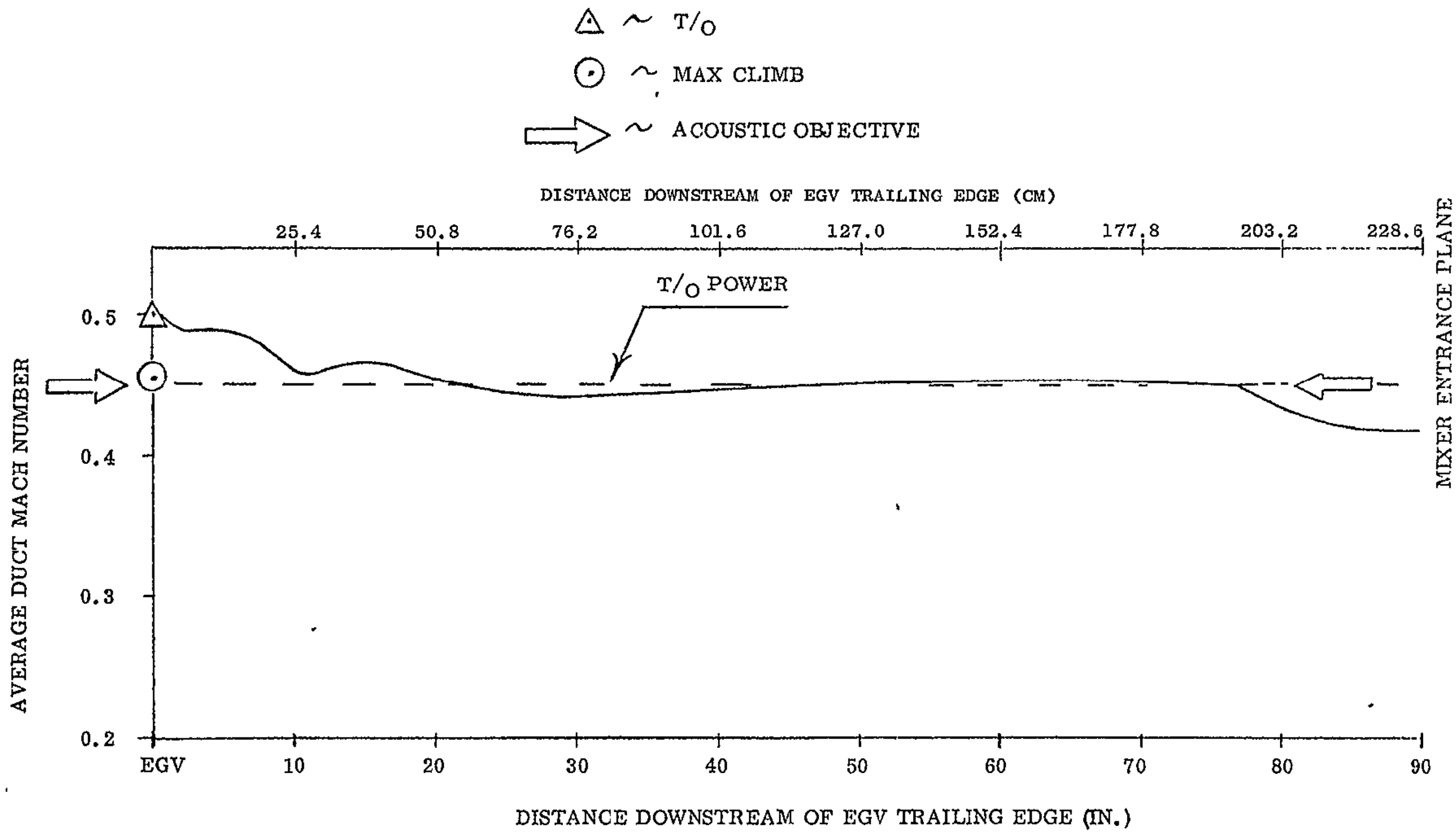

Figure VI-13. Task II GE19/F2C1 & F2C2 Fan Exhaust Duct Mach Number Distribution.

The inlet and exhaust area and Mach number distributions were used to estimate internal losses. A detailed breakdown of the inlet fan and core exhaust losses is listed in Table VI - 12, at the important takeoff condition. A nominal multiplyer of 1.375 was used to compute the additional skin friction drag on acoustically treated duct surfaces.

In order to gain additional insight about thrust reverser utilization vs. thrust reverser noise, a simple airplane braking study was carried out to examine these effects. The trend curve shown in Figure VI - 9 illustrates the trades between engine-provided braking force and airplane braking force (runway friction) required to retain the 0.35 g deceleration level indicated in the Task II study guidelines. As expected, the lower engine power setting during reverse thrust produce significantly lower noise. However, these lower power settings call for more airplane breaking force, which may be achieved by either a better runway surface condition or (for normal dry runway surfaces) utilizing more of the brakes' capability (at some expense in airplane brake life). At this point in time it is not clear where the best compromise between all these factors lies.

The cascade thrust reverser designed to provide the 35% static reverse capability (no reinjection) at aircraft speeds down to 15 knots (7.72 m/sec.) requires a great deal of tailoring of the reverse efflux. The representative cascade efflux pattern selected for the F1 and F2 engines is shown in Figure VI-14.

Table VI-12. Task II Study, GE19/F2C1 (EBF) Installation Loss Breakdown at $\Delta P_T/P_T$ % at T.O. Power.

INLET	
• Lip	.09
• Hardwall and Suppression	.40
• Splitters	.39
• Strut	.03
• Spinner	.07
• Interference	.02
• Total	1.00
FAN DUCT	
• Hardwall and Suppression	.67
• Splitters	1.02
• Strut	.08
• Reverser	.14
• Interference	.20
• Decayer	-
• Nonsymmetric Duct	-
• Total	2.11
• Nozzle Gross Thrust Coefficient ~ C_V	.996
CORE	
• Hardwall and Suppression	.70
• Strut	.09
• Reverser	-
• Total	.79

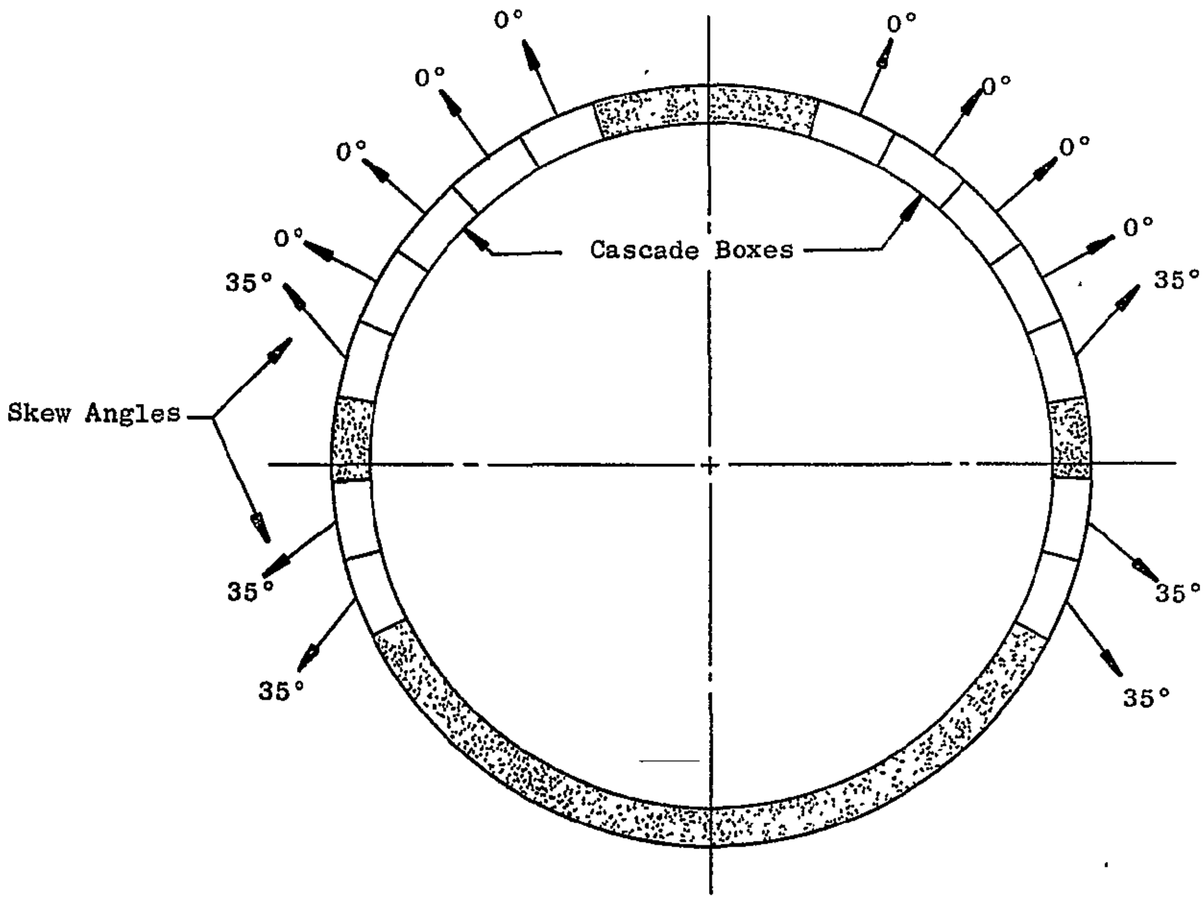

Figure VI-14. GE19/F2C1 & C2 (EBF) Reverse Flow Efflux Pattern.

F2C2

The F2C2 nacelle has the same inlet fan exhaust and thrust reverser as the F2C1. However, it has an external mixer or "decayer" nozzle system, designed to reduce engine exhaust flap interaction noise. The key new feature of this nacelle design concept is shown in Figure VI-2.

The internal mixer lobes have been modified to get more uniform mixing of the fan and core exhaust streams inside the 9 large lobes. Care was taken in positioning these mixing lobes to accommodate a representative EBF engine pylon and to avoid scrubbing the pylon surface with exhaust (to avoid extra scrubbing noise).

The estimated velocity decay characteristics (neglecting the influence of aircraft interference) at static and at 80 knot (41.16 m/sec.) flight speeds are shown in Figure VI-15. Since a design distance for velocity decay level has not been specified, a representative velocity decay ratio (V'/V = 0.88) at 200 inches (508 cm) from the exhaust plane, at 80 kts (41.16 m/sec) flight speed was selected. Task I design experience revealed that velocity decayers designed to give velocity ratios in the 0.5--->0.7 range produced uneconomic designs.

The detailed breakdown of the F2C2 nacelle installation losses shown in Table VI-13 are practically identical to those of the F2C1 with the exception of the decayer duct losses (1.5%) and an incremental loss in exhause nozzle gross thrust coefficient.

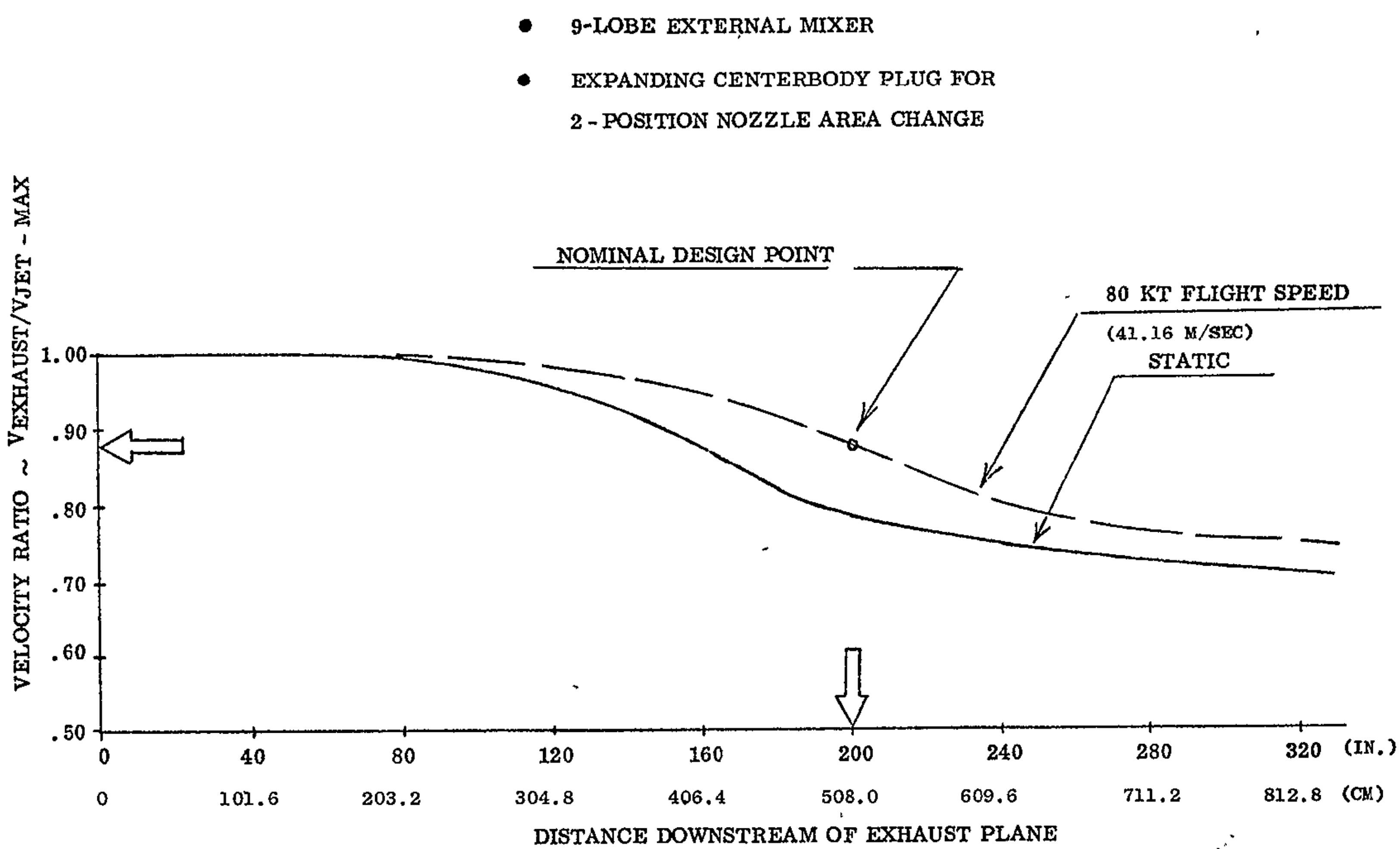

Figure VI-15. Task II GE19/F2C2 Exhaust Velocity Decay Characteristics (Max. Exhaust Velocity Ratio Vs. Distance from Exhaust Plane).

Table VI-13. Task II Study, GE19/F2C2 (EBF & Decayer Installation Loss Breakdown at $\Delta P_T/P_T$ % at T.O. Power.

INLET

•	Lip	.69
•	Hardwall and Suppression	.40
•	Splitters	.39
•	Strut	.03
•	Spinner	.07
•	Interference	.02
•	Total	1.00

FAN DUCT

•	Hardwall and Suppression	.67
•	Splitters	1.02
•	Strut	.08
•	Reverser	.14
•	Interference	.20
•	Decayer	1.5
•	Nonsymmetric Duct	-
•	Total	3.61
•	Nozzle Gross Thrust	.994

CORE

•	Hardwall and Suppression	.70
•	Strut	.09
•	Reverser	-
•	Total	.79

F2C3

The F2C3 OTW nacelle design shown in Figure VI - 3 has the same inlet as the F2C1 and C2. Since favorable wing shielding effects reduce aft fan and core turbomachinery noise at the 500 ft. sideline location, considerably less fan and core duct suppression treatment was required. The "D" shape nozzle was selected to provide an aerodynamically clean configuration offering the potential for a minimum of wing nacelle interference drag.

In addition, this "D nozzle" arrangement is anticipated to be compatible with a variety of flow deflector or turning devices that may be required to keep the engine exhaust flow attached to the wing surface during "powered lift" flight.

The fan exhaust duct area and Mach number distributions for this design are shown in Figures VI - 16 and VI - 17. Somewhat less engine frame and pylon blockage area is shown for this OTW nacelle arrangement than was required for the under-the-wing EBF. The relatively modest blockage of the single splitter permits an average duct Mach number of less than 0.45 to be maintained over the major portion of the splitter.

The tabulated installation losses for the over the wing installation are listed in Table VI-14.

As in the case of the under-the-wing EBF nacelle installations (F2C1 and C2), a simple airplane braking study was carried out to get insight as to the influence of reverse thrust engine power setting, and airplane

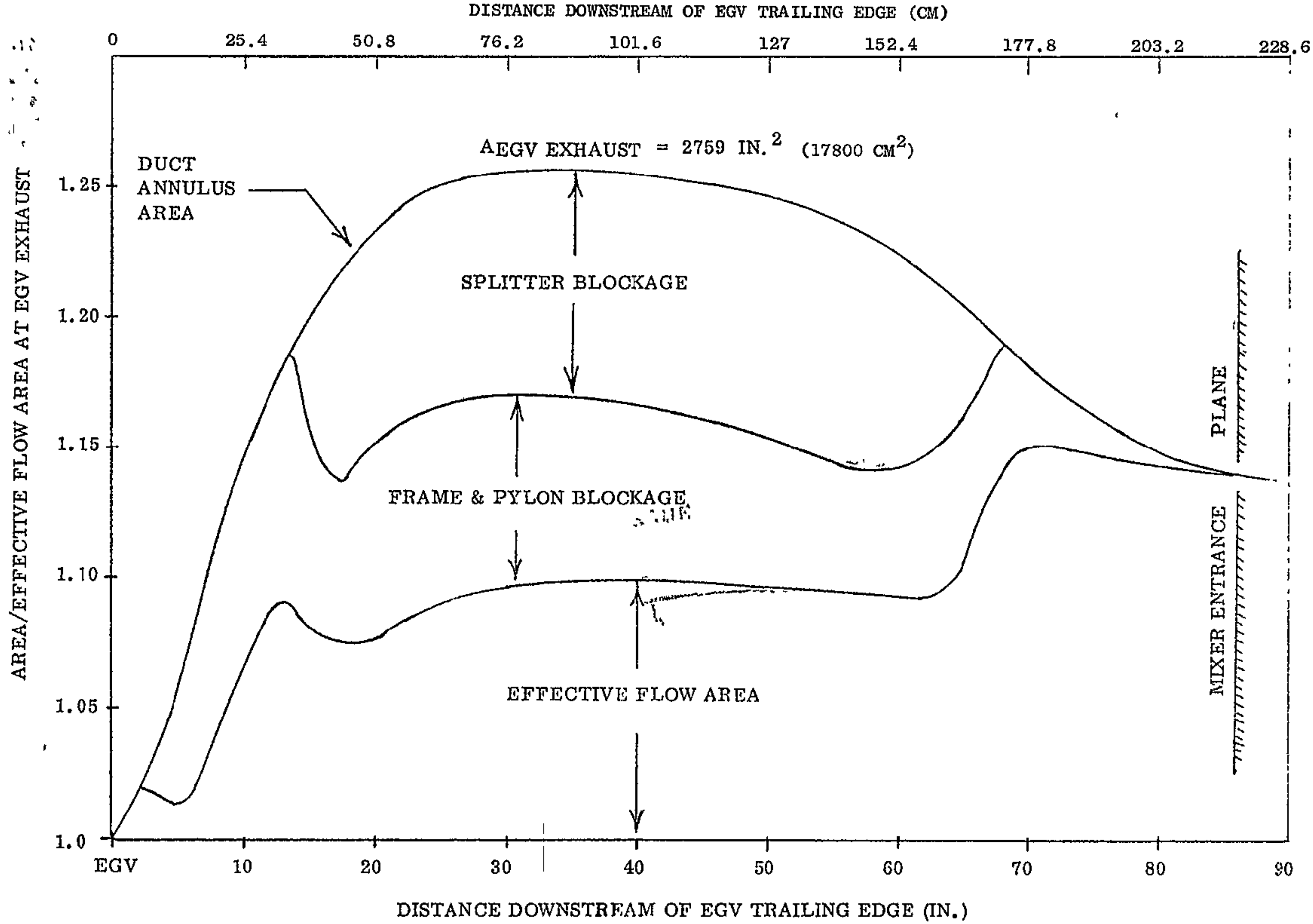

Figure VI-16. Task II GE 19/F2C3 Fan Exhaust Area Distribution.

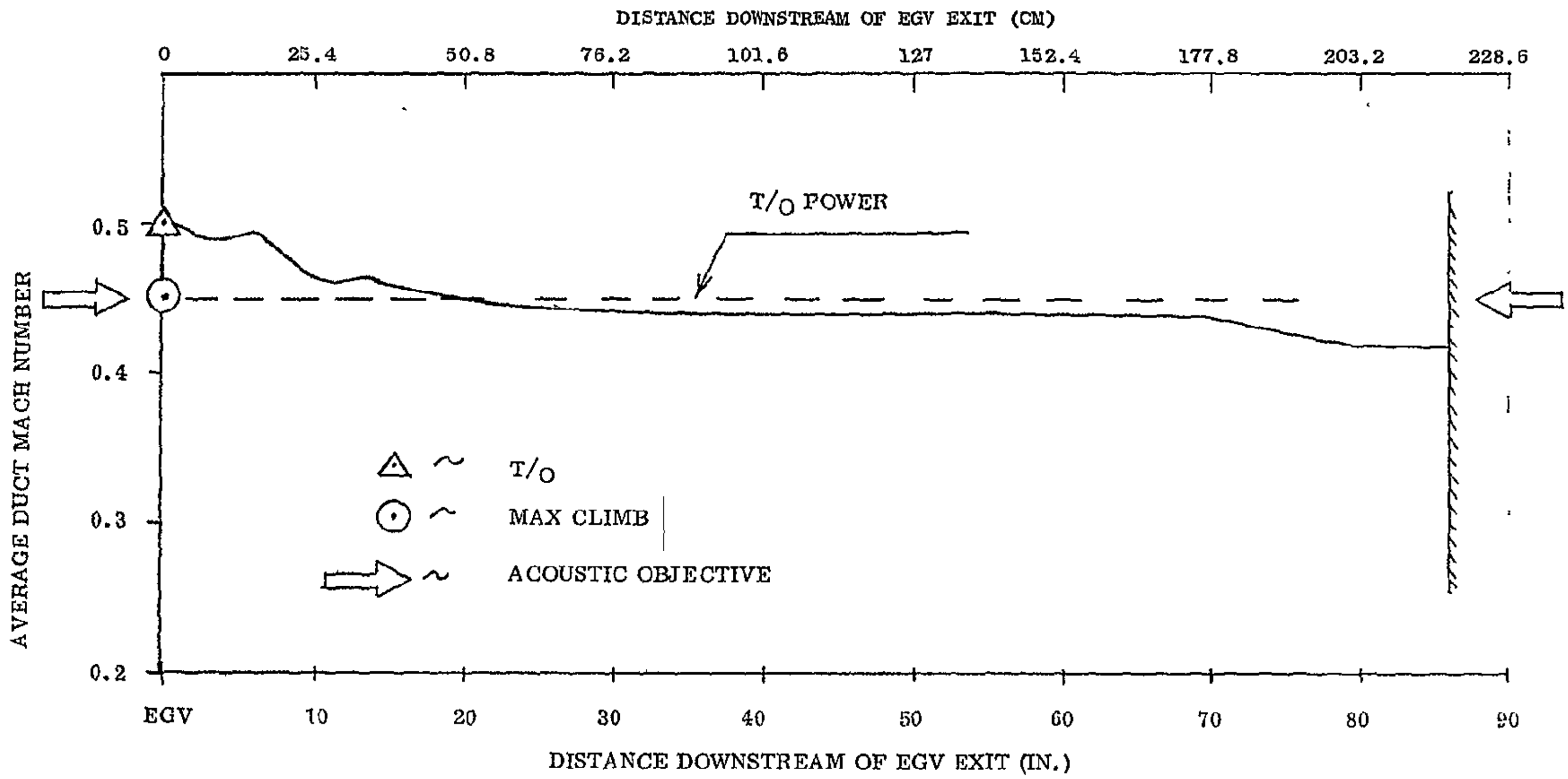

Figure VI-17. Task II GE19/F2C3 Fan Exhaust Duct Mach Number Distribution.

Table VI-14. Task II Study, GE19/F2C3 (OTW) Installation Loss Breakdown at $\Delta P_T/P_T$ % at T.O. Power.

INLET

• Lip	.69
• Hardwall and Suppression	.40
• Splitters	.39
• Strut	.03
• Spinner	.07
• Interference	.02
• Total	1.00

FAN DUCT

• Hardwall and Suppression	.64
• Splitters	.43
• Strut	.08
• Reverser	.14
• Interference	.19
• Decayer	-
• Nonsymmetric Duct	.15
• Total	1.63
• Nozzle Gross Thrust Coefficient ~ C_V	.995

CORE

• Hardwall and Suppression	.56
• Strut	.09
• Reverser	-
• Total	.64

braking on reverse thrust noise. These trends are shown in Figure VI - 18. Since the OTW airplane has a lower power loading than the EBF airplane (0.5 vs. 0.615), the engine-provided braking force is smaller. However, due to the wing shielding effects the reverse thrust noise levels that go with higher engine power settings are relatively low. The representative reverse thrust efflux pattern of the cascade thrust reverser designed to provide 35% static reverse thrust (no reinjestion) is shown in Figure VI - 19. Since the major portion of this efflux pattern is upward, this thrust reverser will provide an additional downward force that will increase the braking capability of the airplane brakes. This favorable effect has not been included to date but may at a later date.

F6E1

The cross section shown in Figure VI-4 illustrates the major aerodynamic and acoustic design features of variable pitch fan nacelle design.

The inlet is relatively similar to the F2C1 design. A combination of high throat region Mach number and acoustically treated wall surfaces utilized to suppress forward-radiated fan noise at takeoff. Since the source noise of the fan is lower, the combination of wall treatment on the outer wall and on a fixed centerbody plug provides sufficient surface area.

As in the case of the F2 fixed pitch fan inlets, care was taken to tailor inlet wall angles and area distribution so as to minimize aerodynamic losses. The area distribution curve shown in Figure VI - 20 illustrates

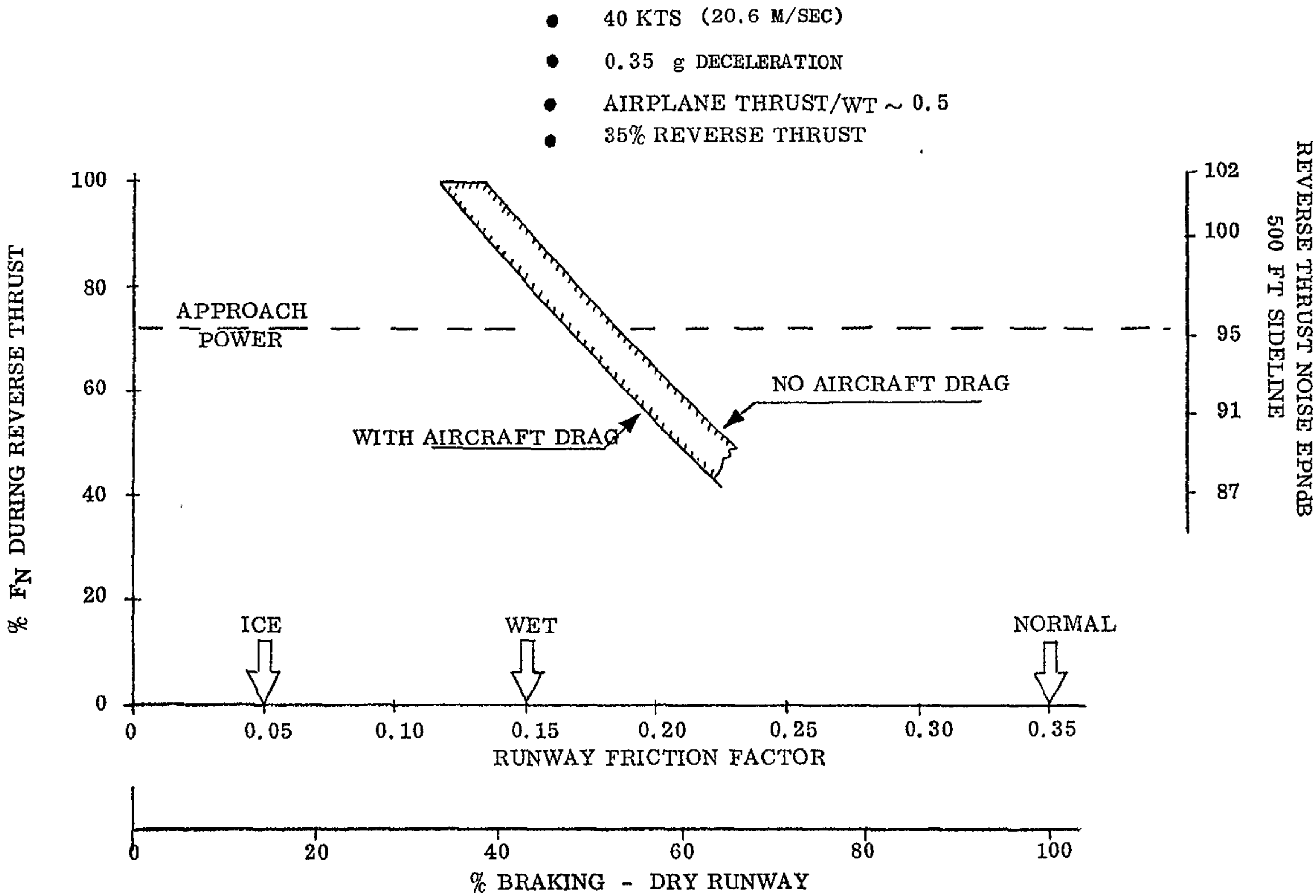

Figure VI-18. Task II GE19/F2C3 (OTW) Reverse Thrust, Noise, and Aircraft Brake Trades.

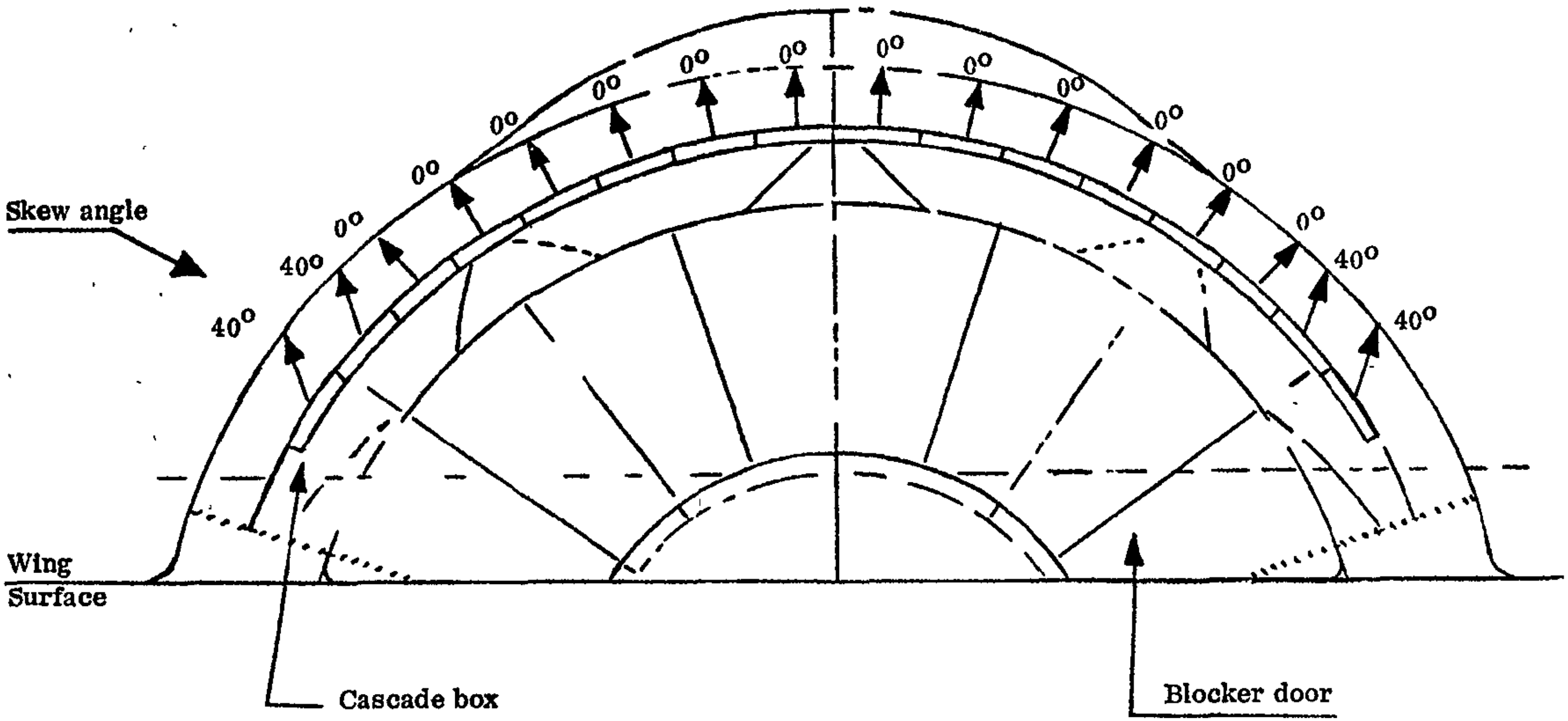

Figure VI-19. GE19/F2C3 (OTW) Reverse Flow Efflux Pattern.

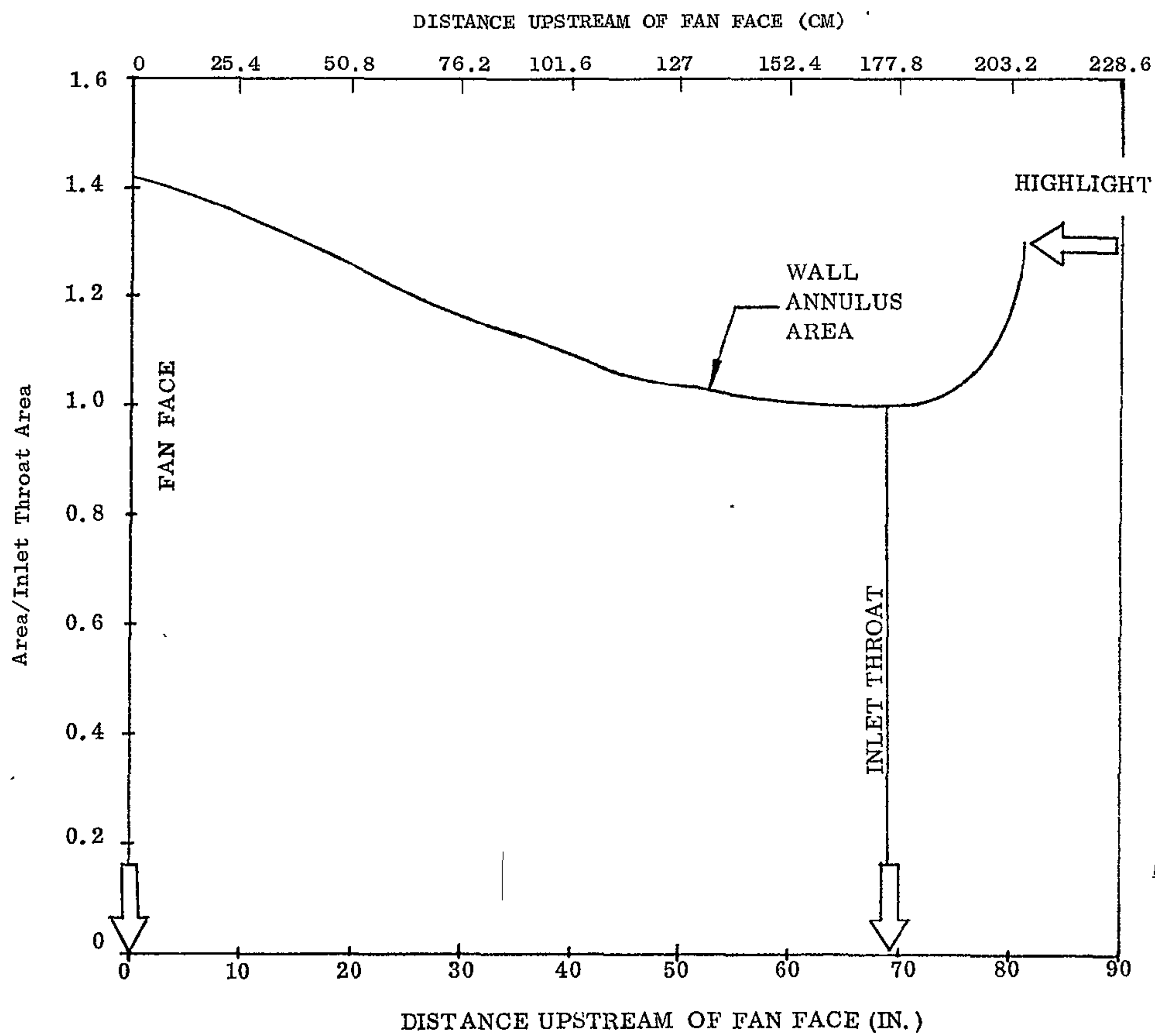

Figure VI-20. Task II GE19/F6E Inlet Area Distribution, Throat Area ≈ 3830 inch^2 (24710 cm^2).

the small wall angles and modest diffusion. Recent NASA-Lewis test data on an extended centerbody plug inlet for a low pressure ratio fan indicates that large losses in recovery can be avoided by using the wall angles shown.

The inlet lip geometry shown in Figure VI-4 is similar to that shown for the F2 series of engines, for the same reasons.

The inlet recovery characteristics at sea level 80 knots (41.16 m/sec.) plus flight speed are shown in Figure VI-21 as a function of inlet flow ratio. The recovery levels at the lower Reynolds number altitude cruise conditions will be somewhat lower as indicated by the included equation. The recovery of the F6D1 inlet is 0.02% higher than the F6E1 levels shown in Figure VI-21.

The fan exhaust duct area distribution and takeoff Mach number distributions are shown in Figure VI-22 and Figure VI-23. The shorter engine design that comes with the integral frame EGV design leaves less room in which to place the fan duct splitters.

Since the length of the splitter is a major factor in setting the length of the fan duct, the leading edge of the splitter was placed as close to the E.G.V. exit plane as was considered practical. The resulting splitter blockage, shown on Figure VI-22, resulted in the local peak in the duct Mach number at the 9 inch (22.9 cm) duct location. As indicated in Figure VI-23, a significant portion of the exhaust duct flow field has an average Mach number greater than 0.45.

The variable geometry fan nozzle (nozzle area is shown in Figure VI-23) has been designed to accommodate engine cruise and takeoff performance

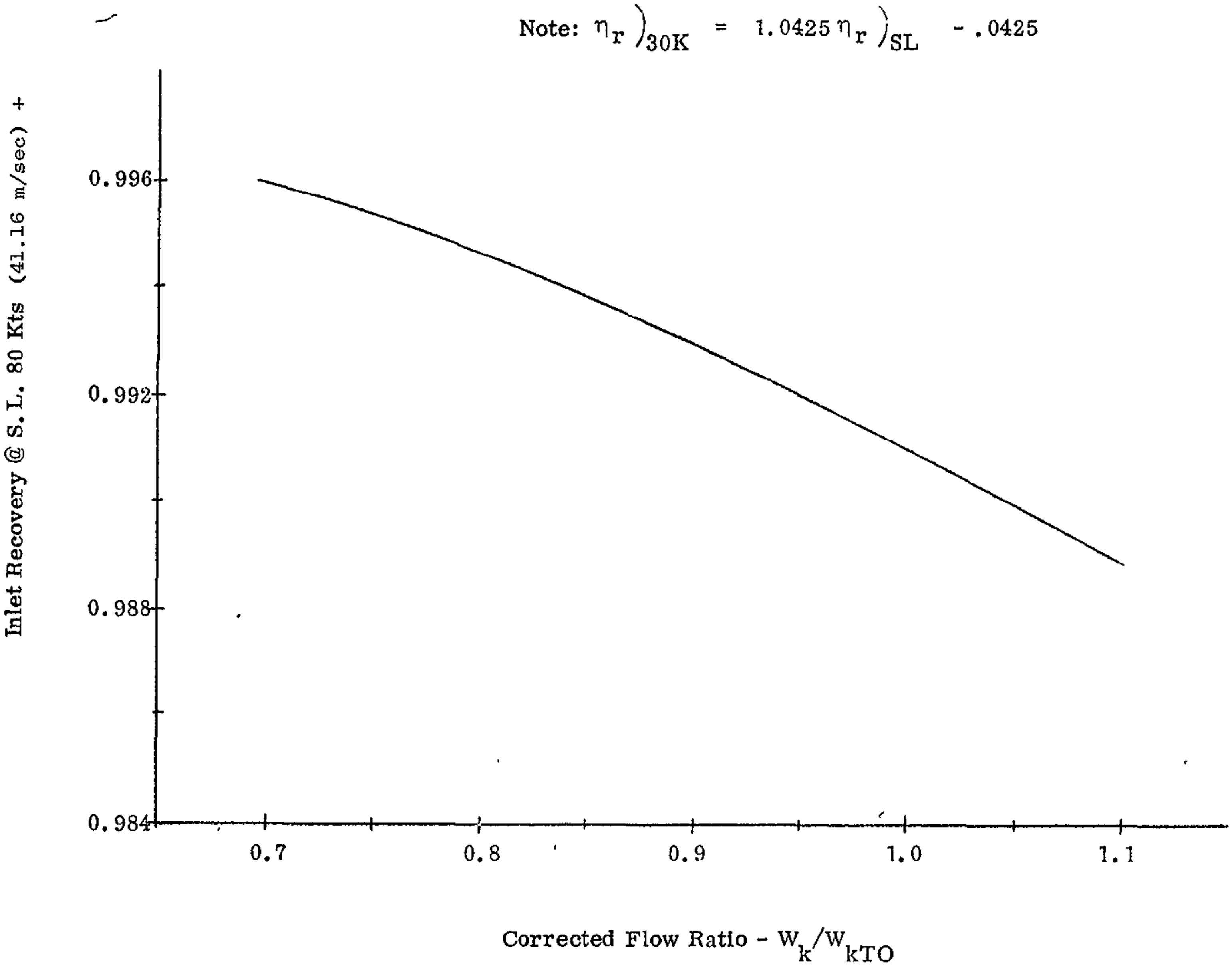

Figure VI-21. Task II GE19/F6E1 Inlet Recovery Vs. Corrected Flow.

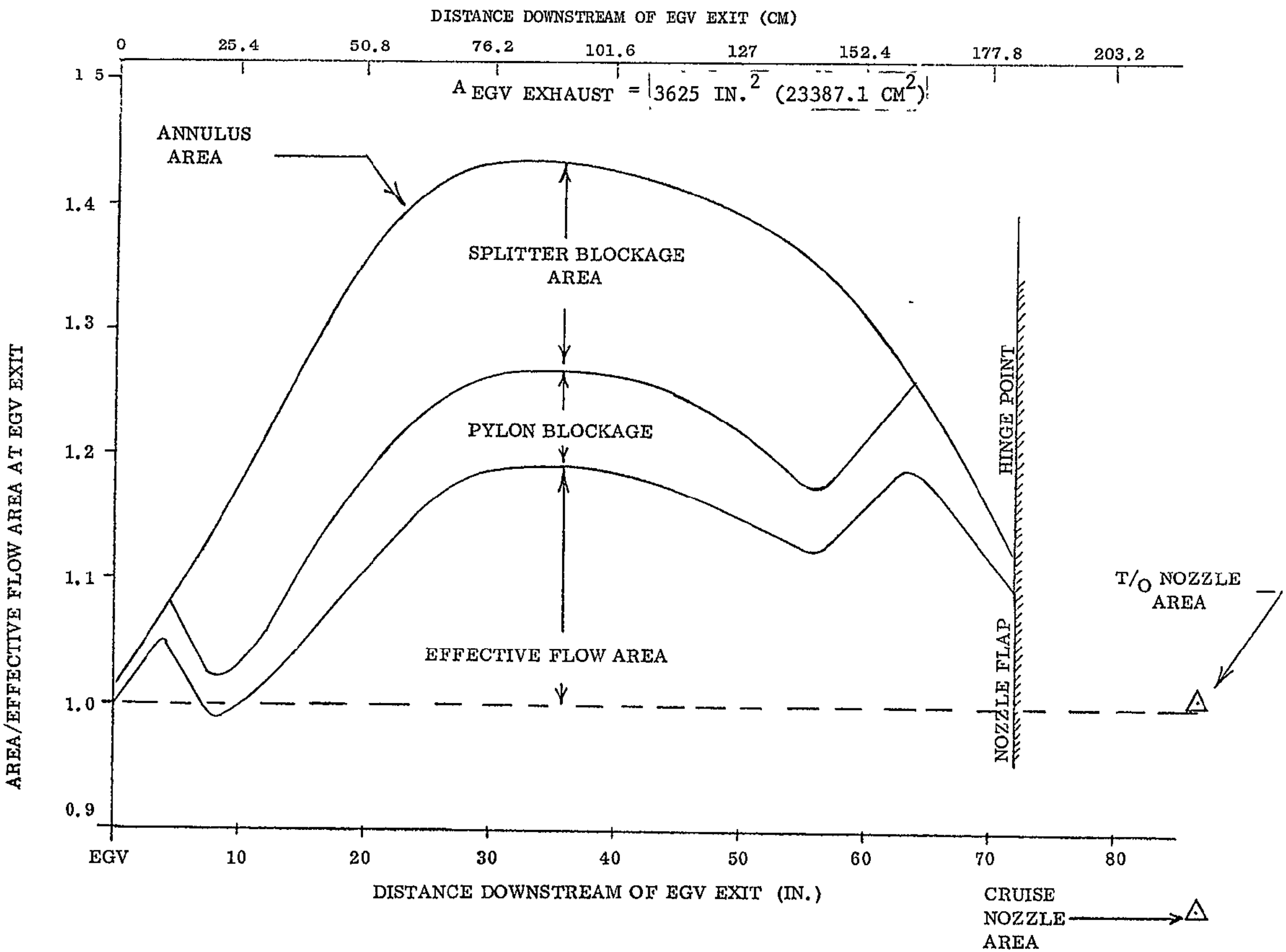

Figure VI-22. Task II GE19/F6 Fan Exhaust Duct Area Distribution.

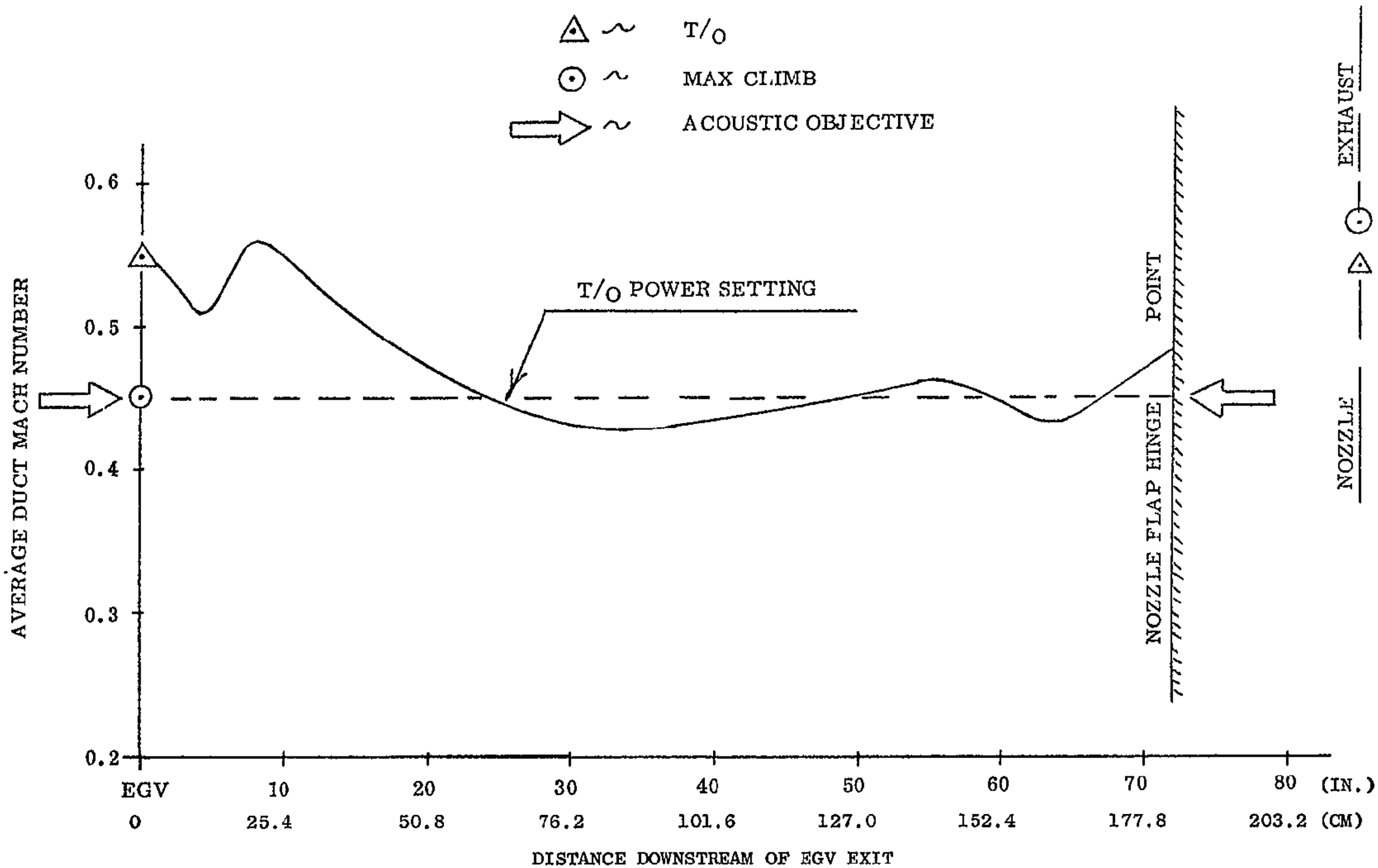

Figure VI-23. Task II GE19/F6 Fan Exhaust Average Mach Number Distributions.

requirements and also to serve as an inlet during reverse pitch fan operation. It has been reported by Hamilton Standard that recent wind tunnel data indicate that satisfactory reverse pitch thrust performance can be accomplished by simply opening up the nozzle flap as shown in Figure VI-4.

These inlet and fan exhaust area and Mach number distributions have been used in formulating the internal performance loss breakdown shown in Table VI-15.

As in the case of the F2 series a simplified airplane deceleration analysis was carried out to gain insight as to the relative influence of engine-provided reverse thrust and airplane-provided braking on reverse thrust noise. The trends shown in Figure VI - 24 show that sufficient airplane stopping force can be realized at less than 100% engine reverse thrust power setting.

The curve in Figure VI - 25 indicates what percentage of the fan thrust capability must be realized in reverse to accomplish the NASA-specified minimum. The fact that the engine reverse thrust is very nearly equal to the % of fan stream thrust applied in reverse means that the inlet ram drag at 40 knots is very nearly equal to the thrust of the core stream.

F6D1

The variable pitch fan with a gear rather than a multistage fan turbine drive system shown in Figure VI - 5 has a nacelle very similar to the F6E1 design. The inlet is 5 inches (12.7 cm) shorter due to the lower source noise level of the gear-driven fan. The fan exhaust duct and nozzle are identical. The

Table VI-15. Task II Study, GE19/F6E1 (Direct Drive) Installation Loss Breakdown at $\Delta P_T/P_T$ % at T.O. Power.

<u>INLET</u>

• Lip	.10
• Hardwall and Suppression	.41
• Splitters	-
• Strut	.03
• Spinner	.12
• Interference	.01
• Total	.67

<u>FAN DUCT</u>

• Hardwall and Suppression	.66
• Splitters	.46
• Strut	-
• Reverser	-
• Interference	.01
• Decayer	-
• Nonsymmetric Duct	-
• Total	1.07
• Nozzle Gross Thrust Coefficient ~ C_V	.996

<u>CORE</u>

• Hardwall and Suppression	1.59
• Strut	.09
• Reverser	-
• Total	1.68
• Nozzle Gross Thrust Coefficient ~ C_V	.996

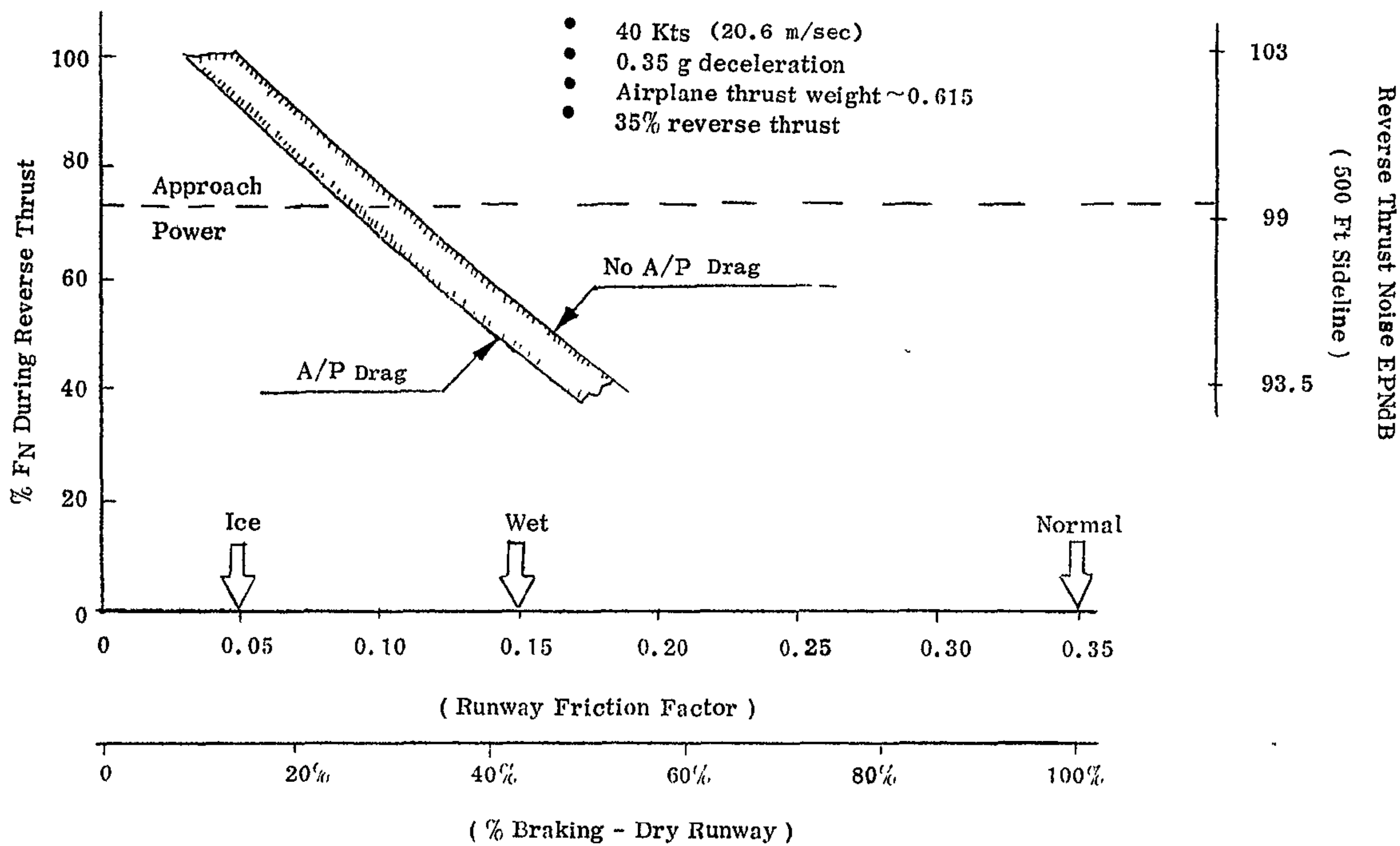

Figure VI-24. Task II GE19/F6E & D (EBF) Reverse Thrust, Noise, and Aircraft Brake Trades.

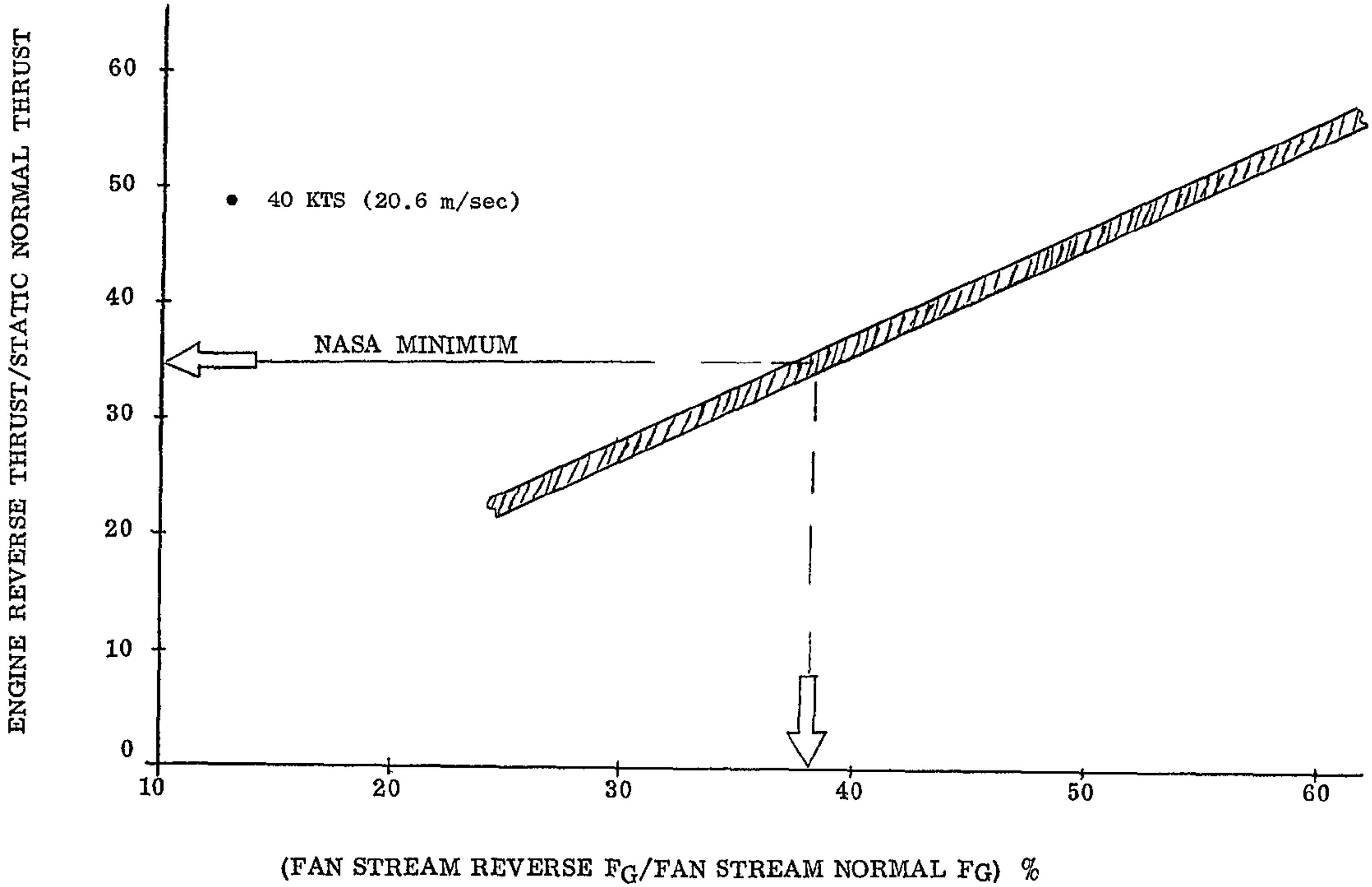

Figure VI-25. Task II VP Reverse Thrust Capability Trends.

core exhaust duct for the gear-driven system is a bit longer. It was not possible to take advantage of the shorter and smaller diameter fan turbine to reduce the nacelle diameter or length without going to excessive fan cowl boattail angles.

The breakdown of F6D1 installation losses given in Table VI - 16 show slightly lower inlet losses and identical fan and core exhaust duct losses.

The average exhaust velocity and total temperatures for both the direct and gear driven fans are tabulated in Table VI - 17. The resulting exhaust plume velocity and total temperature profiles are shown in Figure VI - 26 at static 80 and 130 knot flight speeds.

F9A2

A cross section of the augmentor wing engine nacelle is shown in Figure VI - 6. The wing and cruise nozzle lines shown are representative and were included to help illustrate the complete engine installation. For the purposes of this study the interface between the propulsion system and the aircraft is at the base of the pylon.

Two inlet designs were considered, the fixed geometry arrangement shown in Figure VI - 6 and a variable geometry design. Since the fixed geometry design was found to have lower losses and was lighter, it was selected as the primary design.

The inlet design shown in Figure VI - 6 is similar in many respects to the design approach used for the F2 series of engine installations. A

Table VI-16. Task II Study, GE19/F6D1 (Geared Drive) Installation Loss Breakdown at $\Delta P_T/P_T$ % at T.O. Power.

<u>INLET</u>

• Lip	.12
• Hardwall and Suppression	.38
• Splitters	–
• Strut	.03
• Spinner	.11
• Interference	.01
• Total	.65

<u>FAN DUCT</u>

• Hardwall and Suppression	.60
• Splitters	.46
• Strut	–
• Reverser	–
• Interference	.01
• Decayer	–
• Nonsymmetric Duct	–
• Total	1.07
• Nozzle Gross Thrust Coefficient ~ C_V	.996

<u>CORE</u>

• Hardwall and Suppression	1.59
• Strut	.09
• Reverser	–
• Total	1.68
• Nozzle Gross Thrust Coefficient ~ C_V	.996

Table VI-17. Task II Study, GE19/F6E1 and F6D1 Exhaust Velocity and Total Temperatures (Installed).

	0	80 kts (41.16 m/sec)	130 kts (66.88 m/sec)
Fan Exhaust Velocity (ft/sec)	620	640	650
(m/sec)	189	195.1	198.1
Fan-Exhaust Total Temp (^{o}R)	550^{o}	555^{o}	560^{o}
($^{\circ}$K)	287.78	290.56	293.33
Core Exhaust Velocity (ft/sec)	700	710	720
(m/sec)	167.6	216.4	219.5
Core Exhaust Total Temp (^{o}R)	1570^{o}	1565^{o}	1560^{o}
($^{\circ}$K)	854.44	851.67	848.89

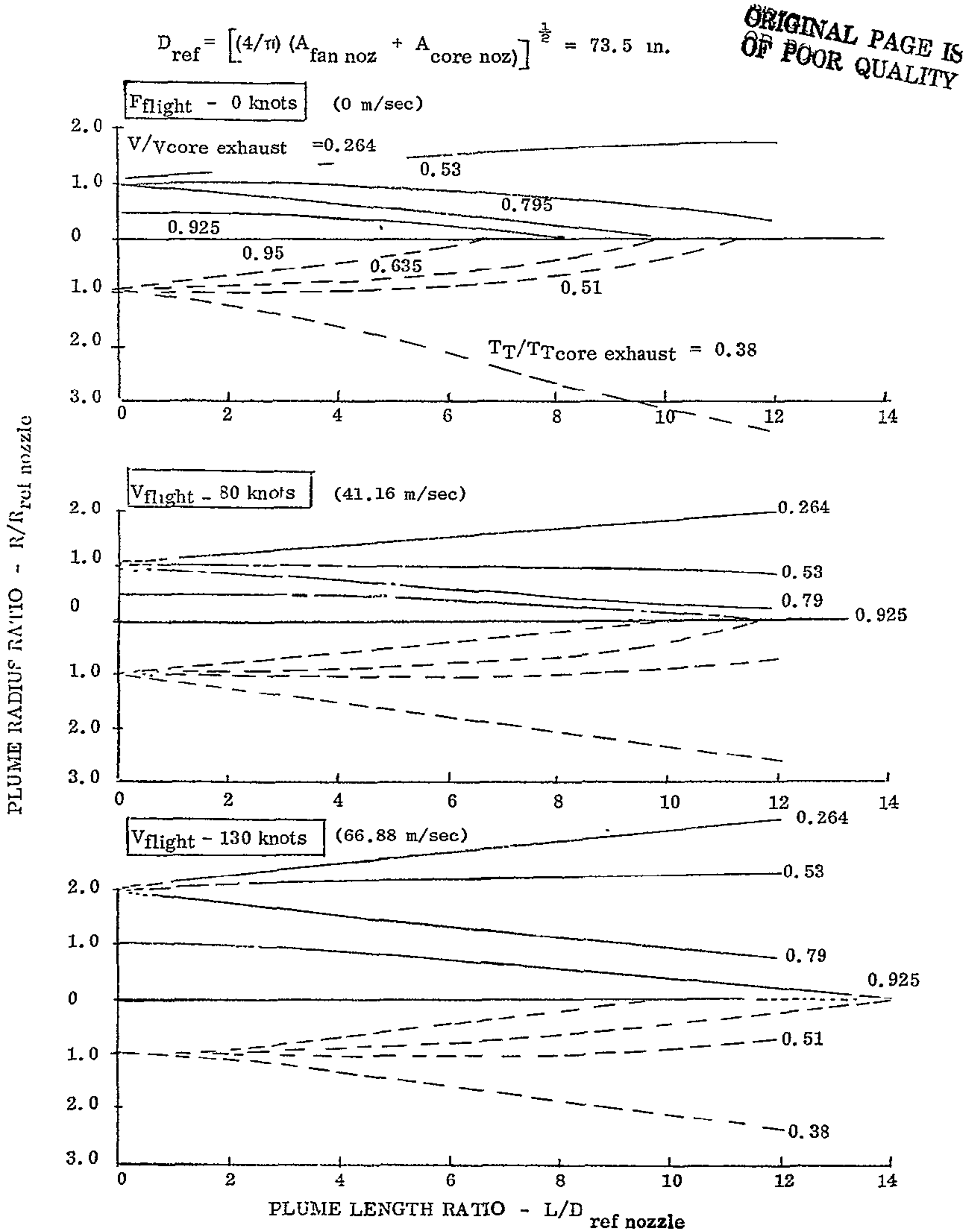

Figure VI-26. Task II GE19/F6E1 & D1 Exhaust Plume Velocity and Temperature Profiles.

combination of higher throat region Mach number and acoustic treatment is used to suppress fan noise at takeoff conditions. The combination of a single acoustically treated splitter and a fixed treated centerbody plug is used to provide the required surface area. The same lip design philosophy used on the F2 series is applied to this installation ($D_{HL}/D_T = 1.14$ on top and $D_{HL}/D_T = 1.2$ on bottom). The inlet area distribution is shown in Figure VI - 27. The estimated takeoff recovery characteristics for 80 kt. [for 80 kt. (41.16 m/sec.) + flight speed] of this inlet concept are shown in Figure VI-28. An equation has been included on this figure to facilitate estimating the altitude cruise recovery levels.

The trend curve shown in Figure VI - 29 illustrates the trades between engine reverse thrust and airplane-applied braking force required to maintain the specified 0.35 g landing deceleration rate.

The reverse thrust noise levels for this engine installation are significantly higher than those of the other propulsion systems. As specified by the Task II study guidelines, the thrust reverser was engine mounted. In order to get the required amount of reverse thrust (35% at 40 knots), it was necessary to reverse the high pressure wing flow stream. As indicated in Figure VI - 6 a simple cascade system was selected. The large pylon, and the high pressure of the wing flow stream and the shape of the wing flow collector duct led to the cascade and reverse eflux pattern shown in Figure VI - 30.

A 30% variation in core nozzle exhaust area was required to satisfy engine operating requirements and to limit jet noise at takeoff. Since thrust

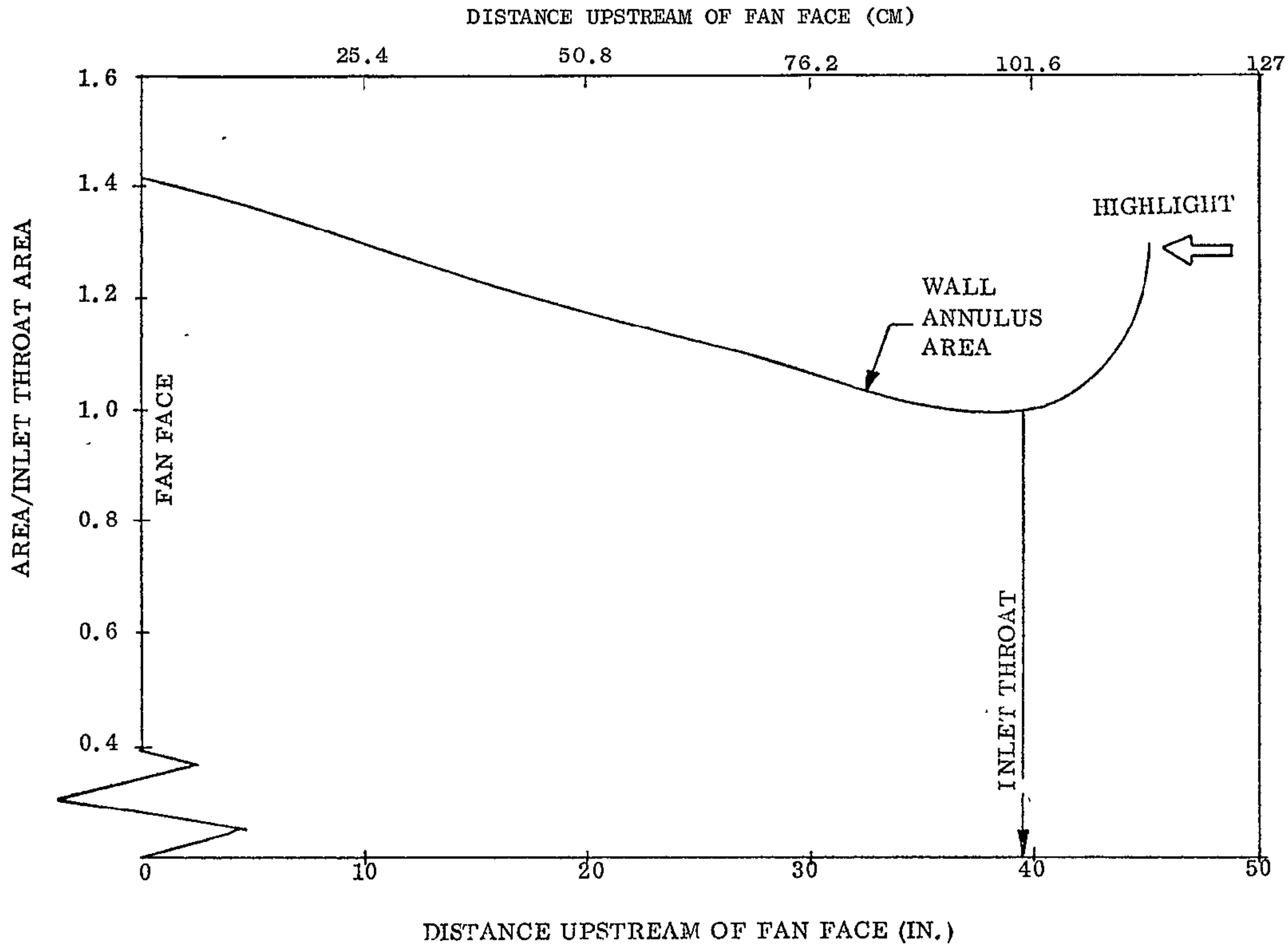

Figure VI-27. Task II GE19/F9A2 Inlet Area Distribution, Throat Area ≈ 1120 inch^2 (7225.8 cm^2).

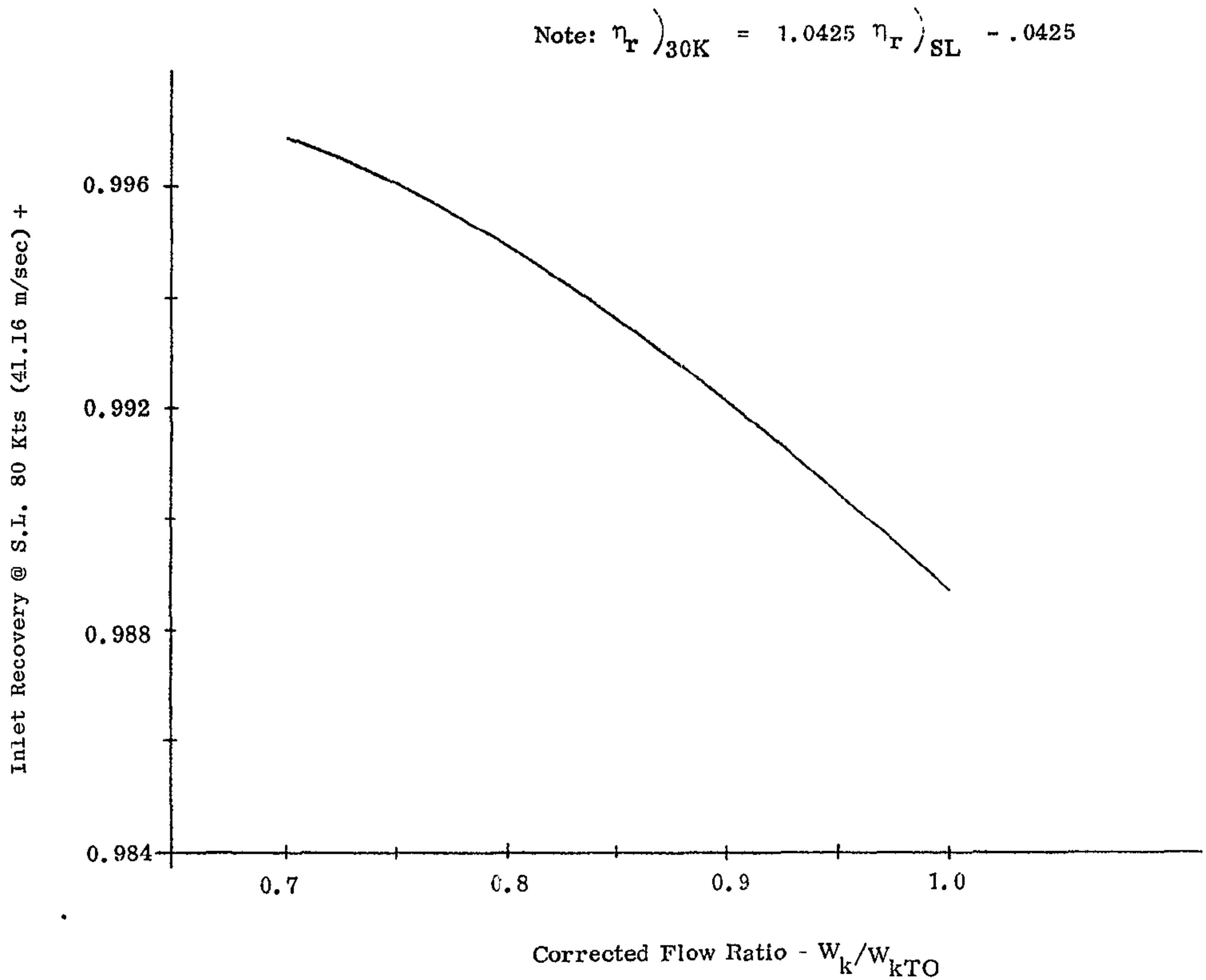

Figure VI-28. GE19/F9A2 Inlet Recovery Vs. Corrected Flow.

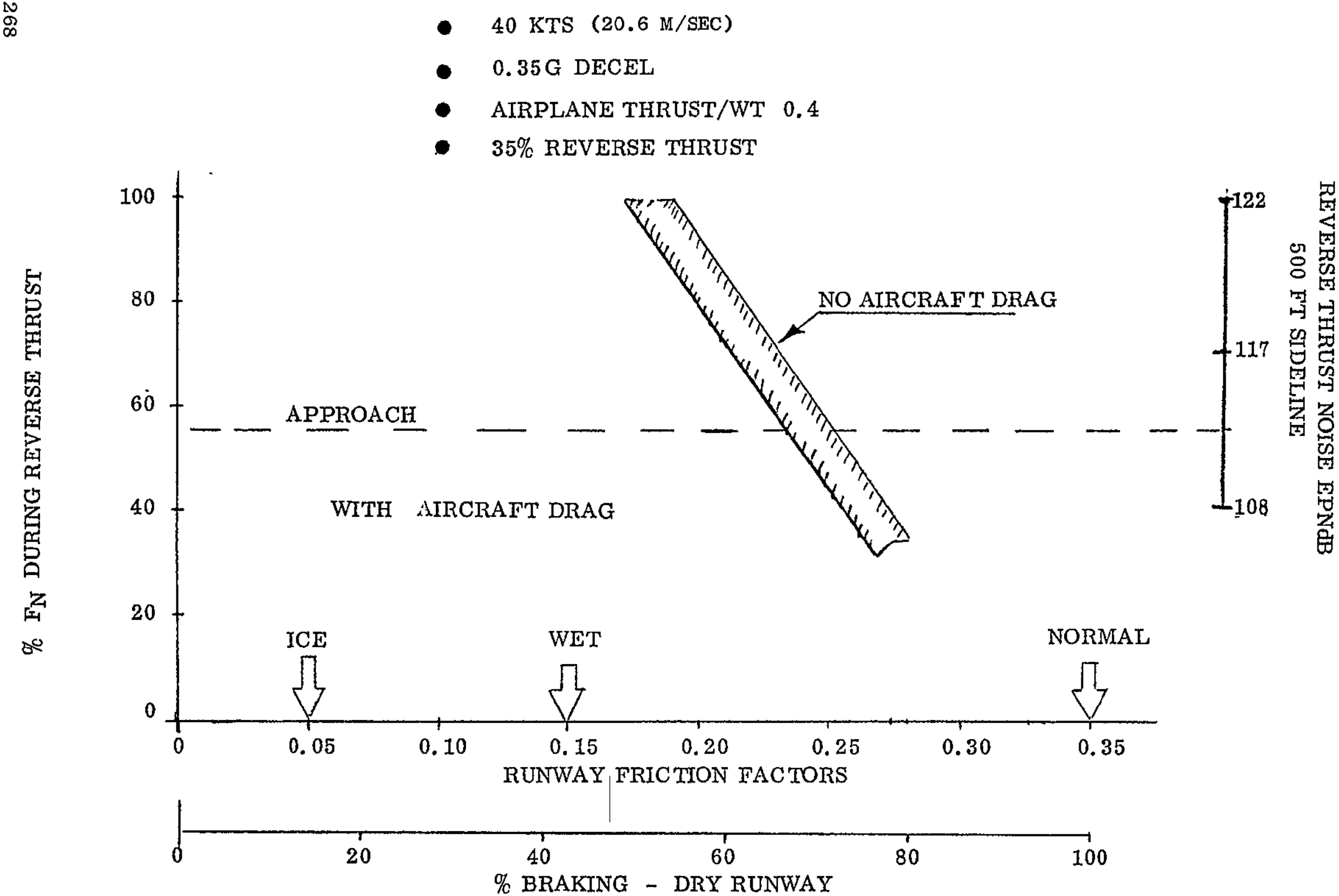

Figure VI-29. Task II AW Reverse Thrust, Noise, and Aircraft Braking Trades.

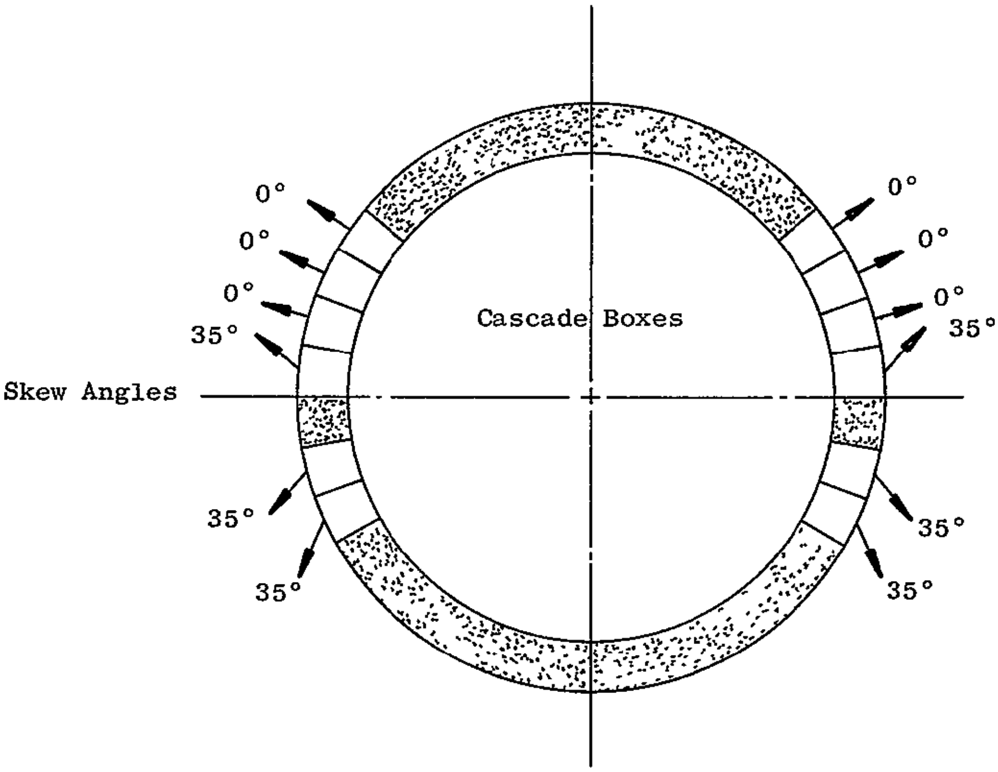

Figure VI-30. GE19/F9A2 & A3 (AW) Reverse Flow Efflux Pattern.

reverser requirements dictated that the thrust of the core exhaust be spoiled, the 2-position nozzle flaps were designed to also serve as blocker doors for the core thrust spoiler.

A breakdown of the inlet, and exhaust installation duct losses is listed in Table VI - 18. The 4% wing flow duct loss value was selected as being representative of the results of available NASA-sponsored studies of augmentor wing aircraft.

F9A3

A cross section of the augmentor wing engine nacelle and the alternate variable geometry inlet is shown in Figure VI - 7. The translating centerbody approach shown was selected as the most promising variable geometry design concept after reviewing the results of available NASA-sponsored design and experimental study programs.

The inlet noise suppression requirements at takeoff and approach are shown in Figure VI - 31, along with the inlet airflow characteristics. Less suppression is required at approach than at the full power takeoff. The airflow variation between takeoff and approach conditions is an indicator of the amount of inlet throat area variation that may be required.

Since the penalties for lining available inlet surface areas with acoustic treatment are small, the most effective design utilized a combination of wall treatment and high throat region Mach number to achieve the desired suppression. Trend data like that shown in Figure VI - 32 were used to formulate

Table VI-18. Task II Study, GE19/F9A2 Installation Loss Breakdown at $\Delta P_T/P_T$ % at T.O. Power.

INLET

•	Lip	.12
•	Hardwall and Suppression	.49
•	Splitters	.50
•	Strut	.06
•	Spinner	.11
•	Interference	.03
•	Total	1.31

FAN DUCT

•	Hardwall and Suppression	4%
•	Splitters	T
•	Strut	O
•	Reverser	
•	Interference	T
•	Decayer	A
•	Nonsymmetric Duct	
•	Total	L

CORE

•	Hardwall and Suppression	.82
•	Strut	.09
•	Reverser	.12
•	Total	1.03
•	Nozzle Gross Thrust Coefficient ~ C_V	.996

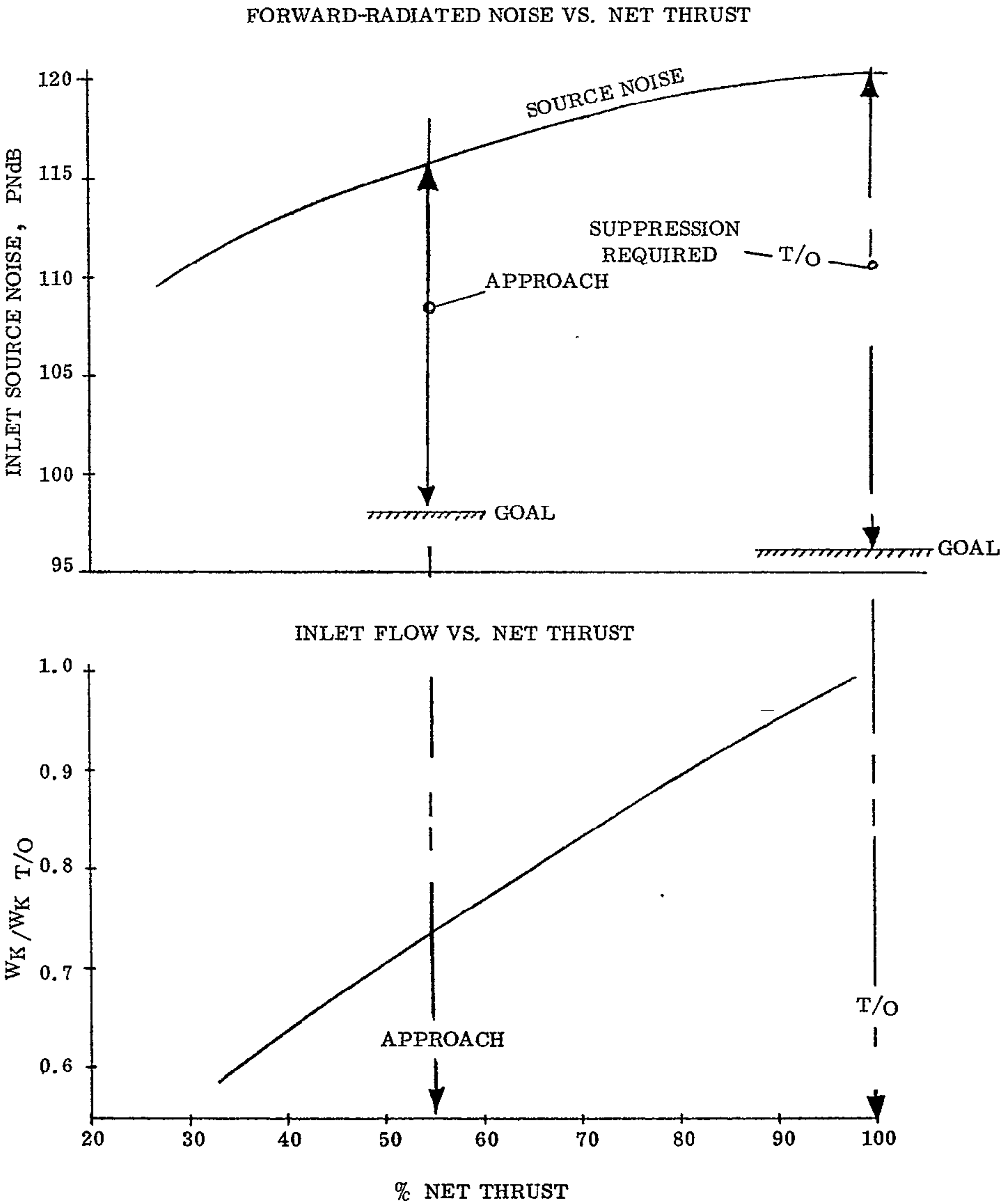

Figure VI-31. Task II GE19/F9 Inlet Suppression and Airflow Characteristics.

a number of different designs utilizing various combinations of wall treatment and high throat Mach number to achieve the desired suppression.

An additional factor that had to be considered in formulating these concepts was the loss in high Mach throat region suppression effectiveness at high inlet incidence angles. After reviewing the results of some recent NASA-Lewis Research Laboratory tests on small scale models, the takeoff and approach high Mach suppression correction factors shown in Figure VI - 33 were formulated.

The results of these different translating plug inlet configuration studies are summarized in Figure VI - 34. An inlet design that utilizes a high average throat Mach number at takeoff does not require much length of acoustic treatment to meet its suppression objectives. However, relatively large area changes are required to satisfy the approach suppression requirements. Selecting a lower value of average throat Mach number at takeoff required more inlet length for the acoustic treatment but less area variation. The solid line represents the family of designs that will satisfy the suppression goals with no correction for inlet incidence angle effects. The dashed lines represent the family of designs that will meet the suppression goals with a correction for loss of suppression due to incidence angle effects.

After reviewing mechanical design considerations the design giving a takeoff average throat Mach number of 0.92 was selected. At this throat Mach number, the inlet length requirements set by mechanical design

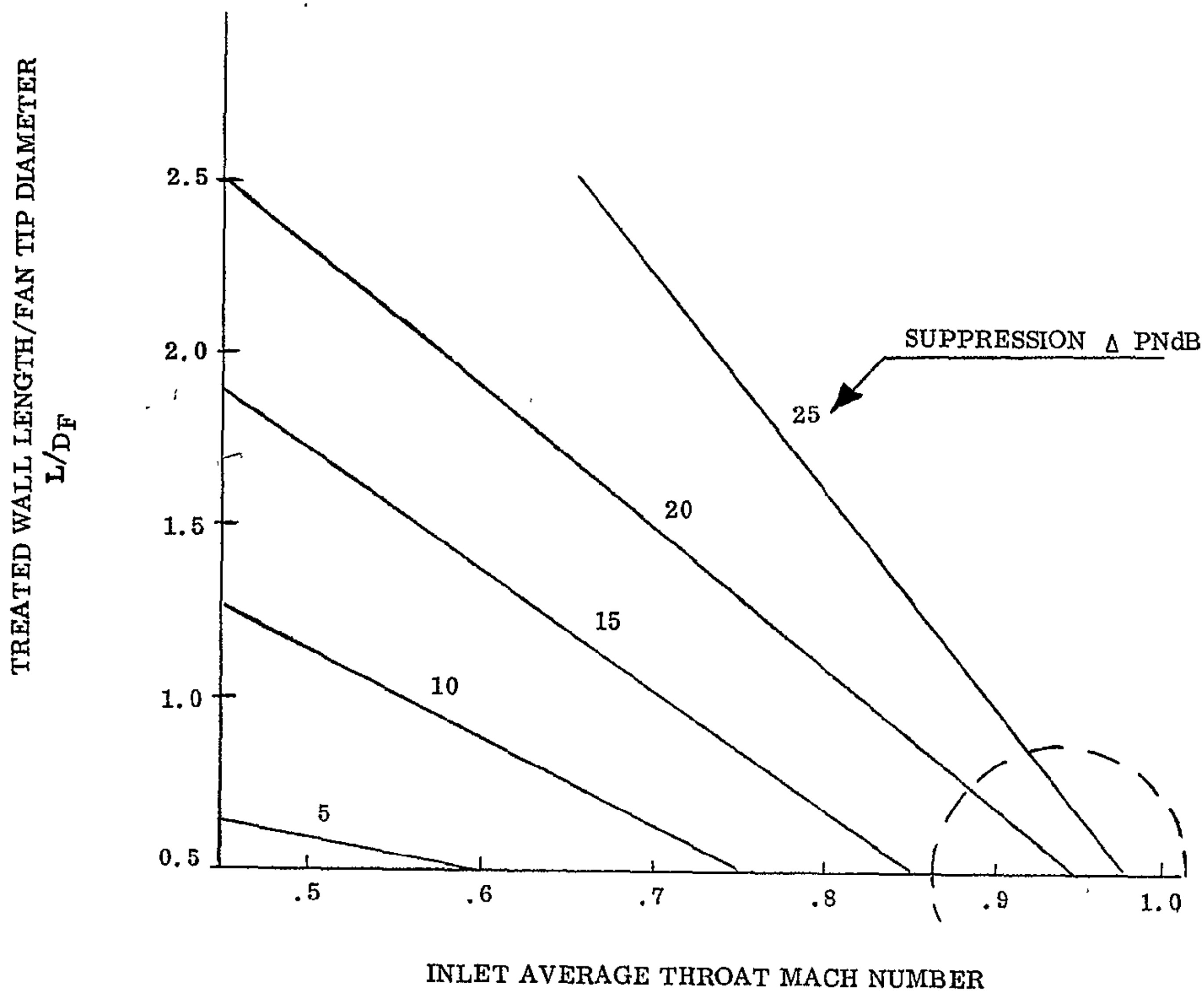

Figure VI-32. Task II GE19/F9A2 Inlet Acoustic Design Trends, Effect of Combined Wall Treatment and High Throat Mach Number on Suppression.

(INLET FLOW INCIDENCE ANGLES REDUCE HIGH MACH SUPPRESSION)

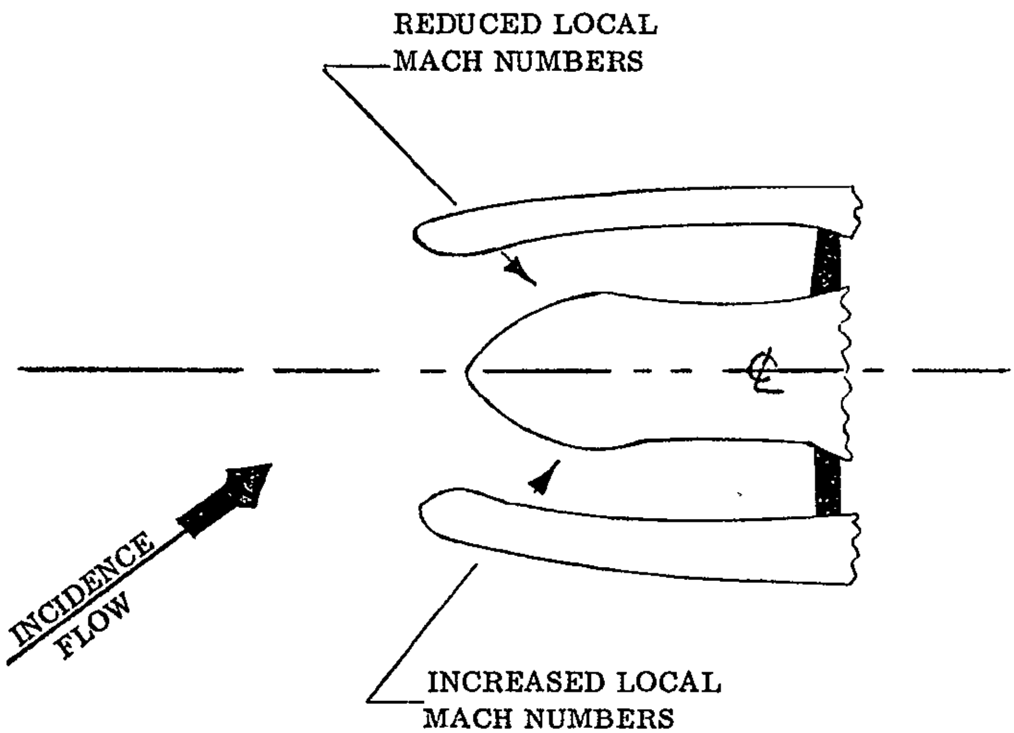

	AVERAGE INCIDENCE ANGLE	LOSS IN SUPPRESSION
T/O	25^{o} --> 35^{o}	- 3 PNdB
APPROACH	35^{o} --> 50^{o}	- 5 PNdB

Figure VI-33. Task II GE19/F9A3 Inlet Installation Aero Design Considerations.

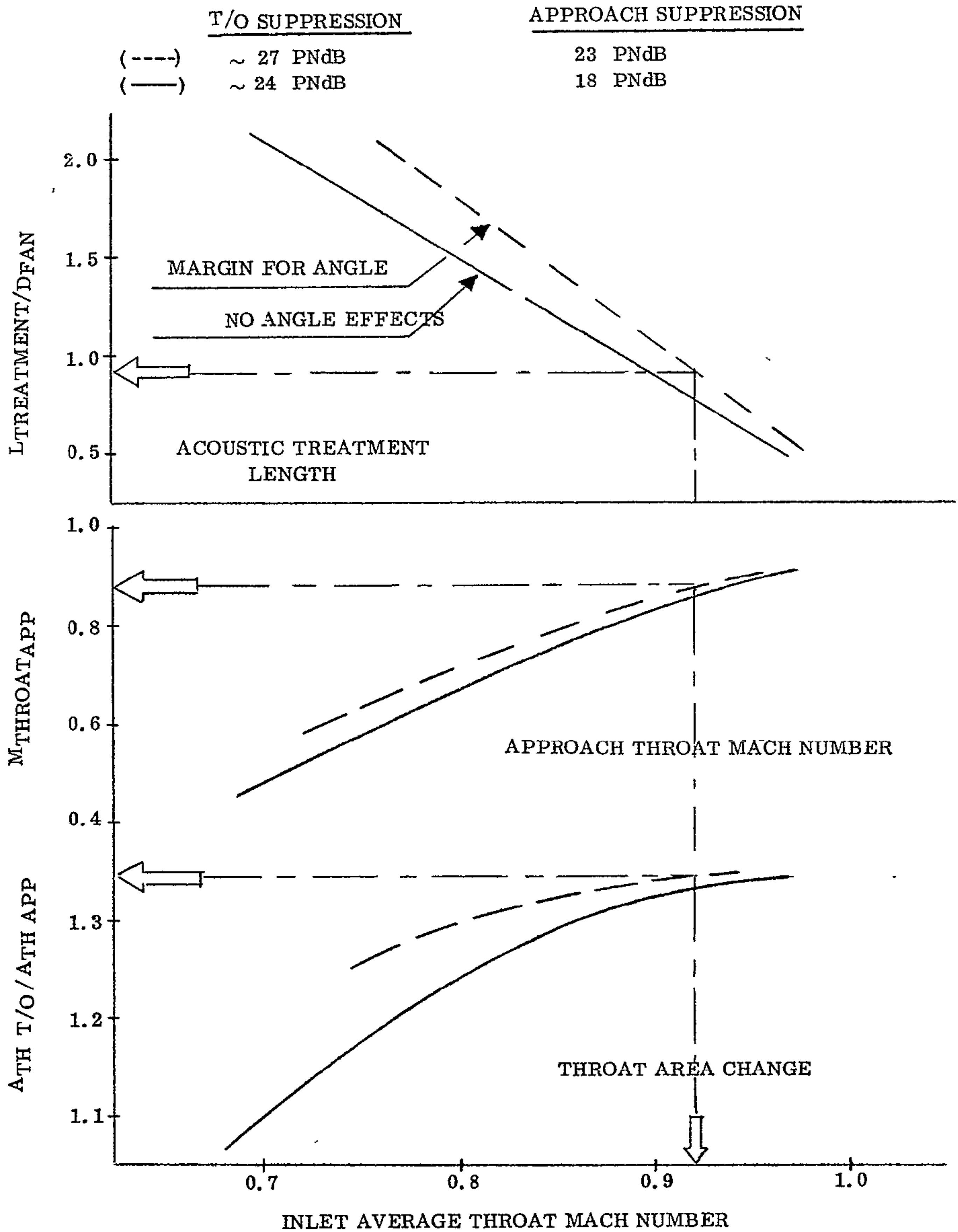

Figure VI-34. Task II GE19/F9A3 Inlet Aero & Geometric Design Trends.

and diffusion wall angle considerations were very nearly equal to the wall treatment requirements.

Care was taken in selecting centerbody plug shape and cowl wall diffusion angles that would avoid separation and abrupt movements in throat location and area with plug position.

Figure VI - 35 illustrates the selected contours and shows the plug in its 3 design positions. The resulting net area distributions and average Mach number distributions are shown in Figures VI - 36 and 37. The additional plug translation at the max. cruise flight condition was incorporated to reduce the length of the high Mach number section in order to help increase cruise recovery levels. The resulting inlet recovery characteristics are shown in Figure VI - 38.

A breakdown of the T/O installation losses for this nacelle installation are listed in Table VI - 19. The inlet losses for this variable geometry design are significantly higher than those of the simpler fixed geometry design.

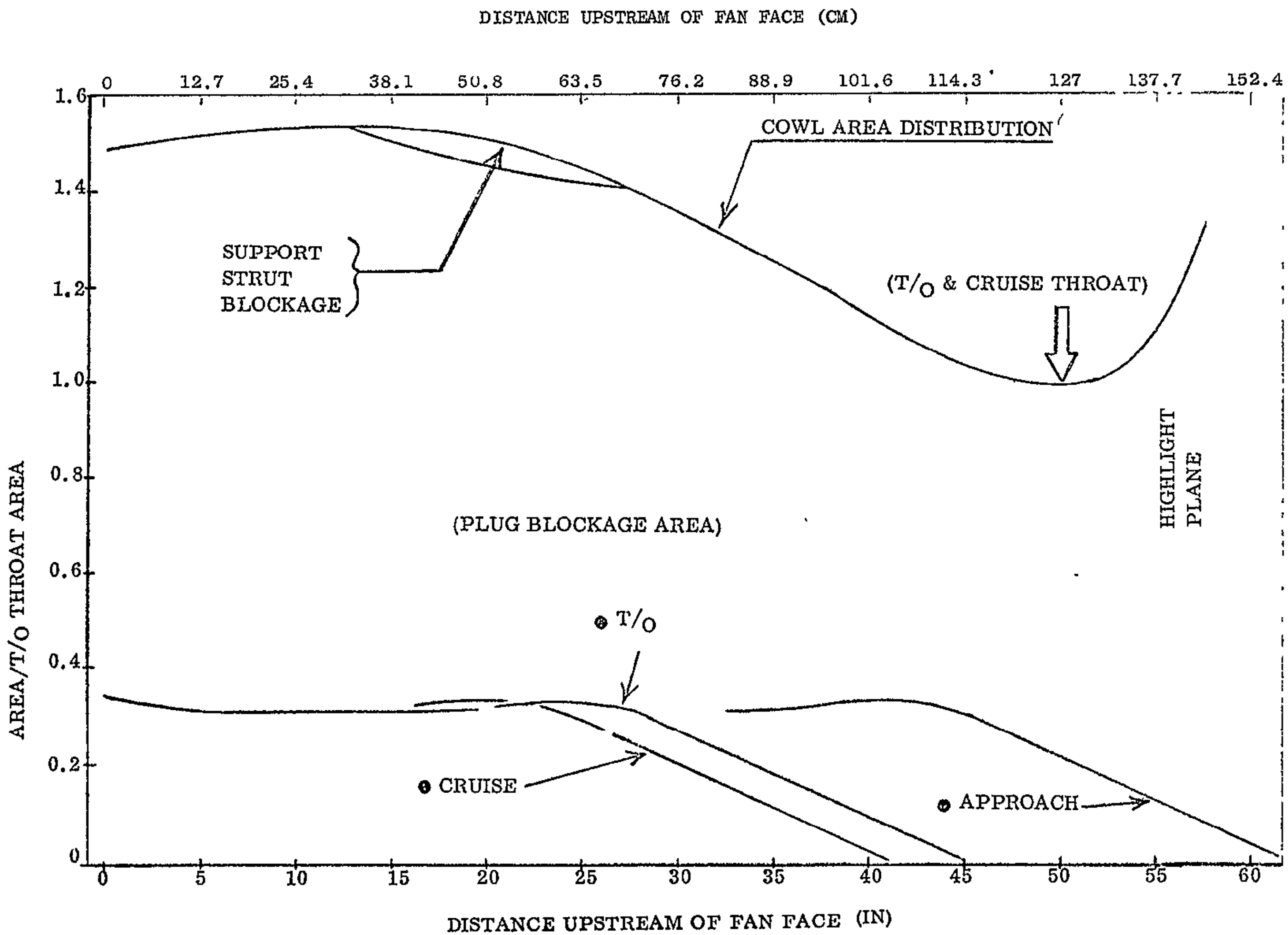

Figure VI-35. Task II GE19/F9A3 Inlet Area Design Factors, T/O and Cruise Inlet Throat Area ≈ 1080 inch^2 (6967.7 cm^2).

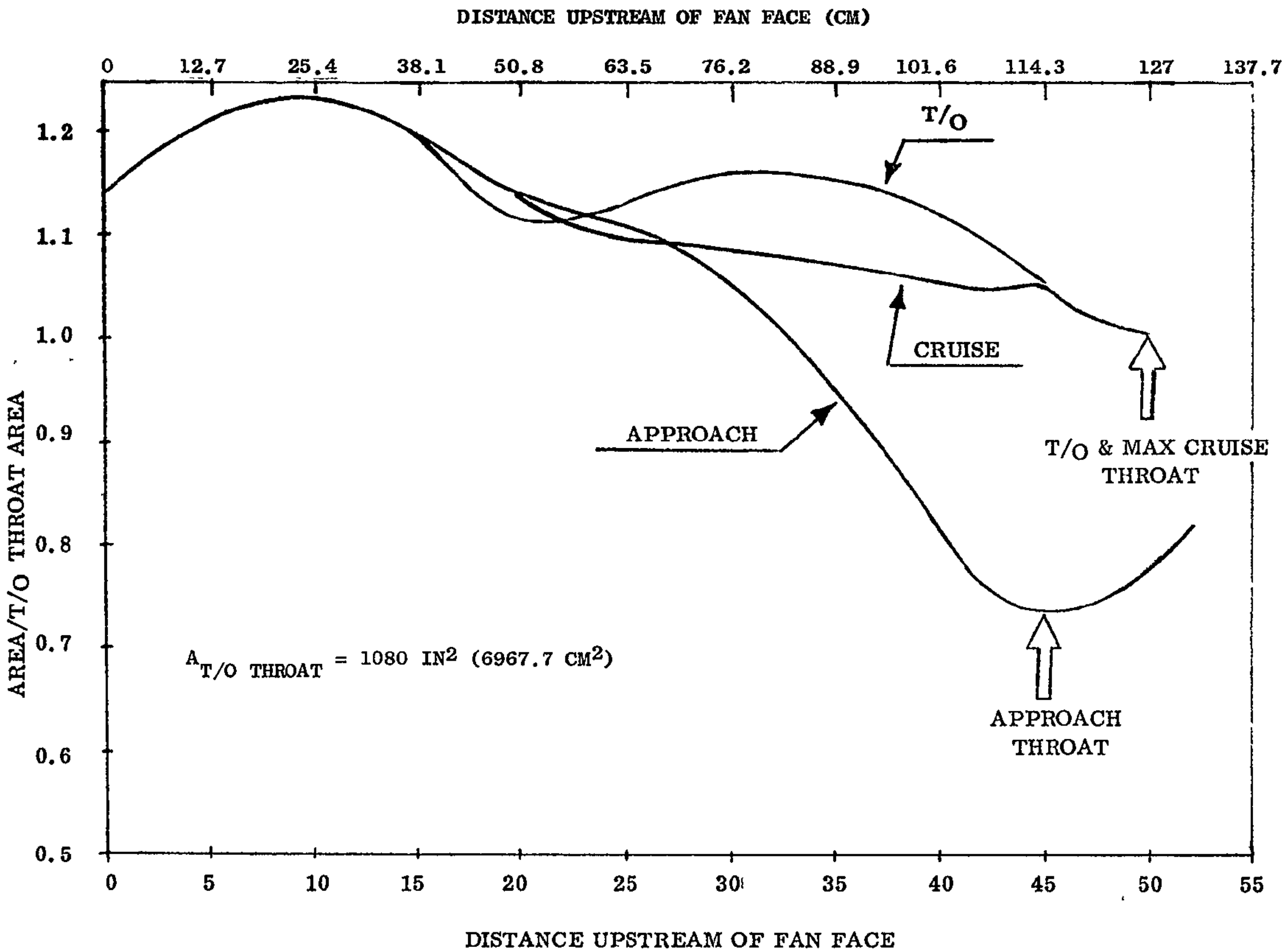

Figure VI-36. Task II GE19/F9A3 Inlet Flow Area Distributions.

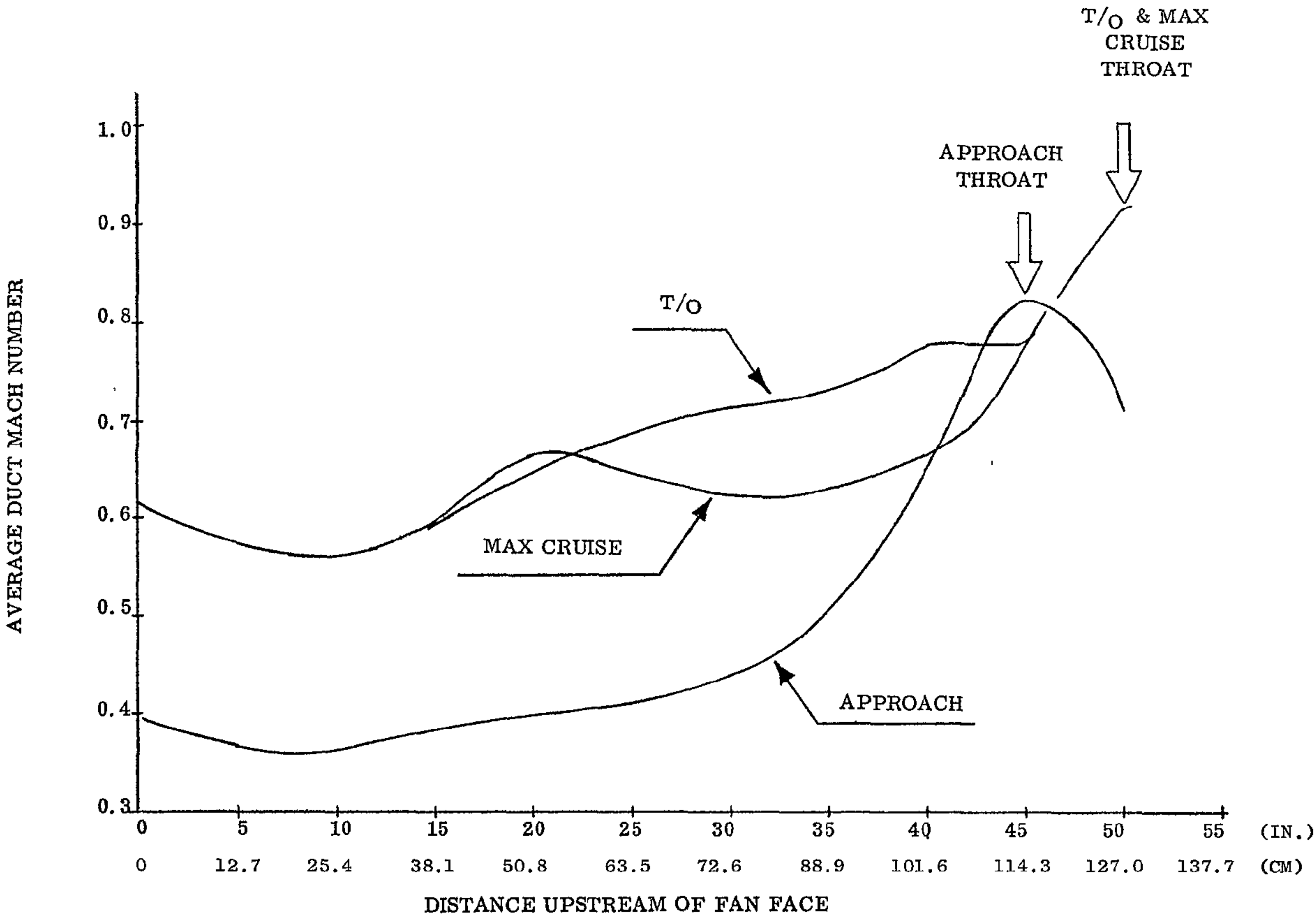

Figure VI-37. Task II GE19/F9A3 Inlet Mach Number Distribution.

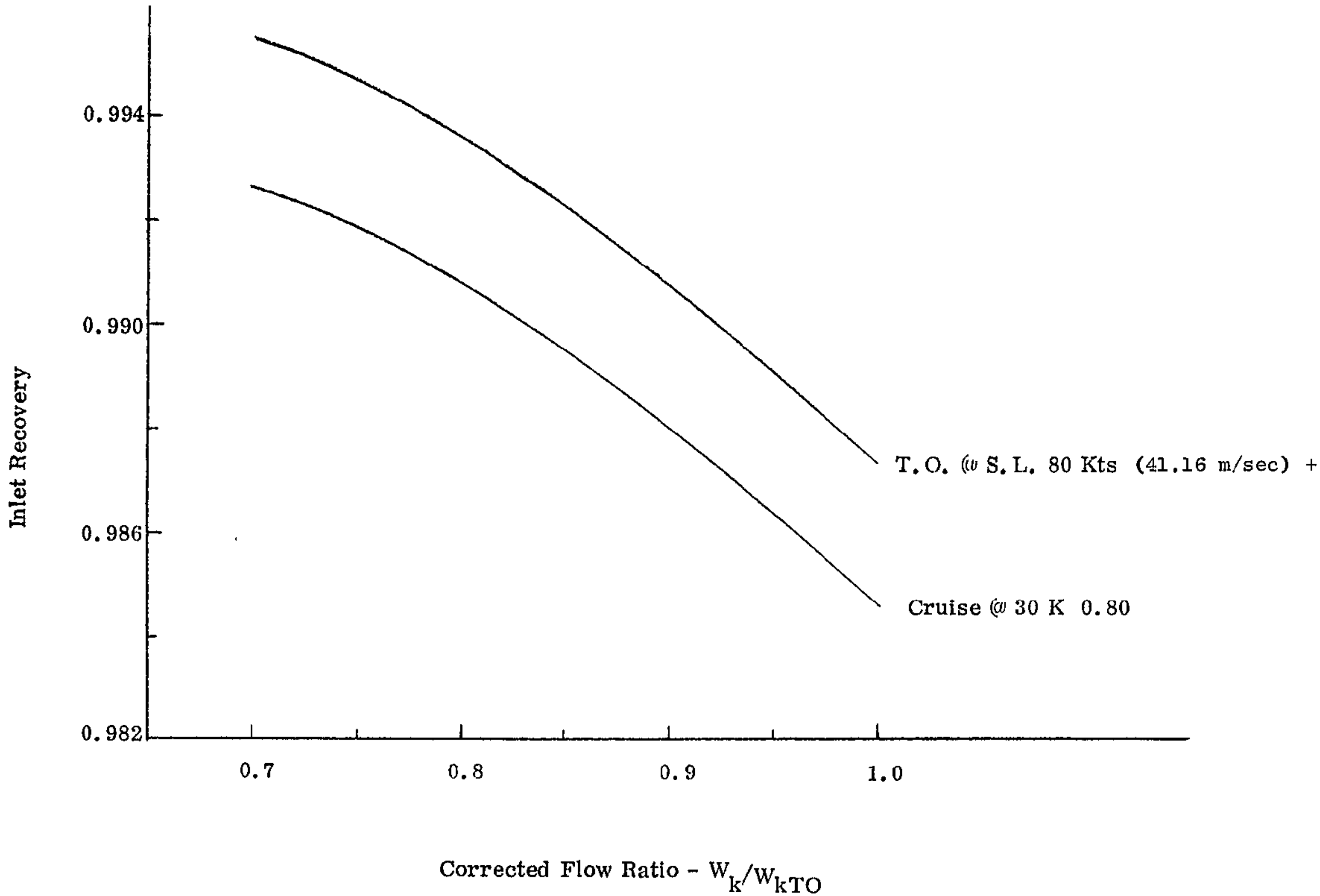

Figure VI-38. GE19/F9A3 Inlet Recovery Vs. Corrected Flow.

Table VI-19. Task II Study; GE19/F9A3 (Alternate Inlet) Installation Loss Breakdown at $\Delta P_T/P_T$ % at T.O. Power.

INLET

• Lip	.12
• Hardwall and Suppression	.83
• Splitters	-
• Strut	.04
• Spinner	.27
• Interference	.01
• Total	1.27

FAN DUCT

• Hardwall and Suppression	4%
• Splitters	T
• Strut	
• Reverser	O
• Interference	T
• Decayer	
• Nonsymmetric Duct	A
• Total	L

CORE

• Hardwall and Suppression	.82
• Strut	.09
• Reverser	.12
• Total	1.03
• Nozzle Gross Thrust Coefficient ~ C_V	.996

VII - INSTALLATION MECHANICAL DESIGN

AUGMENTOR WING ENGINES

The nacelles of the two augmentor wing engines are identical, except the GE19/F9A2 has an acoustically treated inlet and the GE19/F9A3 has a high Mach variable plug inlet. The nacelle construction is 1972 state of the art. The inlet structures are designed to meet FAA requirements for anti-icing and ingestion. The inlet loads are taken in the forward flange of the fan casing with latches; and, for accessibility on the wing, it is hinged to the pylon. The remainder of the cowling is designed to open allowing the engine to drop vertically for removal and replacement with a minimum of time. The CF6 ease of maintenance features have been factored into the nacelle design where applicable. A pressure vessel forms the air passage from the fan discharge to the pylon and is a hinged casing split at the bottom for engine removal. The aircraft duct is bolted directly to a flange on top of the nacelle which avoids the large piston forces which would develop with a flexible joint. The inner wall of the annular pressure vessel is formed by the core engine casing. The thrust reverser consists of two 70° louvered sections on each side of the pressure vessel which also forms the nacelle. The sealed external doors slide aft for thrust reversal synchronized with a shutoff valve in the aircraft duct.

A thrust spoiler is built into the core exhaust similar to the CF6-50.

EBF MIXED FLOW ENGINE INSTALLATION

The GE19/F2C1 and F2C2 are mixed flow EBF engines. The F2C1 has a conical nozzle and the F2C2 has an external mixer; otherwise, the nacelles are identical.

The nacelle designs are 1972 state of the art with desirable maintenance features similar to the CF6 engines. The cascade thrust reverser is located on each side of the nacelle on a 95° arc chosen to minimize hot gas ingestion and gas impingement on the aircraft and runway. The thrust reverser is similar to the CF6 in that the aft section of the nacelle moves back actuating fan flow blocker doors and exposing the cascades. This is shown on the lower half of the drawing. The large exhaust area minimizes core thrust during reversal.

USB Mixed Flow Nacelle, GE19/F2C3

The forward section of the nacelle is identical to F2C1 and F2C2. The fan exhaust has one acoustic splitter instead of three. The pylon and "D" support structure are integrated with the nacelle for vertical engine removal.

The estimate Δ weight of the "D" support structure and pylon is 248 lb (112.5 kg) which is offset by a 54 lb (24.5 kg) saving in the nacelle structure and a 175 lb (79.4 kg) saving in the thrust reverser structure, giving a net weight increase of 19 lb (8.6 kg). The cascade thrust reverser is aft of the pylon support "D" structure covering an arc of 160° which is also integrated with the variable A_8 nozzle.

EBF Separate Flow VP Fan Nacelle

The nacelles for the GE19/F6D1 geared fan VP engine and GE19/F6E1 direct drive VP engine are similar. The technology and maintenance features developed for the CF6 are incorporated in these nacelles as well as the FAA requirements.

Installation Weights

The installation weights of the QCSEE Task II configurations are given in Table VII - I with additional detail given in Tables VII - 2 through VII - 4. These weights do not include engine buildup weights such as aircraft-engine-driven accessories, fire protection system, aircraft piping or pylon, etc.

Weights shown are based on conventional materials and manufacturing techniques as follow:

Inlet

Outer skins .050" (0.127 cm) thick aluminum with a titanium skin 0.040" (0.102 cm) thick in the anti-iced region. It is a rib-fabricated construction. Sound treatment is aluminum honeycomb.

Fan Cowl

The fan cowl is one inch thick (2.54 cm) aluminum honeycomb with 0.040" (0.102 cm) thick outer skin and 0.020" (0.051 cm) thick inner skin.

Aft O. D. Cowl

The aft O. D. cowl is 0.040" (0.102 cm) thick titanium with structural reinforcement 0.60" (0.152 cm) thick.

Core Cowl

Aluminum honeycomb coated on the inner surface with fireproof material.

Turbine Exhaust

Steel honeycomb fabrication.

Acoustic Splitters

Aluminum honeycomb construction.

Advanced developments in composite materials and fabrication methods within the next ten years can reduce these nacelle weights approximately 15 to 20%.

Table VII-1. Task II Study, Installation Weight Breakdown, Lbs.

	AW, 3.0 P/P		1.35 P/P			1.25 P/P V.P.	
			EBF	EBF	USB	Ungeared	Geared
	F9A2	F9A3	F2C1	F2C2	F2C3	F6E1	F6D1
Nacelle including acoustic treatment	683 (309.8 kg)	914 (414.6 kg)	2070 (938.9 kg)	1758 (797.4 kg)	1975 (895.8 kg)	2160 (979.8 kg)	2090 (948 kg)
Mixers and nozzles	56 (25.4 kg)	56 (25.4 kg)	235 (106.6 kg)	922 (418.2 kg)	245 (111.1 kg)	243 (110.2 kg)	243 (110.2 kg)
Engine mounting	67 (30.4 kg)	67 (30.4 kg)	86 (39 kg)	86 (39 kg)	86 (39 kg)	97 (44.8 kg)	86 (39 kg)
Reverser and spoiler	694 (314.8 kg)	694 (314.8 kg)	1154 (523.4 kg)	1193 (541.1 kg)	765 (347 kg)	---	---
Totals	1500 (680.4 kg)	1731 (785.2 kg)	3545 (1608 kg)	3959 (1795.8 kg)	3071 (1393 kg)	2500 (1134 kg)	2419 (1097.2 kg)

Table VII-2. Task II Study, Nacelle Weight Breakdown, Including Acoustic Treatment, Lbs.

	AW, 3.0 P/P		1.35 P/P			1.25 P/P V.P.	
			EBF	EBF	USB	UNGEARED	GEARED
	F9A2	F9A3	F2C1	F2C2	F2C3	F6E1	F6D1
* INLET SYSTEM	337 (152.9 kg)	568 (257.6 kg)	732 (332 kg)	732 (332 kg)	732 (332 kg)	807 (366 kg)	757 (343.4 kg)
INLET SPLITTERS	(81) (36.7 kg)	(0)	(170) (77.1 kg)	(170) (77.1 kg)	(170) (77.1 kg)	(0)	(0)
* FAN COWL + DUCT	206 (93.4 kg)	206 (93.4 kg)	1130 (512.6 kg)	832 (377.4 kg)	1038 (470.8 kg)	881 (400 kg)	861 (390.5 kg)
DUCT SPLITTERS	(0)	(0)	(375) (170.1 kg)	(375) (170.1 kg)	(171) (77.2 kg)	(236) (107 kg)	(236) (107 kg)
CORE COWL	7 (3.2 kg)	7 (3.2 kg)	141 (64 kg)	153 (69.4 kg)	133 (60.3 kg)	356 (161.5 kg)	356 (161.5 kg)
CORE INNER FLOWPATH	4 (1.8 kg)	4 (1.8 kg)	67 (30.4 kg)	41 (18.6 kg)	72 (32.7 kg)	116 (52.6 kg)	116 52.6 kg)
FAN EXHAUST PRESSURE VESSEL	129 (58.5 kg)	129 (58.5 kg)	---	---	---	---	---
TOTAL WEIGHT	683 (309.8 kg)	914 (414.6 kg)	2070 (938.9 kg)	1758 (797.4 kg)	1975 (895.8 kg)	2160 (979.8 kg)	2090 (948 kg)

* INCLUDES SPLITTER WEIGHT

Table VII-3. Task II Study, Cascade Thrust Reverser Δ Weight.

		AW, 3.0 P/P		1.35 P/P		
				EBF		USB
		F9A2	F9A3	F2C1	F2C2	F2C3
Flow Area*	In.^{2}	305	305	2543	2628	2831
	Cm^2	(1967.7)	(1967.7)	(16406.4)	(16954.8)	(18264.5)
Blocker Doors, Actuators and Links	Lbs	10	10	191	197	213
	Kg	(4.5)	(4.5)	(86.6)	(89.4)	(96.6)
Cascade Boxes	Lbs	13	13	169	175	188
	Kg	(5.9)	(5.9)	(76.7)	(79.4)	(85.3)
Configuration + Δ Structure	Lbs	169	169	794	821	366
	Kg	(76.7)	(76.7)	(360)	(372.4)	(166)
Total Δ Weight	Lbs	192	192	1154	1193	767
	Kg	(87.1)	(87.1)	(523.4)	(541)	(347.9)

Table VII-4. Task II Study, Thrust Spoiler Weight Breakdown, AW, 3.0 P/P, GE19/F9A2 and GE19/F9A3.

ITEM	WEIGHT Lbs	WEIGHT Kg
TRANSLATING COWL, BLOCKER DOORS AND LINKS	231	104.8
FIXED STRUCTURE CASCADES	132	59.9
CENTERBODY	59	26.8
MISCELLANEOUS HARDWARE	17	7.7
C & A	63	28.6
TOTAL	502	227.7

MAINTAINABILITY

The mechanical design effort in Task I was for nacelles utilizing CF6 technology. In Task II, investigations were conducted to determine the weight savings that would be deemed practical for a 1980 service engine. In addition, more detailed investigations were conducted to improve the noise, performance, maintainability, and weight integration.

To put the point of departure in perspective, the CF6 nacelle is the best integrated nacelle design in airline service, according to the using airlines.

General Electric has the responsibility of guaranteed installed performance and noise of this nacelle installation besides being responsible for the detail design and manufacture of the fan thrust reverser including the fan nozzle and inner cowl and the primary thrust reverser including the primary exhaust and centerbody. Rohr manufactures the inlet, the fan cowl door , and the aft core door.

The inlet has a titanium anti-iced inletlip, aluminum sheet and stringer inlet outer wall and an integrated aluminum honeycomb acoustic treatment inner wall.

The fan cowl door is of aluminum honeycomb construction and contains separate access doors for normal line service access as shown on Figure VII - 1. This door is a single layer door, light enough for one man access, in and out, in 3 minutes, for accessibility to 72% of the line replaceable items as shown on Figure VII - 2.

The thrust reverser is split and is hinged at the pylon to allow access to the core for maintenance and engine removal without the reverser and without requiring

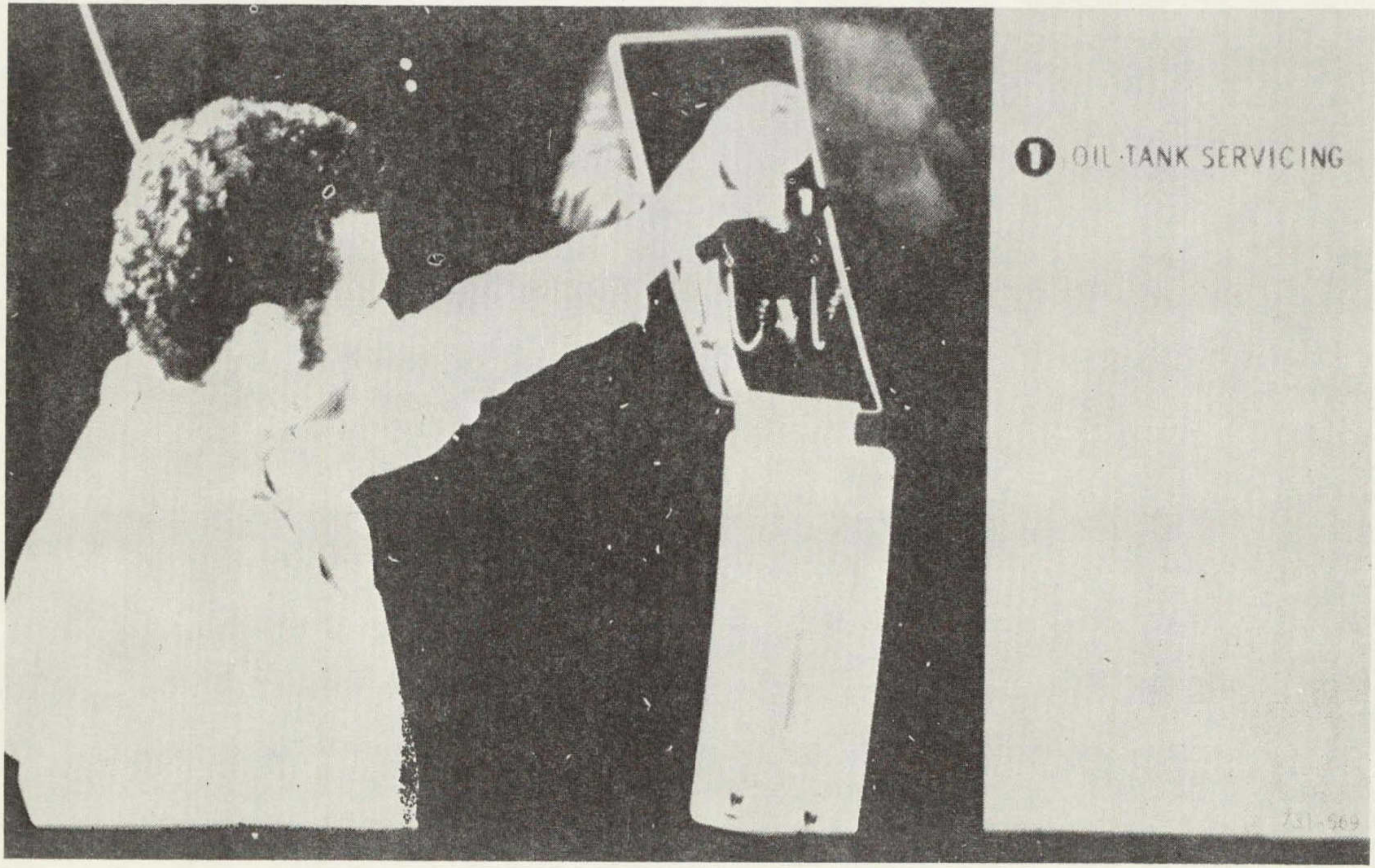

Figure VII-1. CF6 Nacelle, Accessibility, Oil Tank Servicing.

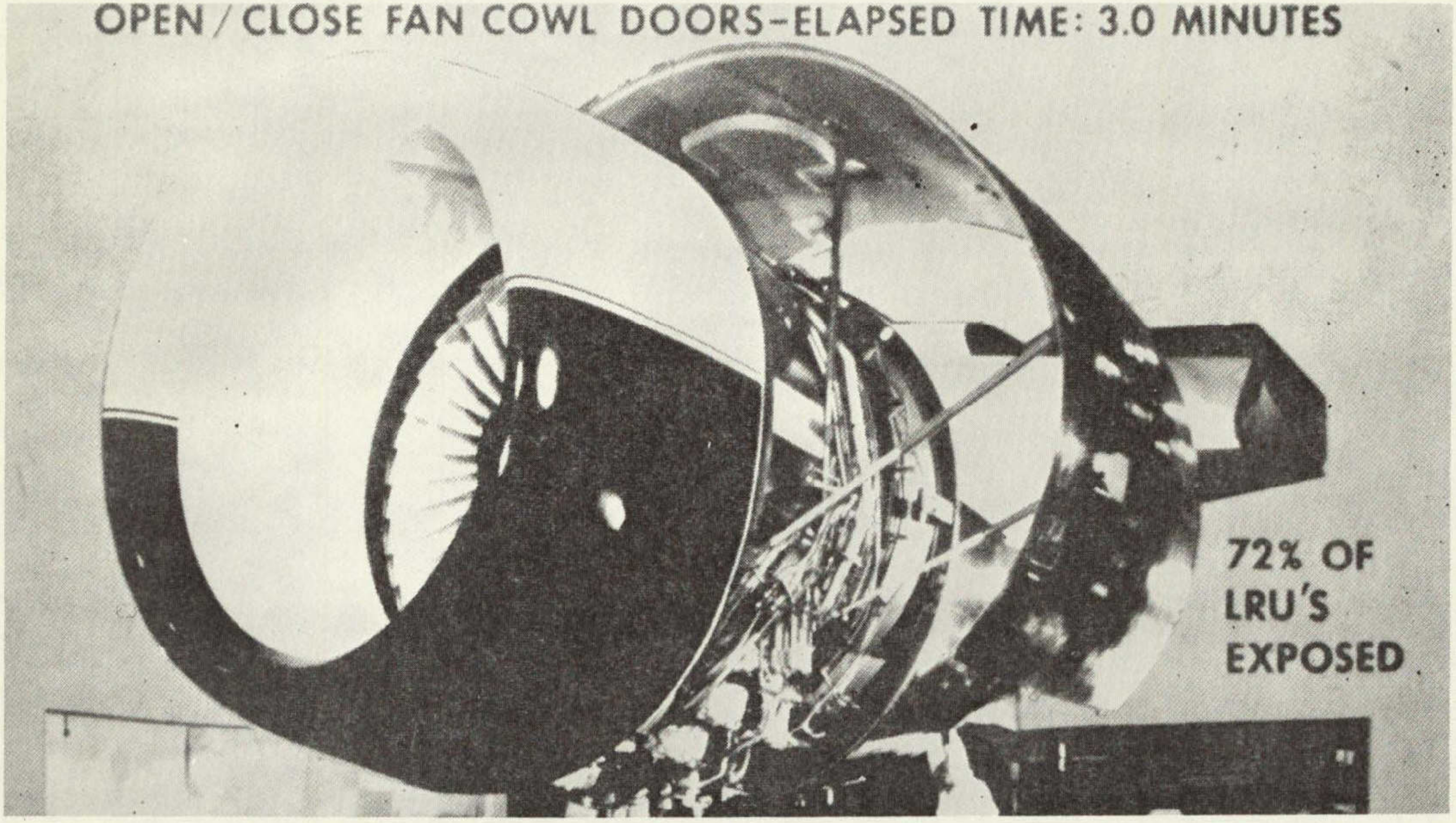

Figure VII-2. CF6 Nacelle, Quick Access.

buildup on the engine as a QEC item. These doors require power actuation due to their size. With these and the aft core cowl doors open, all LRU's are accessible without removal of any QEC items as shown on Figures VII - 3 and 4. The thrust reverser outer wall treatment is double-degree-of-freedom composite material built in panels and is not integrated into the structure. QCSEE weight estimates have all been made assuming integrated acoustic treatment like the inner wall and blocker doors of the CF6 thrust reverser.

The core nozzle and core thrust reverser are made of steel with combinations of sheet and stringer and steel honeycomb construction.

As a result of the CF6 work, GE established the pod system requirements for QCSEE as shown on Tables VII - 5, 6. The weights shown are consistent with nacelles meeting these requirements. The acoustic material used throughout the design comply with the requirements shown on Table VII - 6. Whenever practicable, the acoustic material is integrated into the structure.

Maintenance requirements for the installed engine were established in order to determine door locations and the accessibility requirements. Component change time objectives are shown on Table VII - 7, while module and LRU change time objectives are shown on Table VII - 8. Similar objectives have been demonstrated on the CF6 installation.

Isometric drawings showing the door locations and accessibility features for each of the three basic different engines are shown on Figures VII - 5 through 10. The features for the EBF installation are quite similar to the CF6. The over-the-wing installation requires a three-piece fan exhaust cowl door if the wing is close

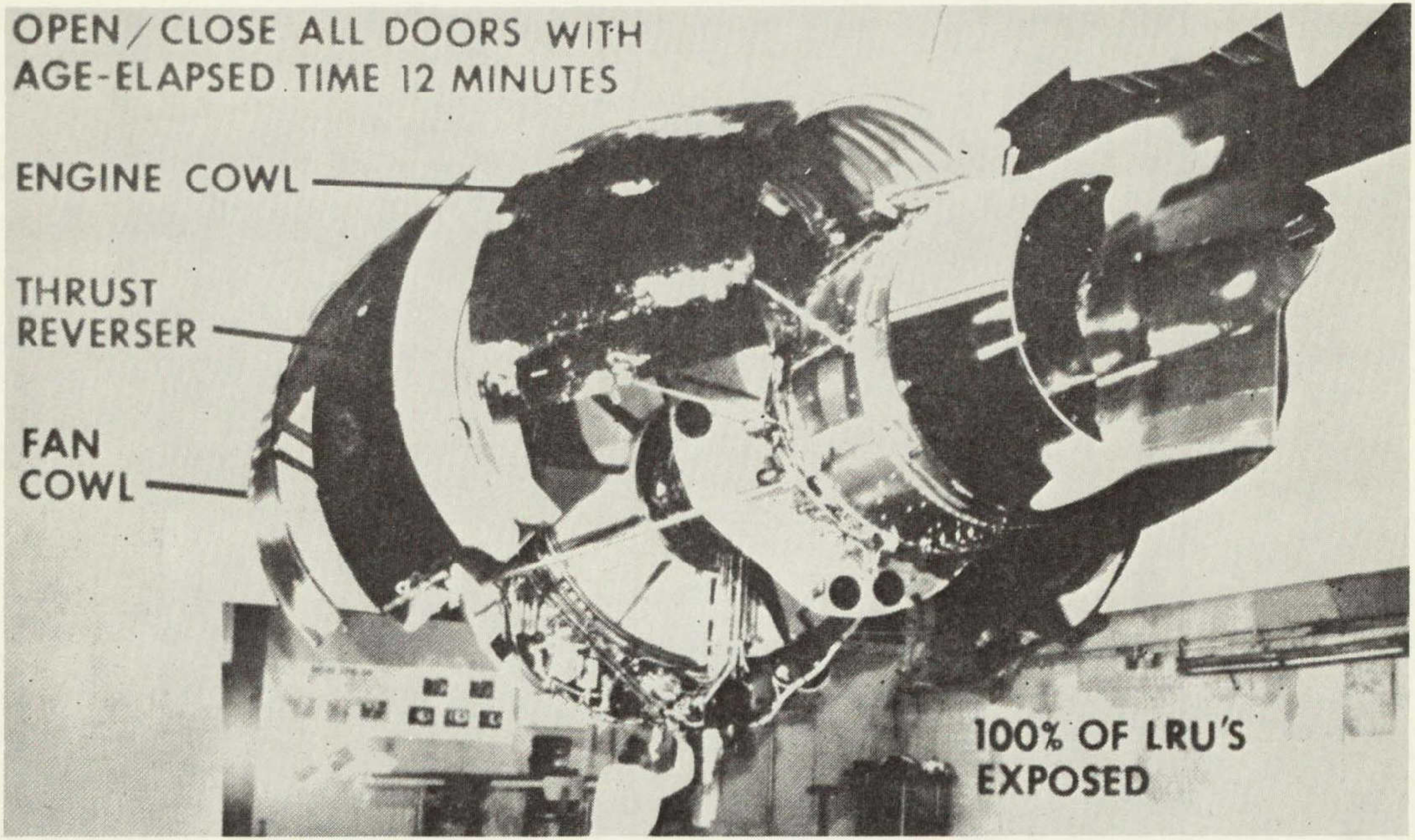

Figure VII-3. CF6 Nacelle Quick Access.

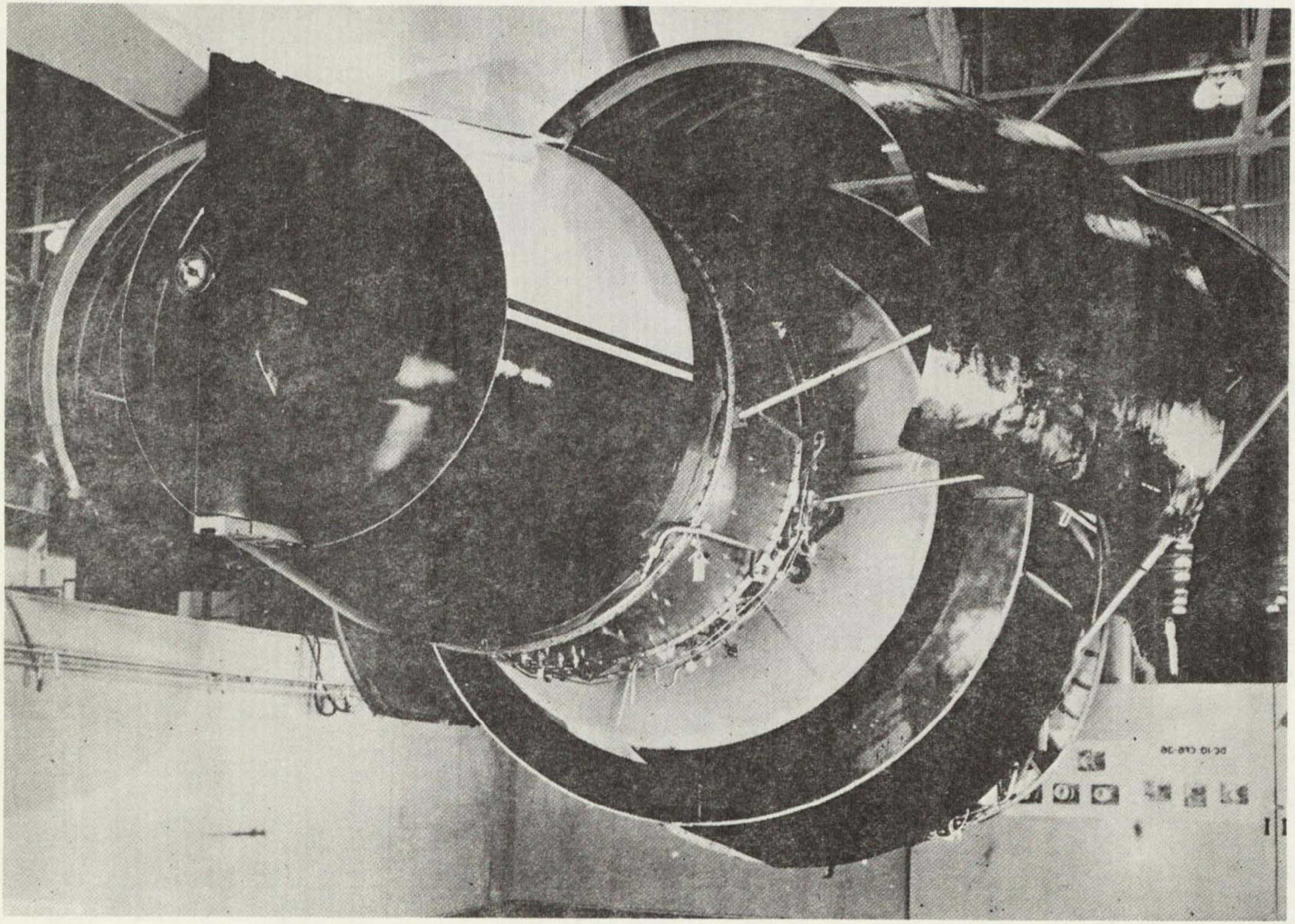

Figure VII-4. CF6 Nacelle.

Table VII-5. Task II Study, POD System Requirements.

- Pod designed for 36,000 hours with repair.
- All nacelle components to stay on the aircraft and not be part of QEC buildup.
- Mounting on aircraft to be with vertical movement only.
- No handing of engine -- 45 minutes elapsed time for buildup of handed QEC from neutral QEC.
- No QEC items to require removal for:
  - Normal engine maintenance
  - Removal of any accessory
  - Borescoping each stage
  - Separating the engine into modules
  - Radiographic inspection of complete engine (with exception of nose bullet access)
- Separate access doors for:
  - Engine and CSD oil servicing
  - Hydraulic filters
  - Starter air valve bypass
- Single layer door, manually operated, for access to gearbox and major number of LRU's.
- All doors of more than 140 pounds to be power operated by built-in actuators or simple AGE.
- Inspection doors and panels to be unstressed.
- Mounting structure to be failsafe.
- Fire walls to be provided to isolate all "fire zones" from other components and primary aircraft structure.
- No electrical components below or downstream of cooling or ventilating flows from fuel or oil components.
- Double-wall vented fuel lines in all areas where casings or ventilating air temperatures exceed ignition temperature.
- All pneumatic system components in fire zones to be fireproof.
- No overboard fuel drainage.
- No unlike fluids drained in common line.
- All drains separable at common location for troubleshooting.

Table VII-6. Task II Study, Mechanical Design Requirements, Acoustic Components.

- Structural parts 36,000 hr life with repair.
- Material non-wicking.
- Material cleanable to restore full acoustic properties.
- Provisions to drain fluids to be provided.
- Inlet splitters and support struts to have evaporative leading edge anti-icing.
- Inlet splitters to retain structural integrity when struck with one 4-lb (1.8-kg) bird and one 2-in. (5.08-cm) ice ball per 400 sq in. (2580.6 cm^2) of inlet area at flight speeds.
- Inlet splitter design to allow access to change or repair fan blades in 6 minutes or less.

Table VII-7. Task II Study, Maintenance Objectives, Component Change Time On-Wing.

	Minutes
Anti-Icing Valve	15
CSD/Generator	30
Hydraulic Pump	15
Starter	15
Starter Valve	10
Fuel Injector	15
Fuel Control	45
Lube & Scavenge Pump	20
Ignition Cable	15
Igniter Plug	5
Fan Blade FP	15
Fan Blade VP	45

Table VII-8. Task II Study, Maintenance Objectives, Module Change Time.

	Hours
Fan Rotor	3
Combustor	7.5
HP Turbine	6.5
LP Turbine	3.5
Accessory Drive	3.0
Thrust Reverser	1.0
Gearbox (for VP F6D Series)	4.0
VP Mechanism	1.5

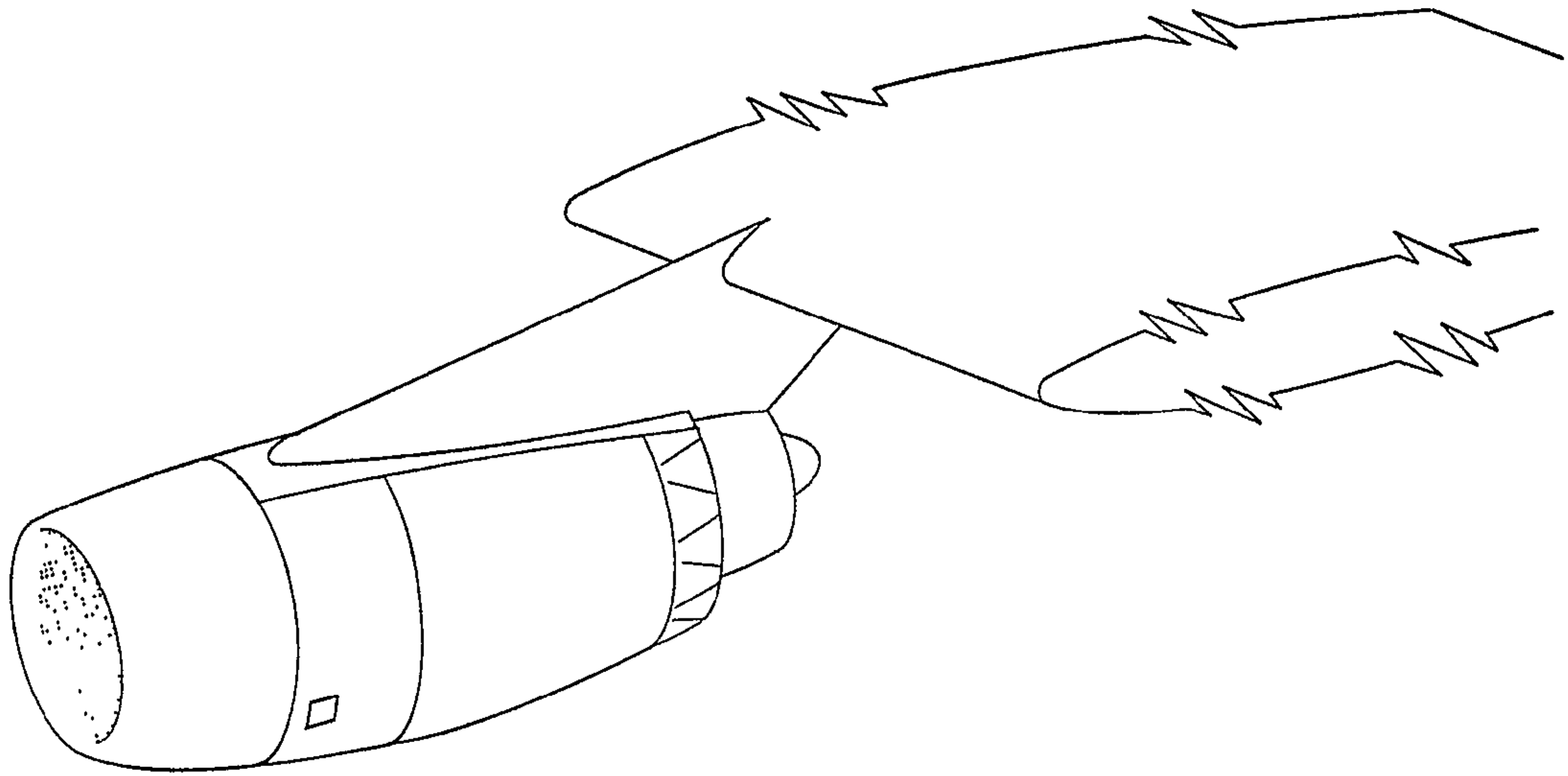

Figure VII-5. GE EBF Engine on Wing Maintainability, Overall.

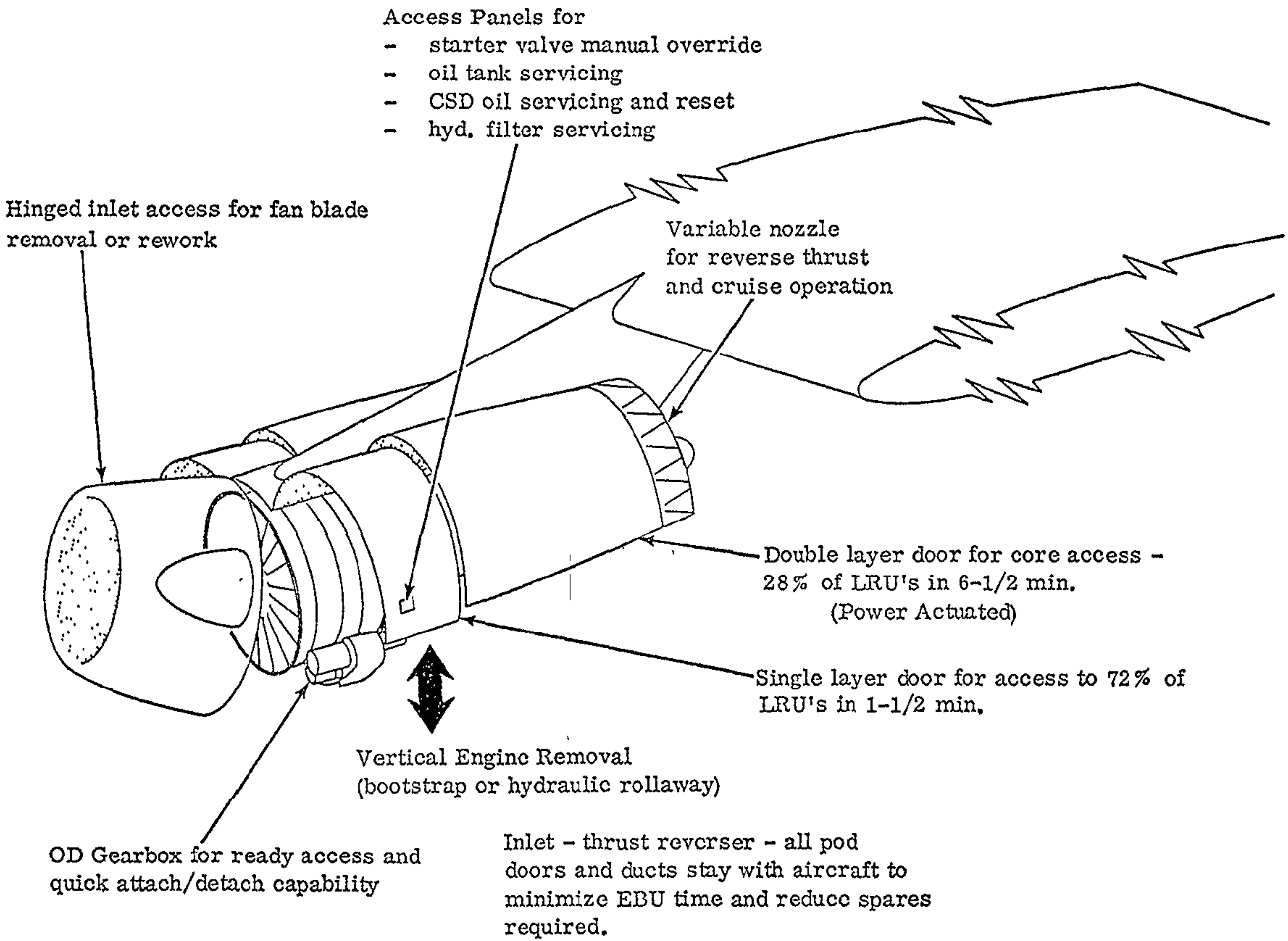

Figure VII-6. GE EBF Engine on Wing Maintainability, Detailed.

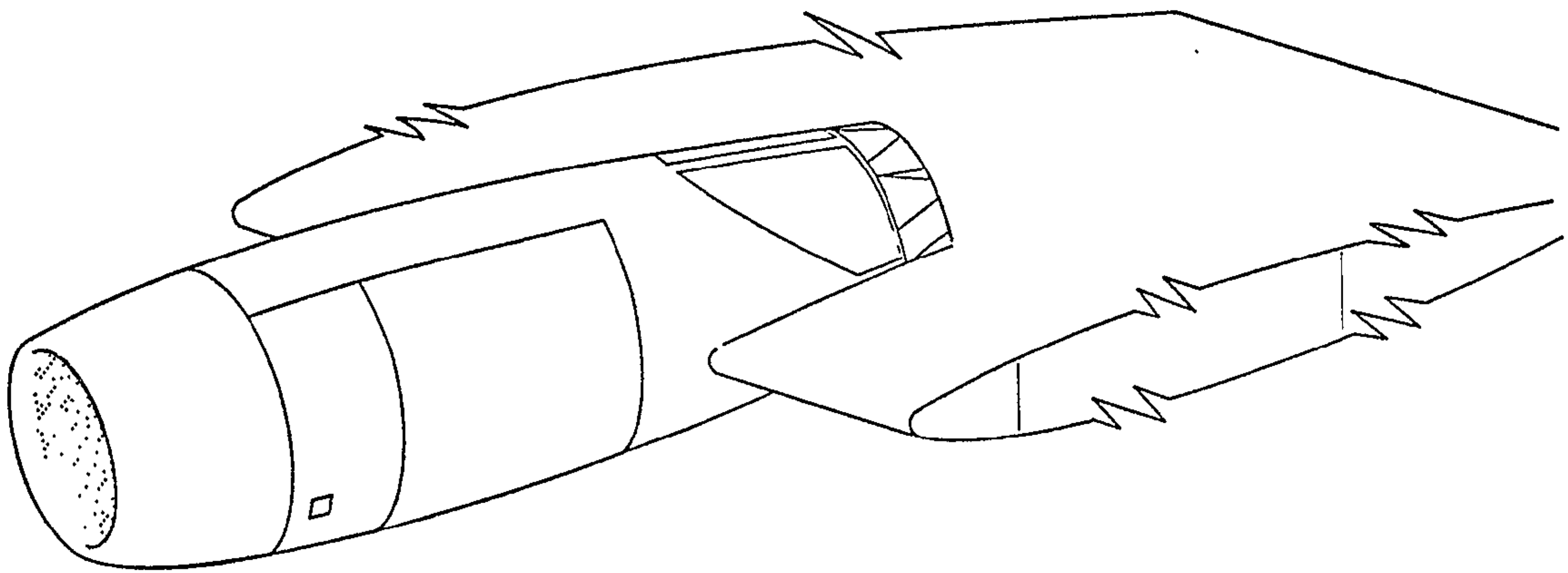

Figure VII-7. GE OTW Engine on Wing Maintainability, Overall.

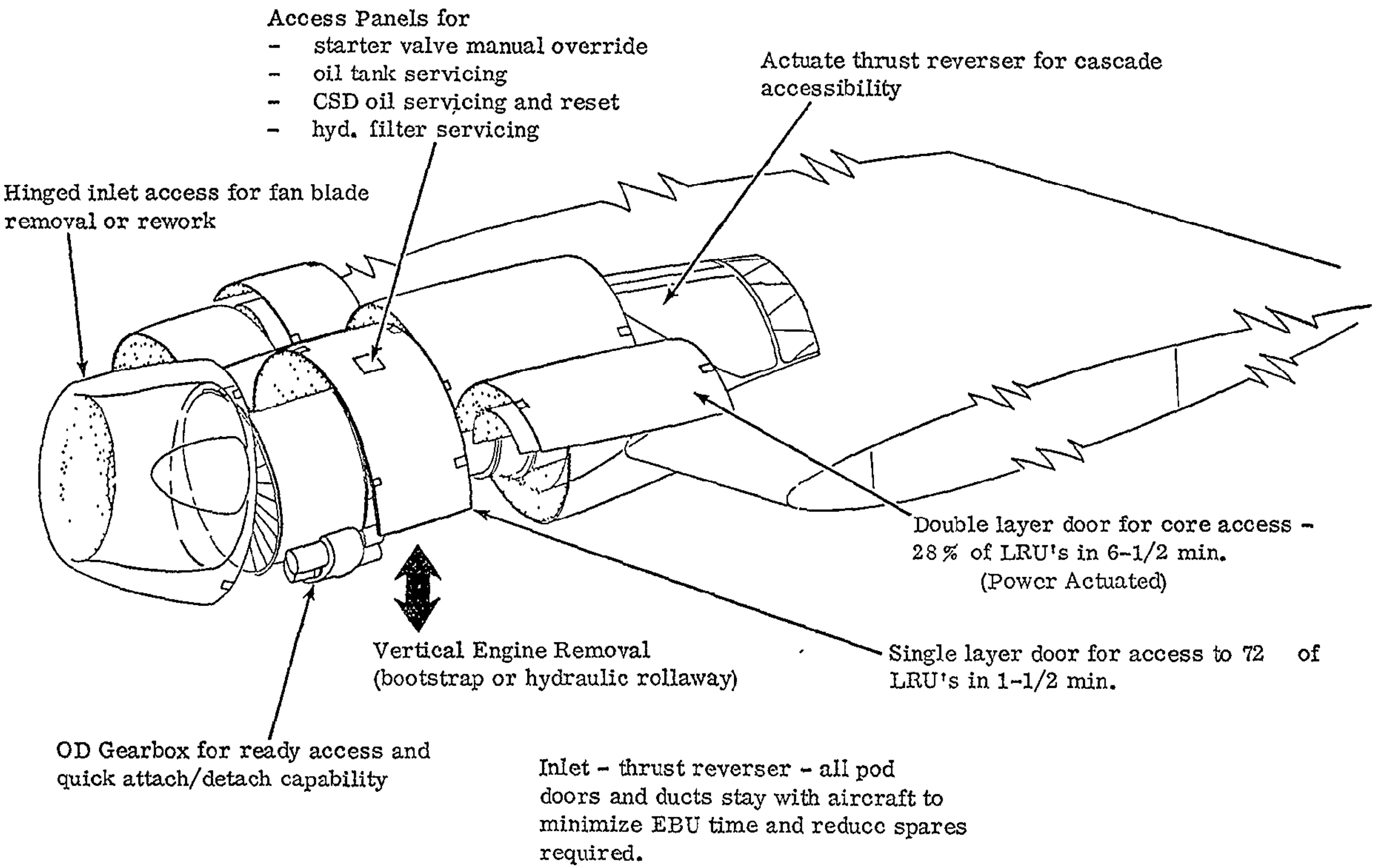

Figure VII-8. GE OTW Engine on Wing Maintainability, Detailed.

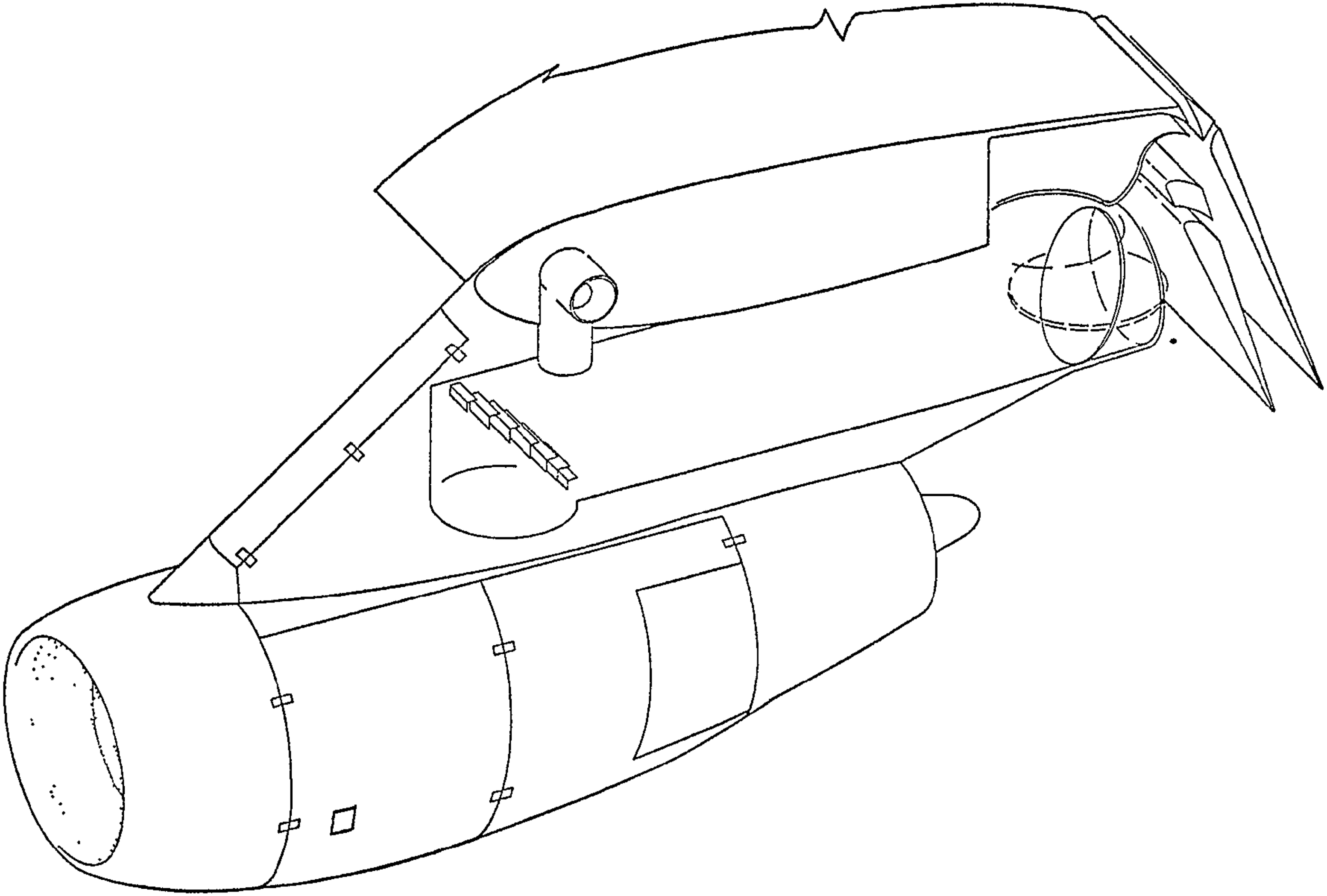

Figure VII-9. GE AW Engine on Wing Maintainability, Overall.

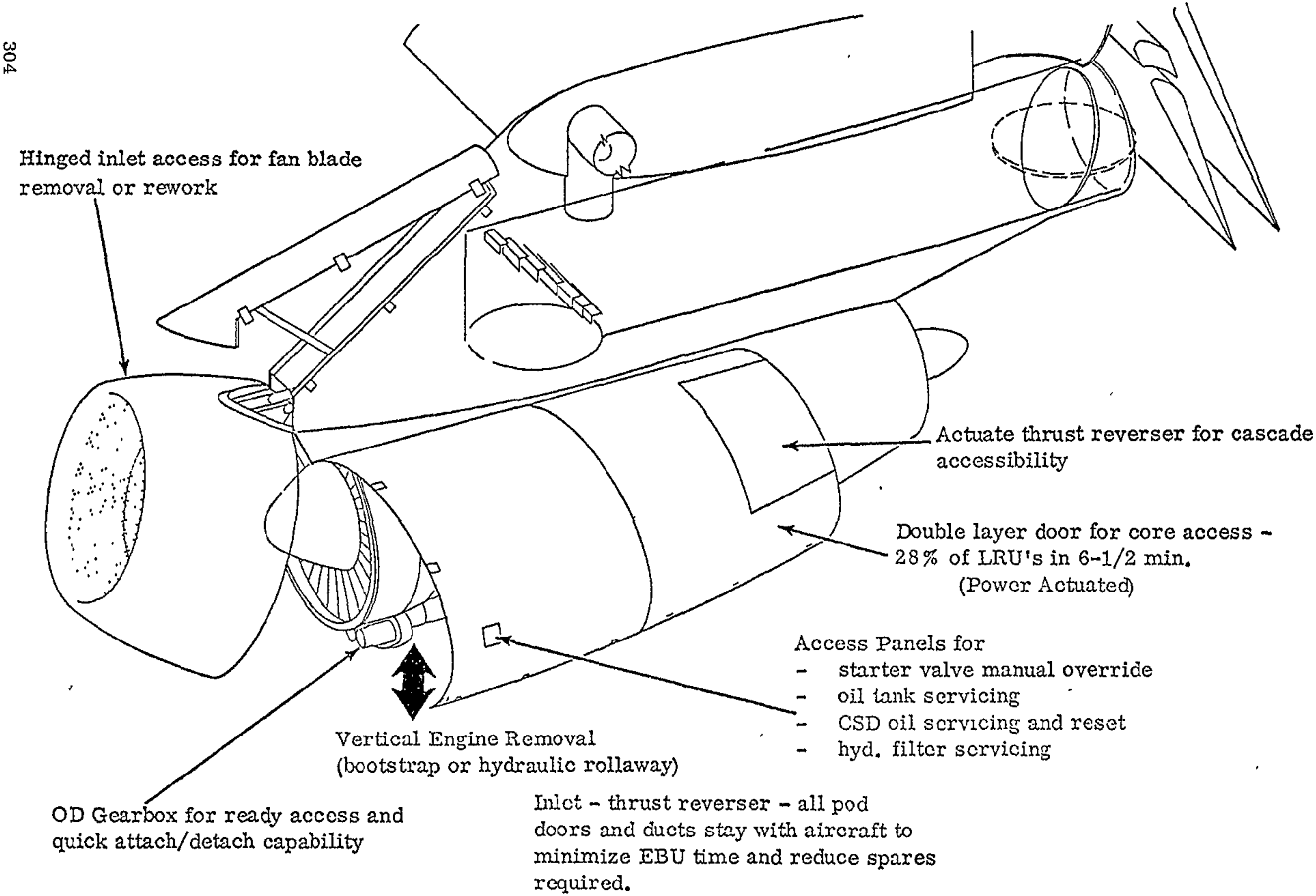

Figure VII-10. GE AW Engine on Wing Maintainability, Detailed.

enough to the ground so a 3/4 door would have insufficient ground clearance. The 3/4 door is required to clear the leading edge of the wing on the inboard side due to the wing sweep. For the over-the-wing installation the best support scheme studied to date is the top pylon D ring scheme shown on Figure VII - 11. The integration of this with the thrust reverser and nozzle support provides a weight saving, and the top pylon provides sufficient accessibility.

Since there were some questions raised on the weight estimates of the Task I pods, an independent check of the weight estimates was made by MDC, Rohr, and Boeing-Wichita. These estimates confirmed the GE weights as shown on Table VII - 9.

The weight improvements in Task II, due to design refinements and investigations of new structural materials and techniques, are shown on Table VII - 10. Table VII - 11 provides a breakdown by weight sections of the potential weight savings of composite construction. General Electric has demonstrated a weight saving of 35% on some major pod parts under other contracts.

The Task II pod weights for each of the 7 Task II engines are shown on Table VII - 12.

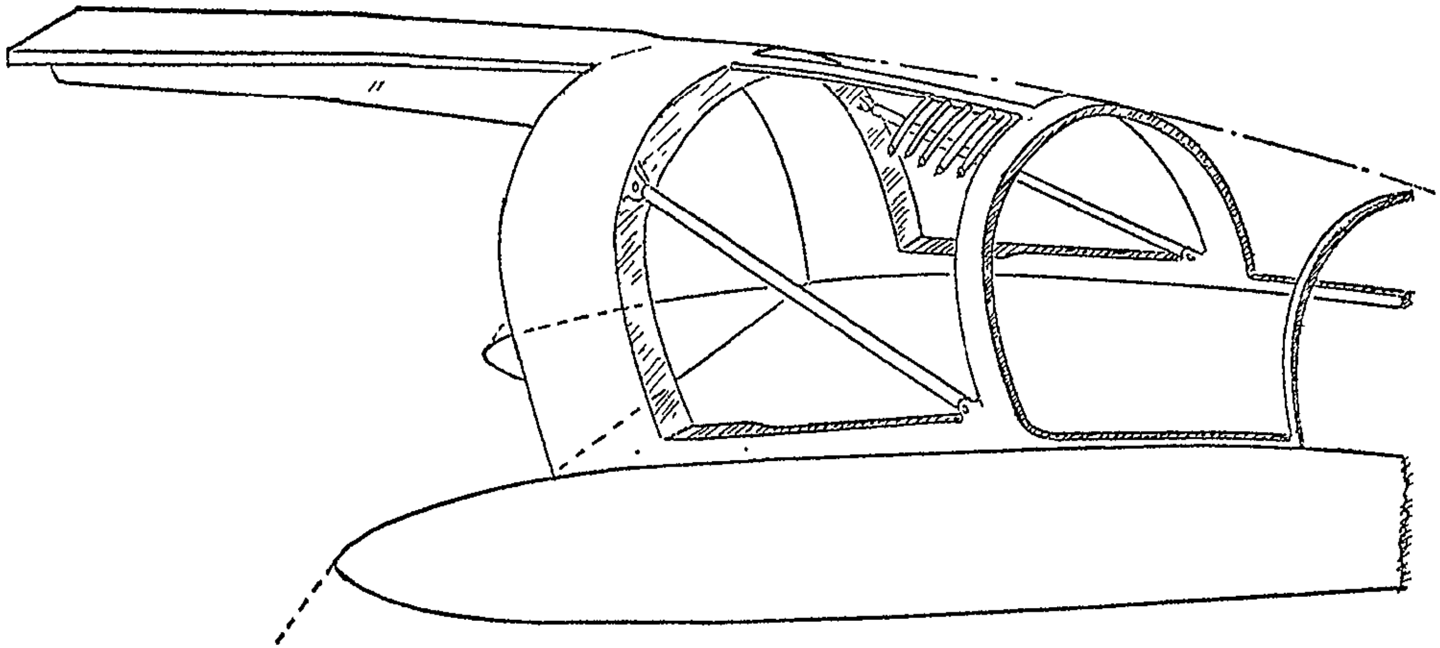

- Ties into main wing spar.
- Allows normal top pylon engine support and vertical engine removal.
- Provides structure for thrust reverser support.
- Replaces section of pod wall.
- Avoids extra struts through flowpath.
- Large weight savings possible with composites.

Figure VII-11. GE OTW Support.

Table VII-9. EBF Pod Weight Substantiation, CF6 Technology, No Pylon or Aircraft Systems.

GE19/F6A3 (1.25 VP 22,000 lb (97861 N) F_N)		Task I
GE Weight Estimate	Lb Kg	2750 (1247.4)
McDonnell-Douglas Weight Estimate of GE Aero/Acoustic Design	Lb Kg	2725 (3972.8)
McDonnell-Douglas Weight Estimate of MDC Aero/Acoustic Design	Lb Kg	2905 (1317.7)
Boeing-Wichita Weight Estimate of GE Aero/Acoustic Design		Within few % of GE estimate
GE19/F6A3-1 (1.25 VP 22,000 lb (97861 N) F_N with Shorter Inlet)		
GE Weight Estimate	Lb Kg	2325 (1054.6)
Rohr Weight Estimate of GE Aero/Acoustic Design	Lb Kg	2380 - 2600 (1079.5 - 1179.3)

ORIGINAL PAGE IS
OF POOR QUALITY

Table VII-10. Pod Weight Improvement, 1.25 VP Fan Engine.

- Task I Pod Weight (CF6 Technology Level - 1970) = 2750 lb (1247.4 kg) [for 22,000 (97861 N)]

  $F_N/Wt = 8.0$

- Task II Pod Weight (CF6 Technology Level - 1970) = 2500 lb (1134 kg) [for 24,000 (106756 N)]

  $F_N/Wt = 9.6$

- Weight Improvement Task II - Task I = 19%

- Improved by
  - More effective acoustic design
  - Simpler reverse thrust inlet
  - Better integrated mechanical design

- Task II Pod Weight with Advanced Technology - (1980) = 2055 (932.1 N) (Preliminary)

  $F_N/Wt = 11.4$

Table VII-11. GE19/F6E1 Preliminary Pod Weight Technology.

	Weight CF6 Tech			Weight 1980 Tech			
	Lbs	Kg	Material	Lbs	Kg	Material	% Weight Reduction
Inlet							
Inlet Cowl & Anti-Icing	675	306.2	Al	465	211	Carbon/Glass	31
Inlet Centerbody Support	115	52.2	Al	75	34	Carbon/Glass	35
Inlet Wall Treatment	15	6.8	Al Honeycomb	15	6.8		
Aft Fan Cowl							
Outer Fan Duct	620	281.2	Al Honeycomb	495	224.5	Carbon/Glass	20
Inner Core Cowl	95	43.1	Al Honeycomb	75	34.0	Carbon/Glass	20
Fan Exhaust Rings	235	106.6	Al Honeycomb	185	83.9	Carbon/Glass	21
Wall Treatment	45	20.4	Al Honeycomb	45	20.4	Al Honeycomb	---
Nozzle Actuation of Control	245	111.1	---	245	111.1	---	---
Primary Exhaust							
Nozzle & Aft Core Cowl	230	104.3	Stressskin	230	104.3	Stressskin	---
Plug	110	49.9	Stressskin	110	49.9	Stressskin	---
Primary Noise Treatment	15	6.8	Steel Honeycomb	15	6.8	Steel Honeycomb	---
Mounting	100	45.4	Steel	100	45.4	Steel	---
Total Pod Weight (Exclusive of Pylon and Equipment)	2500	1134		~2055	932.1		~18
Delta Weight for Advanced Technology				~445	201.8		

Table VII-12. GE19 Pod Weight, Exclusive of Pylon and Equipment.

		Fixed Pitch			Variable		AW	
		F2C1	F2C2	F2C3	F6D1	F6E1	F9C2	F9C3
		EBF	EBF Decayer	OTW	Geared	Direct	Splitter Type	Choked Inlet
CF6 Technology (1970)	Lb	3545	3960	3070*	2420	2500	1500	1730
	Kg	(1608)	(1796.2)	(1392.5)	(1097.7)	(1134)	(680.4)	(784.7)
Advanced Technology (1980)	Lb	2805	3265	2535*	2000	2055	1280	1350
	Kg	(1272.3)	(1481.0)	(1149.9)	(907.2)	(932.1)	(580.6)	(612.3)
% Weight Improvement for Advanced Technology		21%	18%	17%	17%	18%	15%	22%

* Includes credit for portion of support structure replacing section of outer fan cowl.

VIII - COMPARISONS

The primary results of the Task II study are the propulsion system designs including their performance, weight, dimensions, noise and emissions characteristics previously described. However, there are several interesting comparisons and observations which can be made.

COMPARISON WITH GE13 & CF6

Table VIII - 1 compares the variable and fixed pitch GE19 engines with two other engines, one the GE13/F10 which was the engine proposed by GE in the USAF ATE-STOL competition, and the other the CF6-6 which can be considered a typical modern CTOL engine. Of particular interest are the fan pressure ratios at takeoff and cruise, the thrust-to-weight ratios and the cruise to takeoff thrust ratios.

F101 CORE

The F101 core used in the GE19 engines is designed as a commercial core as indicated on Table VIII - 2. The only area in which the supersonic requirements of the F101 make a clear difference is in the materials selection on the compressor. Ti could be used on two stages which are now steel if the engine were designed for subsonic operation only. Note that growth of the engine will utilize whatever core capability is available beyond that utilized at the initial ratings.

Table VIII-1. Task II Study, Engine Comparisons.

	NASA QCSEE		USAF ATE-STOL	Current CTOL
	GE19/F6E VP	GE19/F2C	GE13/F10	CF6-6
Rated Thrust	24,000 (106757 N)	24,000 (106757 N)	24,000 (106757 N)	39,300 (174815 N)
Fan P/P - T O	1.25*	1.35*	1.52	1.56
Fan Tip Diameter	83" (210.8 cm)	70" (177.8 cm)	68.3" (173.5 cm)	86.4" (219.5 cm)
$W\sqrt{\theta}/\delta$ - T O	1200	969	850	1310
T 4 / day - day	2440°F/90°F (1337.8°C/32.2°C)	2400°F/90°F (1315.6°C/32.2°C)	2510°F/103°F (1376.6°C/39.4°C)	2370°F/86°F (1298.9°C/30°C)
T O Thrust / Weight	5.7	6.7	7.0 **	5.2
M = .8, 30K Max. Cr. Thrust	4900 (21796.3 N)	5800 (25799.7 N)	5700 (25354.9 N)	10,500 (46706.3 N)
Cruise Thrust / Wt.	1.2	1.6	1.7	1.4
Cruise Thrust / 80 knts (41.16 m/sec) Thrust	0.22	0.26	0.28	0.29
Fan P/P - Cruise	1.33*	1.42*	1.54	1.68
Bypass Ratio - Cruise	14.4	8.3	6.5	5.9
Overall P/P - Cruise	18.2	25	26.5	27

* 2-Position Nozzle

** No Containment

ORIGINAL PAGE IS OF POOR QUALITY

Table VIII-2. Task II Summary, F101 Core Characteristics.

- Original proposed F101 core fan B1 did not quite meet civil subsonic transport life and maintainability requirements for civil transport.

  Supersonic B1 parts requirements came closer to meeting civil requirements than a fighter engine, but still missed somewhat.

- In 1970 GE negotiated with the USAF the addition of ~80 lbs (36.3 kg) for increased B1 life and maintainability and at the same time met civil transport requirements. For Example:
  - Borescope parts at each stage
  - Additional modular maintenance features
  - Provisions for condition monitoring
  - Thicker flanges for repairability
  - Wear bushing and strip
  - Rabbeted flanges

- F101 core is considered optimum core for ~24,000 lbs (106757 N) Fn civil CTOL and STOL engines --- with 20% growth.
  - Not significantly penalized by B1 supersonic requirement.

GROWTH

Table VIII-3 summarizes the effects on noise of a thrust growth of 25% for each of the engines. The case where fan diameter is held constant is felt to be the most meaningful. Although an increase in diameter of 10% can limit the noise increase to 1 to 1-1/2 EPNdB, the installation would require a complete redesign, and the aircraft may require modification to use the larger engines. If the fan diameter is held constant, the changes are restricted to the engine itself, and the growth becomes directly useful for increased gross weight versions of a given aircraft design. Note that the fan pressure ratio of the augmentor wing engine gets out of hand for 25% growth at constant diameter, 10 - 15% growth is probably the limit in this case.

On a consistent basis, the noise increases 4 to 4-1/2 EPNdB for 25% thrust growth at constant diameter. However, for the time period when the 25% growth will be needed, it is believed there would be improvement in flap/jet noise, and fan and core noise control achieved. On Table VIII-3 is shown the effects of a possible improvement (by suppression or otherwise) of these noise sources. The result is that the noise increase would be limited to the 1-1/2 to 2 EPNdB level which should be acceptable for the higher gross weight aircraft that would utilize the 25% growth.

VARIABLE PITCH CONSIDERATIONS

The primary reason for going to variable pitch is to utilize the fan for reverse thrust. A major choice to be made is the direction through which the blades are to be reversed. The problems associated with each direction

Table VIII-3. Task II GE19 Growth Summary.

BASE ENGINE	F2C			F6D			F6E			F9A		
% THRUST INCR. @ TO	15	25	25	15	25	25	15	25	25	15	25	25
FAN DIAM. INCREASE	0	0	+10%	0	0	+10%	0	0	+10%	0	0	+10%
FAN P/P	1.425	1.50	1.365	1.28	1.33	1.25	1.28	1.33	1.25	3.9	*	2.9
ΔEPNdB - EVUIV. SUPPR.	+2	+4½	+1	+2	+4	+1½	+2	+4	+1½	+2½	-	+1
ΔEPNdB - WITH STATE-OF-ART REDUCTIONS -3 PNdB - FLAP @ CORE NOISE	-½	+2	-2	-½	+1½	-1	-	+1½	-1	+1½	-	-1

* EXCESSIVE

are listed on Table VIII - 4. A question in varying blades through fine pitch is the magnitude of reverse thrust obtainable since the blades are cambered in the wrong direction in reverse. Hamilton Standard has reported some data on a scale model fan with low tip speed (775 fps) (236.2 m/sec) which showed inadequate reverse thrust for this case. It is expected that the higher tip speed GE19 variable pitch fans will be better since the camber is much lower and since the higher tip speed will enable the blade to absorb the energy available from the core. This is borne out on Dowty Rotol reverse thrust experiments in 1971-1972. Note that the Hamilton Standard data showed the fan absorbed only a portion of the design energy input when reversed through fine pitch.

A second limitation is that of hub solidity. If normal loadings are observed, about 4% higher fan hub pressure ratio could be obtained if the hub chords were increased to raise the solidity from 0.95 to 1.5 for an 1100 fps (335.3 m/sec) fan. The efficiency would be no better, low solidity being desirable for subsonic mach numbers. We have concluded that designing the fan for unity solidity does not represent a penalty for a fan in the 900 to 1100 fps (274.3 to 335.3 m/sec) range.

The primary risk in reversing blade through feather is the high aerodynamic exitation in stall and the effect on blade stresses. In addition, blade operation in and out of stall involves uncertainty, normally hysterisis effects are observed. A means of avoiding these problems is to limit fan rpm while blades are being reversed but this would be at the expense of

Table VIII-4. Task II Study, Direction of Reverse for VP Fans.

THRU FINE PITCH	THRU FEATHER (STALL)
1. REVERSE THRUST CAPABILITY? - HAM. STD. DATA VS DOWTY ROTOL DATA - HIGHER TIP SPEED EXPECTED TO BE BETTER • LOWER CAMBER • GREATER ENERGY INPUT CAPABILITY	1. BLADE MECHANICAL OPERATION IN STALL? 2. FAN AERO. IN AND OUT OF STALL? 3. RESPONSE TIME TO REVERSE (IF ENGINE THROTTLED BACK). 4. ACTUATION SYSTEM WEIGHT.
2. HUB PRESSURE RATIO LOWER (SOLIDITY).	5. THRUST TRANSIENT INTO REVERSE?

response time. Actuation system weight tends to be greater primarily because of the greater angle change required. The approach that is taken is to design the fan with a solidity that will enable the fan to be reversed through fine pitch. However, it is suggested that fan component program be run to test out the limiting problems for both directions of reverse and a decision made on the basis of those results as to the direction to be utilized in the engine.

In addition to reverse thrust, there are other potential uses of variable pitch as indicated on Table VIII - 5. There is an .8 sec. advantage in thrust response for wave off as described earlier in the report, but this must involve high fan speed and off-incidence operation of the fan during landing with implications on approach noise. Experimental results are required to evaluate this noise increase together with further study of the need for very rapid thrust response before a decision can be made whether to utilize this concept.

The Task II VP engine performance was generated assuming a fixed position of the blade with the jet nozzle areas set so that near-peak efficiency operation was obtained at both takeoff and cruise. Once experimental results are available, it may prove possible to obtain a modest improvement in fan efficiency at one condition by adjusting the blade angle slightly. A high fan flow and pressure ratio at cruise is assumed necessary to achieve an adequate level of cruise thrust. There is a

Table VIII-5. _Task II Study, Other Uses of Variable Pitch.

1. TRANSIENT RESPONSE IMPROVEMENT FOR WAVE-OFF

   - FAN BLADES CLOSED TO HOLD FAN SPEED AT 100% DOWN TO 50% FN.

   - AT 50% FN, FLOW REDUCED 25%, BLADES CLOSED $\sim 12^{\circ}$.

   - WILL INCREASE FAN NOISE FOR LANDING.

   - COMPATIBLE WITH REVERSE THRU FINE PITCH.

2. PERFORMANCE IMPROVEMENT

   - CURRENT STUDY ASSUME FIXED ANGLE FOR NORMAL ENGINE OPERATION.

   - FAN EFFICIENCY TRIMMING - WILL REQUIRE EXPERIMENTAL RESULTS.

   - FAN R P M LIMITING AT CRUISE.

3. WINDMILLING DRAG REDUCTION

   - MARGINAL USE OF VP.

   - COMPATIBLE WITH REVERSE THRU FEATHER.

tendency for the highest fan physical speed to occur at maximum climb and cruise conditions , and the use of an open blade setting would reduce the fan rpm but at the expense of stall margin.

A final use of variable pitch is the reduction in windmilling drag, but this feature was not designed into the Task II VP engines.

The payoff of variable pitch is that it reduces the weight penalty of achieving reverse thrust on a low fan pressure ratio engine. This is illustrated on Table VIII - 6 for fan p/p = 1.3 engines. On the right hand side is shown the weight penalty of a cascade type reverser system for an OTW installation which totals 840 lbs (381 Kg). This penalty would be higher for an under-the-wing STOL partial arc reverser installation but lower for a CTOL more complete arc reverser installation. There is an equivalent penalty for the variable pitch engine as shown on the left side of Table VIII - 6. Here the base engine is a fixed pitch design with a tip-shrouded Ti fan. The composite VP fan engine and installation then results in a weight penalty of 570 lbs (358.5 Kg) which is considerably less than the reverser penalty for the fixed pitch engine. If a Ti variable pitch blade had to be used, the weight penalty would be considerably larger and a conventional reverser would be preferable. Note this trade will be affected by fan pressure ratio, the lower fan pressure ratios favoring reverse pitch.

TIP SPEED AND GEARING CONSIDERATIONS

Selection of tip speed has an effect upon the system characteristics. The difference in MPT noise can be taken into account by appropriate

Table VIII-6. Task II Study, Weight Penalties of Reverse Thrust, 24,000-lb Engines.

1.3 Fan P/P Variable Pitch EBF

Fan Design	FP	VP	VP
Material	Ti	Composite	Hollow Ti
Shrouds	Tip	None	None
Tip Speed, fps m/sec	1100 335.3	1100 335.3	1100 335.3
Weight Changes			
Fan Blades	Base	+30 (13.6 kg)	+190 (86.2 kg)
Blade Retention	Base	+130 (59 kg)	+190 (86.2 kg)
Disc and Shafting	Base	+40 (18.1 kg)	+140 (63.5 kg)
Actuation (VP)	Base	+230 (104.3 kg)	+290 (131.5 kg)
Casing and Guard	Base	+80	+230
C & A	Base	+10	+10
Total Basic Engine	Base	+520 (235.9 kg)	+1050 (476.3 kg)
Installation (3rd position on nozzle)	Base	+50 (22.7 kg)	+50 (22.7 kg)
Total Installed Penalty of Reverse VP Feature	Base	+570 (258.3 kg)	+1100 (499 kg)

1.3 Fan P/P Fixed Pitch OTW

Weight Changes (Vs. No Reverser)

Basic Engine Ti None

Installation (No Composites)

	Lbs	kg
Cascade Boxes	+140	63.5
Blocker Doors	+90	40.8
Actuation (Reverser)	+120	54.4
Configuration	+50	22.7
Structure Weight	+440	199.6
Total Installed Penalty of Reverser	+840*	381

* Would be more for EBF, upward arc would be less for CTOL, more complete arc.

design of inlet suppression. A minimum tip speed of about 900 fps (274.3 m/sec) is believed necessary for the 1.25 pressure ratio VP fan for several reasons. The most important of these is the ability of the fan to meet the required pressure ratio at design speed, particularly with the distortion levels to be encountered in the STOL application. A higher tip speed in the 1100 fps (335.3 m/sec) range makes the use of a reduction gear unnecessary. It provides more pressure ratio capability for growth and makes boosters more productive in supercharging the core.

A major issue for the variable pitch engine is the geared vs. direct drive question. Table VIII - 7 lists the comparative results of the current study. The higher inlet MPT noise of the direct-drive design was taken into account in the inlet and suppression design with an associated weight penalty. The basic engine weight is somewhat lower for this advanced geared design with 2 stage LP turbine. Performance is very nearly a tradeoff as indicated on Table VIII - 7. The somewhat lower supercharging achieved with the single booster of the geared design required a 20° higher turbine inlet temperature to achieve the same thrust as for the direct-drive engine. The engine price was estimated to be a standoff, and the net effect of the above on mission merit factor was approximately a 1% better DOC for the geared design, weight being the primary factor.

A survey of commercial transport experience on gearsets in turboprop engines was made. Table VIII - 8 illustrates the situation. The premature

Table VIII-7. Task II Study, Advanced Geared Vs. Direct Driven for 1.25 P/P VP Engine Summary.

Noise	- Difference in MPT noise suppressed in inlet		
Weight	- Basic engine	Up to 150 lbs (68.0 kg) lighter for geared [used lightweight 240 lb (108.9 kg) gearset + 2-stage LP turbine.]	
	- Inlet	Up to 80 lbs (36.3 kg) lighter for geared.	
Performance	- Fan Eff	+ 1%	
	- LP Turb.	Same	
	- Gear Loss	1%	T O Fn same -
	- Cooler Loss	Small	Cruise sfc ~1/2% better for geared
	- Inlet Loss	Small	
	- Cycle P/P	- 5%	
	- T_4	+ 20° F (+11.1° C)	
Engine Price	- Approximately the same		
Reliability	- Better for Direct Drive		
Maintenance Costs	- Estimated to be higher for geared design		
Merit Factor	- Up to 1% better DOC for geared at 1.25 fan P/P might be possible.		
QCSEE Program	- Comparable costs		

Table VIII-8. Task II Study, Geared Vs. Direct-Driven, Current Experience and Projected Reliability, Airline Experience.

CURRENT EXPERIENCE AND PROJECTED RELIABILITY

AIRLINE EXPERIENCE

	GEARSET (ALLISON 501D - AL)	LP TURBINE P&W JT8D (3-STAGE UA)
PRR	.058/1000 HRS.	.0073/1000 HRS.

PROJECTED EXPERIENCE - GE19/F6 ENGINES

	GEARSET + 2-STAGE TURBINE	5-STAGE LP TURBINE
PRR	.0173	.0087 (SAME AS CF6-6 PROJECTION)

removal rate (PRR) experience on a gearset in airline service compared with that of a typical three-stage fan turbine at the top of the chart. The projection of this experience to the GE19 engines is shown at the bottom. An improvement in the gearset reliability was estimated and added to that of a two-stage turbine. The five-stage turbine reliability of the direct-drive engine is the same as projected for the five-stage CF6-6 turbine. The net result is that both engines can have satisfactory gear set plus LP turbine or LP turbine-only reliability, but that the direct-drive engine has the advantage which will be reflected in lower maintenance costs.

MERIT FACTOR COMPARISON

Figure VIII - 1 is an attempt to compare the various propulsion systems on a direct operating cost basis. The left side involves the under-the-wing EBF system and the right side the OTW power lift system, both for 2000' (609.6 m) STOL. The reference propulsion system was taken as the GE19/F2C1, 1.35 fan p/p fixed-pitch engine. The effect of differences in installed weight, performance and cost was then determined for engines scaled to a common installed thrust. Mission trade factors from Task I were then used to determine the impact upon DOC and the results plotted vs. takeoff noise. Note that the OTW cases were treated in the same manner; the results, therefore, do not take into account differences in aircraft life performance, drag or weight.

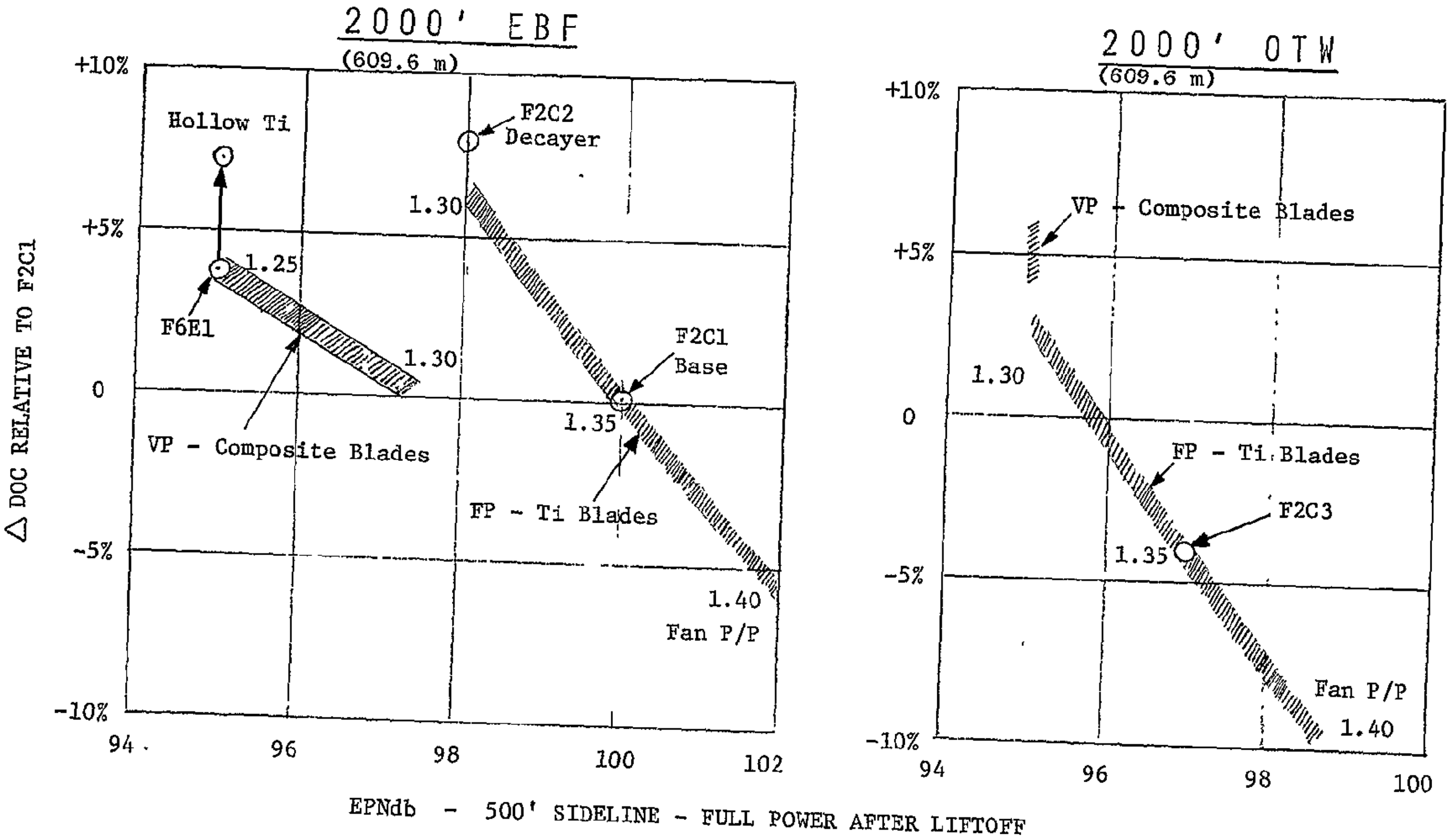

Figure VIII-1. Task II Merit Factor Comparisons, Propulsion System Effects Only.

The open symbols on Fig. VIII - 1 refer to specific Task II engines as indicated. The shaded areas are trends derived from Task I results. It is seen that the variable pitch engine at 1.25 fan p/p can meet 95 EPNdB with only a 3 1/2% DOC penalty relative to the 1.35 fan p/p fixed-pitch engine at 100 EPNdB in the EBF aircraft. Reducing fan p/p of the fixed-pitch engine to reduce noise results in a rapid loss in DOC.

In the case of the OTW installation of the 1.35 p/p fixed-pitch engine, an improvement is obtained in both noise and DOC considering propulsive effects only. Note that the footprint area of the F2C3 with its 97 EPNdB sideline noise in the OTW installation is about the same as that of the F6E1 (VP) engine with its 95 EPNdB sideline noise in the EBF installation. If the fan p/p of the OTW engine is reduced to meet 95 EPNdB on a sideline basis, its merit factor is comparable to that of the VP under-the-wing engine. Both approaches involve areas of risk. For the VP engine, this involves reverse thrust levels and fan operation in reverse; and, for the OTW installation, this involves lift performance for landing. But risk must be accepted in order to achieve a 95 EPNdB system with reasonable economics.

IX. SYMBOLS

Latin

A	Flow area, ft.^{2}
A_A	Annulus area
A_{28}	Duct nozzle area
AGB	Accessory gearbox
Aw	Wetted area - ft.^{2}
AW	Augmentor wing
ALT	Altitude, ft.
BETA	Bypass ratio
C_f	Friction drag coefficient
c	Chord, inches
C_F	Nozzle flow coefficient
CDP	Compressor discharge bleed pressure
C_d	Drag coefficient
C_v	Nozzle velocity coefficient
C_z	Axial velocity, ft./sec.
CTOL	Conventional T/O and landing
D	Diameter, inches
D_f, D.F.	Diffusion factor
D_{HL}	Highlight diameter
DOC	Direct operating cost
D_{ref}	Reference diameter
D_T	Throat diameter
ETAR	Ram recovery
EBF	Externally blown flap

FG	Resultant gross thrust - lb.
FD	Ram drag (W_o/g) - lb.
Fn	Net thrust
FP	Fixed pitch
fps	Feet/second
g	Gravitational constant
GPM	Gallons per minute
H	Height, inches
HP	Horsepower
h	Enthalpy, BTU/lb., or Btu/lb.
i	Incidence angle, deg.
ID	Identification number
ID	Inside diameter
I/S	Interstage
J	Mechanical equivalent of heat
KS	Derivative
KVA	Kili volt amperes
L	Length, inches
LP	Low pressure
LRU	Line replaceable unit
M	Mach no.
M_N	Mach no.
MDOF	Multiple degree of freedom

MPT	Multiple pure tone
Mo	Flight Mach no.
M_R	Relative Mach no.
Mxcru	Max. cruise power setting
N	Number of stages, and rotor speed, RPM
N_F	Fan speed
N_C	Core speed
OD	Outside diameter
OGV	Outlet guide vane
OTW	Over the wing
P	Pressure, psia
P/P	Pressure ratio
P_o	Ambient pressure, psia
P_2	Fan face total pressure, psia
PLA	Power lever angle
PNdB	Perceived noise, decibels
PPH	Pounds per hour
P/S	Power setting
QEC	Quick engine change
R	Radius, inches
ROI	Return on investment
R_x	Reaction
Sec	Second
SFC	Specified fuel consumption, $\frac{lb/hr}{lb}$
S/D	Shut down

SDOF	Single degree of freedom
SM	Stall margin
SOL	Solidity
SDP232	Scalar on fan hub pressure rise
SDHQ49	Scalar on LPT enthalpy drop
SETA2	Scalar on fan hub efficiency
SETA49	Scalar on LPT odiahatic efficiency
STOL	Short T/O and landing
STD	Standard
SLS	Sea level static
SW2R	Scalar on fan hub corrected flow
SW49R	Scalar on LPT flow function
SXNCR49	Scalar on LPT rotor speed
T	Temperature, ^{o}F
T_o	Ambient temperature, ^{o}R
T_2	Fan face total temperature, ^{o}R
t	Thickness, inches
t_m	Maximum thickness, inches
t_e	Trailing edge thickness, inches
T/Q	Thrust/weight ratio
T/O	Takeoff
T_{41}	HP turbine rotor inlet temperature
TGB	Transfer gearbox
T/R	Thrust reverser

U	Wheel speed, ft/sec
USB	Upper surface blowing
V_o	Flight velocity, ft/sec
VP	Variable pitch
VBV	Variable bleed valve
VSV	Variable stator vane
V_8	Core duct exit velocity, ft/sec
V_{28}	Fan duct exit velocity, ft/sec
W	Weight flow, lb/sec
W_o	Total inlet airflow, lb/sec
W_F	Fuel flow
Wt.	Weight

Greek

α_1	Absolute inlet air angle, deg.
β_1	Relative inlet air angle, deg.
β_2	Relative discharge air angle, deg.
β_m	Stagger angle, deg.
γ	Specific heat ratio
Γ	Swirl angle
Δ	Incremental change
δ	Deviation angle, deg. and inlet pressure correction
η_{ad}	Adiabatic efficiency
η_p	Polytropic efficiency
λ	Wave length
ω	Loss coefficient
φ	Camber
Σ	Sum of
σ	Solidity
θ	Inlet temperature correction
ψ	Turbine loading
ϕ	Glide slope angle
$\Delta P/P_T$	Total pressure loss
α	Power lever angle

FEDD